FULL-STATE AND OUTPUT FEEDBACK CONTROL OF UNCERTAIN NONLINEAR NONSTANDARD MULTIPLE-TIME-SCALE SYSTEMS

A Dissertation

by

DIPANJAN SAHA

Submitted to the Office of Graduate and Professional Studies of
Texas A&M University
in partial fulfillment of the requirements for the degree of

DOCTOR OF PHILOSOPHY

Chair of Committee,	John Valasek
Committee Members,	Suman Chakravorty
	Swaroop Darbha
	Srinivas Vadali
Head of Department,	Rodney Bowersox

December 2018

Major Subject: Aerospace Engineering

ABSTRACT

Nonlinear systems with dynamics evolving in distinct slow and fast time-scales are common in science and engineering. Geometric singular perturbation theory is a powerful tool for controller design for such systems over multiple-time-scales. Aerospace vehicles such as aircraft and spacecraft are examples of nonstandard multiple-time-scale systems, for which the control synthesis is more challenging than for standard systems. Most control methods for nonstandard systems assume deterministic model and full-state feedback. This dissertation extends the current capabilities of multiple-time-scale control for nonstandard systems by developing novel theories of control design for uncertain systems and using output feedback. Both of slow state tracking and simultaneous slow and fast state tracking for nonstandard systems are considered as control objectives. Using the time-scales of the slow states, slow actuators, fast states and fast actuators, the control laws developed over four-time-scales can account for multiplicative and additive uncertainties. The controller uses estimates of the unknown parameters and the unmeasured states, and ensures Lyapunov-stability of the lower-order reduced subsystems. The estimates are updated by an online parameter estimator and a nonlinear state observer respectively. They are designed using the composite Lyapunov analysis. This analysis also proves the boundedness of errors and establishes bounds of time-scale separation to accomplish the same. The theory is applied to perform attitude tracking for a generic spacecraft with uncertain inertias, and large-amplitude combined longitudinal and lateral/directional maneuvers of a nonlinear six-degree-of-freedom aircraft with uncertain inertias, control derivatives and engine time-constant.

DEDICATION

To

my family, friends, teachers and students,

Stephanie and Dr. V,

members of the VSCL family

ACKNOWLEDGMENTS

First and foremost, I would like to express my sincere gratitude to my Ph.D. advisor, Dr. John Valasek. It is his constant guidance, support, planning, insights, encouragement, enthusiasm and humor which made this long journey an exciting and memorable one. Dr. Valasek showed tremendous patience for a long time as I experienced a steep learning curve. He believed in me and stayed with me as I gradually got better at critical thinking, producing new results, meeting deadlines, and communicating my research in the written as well as the oral form. Coming from a non-aerospace background, it is by taking, grading for and teaching multiple times Dr. Valasek's flight dynamics class that I got introduced to and began to appreciate the intellectually rich and complex world of aircraft. None of the aircraft simulations in this dissertation would have been possible without this very necessary exposure. Moreover, the spacecraft simulations in this dissertation could not happen, had he not thought about us writing a paper on spacecraft attitude control. In addition to research and teaching, Dr. Valasek played a significant role in my professional and to a large extent personal development. He gave me many opportunities to strengthen my mentoring and leadership skills. I would also like to thank Dr. Valasek's wife Stephanie, who recognizes and celebrates his consistent attempts to go 'the extra mile', and who is as much a part of our group as Dr. Valasek himself is.

I would like to thank my committee members Dr. Srinivas Vadali, Dr. Suman Chakravorty and Dr. Swaroop Darbha for their valuable time and efforts to review this dissertation and provide insightful comments and feedback to improve the work. From my interactions with them I was able to get a better grasp of the fundamentals and subtleties in the field of dynamics and control. I would also like to acknowledge Dr. Raktim Bhattacharya who provided a MATLAB simulation of a nonlinear six-degree-of-freedom generic F-16A which I used in many examples.

I would like to acknowledge my colleagues who have been part of the Vehicle Systems & Control Laboratory (VSCL) over the years. It is a great pleasure working with all of them. I learnt the fundamentals of nonlinear multiple-time-scale control by reading the Ph.D. dissertation of

VSCL alumnus Dr. Anshu Narang-Siddarth. Dr. Narang-Siddarth and Dr. Valasek subsequently co-authored a book based on her dissertation. This book helped me appreciate and enjoy the field of geometric singular perturbations. The concept of online parameter estimation forms a significant part of the theoretical development in this dissertation. I learnt this technique from my former VSCL colleague Dr. Douglas Famularo whose Ph.D. dissertation is in adaptive control. Part of the aircraft simulations involve data collected from the X-Plane 10 Engineering Flight Simulator, which could not have been possible without VSCL graduate research assistants Josh Harris and Emily Fojtik. In addition, I would like to acknowledge former and current VSCL graduate researchers Jim Henrickson, Cameron Rogers, Jack Lu, Vinicius Goecks and Zeke Bowden who attended my presentations from time to time and helped better the research by asking questions and providing insightful comments. My special thanks go to VSCL undergraduate researcher Charles Noren, who has been a constant source of insightful discussions along with enthusiasm and wholehearted support. There is a long list of VSCL undergraduate researchers who helped me better my research and enjoy my stay. Finally, it has been a great joy working with my mentees: Ritwik Bera, Christopher Leshikar and Md. Mashfique Reza. Ritwik worked with me for only one summer, but together we made significant progress. I have been fortunate to be able to mentor Chris and Mashfique for almost two years. They not only made me a better learner of this field, but also helped accelerate the progress of the research when it was needed. Chris and Mashfique have been my companions right from writing the first few lines of math to running the simulations - in fact all the way up to the time-consuming typing of quite a few equations for this dissertation. I cannot thank them enough.

I would like to express my sincere thanks to the staff of the Aerospace Engineering department at Texas A&M University. In particular, I want to acknowledge our current graduate advisor Ms. Gail Rowe. Gail has helped a lot to keep me updated on what needs to be done by when: the deadlines and the paperwork. I would also like to thank Ms. Rose Sauser. Rose was my go-to person every time I needed help in my advisor's absence, and every time I traveled to a conference. Apart from being a thorough professional with a commendable work ethic, Rose was also a great

friend with whom I enthusiastically shared many personal stories from time to time.

Being the first person in my family to pursue a Ph. D., many times it was hard for me to communicate my learning experiences effectively to my parents. For them it was a steeper learning curve to adjust to my new lifestyle and new ways of thinking. My parents have been incredibly patient and supportive throughout the journey. I had to stay away from my family from many years; I missed many get-togethers and special occasions. I am blessed to have a family which stood by me, believed in me and supported me when I needed the most. My friends in India and in the United States proved to be of great support during my Ph.D. years. At times by offering advice, at times by planning get-togethers, making the environment light and letting me relax, at times by planning trips so we can recharge and get back to work, my friends have played a big role in helping me keep the ball rolling. I am grateful to have teachers who inspired me and instilled in me the virtues of honesty, integrity, dedication and respect. As a graduate teaching assistant and an instructor of record, I have come in contact with bright young minds. Teaching them automatically helped me become better at research.

I am grateful to have in my life so many important people who have made a real difference. Directly or indirectly they made valuable contributions towards my Ph.D. research. I acknowledge all of their contributions as I write this dissertation.

CONTRIBUTORS AND FUNDING SOURCES

Contributors

This work was supported by a dissertation committee consisting of Dr. John Valasek (advisor), Dr. Srinivas Vadali and Dr. Suman Chakravorty of the Department of Aerospace Engineering and Dr. Swaroop Darbha of the Department of Mechanical Engineering.

The nonlinear six-degree-of-freedom MATLAB simulation of the generic F-16A for Chapters 2-4 was provided by Dr. Raktim Bhattacharya. The data of the reference aircraft states for the flight simulator maneuver was collected from the X-Plane 10 Engineering Flight Simulator of the Vehicle Systems & Control Labotatory by Joshua Harris and Emily Fojtik.

All other work conducted for the dissertation was completed by the student independently.

Funding Sources

Graduate study was supported by an assistantship with the Department of Aerospace Engineering at Texas A&M University.

NOMENCLATURE

DOF	Degrees Of Freedom
LPM	Leading Principal Minor
MRP	Modified Rodriguez Parameter
$\mathbb{R}$	Set of real numbers
x	slow states OR kinetic slow states
ξ	kinematic slow states
z	fast states
δ_s	slow actuators
δ_f	fast actuators
x_U	unmeasured slow states
σ	time-scale parameter for slow actuators
ε	time-scale parameter for fast states
ρ	time-scale parameter for fast actuators
p_*, p^*	lower and upper bounds of a time-scale parameter p for a deterministic system with full-state feedback
p_{**}, p^{**}	lower and upper bounds of a time-scale parameter p for an uncertain system with full-state feedback
p_{***}, p^{***}	lower and upper bounds of a time-scale parameter p for an uncertain system with output feedback
$\hat{p}, \hat{\chi}$	estimate of an unknown parameter p or an unmeasured state χ
α_i	weights of individual Lyapunov functions in the composite
θ_i	gains used in the parameter update laws

TABLE OF CONTENTS

Page

LIST OF FIGURES

FIGURE Page

LIST OF TABLES

TABLE Page

1. INTRODUCTION

1.1 Merits of Multiple-Time-Scale Control Using Geometric Singular Perturbation

Dynamics evolving in distinct slow and fast time-scales are observed in systems such as aircraft [1], spacecraft [2], robotic manipulators [3], electrical power systems [4], biochemical reactions [5], nuclear reactors [6], production planning in manufacturing [7], and so on. Geometric singular perturbation theory [8, 9] gives an asymptotic view of the evolution of the states of the system in two different time-scales. In the fast time-scale, the fast states evolve to an equilibrium manifold, while the slow states remain frozen at the initial conditions. In the slow time-scale, the slow states evolve, while the fast states stay on the manifold. Using this physical insight of the dynamics, control laws can be designed in two distinct time-scales. For a two-time-scale system with one state evolving in the slow time-scale and one state in the fast time-scale, the state-space model has a small positive parameter ε such that $0 < \varepsilon << 1$. This parameter is called the *perturbation parameter* or the *time-scale separation parameter*. Two extremes of time-scale separation can be described as follows: the case of infinite separation of time-scales is represented by $\varepsilon = 0$, and the case of no separation is represented by $\varepsilon = 1$. For control law design, geometric singular perturbation theory suggests the use of lower-order reduced subsystems by artificially substituting $\varepsilon = 0$, i.e. assuming infinite time-scale separation. The difference between the full-order dynamics with finite time-scale separation and the reduced-order dynamics with infinite time-scale separation is taken care of by a separate stability analysis, called the composite Lyapunov analysis [10]. This analysis produces bounds of the time-scale separation parameter ε within which the control law is guaranteed to keep the closed-loop system stable. In addition to slow and fast system states, a system can have actuators working in slow and fast time-scales. For example, aircraft have velocity and aerodynamic and kinematic angles as slow states, while angular rates are fast. Aircraft also have slow engine dynamics, and fast dynamics of the aerodynamic control surfaces. Inclusion of actuator dynamics is an important consideration for control design, and it may lead to additional

time-scales in the model. In such cases, the concepts from the geometric singular perturbation theory can be extended to state-space models with more than one perturbation parameters, and the control law can be designed in more than two time-scales [11].

Controller design using the geometric singular perturbation approach has a few major benefits. First, it results in a nonlinear controller for a nonlinear system, and does not involve any linearization or gain-scheduling in the development. This is of particular advantage for aircraft control design, since it does not require approximate linear models using short-period and phugoid approximations followed by gain-scheduling. Second, this approach does not treat the slow and the fast dynamics as two completely isolated subsystems; it rather takes care of the coupling between them in different time-scales. Third, the use of reduced subsystems obtained by artificially substituting $\varepsilon = 0$ makes the control design mathematically easier. However, the control law still works on the full-order dynamics as long as the perturbation parameter ε is within the bounds determined by composite Lyapunov analysis. Fourth, for systems like aircraft, the time-scale separation parameter is not a function of system parameters. It is not known exactly, and added artificially in the model to separate the slow and the fast states. If it is possible to design a compensator which does not require explicit time-derivatives with respect to the fast time-scale, the control design does not require exact knowledge of the time-scale separation parameter ε. However, closed-loop stability can still be guaranteed as long as ε is within a bound established by the composite Lyapunov analysis.

1.2 Literature Review

A review of the important historical developments in singular perturbation and its applications in control theory can be found in the works of Kokotovic *et. al.* [12], Naidu and Calise [13], Naidu [14], and O'Malley [15, 16]. The concept of singular perturbation originated as an integral part of Prandtl's boundary layer theory in the field of fluid dynamics. For high Reynolds numbers the velocity profile in an incompressible viscous flow past an object changes very rapidly from zero at the boundary to the value as given by the solution of the Navier–Stokes equation. This

change takes place in a region near the wall, called the *boundary layer*. The thickness of this boundary layer is inversely proportional to the square root of the Reynold's number. The works of Tikhonov [17] and Vasileva [18] on systems of differential equations containing small parameters multiplying the derivatives of the highest order built some of the most important foundations of the singular perturbation theory.

In the second half of the twentieth century singular perturbation methods became popular in control theory, particularly for systems described by stiff high-order differential equations. The source of the stiffness and high order is the presence of some "parasitic" parameters such as small time constants, resistances, inductances, capacitances, moments of inertia, Reynolds number, etc. Each of these parasitic parameters can be small or large. If the original parameter is large such as the Reynold's number, the reciprocal of the original parameter can be thought of as a small parameter. In case a small parameter multiplies the highest-order derivative of a differential equation, equating the parameter to zero results in a degenerate lower-order differential equation. This indicates a singularity, since a lower-order differential equation cannot satisfy all the initial or boundary conditions for the original higher-order differential equation. Tikhonov's theorem [17] enabled the analysis of such high-order systems as a combination of two lower-order subsystems working in two different time-scales: an 'outer layer' subsystem evolving in a slower time-scale, and a 'boundary layer' subsystem evolving in a faster time-scale. This is how singular perturbation began to serve as a powerful model reduction technique in systems and control. Model order reduction using singular perturbation is the focus of Refs. [19, 20]. Singular perturbation techniques were first applied in optimal control problems in the works of Kokotovic and Sannuti [21–23]. Both of the open-loop formulation leading to two-point boundary value problems and the closed-loop formulation leading to the matrix Riccati equation were studied. Further work on the application of singular perturbation on optimal control problems can be found in Refs. [24–26]. In addition to continuous-time systems, singular perturbation techniques were applied for control of discrete-time systems in Refs. [27, 28]. A recent work of Zheng *et. al.* [29] focused on system identification and control of nonlinear singularly perturbed systems.

The work of Lagerstrom and Casten [30] provided a review of the method of asymptotic expansion to solve singularly perturbed differential equations. In contrast, Fenichel [8] proposed a geometric approach which gave a physical insight into the time-scale evolution of singularly perturbed systems. This approach introduced the notion of the 'equilibrium manifold'. It was seen previously that suppressing the time-scale separation parameter ε for a two-time-scale system results in the fast dynamics reducing to a system of algebraic equations. Tikhonov's theorem [17] mentioned the existence of an isolated real root for the fast states, obtained by solving the system of algebraic equations. The geometric approach established the notion of the 'equilibrium manifold' of the fast states as a physical equivalent of the 'isolated real root'. Following the geometric approach, a control synthesis technique called *composite control* [10] was developed for two-time-scale systems. This technique assumed a structure of the control as a sum of a slow component and a fast component. The slow component was present in both of the slow and the fast time-scales, and ensured that the slow states evolved to their desired reference. The fast component, present only in the fast time-scale, ensured that the fast states evolved to their 'equilibrium manifold'.

A major limitation of the analysis and control methods developed so far was that they relied on the existence of an isolated real root or an equilibrium manifold. This was obtained by solving the algebraic equation resulting from setting the time-scale separation parameter to zero. The implicit function theorem [31] states a sufficient condition for the existence of such isolated real roots. One of the ways the existence of a manifold is guaranteed for a two-time-scale system is when the fast dynamics are linear in the fast states. On the other hand, if the fast dynamics are nonlinear in the fast states, the existence of a unique equilibrium manifold is not always guaranteed. At this point singularly perturbed systems were classified as standard and nonstandard, depending on whether the existence of an "isolated real root" for the fast states is guaranteed or not. The angular rates are the fast states for aircraft and spacecraft. Their evolution equations have inertial coupling, which involve products of angular rates. As a consequence aircraft and spacecraft are examples of nonstandard systems. The control synthesis tools based on Tikhonov's theorem are

not applicable for nonstandard systems. Several works of Narang-Siddarth and Valasek [11, 32–34] developed control techniques for nonstandard systems. Their works considered two different control objectives: (1) slow state tracking, (2) simultaneous slow and fast state tracking.

The fundamental idea behind the design of slow state tracking controllers is to drive the fast states to a suitable equilibrium manifold in the fast time-scale, and then drive the slow states to their reference in the slow time-scale. For nonstandard systems, finding a suitable equilibrium manifold is a challenge. Depending on how the manifold is selected, slow state tracking controllers have been developed for nonstandard systems using two different methods. The method of modified composite control *approximates* the manifold. This is a two-stage design method in which the nonlinear control law is designed as a sum of slow and fast components. In essence it is an extension of the regular composite control method [10] for standard systems, except for the fact that an approximate solution for the manifold is obtained using ideas based on the center manifold theorem [11,32]. Subsequently the stability of the closed-loop system is established using Lyapunov analysis. However, it is not always straightforward to find an approximation of the manifold. To avoid this issue, an alternative method called sequential control *specifies* the manifold of the fast states as an intermediate control variable to achieve slow state tracking, and then designs the control so the fast states can be stabilized on the manifold. In addition to being mathematically more convenient, sequential control has another major advantage over modified composite control. In modified composite control the slow and fast components of the controller are selected using any nonlinear control synthesis technique, and subsequently the stability is investigated using Lyapunov analysis. On the other hand, sequential control is a Lyapunov design method. The manifold of the fast states and the control are designed such that the equilibrium points for the reduced subsystems are guaranteed to be Lyapunov-stable. The subsequent Composite Lyapunov analysis helps establish the stability of the full-order system. These advantages make the sequential control method suitable to extend to more than two time-scales. In the literature the method of sequential control was extended to include slow and fast actuator dynamics in addition to slow and fast system states, thus increasing the number of time-scales from two to four [11].

Several aerospace applications of these slow state tracking control methods can be found in the literature. Modified composite control was implemented on a nonlinear six-degree-of-freedom (6-DOF) generic F/A-18A commanded to perform a 45 degree left turn [33]. It was seen that the controller could track the three commanded states: angle-of-attack, sideslip angle and heading angle. However, the aircraft lost almost half of its initial airspeed as it completed the turn. This was because velocity was not considered for tracking. The slow engine dynamics were not accounted for, and throttle was kept constant. In order to have better control over velocity, it was necessary to consider the slow dynamics of the engine and the fast dynamics of the aerodynamic actuators. This needed an application of the four-time-scale version of sequential control which accounts for slow and fast actuator dynamics. The work of Saha *et. al.* [35] developed a four-time-scale sequential controller to accomplish a large-amplitude combined longitudinal and lateral/directional maneuver of a generic F-16A. For an evaluation maneuver comprising of a 90 degree left turn followed by a 90 degree right turn [36], it was observed that the inclusion of slow and fast actuator dynamics in the control synthesis reduced the loss of airspeed during turn from 50% to 5%. In addition, the velocity came back to the commanded value as each turn was complete.

In contrast to slow state tracking, the sequential approach does not work when it is required to track simultaneously both the slow and fast states of a nonlinear, nonstandard two-time-scale system. For this problem, the fast states have to reach a commanded reference trajectory. This reference trajectory may not be a suitable equilibrium manifold to enable the slow states to evolve to their reference. As a result, the state-of-the-art for simultaneous slow and fast state tracking is a coupled two-stage design of the control instead of the sequential design [11]. The control is assumed to be a sum of two components. One component is present in both the slow and the fast time-scales, and it is designed such that the slow states track their reference in the slow time-scale. An additional component is present only in the fast time-scale, and it is designed such that the fast states track their reference. The stability of the full-order closed-loop system is then established using Composite Lyapunov analysis. This method was applied on a nonlinear 6-DOF generic F/A-18A aircraft commanded to perform an aggressive climb and roll maneuver [11]. Similar to

the 45 deg turn maneuver, it was seen that the controller could track the three commanded states: sideslip angle, body-axis roll rate and pitch rate. However, velocity was not tracked, and throttle was kept constant. As a result, the aircraft lost almost 50% of its airspeed as it climbed. A later work of Saha and Valasek [37] followed the two-stage design method to develop a simultaneous slow and fast state tracking controller for a nonlinear 6-DOF generic F-16A. This paper showed that the inclusion of velocity as a commanded state and throttle as an automatic control was able to reduce the loss of airspeed from 50% to 25% using military thrust. The controller was able to reduce the loss of airspeed even further using the afterburner thrust level. Moreover, the velocity came back to its commanded value as the aircraft completed the climb.

1.3 Contributions of this Dissertation

This dissertation significantly extends the capabilities of the control synthesis techniques for finite-dimensional, affine in control, nonlinear, nonstandard, multiple-time-scale systems by addressing a few major limitations of the previous methods, and developing new theories to overcome them. The new development seeks to fulfill three different research objectives.

The first objective the current research seeks to address is to investigate a theory of slow state tracking control law design for finite-dimensional, affine in control, nonlinear, nonstandard multiple-time-scale systems with multiplicative and additive uncertainties, and slow and fast actuator dynamics, assuming full-state feedback. A major limitation of the current sequential design approach for slow state tracking is that it assumes the model to be deterministic. In practice it is not possible to have a perfect knowledge of the model structure and parameters. The stability guarantees for a deterministic model may not hold if one or more parameters of the system are not known exactly, or if there are additive uncertainties. For aircraft, it is often difficult to obtain accurate values of the inertias. Moreover, the aerodynamics are modeled using stability and control derivatives. While both types of derivatives are difficult to obtain accurately, in particular it is more difficult to obtain accurate values of the control derivatives than those of the stability derivatives. Furthermore, the throttle is a slow actuator due to the slow engine dynamics. While the turbomachinery can be modeled as a first-order actuator, the time-constant

of the engine is difficult to obtain accurately. In addition, additive uncertainties appear as the aerodynamic forces and moments are *approximated* using first-order Taylor series expansions, with the partial derivatives being the stability and control derivatives. Therefore, it is needed to develop a new theory to account for multiplicative and additive uncertainties, and establish new bounds of the time-scale separation parameters for stability of the full-order nonlinear system.

In the literature there are some works where the singular perturbation approach has been used for controller design for uncertain nonlinear systems. For a nonlinear system in strict feedback form with nonlinear input uncertainties, a high gain scaling control design was developed in Krishnamurthy and Khorrami [38]. To recover the trajectories of a nominal control design in presence of uncertain nonlinearities, time-scale separation based robust redesign techniques are proposed in Chakrabortty and Arcak [39]. Insights from this approach were utilized in the control design with high gain filters for a nonlinear system with matched and unmatched uncertainties in Asadi and Khayatiyan [40]. This approach creates time-scales for the control design such that the uncertainty is estimated in a faster time-scale, and the nominal controller works in a slower time-scale. However, this approach does not consider time-scales in the dynamics of the system. The first objective of the current research addresses time-scales in the model itself, along with model uncertainties and actuator dynamics.

Figure 1.1 shows a schematic of the slow state tracking controller design over four time-scales. The numbers in Figure 1.1 indicate the order in which the design variables are selected. In the slowest time-scale, the manifold of the fast states and that of the slow actuators are chosen as intermediate control variables such that the slow states reach the desired reference. In the second slowest time-scale, the slow controls are selected such that the slow actuators reach their manifold. In the second fastest time-scale, the manifold of the fast actuators is selected such that the fast states reach their manifold. Finally, in the fastest time-scale, the fast controls are selected such that the fast actuators go to their manifold.

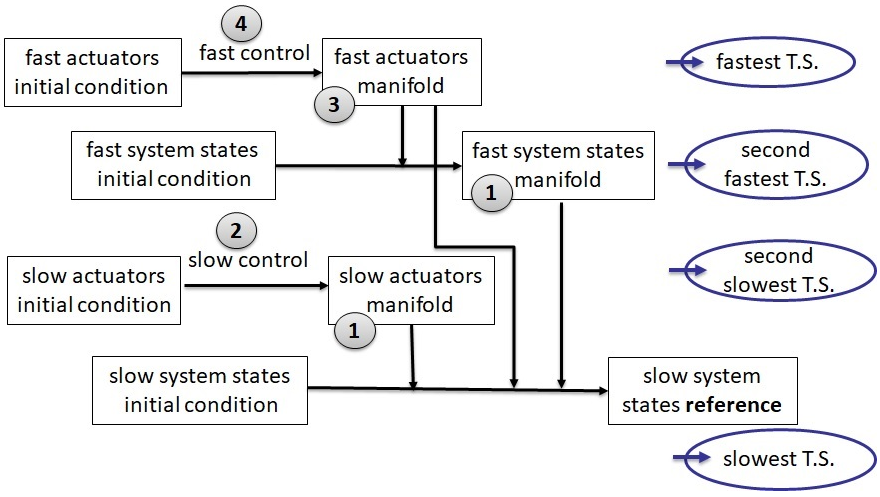

Figure 1.1: Slow state tracking control design approach

The novelty of this work for slow state tracking is to develop a theory such that multiplicative and additive uncertainties in the nonlinear nonstandard model can be accounted for. Multiplicative uncertainties are parametric, and to address the same the four-time-scale sequential controller shown in Figure 2.18 uses the estimates of the unknown parameters. An online parameter estimator updates the estimates. The additive uncertainties are handled by the composite Lyapunov analysis. Moreover, the slow states to be tracked are divided into kinetic and kinematic slow states. The idea came from the development of the four-time-scale aircraft controller in Saha *et. al.* [35]. The classification of slow states as kinetic and kinematic made it possible to decouple the selections of the manifolds of the fast states and the slow actuators. The utility of this classification to handle uncertainties was mentioned as a comment in Ref. [41], and used as a fundamental consideration in Refs. [42, 43]. The evolutions of the kinematic states describe only the properties of the motion, and therefore do not have any uncertainty. Kinetic states, however, have uncertainties in their evolution.

The first objective of the current research seeks to develop following for slow state tracking of nonstandard multiple-time-scale systems with uncertainties and actuator dynamics using full-state feedback:

- a procedure to construct reduced subsystems in presence of uncertainties
- a method to design the slow and fast control commands to achieve slow state tracking and guarantee Lyapunov-stability of the reduced subsystems in presence of uncertainties
- a method to design the online parameter estimator: which parameter needs to be updated in which time-scale, and parameter update laws
- a proof that the tracking errors, manifold errors and parameter estimation errors are bounded: conditions needed on the system parameters, functions, matrices, controller gains, and lower and upper bounds of the three perturbation parameters to ensure the boundedness of errors.

The development starts with a two-time-scale spring-mass-damper system, and complexity of the class of systems is increased progressively. Attitude tracking of a rigid spacecraft with uncertain inertias is shown as a three-time-scale example, and large-amplitude combined longitudinal and lateral/directional maneuvers of aircraft are shown as four-time-scale examples.

The second objective of the current research is to investigate a theory of simultaneous slow and fast state tracking control design for finite-dimensional, affine in control, nonlinear, nonstandard multiple-time-scale systems with multiplicative and additive uncertainties, and slow and fast actuator dynamics, assuming full-state feedback. There are two major limitations of the existing two-stage design used for simultaneous slow and fast state tracking. This method can handle slow and fast system states, but all actuators are assumed infinitely fast. Even in the case of the improved performance shown in the work of Saha and Valasek [37], the closed-loop speeds of response of the states were adjusted with the controller gains, and actuator dynamics were included only in simulation. A new theory is needed to account for the actuator dynamics realistically in the control synthesis. Since the actuators do not have a reference, they can be commanded to go to any suitable equilibrium manifold so the states can track their reference. Unlike the sequential method for slow state tracking, it is not straightforward to extend the two-stage design method to add actuator dynamics. A second limitation of the existing two-stage design is the assumption of a deterministic model. Similar to the case of slow state tracking, it is possible that the

stability guarantees derived for a deterministic system may not hold in presence of uncertainties. Therefore, a new theory needs to be developed accounting for model uncertainties in the design.

Figure 1.2 shows the new approach developed in this work to accomplish simultaneous slow and fast state tracking in four time-scales. The numbers 1,2,3,4 indicate the sequence in which they are selected. In the fastest time-scale, the fast actuators evolve from their initial condition to their equilibrium manifold. This equilibrium manifold acts as an intermediate control variable which drives the fast states to their reference trajectory in the second-fastest time-scale. In the second slowest time-scale, the slow actuators evolve from their initial conditions to their equilibrium manifold. Finally, in the slowest time-scale, the manifolds of the slow and fast actuators and the reference for fast states drive the slow states to their reference.

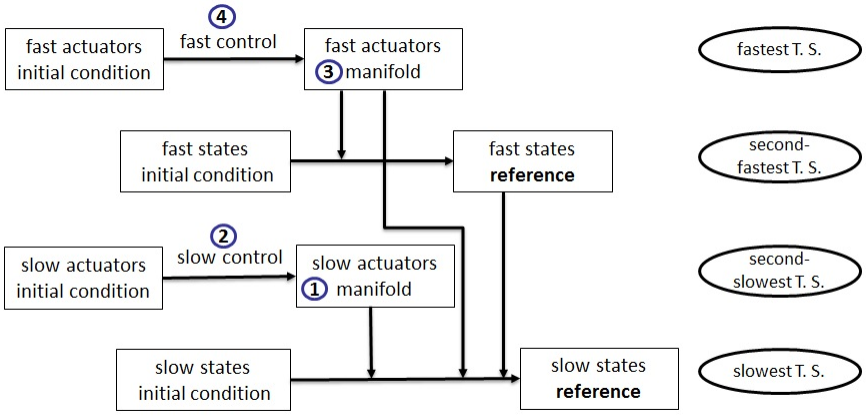

Figure 1.2: Simultaneous slow and fast tracking control design approach

The new approach is in essence a sequential approach for slow and fast state tracking. This is to some extent similar to slow state tracking, except for the fact that no kinematic slow state is considered for tracking. Only the kinetic slow states and the fast states are tracked. Furthermore, to address the issue of multiplicative or parametric uncertainties an online parameter estimator is designed. The parameter update laws chosen from the composite Lyapunov analysis. The additive uncertainties are handled directly by the composite Lyapunov analysis.

The second objective of the current research seeks to develop the following for simultaneous slow and fast state tracking of nonstandard multiple-time-scale systems with uncertainties and actuator dynamics using full-state feedback:

- a procedure to construct reduced subsystems in presence of uncertainties
- a method to design the slow and fast control commands to achieve simultaneous slow and fast tracking and guarantee Lyapunov-stability of the reduced subsystems
- a method to design the online parameter estimator: which parameter needs to be updated in which time-scale, and parameter update laws
- a proof of boundedness of the tracking errors, manifold errors and parameter estimation errors: conditions needed on the system parameters, functions, matrices, controller gains, and lower and upper bounds of the three perturbation parameters to ensure boundedness of errors.

The application considered for this objective is a large-amplitude combined longitudinal and lateral/directional maneuver of a nonlinear 6-DOF aircraft. The controller tracks the same reference used for the climb and roll maneuver in Saha and Valasek [37] in presence of slow and fast actuator dynamics and uncertainties in the following: inertias, control derivatives and engine time-constant.

The third objective of the current research is to investigate a theory of output feedback control design for slow state tracking as well as simultaneous slow and fast state tracking of finite dimensional, affine in control, nonlinear, nonstandard multiple-time-scale systems with multiplicative and additive uncertainties, and slow and fast actuator dynamics. A major limitation of most control design approaches for nonlinear, nonstandard multiple-time-scale systems is the requirement of full-state feedback. In practice, measurement of all the states may not always be possible, and hence is the need for output feedback. One way of dynamic compensation using output feedback is to use state observers to feed the estimates of the states to the controller designed assuming full-state feedback. For linear systems, the well-known separation principle

enables controller and observer to be designed independently of each other. For nonlinear systems, the separation principle does not work, and the designs are likely to be coupled. In literature there are some works on observer-based feedback design for two-time-scale systems. For a robotic manipulator, a linear observer for the fast state is proposed in the works of Ashayeri *et al.* [44] and Tavasoli *et al.* [3]. For a discrete linear two-time-scale system, an output feedback control scheme based on genetic algorithm is proposed in Pan and Chen [45] and Pan *et al.* [46]. A Linear Quadratic Gaussian (LQG) controller in two time-scales is developed for a missile autopilot in Moghaddam and Zarabadipour [47]. Design of observer-based controllers for linear time-delay systems with two-time-scale dynamics is discussed in Chiou [48]. Observer design for linear two-time-scale systems with Lipschitz constraint is considered in Wang and Liu [49]. Hofmann and Sanders [50] present an observer-based torque control of an induction machine. In all of the above works, the observer design is based on the system dynamics being linear or linearized, and standard. For a nonlinear two-time-scale spring-mass-damper with one slow and one fast states, both of the controller and the observer were designed in two time-scales [51]. This observer-based feedback design was an extension of the method of sequential control developed earlier with the assumption of full-state feedback [11]. The Lyapunov design of observers in two time-scales led to guaranteed stability of the corresponding reduced subsystems. A total of six cases - two different cases of dynamics and three difference cases of measurement - were described, and results were presented for four of them. The cases of dynamics were (a) high damping and (b) high stiffness. The cases of measurement were (a) only the slow state measured, (b) only the fast state measured, (c) a linear combination of the states measured. While this paper demonstrated how the sequential control can be extended to observer-based feedback, the stability of the full-order nonlinear system including the controller and the observer in the loop was not investigated. For one of the four cases in this paper, the procedure was extended further to a nonlinear spring-mass-damper with multiple slow and fast states [52]. This work showed an approach to analyze closed-loop stability of the full-order system by using an extension of the composite Lyapunov analysis. The composite Lyapunov function for the full-order system was a linear combinations of the individual Lyapunov

functions used to design the controller and the state observer.

While the previous works of the authors [51, 52] addressed the controller and observer design using reduced subsystems in two time-scales, a few issues have not been investigated yet. One of the previous works [52] established an acceptable range of the time-scale separation parameter graphically by plotting the eigenvalues of a matrix. Moreover, there was no guideline on acceptable ranges of gains to obtain a suitable bound of time-scale separation. A more rigorous analytical treatment of the composite Lyapunov analysis is needed for output feedback. In addition, the model used in this work [52] is such that the nonlinearity is present in the reduced subsystems. This nonlinearity can be canceled in part by the controller design. However, the analysis becomes more challenging when the nonlinearity is present in the full-order dynamics but is not captured in the reduced subsystems. The cases of high damping in the authors' another previous work [51] fall under this category, and the stability analysis for them is yet to be investigated. Furthermore, how the different cases of measurement alter the bounds of stability is yet to be investigated.

Moreover, none of the authors' previous works considered output feedback in the presence of uncertainties and slow and fast actuator dynamics. Intuitively, one way of control synthesis for such a system is to have a controller which uses the estimates of the unknown parameters and unmeasured states. An online parameter estimator updates the parameter estimates, and a nonlinear observer updates the estimates of the unmeasured states. In the literature there are some works on design of nonlinear observers for simultaneous parameter and state estimations of nonlinear systems [53] and adaptive output feedback control [54, 55], but the problem of multiple-time-scale output feedback design for uncertain nonlinear, nonstandard systems have not been investigated. The third objective of the current work seeks to develop the following for slow state tracking as well as simultaneous slow and fast state tracking of uncertain nonstandard multiple-time-scale systems with uncertainties and actuator dynamics using output feedback:

- how the system dynamics should be modified from the one used for the first two objectives, and how to select the measurement vector so output feedback with observer can be used
- a method to design the slow and fast controls to guarantee Lyapunov-stability of the reduced

subsystems in presence of uncertainties

- a method to select the parameter update laws for an online estimator as well as the state observation laws for a nonlinear observer

- a proof of boundedness of the tracking errors, manifold errors, parameter estimation errors, state observation errors: conditions needed on the system parameters, functions, matrices, controller gains, and lower and upper bounds of the three perturbation parameters to ensure boundedness of errors.

The application considered for this objective is a large-amplitude combined longitudinal and lateral/directional maneuver of a nonlinear 6-DOF aircraft. The output feedback controller performs all of the maneuvers considered for full-state feedback, when the angle-of-attack and the sideslip angle are not measured. The controller works in presence of slow and fast actuator dynamics and uncertainties in the following: inertias, control derivatives and engine time-constant.

1.4 Organization of the Dissertation

The theoretical developments and applications in this dissertation are organized as follows. The first research objective of slow state tracking in the presence of uncertainties and actuator dynamics using full-state feedback is the focus of Chapter 2. Chapter 3 deals with simultaneous slow and fast tracking using full-state feedback for uncertain multiple-time-scale systems. Output feedback design is in Chapter 4. Chapter 5 discusses the conclusions based on the results in Chapters 2-4. Future directions of research are in Chapter 6.

2. SLOW STATE TRACKING IN THE PRESENCE OF UNCERTAINTIES AND ACTUATOR DYNAMICS WITH FULL-STATE FEEDBACK

2.1 Introduction

This chapter addresses the first objective of slow state tracking control for nonlinear, nonstandard multiple-time-scale systems with uncertainties and actuator dynamics, using full-state feedback. The complexity of the class of systems is progressively increased in this chapter. To show how the current work makes improvements over the previous work, the control law development for a deterministic two-time-scale system is reviewed in Section 2.2. With uncertainties added in the fast dynamics of a two-time-scale system, a new theory is developed in Section 2.3. Section 2.4 extends the theory when a two-time-scale system contains uncertainties both in the fast dynamics and in the control distribution. Section 2.5 shows how the theory is extended when there is an increment in the number of time-scales from two to three as actuator dynamics are included. Attitude control of a rigid spacecraft with uncertain inertias is shown as an example of a three-time-scale control problem. Section 2.6 extends the theory when the system has a total of four time-scales: one time-scale each for slow states, slow actuators, fast states and fast actuators. The uncertainties are assumed more generic. Both the slow and fast dynamics are assumed to have multiplicative and additive uncertainties. In addition, the actuator dynamics have multiplicative uncertainties. This Section also demonstrates the application of the theory to a nonlinear, 6-DOF aircraft commanded to perform a large-amplitude combined longitudinal and lateral/directional maneuver. Concluding remarks are in Section 2.7.

2.2 Review of Sequential Control: Slow State Regulation of a Deterministic Nonstandard System with Two Time-Scales

In the literature the method of composite control was developed for standard singularly perturbed systems [10]. This method assumed a structure of the control variable as a sum of a slow component and a fast component, and relied on the fast states being stabilized on an “isolated real root" or

manifold in the fast time-scale. However, for nonstandard systems, a unique manifold for the fast states may not be found analytically. A modified composite control approach was developed in the work of Narang-Siddarth and Valasek [11] to extend the ideas of composite control to nonstandard systems. This method relied on finding an approximation of the manifold, which can often be cumbersome. A new method called sequential control was developed [11] to avoid this approximation. In this method the manifold of the fast states was designed as an intermediate control variable to achieve slow state regulation or tracking. Part of the work in Saha and Valasek [51] showed how the method of sequential control can be applied for slow state regulation of a nonstandard spring-mass-damper system. A modified version of the work is presented in this Section as a review of how sequential control works, and what its limitations are. Saha and Valasek [51] considered two different cases of dynamics for a nonlinear spring-mass-damper: (1) when the damping is significantly higher than the spring stiffness, and (2) when the spring stiffness is significantly higher than the damping. Mathematically, the two cases differ in where the time-scale separation parameter ε appears in the fast dynamics. The class of systems in this section is similar to the second case, with a more generic form of the nonlinearity. The two-time-scale model is

$$\begin{aligned} \dot{x} &= z \\ \varepsilon \dot{z} &= b_z f(x,z) - \varepsilon z + u \end{aligned} \tag{2.1}$$

where displacement x is the slow state, velocity z is the fast state, b_z is a known constant parameter, $f(x,z)$ is a known function which can be nonlinear in both x and z, and the control input is u. The fast dynamics in (2.1) can be nonlinear in the fast state z, and it may not be possible to obtain an analytical solution z^0 by substituting $\varepsilon = 0$ in the fast dynamics. Therefore, the system is nonstandard. To accomplish the control objective of driving the slow state x from its initial condition $x(0)$ to the origin, a sequential controller can be designed over two-time-scales according to the following procedure.

2.2.1 Development of Control Law Using Lower-Order Reduced Subsystems

2.2.1.1 Step I: Design of Manifold in the Slow Time-Scale

The artificial substitution of $\varepsilon = 0$ in (2.1) converts the $\dot{z}$ equation from a differential to an algebraic one. Physically it means the following: the fast state z has evolved infinitely fast to an equilibrium manifold, say z^0, and is not evolving independently any more. At the same time, it results in a reduced-order subsystem which dictates how the slow state x evolves, given the fast state z is on its manifold z^0. In the first step, this manifold z^0 is designed as an intermediate control variable which ensures that the slow state x reaches the origin. To design the manifold, the reduced slow subsystem is obtained by setting $\varepsilon = 0$ in (2.1) as

$$\begin{aligned} \dot{x} &= z^0 \\ 0 &= b_z f(x, z^0) + u^0 \end{aligned} \tag{2.2}$$

where u^0 is the effective component in the slow time-scale of the control u. In order that the slow state x reaches the origin, a positive-definite candidate Lyapunov function for the reduced slow dynamics is selected as

$$V_{s_c} = \frac{1}{2}x^2. \tag{2.3}$$

Its time-derivative for the reduced slow subsystem (2.2) is

$$\dot{V}_{s_c}|_{(2.2)} = x\dot{x}|_{(2.2)} = xz^0 \tag{2.4}$$

where the notation $f(.)|_{(i)}$ stands for the value of the function $f(.)$ for the system denoted by equation (i). If the manifold is selected as

$$z^0 = -k_1 x \tag{2.5}$$

where $k_1 > 0$ is a gain, the time-derivative (2.4) becomes

$$\dot{V}_{s_c}|_{(2.2)} = -k_1 x^2 \tag{2.6}$$

which is negative-definite. Therefore, the equilibrium $x = 0$ of the reduced slow subsystem (2.2) is Lyapunov-stable.

2.2.1.2 Step II: Design of Control in the Fast Time-Scale

In the second step, the control is designed such that the fast state z reaches the manifold z^0 designed in the previous step. In the fast time-scale $\tau = \frac{t}{\varepsilon}$ the full-order dynamics (2.1) become

$$\begin{aligned} x' &= \varepsilon z \\ z' &= b_z f(x, z) - \varepsilon z + u \end{aligned} \tag{2.7}$$

where the 'prime' denotes differentiation with respect to the fast time-scale τ. The artificial substitution of $\varepsilon = 0$ in (2.7) results in another reduced-order model, the reduced fast subsystem:

$$\begin{aligned} x' &= 0 \\ z' &= b_z f(x, z) + u. \end{aligned} \tag{2.8}$$

This reduced subsystem physically indicates the following: in the fast time-scale, the slow state x is 'frozen' at its initial condition while the fast state z is evolving. Since the fast state z needs to go to its equilibrium manifold z^0, a positive-definite candidate Lyapunov function for the reduced fast subsystem is selected as

$$V_{f_c} = \frac{1}{2}(z - z^0)^2. \tag{2.9}$$

Its time-derivative for the reduced fast subsystem (2.8) is

$$\begin{aligned} V'_{f_c}|_{(2.8)} &= (z - z^0)(z'|_{(2.8)} - z^{0'}|_{(2.8)}) \\ &= (z - z^0)(z'|_{(2.8)} + k_1 x'|_{(2.8)}) \\ &= (z - z^0)(b_z f(x, z) + u + 0) \\ &= (z - z^0)(b_z f(x, z) + u). \end{aligned} \tag{2.10}$$

If the control u is selected as

$$u = -b_z f(x, z) - k_2(z - z^0) = -b_z f(x, z) - k_1 k_2 x - k_2 z \tag{2.11}$$

where $k_2 > 0$ is another gain, the time-derivative (2.26) becomes

$$V'_{f_c}|_{(2.8)} = -k_2(z - z^0)^2 \tag{2.12}$$

which is negative-definite. Therefore, the equilibrium $z = z^0$ of the reduced fast subsystem (2.8) is Lyapunov-stable.

2.2.2 Stability Analysis of the Full-Order System: The Bound of Time-Scale Separation

Having designed the manifold and control with the artificial substitution of $\varepsilon = 0$, or from a physical standpoint, using the asymptotic behavior of the system under infinite time-scale separation, the question now is this: is the control law guaranteed to work for finite time-scale separation? In other words, within what bounds of time-scale separation ε is the control law guaranteed to ensure stability of the full-order system? This Subsection performs a composite Lyapunov analysis [10] to establish the bound ε^* of the time-scale separation parameter ε such that the stability of the full-order system (2.1) under the full-state feedback control law (2.11) is guaranteed

for $0 < \varepsilon < \varepsilon^*$. A candidate composite Lyapunov function for the full-order system (2.1) is

$$V_c = \alpha_1 V_{s_c} + \alpha_2 V_{f_c} \tag{2.13}$$

which is positive-definite for any $\alpha_1, \alpha_2 > 0$. Along the trajectories of the full-order dynamics (2.1) or equivalently (2.7), the time-derivative of this composite Lyapunov function is

$$\dot{V}_c|_{(2.1)} = \alpha_1 \dot{V}_{s_c}|_{(2.1)} + \frac{\alpha_2}{\varepsilon} V'_{f_c}|_{(2.7)}. \tag{2.14}$$

Introducing the reduced subsystems for which the time-derivatives of the individual Lyapunov functions V_{s_c} and V_{f_c} are known, equation (2.14) becomes

$$\begin{aligned}
\dot{V}_c|_{(2.1)} &= \alpha_1 \dot{V}_{s_c}|_{(2.2)} + \frac{\alpha_2}{\varepsilon} V'_{f_c}|_{(2.8)} + \alpha_1(\dot{V}_{s_c}|_{(2.1)} - \dot{V}_{s_c}|_{(2.2)}) + \frac{\alpha_2}{\varepsilon}(V'_{f_c}|_{(2.7)} - V'_{f_c}|_{(2.8)}) \\
&= -\alpha_1 k_1 x^2 - \frac{\alpha_2}{\varepsilon} k_2 (z - z^0)^2 + \alpha_1 x(\dot{x}|_{(2.1)} - \dot{x}|_{(2.2)}) \\
&\quad + \frac{\alpha_2}{\varepsilon}(z - z^0)[(z'|_{(2.7)} - z'|_{(2.8)}) - (z^{0\prime}|_{(2.7)} - z^{0\prime}|_{(2.8)})] \\
&= -\alpha_1 k_1 x^2 - \frac{\alpha_2}{\varepsilon} k_2 (z - z^0)^2 + \alpha_1 x(z - z^0) + \frac{\alpha_2}{\varepsilon}(z - z^0)[-\varepsilon z + k_1 \varepsilon z] \\
&= -\alpha_1 k_1 x^2 - \frac{\alpha_2}{\varepsilon} k_2 (z - z^0)^2 + \alpha_1 x(z - z^0) + \alpha_2(k_1 - 1)(z - z^0) z \\
&= -\alpha_1 k_1 x^2 - \frac{\alpha_2}{\varepsilon} k_2 (z - z^0)^2 + \alpha_1 x(z - z^0) + \alpha_2(k_1 - 1)(z - z^0)(z - z^0 - k_1 x) \\
&= -\alpha_1 k_1 x^2 - \alpha_2[\frac{k_2}{\varepsilon} - (k_1 - 1)](z - z^0)^2 - [\alpha_2 k_1(k_1 - 1) - \alpha_1] x(z - z^0) \\
&= -\begin{bmatrix} x & z - z^0 \end{bmatrix} \begin{bmatrix} \alpha_1 k_1 & \frac{1}{2}(\alpha_2 k_1(k_1 - 1) - \alpha_1) \\ \frac{1}{2}(\alpha_2 k_1(k_1 - 1) - \alpha_1) & \alpha_2[\frac{k_2}{\varepsilon} - (k_1 - 1)] \end{bmatrix} \begin{bmatrix} x \\ z - z^0 \end{bmatrix}.
\end{aligned} \tag{2.15}$$

The time-derivative of the composite Lyapunov function, represented by equation (2.15), will be negative-definite if the 2×2 matrix $\begin{bmatrix} \alpha_1 k_1 & \frac{1}{2}(\alpha_2 k_1(k_1 - 1) - \alpha_1) \\ \frac{1}{2}(\alpha_2 k_1(k_1 - 1) - \alpha_1) & \alpha_2[\frac{k_2}{\varepsilon} - (k_1 - 1)] \end{bmatrix}$ is positive-definite; i.e. its 1×1 and 2×2 Leading Principal Minors (LPMs) are positive. Since α_1

and k_1 are positive by design, the 1×1 LPM is already positive. The 2×2 LPM is positive if

$$\begin{aligned}
&\alpha_1 k_1 \alpha_2 [\frac{k_2}{\varepsilon} - (k_1 - 1)] > \frac{1}{4}(\alpha_2 k_1 (k_1 - 1) - \alpha_1)^2 \\
\Leftrightarrow &\frac{4\alpha_1 \alpha_2 k_1 k_2}{\varepsilon} > (\alpha_2 k_1 (k_1 - 1) - \alpha_1))^2 + 4\alpha_1 \alpha_2 k_1 (k_1 - 1) \\
\Leftrightarrow &\frac{4\alpha_1 \alpha_2 k_1 k_2}{\varepsilon} > (\alpha_2 k_1 (k_1 - 1) + \alpha_1)^2 \\
\Leftrightarrow &\varepsilon < \frac{4\alpha_1 \alpha_2 k_1 k_2}{(\alpha_2 k_1 (k_1 - 1) + \alpha_1)^2}
\end{aligned} \tag{2.16}$$

Therefore, the equilibrium $x = 0, z = z^0$ of the full-order system (2.1) will be globally asymptotically stable for all ε in the range $0 < \varepsilon < \varepsilon^*$, where $\varepsilon^* := \frac{4\alpha_1 \alpha_2 k_1 k_2}{(\alpha_2 k_1 (k_1 - 1) + \alpha_1)^2}$.

2.2.3 Numerical Results

This subsection shows in simulation slow state regulation using the control law developed in Subsection 2.2.2 on the nonlinear, nonstandard system (2.1). The initial conditions, parameter, nonlinear function in the fast dynamics, and controller gains are: $x(0) = 1, z(0) = 1, b_z = -0.1, f(x, z) = x^2 z^3 \sin^2 z, k_1 = 1, k_2 = 1$. The time-scale separation parameter ε is assumed 0.01 for the simulation.

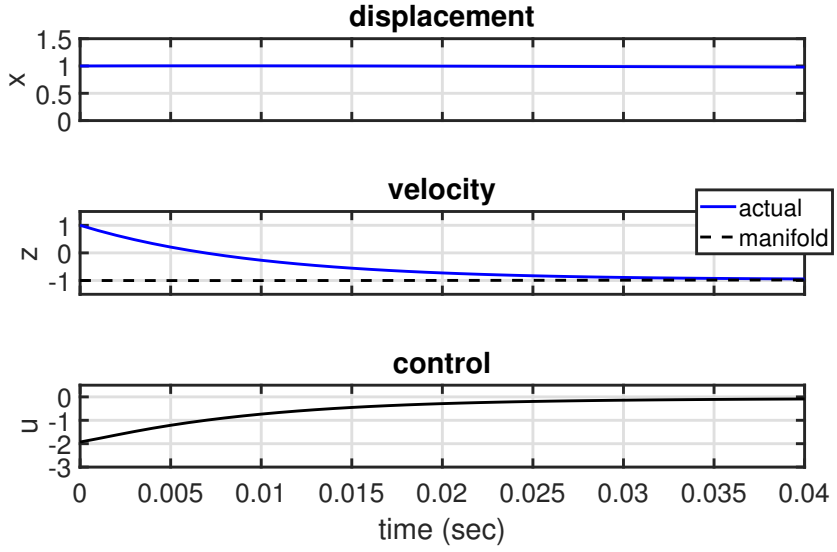

Figure 2.1: States and control in the fast time-scale

Figure 2.1 shows the states and the control in the fast time-scale. It can be seen that the displacement x is almost frozen at its initial condition $x(0) = 1$, and that the velocity z evolves to its equilibrium manifold $z^0 = -k_1 x = -x$. Figure 2.2 shows the states and the control in the slow time-scale. It can be seen that the velocity now stays on its manifold $z^0 = -k_1 x = -x$, and that the displacement evolves to its desired value of zero.

For the controller gains $k_1 = 1, k_2 = 1$ and choosing the weights α_1, α_2 in the composite Lyapunov function as $\alpha_1 = 1, \alpha_2 = 1$, the upper bound of time-scale separation is obtained as $\varepsilon^* = 4$. In addition to the controller gains k_1, k_2, the weights α_1, α_2 are the 'tuning knob's which can be varied to obtain a desired bound of time-scale separation for stability.

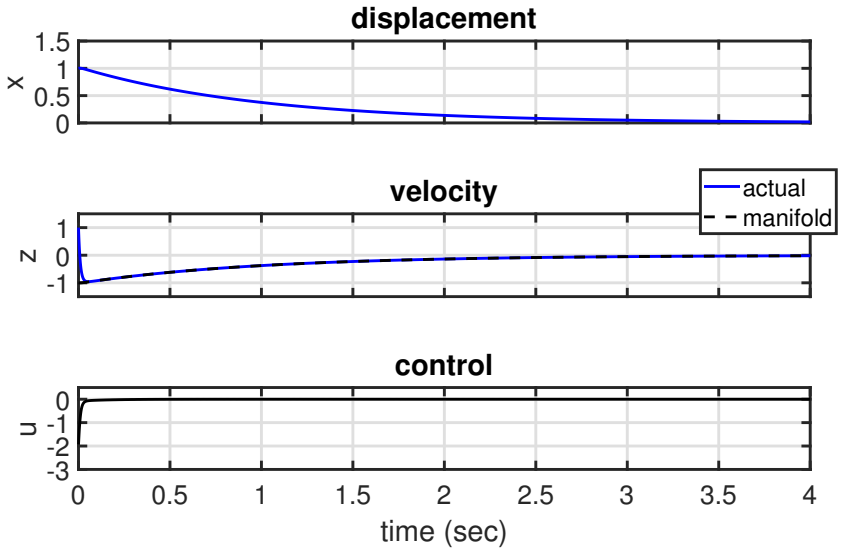

Figure 2.2: States and control in the slow time-scale

2.2.4 Limitations of the Approach

While sequential control has the advantages of convenient design of the manifold and guaranteed Lyapunov-stability of the reduced subsystems as well as the full-order system, the major limitations of this method are as follows:

1. **Assumption of a deterministic model:** While applying the method of sequential control, it

is assumed that the model structure and parameters are known exactly. In practice, however, every model is imperfect. A new theory is needed to address uncertainties in model structure and parameters. This will be the focus of the rest of Chapter 2.

2. **Assumption of full-state feedback:** The method of sequential control assumes that all the states are available for feedback. In practice, some states may be difficult to measure, or sometimes a linear combination of the states may be easier to measure than the individual states themselves. A new theory of output feedback is needed to address this. This will be the focus of Chapter 4.

2.3 Slow State Regulation of a Nonstandard Two-Time-Scale System with Uncertainties in the Fast Dynamics

[1] This section develops a theory of control design when uncertainties are included in the model structure and parameters of a class of nonlinear, nonstandard two-time-scale systems. This class was investigated in Saha *et. al.* [56]. It is similar to the nonlinear spring-mass-damper investigated in the authors' previous work [51], but the nonlinearity of the spring is assumed differently. It is assumed that the spring force is a sum of two uncertain components: one with a known functional form and a constant but unknown parameter, and another with an unknown function of the slow state. The nonlinear state equations are

$$\begin{aligned} \dot{x} &= z \\ \varepsilon \dot{z} &= b_z f(x,z) + \Delta(x) z - \varepsilon z + u. \end{aligned} \tag{2.17}$$

In (2.17), the position of the mass is the slow state x. The velocity of the mass is the fast state z. u is the force acting on the mass. b_z is the constant but unknown parameter. $f(x,z)$ is a known smooth function that can be nonlinear in both x and z, and bounded when x and z are bounded. $\Delta(x)$ is an unknown function with a known upper bound D, and its first-order derivative with respect to x is bounded when x is bounded. The parameter ε satisfying $0 < \varepsilon << 1$ represents

[1] Section 2.3 of this dissertation is from Saha *et. al.* [56], ©2018 IEEE, reprinted with permission from IEEE.

how well-separated the slow and the fast time-scales are. It can be seen that for $\varepsilon = 0$, the fast dynamics reduce to an algebraic equation, indicating infinite time-scale separation and a singularity in the model. Similar to Section 2.2, it can also be seen that the presence of the generic nonlinear function $f(x, z)$ in the fast dynamics makes the system nonstandard.

The control objective is to drive the slow state x from its initial condition x_0 to the origin in the presence of the uncertainties present in the model (2.17). To achieve this, the control must also ensure that the fast state z reaches a suitable equilibrium manifold and stay there. Using a formulation similar to the sequential control developed in the work of Narang-Siddarth and Valasek [11] but taking care of the uncertainties present in the fast dynamics of (2.17), the control law is developed over two time-scales as follows.

2.3.1 Development of Control Law Using Reduced Subsystems

2.3.1.1 Step I: Design of Manifold in the Slow Time-Scale

In the slow time-scale, the fast state z is assumed to have reached its manifold z^0, and stay on the same. The manifold z^0 is designed as an intermediate control which ensures that the slow state x reaches the origin. The manifold is designed on the reduced slow subsystem. For a deterministic model, the reduced subsystem is obtained by simply setting $\varepsilon = 0$ in the full-order dynamics. However, in presence of uncertainties it must be considered how the uncertain terms will be handled in the reduced subsystems. A way to add the uncertain terms is to use the best estimate for the uncertain parameter b_z and the worst-case scenario for the uncertain function $\Delta(x)$. As a result the reduced slow subsystem is obtained from the full-order system (2.17) as

$$\begin{aligned} \dot{x} &= z^0 \\ 0 &= \hat{b}_z f(x, z^0) + Dz^0 + u^0 \end{aligned} \tag{2.18}$$

where $\hat{b}_z$ is the best estimate of the unknown parameter b_z, and u^0 is the effective component in the slow time-scale of the control u. In order that the slow state x reaches the origin, a positive-definite

candidate Lyapunov function for the reduced slow dynamics is selected as

$$V_{s_c} = \frac{1}{2}x^2. \tag{2.19}$$

Its time-derivative for the reduced slow subsystem (2.18) is

$$\dot{V}_{s_c}|_{(2.18)} = x\dot{x}|_{(2.18)} = xz^0. \tag{2.20}$$

If the manifold is selected as

$$z^0 = -k_1 x \tag{2.21}$$

where $k_1 > 0$ is a gain, the time-derivative (2.20) becomes

$$\dot{V}_{s_c}|_{(2.18)} = -k_1 x^2 \tag{2.22}$$

which is negative-definite. Therefore, the equilibrium $x = 0$ of the reduced slow subsystem (2.18) is Lyapunov-stable.

2.3.1.2 Step II: Design of Control in the Fast Time-Scale

The control is designed such that the fast state reaches the manifold z^0 which was designed in the previous step. In the fast time-scale $\tau = \frac{t}{\varepsilon}$ the full-order dynamics (2.17) become

$$\begin{aligned} x' &= \varepsilon z \\ z' &= b_z f(x,z) + \Delta(x)z - \varepsilon z + u \end{aligned} \tag{2.23}$$

where the 'prime' denotes differentiation with respect to the fast time-scale τ. Setting $\varepsilon = 0$ in (2.7), using the best estimate of the parameter b_z and the worst-case scenario for the function $\Delta(x)$,

the reduced fast subsystem is obtained as

$$\begin{aligned} x' &= 0 \\ z' &= \hat{b}_z f(x,z) + Dz + u. \end{aligned} \tag{2.24}$$

Since the fast state z needs to go to its manifold z^0, a positive-definite candidate Lyapunov function is selected as

$$V_{f_c} = \frac{1}{2}(z - z^0)^2. \tag{2.25}$$

Its time-derivative for the reduced fast subsystem (2.24) is

$$\begin{aligned} V'_{f_c}|_{(2.24)} &= (z - z^0)(z'|_{(2.24)} - z^{0'}|_{(2.24)}) \\ &= (z - z^0)(z'|_{(2.24)} + k_1 x'|_{(2.24)}) \\ &= (z - z^0)(\hat{b}_z f(x,z) + Dz + u + 0). \end{aligned} \tag{2.26}$$

If the control is selected as

$$\begin{aligned} u &= -\hat{b}_z f(x,z) - Dz - k_2(z - z^0) \\ &= -\hat{b}_z f(x,z) - k_1 k_2 x - (D + k_2)z \end{aligned} \tag{2.27}$$

where $k_2 > 0$ is another gain, the time-derivative (2.26) becomes

$$V'_{f_c}|_{(2.24)} = -k_2(z - z^0)^2 \tag{2.28}$$

which is negative-definite. Therefore, the equilibrium $z = z^0$ of the reduced fast subsystem (2.24) is Lyapunov-stable.

2.3.2 Stability Analysis of the Full-Order System

For deterministic dynamics, an approach to analyze the stability of the full-order nonlinear system is to use a composite Lyapunov function [10], which is a linear combination of the two Lyapunov functions used for the control design. In the presence of uncertainties, however, the

control law (2.27) designed using the reduced subsystems uses the best estimate of the unknown parameter. Since this uncertainty appears in the fast dynamics, by intuition the estimate $\hat{b}_z$ should be updated in the fast time-scale. An online parameter estimator is designed for this update. A positive-definite candidate Lyapunov function for the online parameter estimator is selected as

$$V_{f_p} = \frac{1}{2}(b_z - \hat{b}_z)^2. \tag{2.29}$$

Including this Lyapunov function for parameter estimation to the ones used for controller design, a candidate composite Lyapunov function for the full-order system (2.17) is

$$V_c = \alpha_1 V_{s_c} + \alpha_2 V_{f_c} + \alpha_3 V_{f_p}. \tag{2.30}$$

where $\alpha_1, \alpha_2, \alpha_3 > 0$. By this choice the composite Lyapunov function is positive-definite. The following theorem gives the sufficient conditions for stability of the equilibrium $x = 0, z = z^0$ of the full-order nonlinear system (2.17).

Theorem 1. *Let*

$$\begin{aligned}
\varepsilon_{**}^{(1)} &:= \frac{D\alpha_2 k_1}{2\alpha_1} \\
a_2 &:= (\alpha_2 k_1(k_1 - 1) + \alpha_1)^2 \\
a_1 &:= 2(D\alpha_2^2 k_1^2(k_1 - 1) - 2\alpha_1\alpha_2 k_1 k_2) \\
a_0 &:= 2D\alpha_2^2 k_1^2 k_2 \\
\varepsilon_{**}^{(2)} &:= \frac{-a_1 - \sqrt{a_1^2 - 4a_2 a_0}}{2a_2} \\
\varepsilon^{**} &:= \frac{-a_1 + \sqrt{a_1^2 - 4a_2 a_0}}{2a_2}.
\end{aligned} \tag{2.31}$$

Suppose that the gains are selected such that $a_1^2 - 4a_2 a_0 > 0$ *and* $\varepsilon^{**} > \varepsilon_{**}^{(1)}$. *Furthermore, suppose that the estimate of the parameter* b_z *is updated as*

$$\hat{b}_z' = \frac{\alpha_2}{\alpha_3}(z - z^0)f(x, z) = \frac{\alpha_2}{\alpha_3}(z + k_1 x)f(x, z). \tag{2.32}$$

Then the equilibrium $x = 0, z = z^0, \hat{b}_z = b_z$ of the full-order nonlinear system (2.17), (2.32) is stable in the sense of Lyapunov, and $x \to 0, z \to z^0$ as $t \to \infty$ for all ε in the range

$$\max(\varepsilon_{**}^{(1)}, \varepsilon_{**}^{(2)}) < \varepsilon < \varepsilon^{**}. \tag{2.33}$$

Proof. The proof of Theorem 1 is shown over the next two Subsubsections. The first Subsubsection derives the parameter update law and establishes the bounds of ε for stability. The second Subsubsection uses Barbalat's lemma [57] to prove the convergence of the states to their equilibria.

2.3.2.1 Selection of Parameter Update Law and Bounds of Time-Scale Separation

The time-derivative of the composite Lyapunov function (2.30) for the full-order system (2.17), or equivalently (2.23), is

$$\dot{V}_c = \alpha_1 x\dot{x}|_{(2.17)} + \frac{\alpha_2}{\varepsilon}(z - z^0)(z'|_{(2.23)} - z^{0'}|_{(2.23)}) + \frac{\alpha_3}{\varepsilon}(b_z - \hat{b}_z)(0 - \hat{b}_z'). \tag{2.34}$$

This uses the fact that the unknown parameter b_z is constant, so its time-derivative equals zero. Introducing appropriate reduced subsystems and differences between the full-order and reduced-order systems, the time-derivative of the composite Lyapunov function becomes

$$\begin{aligned}\dot{V}_c = {} & \alpha_1 x\dot{x}|_{(2.18)} + \frac{\alpha_2}{\varepsilon}(z - z^0)(z'|_{(2.24)} - z^{0'}|_{(2.24)}) + \alpha_1 x(\dot{x}|_{(2.17)} - \dot{x}|_{(2.18)}) \\ & + \frac{\alpha_2}{\varepsilon}(z - z^0)[(z'|_{(2.23)} - z'|_{(2.24)}) - (z^{0'}|_{(2.23)} - z^{0'}|_{(2.24)})] - \frac{\alpha_3}{\varepsilon}(b_z - \hat{b}_z)\hat{b}_z'.\end{aligned} \tag{2.35}$$

Substituting for all the derivatives leads to

$$\begin{aligned}\dot{V}_c = {} & -\alpha_1 k_1 x^2 - \frac{\alpha_2}{\varepsilon} k_2 (z - z^0)^2 + \alpha_1 x(z - z^0) \\ & + \frac{\alpha_2}{\varepsilon}(z - z^0)[((b_z f(x, z) + \Delta(x)z - \varepsilon z + u) - (\hat{b}_z f(x, z) + Dz + u)) + k_1 \varepsilon z] \\ & - \frac{\alpha_3}{\varepsilon}(b_z - \hat{b}_z)\hat{b}_z'.\end{aligned} \tag{2.36}$$

Separating the quadratic and the other terms, (2.36) becomes

$$\begin{aligned}\dot{V}_c = &-\alpha_1 k_1 x^2 - \frac{\alpha_2}{\varepsilon} k_2 (z - z^0)^2 + \alpha_1 x(z - z^0) + \alpha_2 (k_1 - 1) z(z - z^0) \\ &+ \frac{\alpha_2}{\varepsilon}(b_z - \hat{b}_z)(z - z^0) f(x, z) + \frac{\alpha_2}{\varepsilon}(\Delta(x) - D) z(z - z^0) - \frac{\alpha_3}{\varepsilon}(b_z - \hat{b}_z)\hat{b}'_z.\end{aligned} \tag{2.37}$$

An upper bound of the term $(\Delta(x) - D)z(z - z^0)$ can be found in the following manner.

$$\begin{aligned}(\Delta(x) - D)z(z - z^0) &= (\Delta(x) - D)[(z - \frac{z^0}{2})^2 - \frac{z^{0^2}}{4}] \\ &= (\Delta(x) - D)(z - \frac{z^0}{2})^2 - (\Delta(x) - D)\frac{k_1^2 x^2}{4}\end{aligned} \tag{2.38}$$

Since $-D \leq \Delta(x) \leq D$, $-2D \leq \Delta(x) - D \leq 0$. As a result, $(\Delta(x) - D) \leq 0$ and $-(\Delta(x) - D) \leq 2D$. Therefore, (2.38) reduces to

$$(\Delta(x) - D)z(z - z^0) \leq 2D\frac{k_1^2 x^2}{4}. \tag{2.39}$$

The terms involving $(b_z - \hat{b}_z)$ in (2.37) can be canceled if the update law is selected according to (2.32), i.e.

$$\hat{b}'_z = \frac{\alpha_2}{\alpha_3}(z - z^0) f(x, z) = \frac{\alpha_2}{\alpha_3}(z + k_1 x) f(x, z).$$

Using this parameter update law and the upper bound of the term $(\Delta(x) - D)z(z - z^0)$ found in (2.39), and expressing $z(z - z^0) = (z - z^0)^2 - k_1 x(z - z^0)$, the derivative of the composite Lyapunov function given by (2.37) can be expressed as the following inequality:

$$\begin{aligned}\dot{V}_c \leq &-\alpha_1 k_1 x^2 - \frac{\alpha_2}{\varepsilon} k_2 (z - z^0)^2 + \alpha_1 x(z - z^0) \\ &+ \alpha_2 (k_1 - 1)[(z - z^0)^2 - k_1 x(z - z^0)] + \frac{D\alpha_2}{2\varepsilon} k_1^2 x^2.\end{aligned} \tag{2.40}$$

Grouping terms, (2.40) can be expressed in the following vector-matrix form:

$$\dot{V}_c \leq -\mathbb{X}^T \mathbb{K} \mathbb{X} \tag{2.41}$$

where $\mathbb{K} := \begin{bmatrix} \alpha_1 k_1 - \frac{D\alpha_2 k_1^2}{2\varepsilon} & \frac{1}{2}(\alpha_2 k_1(k_1-1) - \alpha_1) \\ \frac{1}{2}(\alpha_2 k_1(k_1-1) - \alpha_1) & \alpha_2(\frac{k_2}{\varepsilon} - (k_1-1)) \end{bmatrix}$ and $\mathbb{X} := \begin{bmatrix} x & z - z^0 \end{bmatrix}^T$. If $\mathbb{K}$ is positive-definite, the time-derivative of the composite Lyapunov function in (2.41) is *negative semi-definite* since it does not depend on the parameter estimation error $(b_z - \hat{b}_z)$.

To find the conditions under which $\mathbb{K}$ is positive-definite, it can be noticed that the 1×1 Leading Principal Minor (LPM) of $\mathbb{K}$ is positive if

$$\alpha_1 k_1 - \frac{D\alpha_2 k_1^2}{2\varepsilon} > 0. \tag{2.42}$$

Inequality (2.42) yields a possible lower bound $\varepsilon_{**}^{(1)}$ of the time-scale separation parameter:

$$\varepsilon > \varepsilon_{**}^{(1)} = \frac{D\alpha_2 k_1}{2\alpha_1}. \tag{2.43}$$

Furthermore, the 2×2 LPM of $\mathbb{K}$ is positive if

$$(\alpha_1 k_1 - \frac{D\alpha_2 k_1^2}{2\varepsilon})\alpha_2(\frac{k_2}{\varepsilon} - (k_1 - 1)) > \frac{1}{4}(\alpha_2 k_1(k_1-1) - \alpha_1)^2. \tag{2.44}$$

Simplifying, this leads to the following quadratic inequality in ε:

$$a_2\varepsilon^2 + a_1\varepsilon + a_0 < 0 \tag{2.45}$$

where a_0, a_1, a_2 are given by (2.31). Since the coefficient of ε^2 is positive, if the discriminant $a_1^2 - 4a_2a_0 > 0$, the quadratic expression in (2.45) is negative between the two real roots of $a_2\varepsilon^2 + a_1\varepsilon + a_0 = 0$. Hence, the 2×2 LPM of $\mathbb{K}$ is positive for

$$\varepsilon_{**}^{(2)} < \varepsilon < \varepsilon^{**} \tag{2.46}$$

where $\varepsilon_{**}^{(2)}$ and ε^{**} are given by (2.31). If $\varepsilon^{**} > \varepsilon_{**}^{(1)}$ where $\varepsilon_{**}^{(1)}$ is the lower bound obtained from the 1×1 LPM of $\mathbb{K}$, then the time-derivative of the composite Lyapunov function in (2.77) is negative

semi-definite as long as $\max(\varepsilon_{**}^{(1)}, \varepsilon_{**}^{(2)}) < \varepsilon < \varepsilon^{**}$.

$\dot{V}_c$ being negative semi-definite implies that $V_c(t) \leq V_c(0)\ \forall t \geq 0$. Since the Lyapunov function is non-increasing, it can be concluded that the slow state x, the fast state manifold error $(z - z^0)$ and the parameter estimation error $(b_z - \hat{b}_z)$ remain *bounded* as the time t approaches infinity. This alone does not guarantee the convergence of the states x and z to their equilibria. The convergence is addressed in the next Subsubsection.

2.3.2.2 Convergence Using Barbalat's Lemma

The two-time-scale model (2.17) without the control term u is autonomous, since the dynamics do not have explicit dependence on time. However, the control u uses the parameter estimate $\hat{b}_z$, which evolves with time according to the parameter update law (2.32). This makes the closed-loop system non-autonomous. Barbalat's lemma [57] gives sufficient conditions under which the derivative of a function approaches zero as time approaches infinity. The application of Barbalat's lemma to the stability analysis of non-autonomous systems leads to a Lyapunov-like lemma [57] for the case where the time-derivative of the Lyapunov function is negative semi-definite. For this problem, the Lyapunov-like lemma can be used to show the convergence of the fast state z to its manifold z^0 and that of the slow state x to zero. With the parameter update law chosen according to (2.69), the time-derivative of the composite Lyapunov function is

$$\begin{aligned}\dot{V}_c = &-\alpha_1 k_1 x^2 - \frac{\alpha_2}{\varepsilon} k_2 (z - z^0)^2 + \alpha_1 x (z - z^0) \\ &+ \alpha_2 (k_1 - 1) z (z - z^0) + \frac{\alpha_2}{\varepsilon} (\Delta(x) - D) z (z - z^0).\end{aligned} \tag{2.47}$$

Differentiating (2.47) with respect to time and substituting for all the individual derivatives, the second-order derivative of the composite Lyapunov function $\ddot{V}_c$ is

$$\begin{aligned}\ddot{V}_c = &-2\alpha_1 k_1 x z - 2\frac{\alpha_2}{\varepsilon^2} k_2 (z - z^0)(z' - z^{0'}) + [\alpha_1 z + \frac{\alpha_2}{\varepsilon}(k_1 - 1) z' + \frac{\alpha_2}{\varepsilon} \frac{d\Delta(x)}{dx} z^2 \\ &+ \frac{\alpha_2}{\varepsilon^2} (\Delta(x) - D) z'](z - z^0) + [\frac{\alpha_1}{\varepsilon} x + \frac{\alpha_2}{\varepsilon}(k_1 - 1) z + \frac{\alpha_2}{\varepsilon^2} (\Delta(x) - D) z](z' - z^{0'})\end{aligned} \tag{2.48}$$

where the rate changes of z and $z - z^0$ after substituting for the control input u, are

$$\begin{aligned} z' &= (b_z - \hat{b}_z) f(x,z) + (\Delta(x) - D)z - \varepsilon z - k_2(z - z^0) \\ z' - z^{0'} &= (b_z - \hat{b}_z) f(x,z) + (\Delta(x) - D)z + (k_1 - 1)\varepsilon z - k_2(z - z^0). \end{aligned} \tag{2.49}$$

It can be seen from from (2.48) and (2.49) that the second-order derivative consists of terms involving $x, z, (z - z^0)$, the unknown function $\Delta(x)$ and its derivative with respect to x, the parameter estimation error $(\hat{b}_z - b_z)$, the known function $f(x,z)$, the gains k_1, k_2, α_1, α_2 and the time-scale separation parameter ε. Since it is already shown that $(z - z^0)$ is bounded, and $z^0 = -k_1 x$ is bounded since x is bounded, it can be concluded that z is bounded. As a result, the known function $f(x,z)$ is also bounded. Furthermore, $(b_z - \hat{b}_z)$ was also shown to be bounded, and $\Delta(x)$ and its derivative with respect to x were assumed to be bounded. Therefore, the second-order derivative $\ddot{V}_c$ is bounded. Consequently, the first-order derivative $\dot{V}_c$ is uniformly continuous. Using the Lyapunov-like lemma derived from Barbalat's lemma [57], it can be concluded that $\dot{V}_c \to 0$ as $t \to \infty$. Therefore, its upper bound $-\mathbb{X}^T \mathbb{K} \mathbb{X} \to 0$ as $t \to \infty$. Since $\mathbb{K}$ is positive-definite, $-\mathbb{X}^T \mathbb{K} \mathbb{X} \to 0$ implies that $\mathbb{X} \to 0$, i.e. $x \to 0$ and $(z - z^0) \to 0$ as $t \to \infty$. This completes the proof. □

The proof of Theorem 1 reveals the following two insights.

Remark 1. *The time-derivative of the composite Lyapunov function is independent of the parameter estimation error $(b_z - \hat{b}_z)$ and therefore negative semi-definite instead of negative-definite. As a consequence, the closed-loop system is guaranteed to be stable, but not asymptotically stable. Even though asymptotic stability is not guaranteed, it is rigorously proven that the control law (2.63) makes the fast state converge to its manifold and the slow state to its desired value of zero. This is achieved even when the estimated parameter $\hat{b}_z$ does not necessarily converge to the actual parameter b_z. It is guaranteed, however, that the parameter estimation error $(b_z - \hat{b}_z)$ remains bounded.*

Remark 2. *If there is no uncertainty in the model structure, the function $\Delta(x)$ and its upper bound*

D will be zero. For $D = 0$, the possible lower bound of ε coming out of the 1×1 LPM of $\mathbb{K}$ will reduce to $\varepsilon_{**}^{(1)} = 0$. The quadratic inequality coming out of the 2×2 LPM of $\mathbb{K}$ will become $a_2\varepsilon^2 + a_1\varepsilon < 0$, where $a_2 = (\alpha_2 k_1(k_1 - 1) + \alpha_1)^2$ and $a_1 = -4\alpha_1\alpha_2 k_1 k_2$. As a result the bound of ε for closed-loop stability will become $0 < \varepsilon < \varepsilon^{**}$, where $\varepsilon^{**} = \frac{4\alpha_1\alpha_2 k_1 k_2}{(\alpha_2 k_1(k_1-1)+\alpha_1)^2}$. It can be seen that in this special case $\varepsilon^{**} = \varepsilon^*$, where ε^* is the upper bound resulting from the regular composite Lyapunov analysis in the absence of uncertainties in Section 2.2.

2.3.3 Numerical Results

This section demonstrates in simulation the regulator control law on the nonlinear, nonstandard system (2.17). For the simulation, the time-scale separation parameter ε is selected as 0.01. The initial conditions of the states are $x(0) = 1$, $z(0) = 0$. The known function in the fast dynamics is $f(x, z) = x^2 z^3 \sin^2 z$. The unknown function in the fast dynamics is taken as $\Delta(x) = 0.1\cos(x + \frac{\pi}{4})$, so its known upper bound is $D = 0.1$. The actual value of the constant but unknown parameter b_z is -0.1, and its initial estimate is taken as $\hat{b}_z(0) = 1$. The controller gains are selected as $k_1 = 2$, $k_2 = 2$. The weights of the individual Lyapunov functions in the composite are selected as $\alpha_1 = 0.2$, $\alpha_2 = 0.01$ and $\alpha_3 = 0.25$. The states, control, and estimate of the unknown parameter are shown in Fig. 2.3.

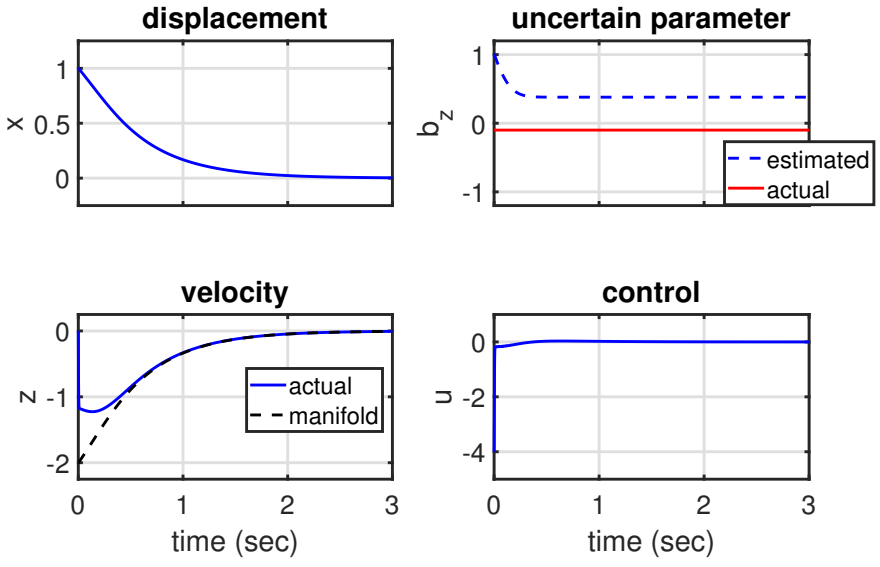

Figure 2.3: Time histories of the states, control, and estimate of the unknown parameter; from Saha *et. al.* [56], ©2018 IEEE, reprinted with permission from IEEE.

It can be seen that the fast state z approaches its equilibrium manifold $z^0 = -k_1 x = -2x$ within approximately 0.5 sec into the simulation, and stays at its manifold for the remaining time. The slow state x reaches the origin in spite of the uncertainties. The estimated parameter does not converge to its actual value; however, the controller is able to achieve slow state regulation. The parameter estimation error, as pointed out in the proof of Theorem 1, remains bounded. The control signal remains bounded as well.

For the choice of gains used for the simulation, the sufficient conditions stated in Theorem 1 are satisfied. The bounds of the perturbation parameter obtained are $\varepsilon_{**}^{(1)} = 0.0050, \varepsilon_{**}^{(2)} = 0.0051, \varepsilon^{**} = 0.6545$. Therefore, stability is guaranteed for $0.0051 < \varepsilon < 0.6545$.

2.4 Two-Time-Scale Slow State Regulation with Uncertainties Both in Fast Dynamics and in Control Distribution

Consider a generic nonlinear system

$$\dot{X} = f(X) + g(X)u \tag{2.50}$$

The notion "uncertainty in dynamics" refers to that in $f(X)$, whereas the notion "uncertainty in control distribution" refers to that in $g(X)$. Considering both types of uncertainties, this section develops a two-time-scale controller for slow state regulation of a class of systems which is an extension of the nonlinear spring-mass-damper taken up in [51] and [56]. In the previous Section, uncertainty was assumed in the fast dynamics, but the control distribution term was assumed to be known. However, aerospace applications such as aircraft have uncertainties in control derivatives, which multiply the control surface deflections. In addition, aircraft and spacecraft have inertias as a major source of uncertainty. Both $f(.)$ and $g(.)$ will involve the inverse of the inertia matrix. Therefore, uncertainties in inertias can be reflected as both $f(.)$ and $g(.)$ being uncertain. With this foresight, it is important to address uncertainties in control distribution as well as the dynamics. For the class of systems taken up in this section, uncertainties are assumed in the characteristics of

the nonlinear spring as well as the forcing mechanism. The nonlinear state equations are

$$\begin{aligned} \dot{x} &= z \\ \varepsilon \dot{z} &= b_z f(x,z) + \gamma(x,z) - \varepsilon z + [\lambda g(x,z) + \mu(x,z)]u. \end{aligned} \tag{2.51}$$

In (2.51), the position of the mass is the slow state x. The velocity of the mass is the fast state z. u is the force acting on the mass. The parameter ε satisfying $0 < \varepsilon << 1$ represents the separation between the slow and the fast time-scales. The nonlinear spring is characterized by a sum of two uncertainties. One is a parametric uncertainty represented by a constant but unknown parameter b_z multiplying a known function $f(x,z)$. The second one is a state-dependent uncertainty represented by $\gamma(x,z)$. The forcing mechanism is characterized by a sum of two similar uncertainties. The parametric uncertainty is represented by a constant but unknown parameter λ multiplying a known function $g(x,z)$. The state-dependent uncertainty is represented by $\mu(x,z)$. The known functions $f(x,z)$ and $g(x,z)$ are continuous in both x and z. The functions $\gamma(x,z)$ and $\mu(x,z)$ are assumed to be of the form

$$\begin{aligned} \gamma(x,z) &= \gamma_1(x,z)x + \gamma_2(x,z)z \\ \mu(x,z) &= \mu_1(x,z)x + \mu_2(x,z)z \end{aligned} \tag{2.52}$$

where $\gamma_1(x,z)$, $\gamma_2(x,z)$, $\mu_1(x,z)$, $\mu_2(x,z)$ are unknown functions such that $\left|\gamma_1(x,z)\right| \leq G_1$, $\left|\gamma_2(x,z)\right| \leq G_2$, $\left|\mu_1(x,z)\right| \leq M_1$ and $\left|\mu_2(x,z)\right| \leq M_2$ for all values of x and z. Moreover, they have bounded first-order partial derivatives with respect to x and z. For the class of state-dependent uncertainties represented by (2.52), the nonlinear state equations become

$$\begin{aligned} \dot{x} &= z \\ \varepsilon \dot{z} &= b_z f(x,z) + \gamma_1(x,z)x + \gamma_2(x,z)z - \varepsilon z + [\lambda g(x,z) + \mu_1(x,z)x + \mu_2(x,z)z]u. \end{aligned} \tag{2.53}$$

The $\dot{z}$ equation in (2.53) reduces to an algebraic one for $\varepsilon = 0$, implying a singularity due to infinite separation of the time-scales. Moreover, the presence of several generic functions nonlinear in z in the $\dot{z}$ equation makes the system nonstandard. The control objective is to drive the slow state x

from its initial condition $x(0)$ to the origin in presence of all the parametric and state-dependent uncertainties present in the model (2.53).

2.4.1 Development of Control Law Using Reduced Subsystems

2.4.1.1 Design of Manifold in the Slow Time-Scale

The objective at this step is to design the manifold of the fast state to drive the slow state to origin. Similar to Section 2.3, the reduced subsystems are obtained by substituting $\varepsilon = 0$ and using the best estimates of parametric uncertainties and the upper bounds of state-dependent uncertainties. the reduced slow subsystem is

$$\begin{aligned} \dot{x} &= z^0 \\ 0 &= \hat{b}_z f(x, z^0) + G_1 x + G_2 z^0 + [\hat{\lambda} g(x, z^0) + M_1 x + M_2 z^0] u^0 \end{aligned} \tag{2.54}$$

where $\hat{b}_z$ and $\hat{\lambda}$ are the best estimates of the unknown parameters b_z and λ, and u^0 is the effective component in the slow time-scale of the control u which is yet to be designed. In order that the slow state x reaches the origin, a positive-definite candidate Lyapunov function for the reduced slow dynamics is selected as

$$V_{s_c} = \frac{1}{2} x^2. \tag{2.55}$$

Its time-derivative for the reduced slow subsystem (2.54) is

$$\dot{V}_{s_c}|_{(2.54)} = x\dot{x}|_{(2.54)} = xz^0. \tag{2.56}$$

If the manifold is selected as

$$z^0 = -k_1 x \tag{2.57}$$

where $k_1 > 0$ is a gain, the time-derivative (2.56) becomes

$$\dot{V}_{s_c}|_{(2.54)} = -k_1 x^2 \tag{2.58}$$

which is negative-definite. Therefore, the equilibrium $x = 0$ of the reduced slow subsystem (2.54) is Lyapunov-stable.

2.4.1.2 Design of Control in the Fast Time-Scale

The objective at this step is to design the control such that the fast state z reaches the manifold z^0 specified in the previous step. In the fast time-scale $\tau = \frac{t}{\varepsilon}$ the full-order dynamics (2.53) become

$$\begin{aligned} x' &= z \\ z' &= b_z f(x,z) + \gamma_1(x,z)x + \gamma_2(x,z)z - \varepsilon z \\ &\quad + [\lambda g(x,z) + \mu_1(x,z)x + \mu_2(x,z)z]u. \end{aligned} \tag{2.59}$$

where the 'prime' denotes differentiation with respect to the fast time-scale τ. Setting $\varepsilon = 0$ in (2.59), using the best estimates of the parameters b_z and λ and the upper bounds of the state-dependent uncertainties, the reduced fast subsystem is obtained as

$$\begin{aligned} x' &= 0 \\ z' &= \hat{b}_z f(x,z) + G_1 x + G_2 z + [\hat{\lambda} g(x,z) + M_1 x + M_2 z]u. \end{aligned} \tag{2.60}$$

Keeping in mind that the fast state z needs to go to its equilibrium manifold z^0, a positive-definite candidate Lyapunov function is selected as

$$V_{f_c} = \frac{1}{2}(z - z^0)^2. \tag{2.61}$$

Its time-derivative for the reduced fast subsystem (2.60) is

$$\begin{aligned} V'_{f_c}|_{(2.60)} &= (z - z^0)(z'|_{(2.60)} - z^{0'}|_{(2.60)}) \\ &= (z - z^0)(z'|_{(2.60)} + k_1 x'|_{(2.60)}) \\ &= (z - z^0)(\hat{b}_z f(x,z) + G_1 x + G_2 z \\ &\qquad + [\hat{\lambda} g(x,z) + M_1 x + M_2 z]u). \end{aligned} \tag{2.62}$$

If the control is selected as

$$\begin{aligned} u &= \frac{-\hat{b}_z f(x,z) - G_1 x - G_2 z - k_2(z - z^0)}{\hat{\lambda} g(x,z) + M_1 x + M_2 z} \\ &= \frac{-\hat{b}_z f(x,z) - (G_1 + k_1 k_2)x - (G_2 + k_2)z}{\hat{\lambda} g(x,z) + M_1 x + M_2 z} \end{aligned} \tag{2.63}$$

where $k_2 > 0$ is another gain, the time-derivative (2.62) becomes

$$V'_{f_c}|_{(2.60)} = -k_2(z - z^0)^2 \tag{2.64}$$

which is negative-definite. Therefore, the reduced fast subsystem (2.60) is Lyapunov-stable. It is to note from (2.63) that the following condition needs to hold for all values of $\hat{\lambda}, x, z$ so the control does not become unbounded:

$$\hat{\lambda} g(x,z) + M_1 x + M_2 z \neq 0. \tag{2.65}$$

2.4.2 Stability Analysis of the Full-Order System

Similar to Subsection 2.3.2, this subsection selects the parameter update laws, derives the stability bounds ε_{**} and ε^{**} and proves the converges of the slow and fast states to their respective equilibrium using Barbalat's lemma. An online parameter estimator is designed to update the parameter estimates $\hat{b}_z$ and $\hat{\lambda}$. To this end, a positive-definite candidate Lyapunov function is selected as

$$V_{f_p} = \frac{1}{2} w_1 (b_z - \hat{b}_z)^2 + \frac{1}{2} w_2 (\lambda - \hat{\lambda})^2. \tag{2.66}$$

where $w_1, w_2 > 0$. Including this Lyapunov function for parameter estimator and the ones used for controller design, a candidate composite Lyapunov function for the full-order system (2.53) is

$$V_c = \alpha_1 V_{s_c} + \alpha_2 V_{f_c} + \alpha_3 V_{f_p} \tag{2.67}$$

where $\alpha_1, \alpha_2, \alpha_3 > 0$. By this choice the composite Lyapunov function is positive-definite. The following theorem gives the sufficient conditions for stability of the full-order nonlinear system

(2.53).

Theorem 2. *Suppose that the magnitude limit of the actuator is $\pm U$; i.e. $|u| \leq U$ at all times. Let*

$$\begin{aligned}
a_2 &:= (\alpha_2 k_1(k_1-1)+\alpha_1)^2 \\
a_1 &:= 4\alpha_2\big|\alpha_2 k_1(k_1-1)-\alpha_1\big|\left[(G_1+M_1U)+k_1(G_2+M_2U)\right] \\
&\quad -4\alpha_1 k_1\alpha_2[k_2-2(G_2+M_2U)] \\
a_0 &:= 4\alpha_2^2[(G_1+M_1U)+k_1(G_2+M_2U)]^2 \\
\varepsilon_{**} &:= \frac{-a_1-\sqrt{a_1^2-4a_2a_0}}{2a_2} \\
\varepsilon^{**} &:= \frac{-a_1+\sqrt{a_1^2-4a_2a_0}}{2a_2}.
\end{aligned} \tag{2.68}$$

Suppose that the gains are selected such that $a_1 < -2\sqrt{a_2a_0}$, and that the estimates of the parameters b_z and λ are updated as

$$\begin{aligned}
\hat{b}_z' &= \frac{\alpha_2}{\alpha_3 w_1}(z-z^0)f(x,z) = \frac{\alpha_2}{\alpha_3 w_1}(z+k_1x)f(x,z) \\
\hat{\lambda}' &= \frac{\alpha_2}{\alpha_3 w_2}(z-z^0)g(x,z)u = \frac{\alpha_2}{\alpha_3 w_2}(z+k_1x)g(x,z)u
\end{aligned} \tag{2.69}$$

where u is the control law designed according to (2.63). Furthermore, suppose that the condition (2.65) holds. Then the equilibrium $x=0, z=z^0, \hat{b}_z = b_z, \hat{\lambda}=\lambda$ of the full-order nonlinear system (2.53), (2.69) is stable in the sense of Lyapunov, and $x \to 0, z \to z^0$ as $t \to \infty$ for all ε in the range

$$\varepsilon_{**} < \varepsilon < \varepsilon^{**}. \tag{2.70}$$

Proof. The time-derivative of the composite Lyapunov function (2.157) for the full-order system (2.53), or equivalently (2.59), is

$$\begin{aligned}
\dot{V}_c &= \alpha_1 x\dot{x}|_{(2.53)} + \frac{\alpha_2}{\varepsilon}(z-z^0)(z'|_{(2.59)} - z^{0'}|_{(2.59)}) \\
&\quad + \frac{\alpha_3}{\varepsilon}[w_1(\hat{b}_z-b_z)\hat{b}_z' + w_2(\hat{\lambda}-\lambda)\hat{\lambda}'].
\end{aligned} \tag{2.71}$$

Introducing appropriate reduced subsystems and differences between the full-order and reduced-order systems, the time-derivative of the composite Lyapunov function becomes

$$\begin{aligned}\dot{V}_c &= \alpha_1 x\dot{x}|_{(2.54)} + \frac{\alpha_2}{\varepsilon}(z-z^0)(z'|_{(2.60)} - z^{0'}|_{(2.60)}) + \alpha_1 x(\dot{x}|_{(2.53)} - \dot{x}|_{(2.54)}) \\ &+ \frac{\alpha_2}{\varepsilon}(z-z^0)[(z'|_{(2.59)} - z'|_{(2.60)}) - (z^{0'}|_{(2.59)} - z^{0'}|_{(2.60)})] \\ &+ \frac{\alpha_3}{\varepsilon}[w_1(\hat{b}_z - b_z)\hat{b}'_z + w_2(\hat{\lambda}-\lambda)\hat{\lambda}'].\end{aligned} \tag{2.72}$$

Substituting for all the derivatives leads to

$$\begin{aligned}\dot{V}_c &= -\alpha_1 k_1 x^2 - \frac{\alpha_2}{\varepsilon}k_2(z-z^0)^2 + \alpha_1 x(z-z^0) \\ &+ \frac{\alpha_2}{\varepsilon}(z-z^0)[(b_z - \hat{b}_z)f(x,z) + (\gamma_1(.) - G_1)x + (\gamma_2(.) - G_2)z \\ &- \varepsilon z + [(\lambda-\hat{\lambda})g(x,z) + (\mu_1(.) - M_1)x + (\mu_2(.) - M_2)z]u \\ &+ k_1\varepsilon z] + \frac{\alpha_3}{\varepsilon}[w_1(\hat{b}_z - b_z)\hat{b}'_z + w_2(\hat{\lambda}-\lambda)\hat{\lambda}'].\end{aligned} \tag{2.73}$$

The terms involving $(\hat{b}_z - b_z)$ and $(\hat{\lambda}-\lambda)$ be canceled if the update laws $\hat{b}'_z$ and $\hat{\lambda}'$ are selected according to (2.69). The cancellations lead to

$$\begin{aligned}\dot{V}_c &= -\alpha_1 k_1 x^2 - \frac{\alpha_2}{\varepsilon}k_2(z-z^0)^2 + \alpha_1 x(z-z^0) \\ &+ \frac{\alpha_2}{\varepsilon}(z-z^0)[(\gamma_1(.) - G_1)x + (\gamma_2(.) - G_2)z \\ &+ (k_1-1)\varepsilon z + ((\mu_1(.) - M_1)x + (\mu_2(.) - M_2)z)u].\end{aligned} \tag{2.74}$$

Rewriting $z(z-z^0)$ as $(z-z^0+z^0)(z-z^0) = (z-z^0)^2 + z^0(z-z^0) = (z-z^0)^2 - k_1 x(z-z^0)$

and grouping terms, (2.74) reduces to

$$\begin{aligned}\dot{V}_c = &-\alpha_1 k_1 x^2 - \alpha_2(\frac{k_2}{\varepsilon} - (k_1 - 1))(z - z^0)^2 \\ &- (\alpha_2 k_1(k_1 - 1) - \alpha_1)x(z - z^0) + \frac{\alpha_2}{\varepsilon}(\gamma_1(.) - G_1)x(z - z^0) \\ &+ \frac{\alpha_2}{\varepsilon}(\gamma_2(.) - G_2)(z - z^0)^2 - \frac{\alpha_2 k_1}{\varepsilon}(\gamma_2(.) - G_2)x(z - z^0) \\ &+ \frac{\alpha_2}{\varepsilon}(\mu_1(.) - M_1)x(z - z^0)u + \frac{\alpha_2}{\varepsilon}(\mu_2(.) - M_2)u(z - z^0)^2 \\ &- \frac{\alpha_2 k_1}{\varepsilon}(\mu_2(.) - M_2)x(z - z^0)u.\end{aligned} \tag{2.75}$$

Considering absolute values of the indefinite terms as upper bounds, (2.75) leads to

$$\begin{aligned}\dot{V}_c \leq &-\alpha_1 k_1 |x|^2 - \alpha_2(\frac{k_2}{\varepsilon} - (k_1 - 1))\left|z - z^0\right|^2 \\ &+ \left|\alpha_2 k_1(k_1 - 1) - \alpha_1\right||x|\left|z - z^0\right| + \frac{\alpha_2}{\varepsilon}\left|\gamma_1(.) - G_1\right||x|\left|z - z^0\right| \\ &+ \frac{\alpha_2}{\varepsilon}\left|\gamma_2(.) - G_2\right|\left|z - z^0\right|^2 + \frac{\alpha_2 k_1}{\varepsilon}\left|\gamma_2(.) - G_2\right||x|\left|z - z^0\right| \\ &+ \frac{\alpha_2}{\varepsilon}\left|\mu_1(.) - M_1\right||x|\left|z - z^0\right||u| + \frac{\alpha_2}{\varepsilon}\left|\mu_2(.) - M_2\right||u|\left|z - z^0\right|^2 \\ &+ \frac{\alpha_2 k_1}{\varepsilon}\left|\mu_2(.) - M_2\right||x|\left|z - z^0\right||u|.\end{aligned} \tag{2.76}$$

In order to find bounds of the terms $\left|\gamma_i(.) - G_i\right|$ and $\left|\mu_i(.) - M_i\right|$; $i = 1, 2$, it is to be noted that $\left|\gamma_i(.) - G_i\right| \leq \left|\gamma_i(.)\right| + G_i \leq G_i + G_i = 2G_i; i = 1, 2$. Similarly, $\left|\mu_i(.) - M_i\right| \leq 2M_i; i = 1, 2$. Using these upper bounds and $|u| \leq U$, the time-derivative (2.76) can be expressed in the following vector-matrix form:

$$\dot{V}_c \leq -\mathbb{X}^T \mathbb{K} \mathbb{X} \tag{2.77}$$

where $\mathbb{X} := \begin{bmatrix} |x| & |z - z^0| \end{bmatrix}^T$ and $\mathbb{K} := [K_{ij}]_{2\times 2}$ with its elements given by

$$\begin{aligned} K_{11} &= \alpha_1 k_1 \\ K_{12} &= -\frac{1}{2}[|\alpha_2 k_1(k_1 - 1) - \alpha_1| + \frac{2\alpha_2}{\varepsilon}((G_1 + M_1 U) + k_1(G_2 + M_2 U)] \\ K_{21} &= K_{12} \\ K_{22} &= \alpha_2(\frac{k_2}{\varepsilon} - (k_1 - 1)) - \frac{2\alpha_2 G_2}{\varepsilon} - \frac{2\alpha_2 M_2 U}{\varepsilon} \end{aligned} \tag{2.78}$$

If $\mathbb{K}$ is positive-definite, the time-derivative of the composite Lyapunov function in (2.77) is *negative semi-definite*. To find conditions under which $\mathbb{K}$ is positive-definite, it is to be noted that the 1×1 Leading Principal Minor (LPM) of $\mathbb{K}$ is $K_{11} = \alpha_1 k_1$ which is already positive. The 2×2 LPM of $\mathbb{K}$ will be positive if $K_{11}K_{22} > K_{12}^2$. Expanding and simplifying, it leads to the quadratic inequality

$$a_2\varepsilon^2 + a_1\varepsilon + a_0 < 0 \tag{2.79}$$

where a_2, a_1, a_0 are given by (2.68). Since $a_2, a_0 > 0$, if $a_1 < -2\sqrt{a_2 a_0}$ is satisfied, the quadratic inequality (2.79) will hold between two real positive roots of $a_2\varepsilon^2 + a_1\varepsilon + a_0 = 0$. These roots are ε_{**} and ε^{**} given in (2.68).

Therefore, for all ε satisfying $\varepsilon_{**} < \varepsilon < \varepsilon^{**}$, the time-derivative of the Composite Lyapunov function is negative semi-definite. Hence, the slow state x, the difference between the fast state and its manifold $(z - z^0)$ and the parameter estimation errors $(\hat{b}_z - b_z)$ and $(\hat{\lambda} - \lambda)$ remain bounded.

Differentiating (2.74) with respect to time t, the second-order derivative will involve the following: the states x, z and their derivatives $\dot{x}$, $\dot{z}$; the control u and its derivative $\dot{u}$; the difference between state-dependent uncertainties and their upper bounds $(\gamma_i(.) - G_i)$; $(\mu_i(.) - M_i)$; $i = 1, 2$; the partial derivatives associated with the state-dependent uncertainties $\frac{\partial \gamma_i}{\partial x}$, $\frac{\partial \gamma_i}{\partial z}$.$\frac{\partial \mu_i}{\partial x}$, $\frac{\partial \mu_i}{\partial z}$; $i = 1, 2$; the gains $k_1, k_2, \alpha_1, \alpha_2$ and the time-scale separation parameter ε. It is already shown that x and $z - z^0$ are bounded. Since $z^0 = -k_1 x$, the fast state z remains bounded. Moreover, the parameter estimation errors are shown to be bounded, and the actual parameters are bounded, so the estimated parameters

are bounded. The term $(\hat{\lambda}g(x,z) + M_1 x + M_2 z)$ appears in the denominator of u, and the square of this expression will appear in the denominator of $\dot{u}$. By condition (2.65), this remains bounded. As a consequence, the second derivative of the composite Lyapunov function is bounded, so its first derivative is uniformly continuous. Using Barbalat's lemma [57], the first derivative $\dot{V}_c \to 0$ as $t \to \infty$. Therefore, its upper bound $-\mathbb{X}^T\mathbb{K}\mathbb{X} \to 0$ as $t \to \infty$. Since $\mathbb{K}$ is positive-definite, $-\mathbb{X}^T\mathbb{K}\mathbb{X} \to 0$ implies that $\mathbb{X} \to 0$, i.e. $|x| \to 0$ and $\left|z - z^0\right| \to 0$ as $t \to \infty$. Therefore, the fast state reaches its manifold, and the slow state reaches the origin as time approaches infinity. This completes the proof. □

The proof of Theorem 2 reveals the following two insights.

Remark 3. *Similar to the analysis in [56], the time-derivative of the composite Lyapunov function is negative semi-definite, but not negative-definite. Therefore, the closed-loop system is guaranteed to be stable, but not asymptotically stable. Using Barbalat's lemma, it is shown that the fast state reaches its manifold and that the slow state reaches zero, even though the estimated parameters do not necessarily converge to their actual values. It is guaranteed, however, that the parameter estimation errors remain bounded.*

Remark 4. *In the special case of no state-dependent uncertainty, the constant term a_0 in the quadratic inequality (2.76) will be zero, and (2.76) will reduce to $a_2\varepsilon^2 + a_1\varepsilon < 0$, where $a_2 = (\alpha_2 k_1(k_1 - 1) + \alpha_1)^2$ and $a_1 = -4\alpha_1\alpha_2 k_1 k_2$. As a result the bound of ε for closed-loop stability will become $0 < \varepsilon < \varepsilon^{**}$, where $\varepsilon^{**} = \frac{4\alpha_1\alpha_2 k_1 k_2}{(\alpha_2 k_1(k_1-1)+\alpha_1)^2}$ is the same as the upper bound that would result from the regular composite Lyapunov analysis for the corresponding deterministic system. This is still valid if only parametric uncertainties are considered. Therefore, the bounds of the time-scale separation parameter differ from the deterministic case because of the state-dependent uncertainties, not the parametric uncertainties.*

2.4.3 Numerical Results

This subsection demonstrates in simulation slow state regulation for the nonstandard system (2.53) using the controller developed in Subsections 2.4.1 - 2.4.2. For the simulation, the time-scale

separation parameter ε is selected as 0.01. The initial conditions of the states are $x(0) = 1$, $z(0) = 0$. The parametric uncertainties are assumed as follows. The known function in the fast dynamics is $f(x, z) = x^2 z^3 \sin^2 z$. The actual value of the constant but unknown parameter multiplying $f(x, z)$ is assumed as $b_z = -0.1$, and its initial estimate is $\hat{b}_z(0) = 1$. The known function in the control distribution is $g(x, z) = (1 + x^3)(1 + z^2)$. The actual value of the constant but unknown parameter multiplying this function is assumed as $\lambda = 2$. Its initial estimate is $\hat{\lambda}(0) = 1$. The state-dependent uncertainties in the dynamics and control distribution are assumed as follows: $\gamma_1(x, z) = G_1 e^{-|x|} \sin z; \gamma_2(x, z) = G_1 e^{-3|z|} \cos x; \mu_1(x, z) = M_1 \cos(x + z); \mu_2(x, z) = M_2 \sin(x^2 e^{-z})$. All of the upper bounds G_1, G_2, M_1, M_2 are selected as 0.05. The controller gains are selected as $k_1 = 2, k_2 = 2$. The weights of the individual Lyapunov functions in the composite are selected as $\alpha_1 = 0.2$, $\alpha_2 = 0.01$ and $\alpha_3 = 0.25$. The weights in the parameter estimator Lyapunov functions are selected as $w_1 = 5$, $w_2 = 0.1$. The states, control, and estimates of the unknown parameters are shown in Fig. 2.4.

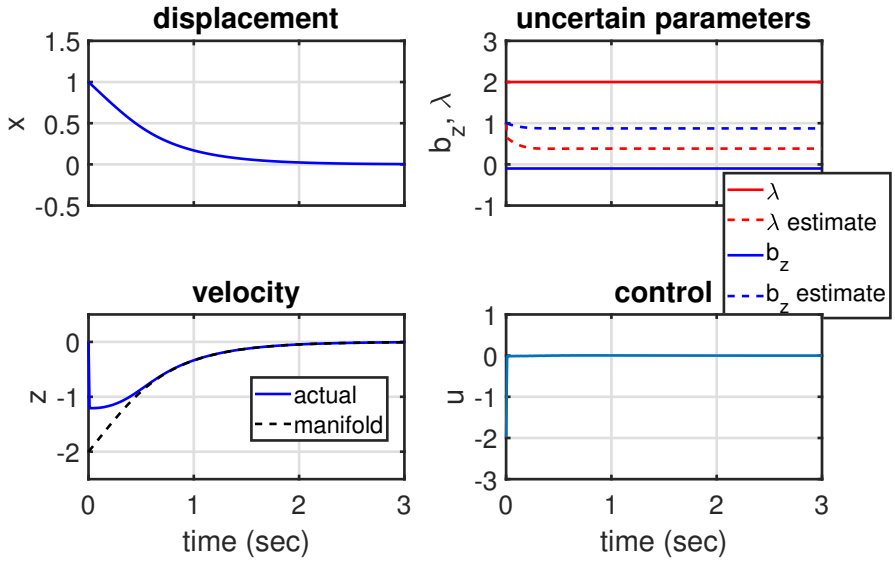

Figure 2.4: Time histories of the states, control, and estimates of the unknown parameters

It can be seen in Figure 2.4 that the fast state z approaches its equilibrium manifold $z^0 = -k_1 x = -2x$ within approximately 0.5 sec into the simulation, and stays at its manifold for the

remaining time. The slow state x reaches the origin in spite of all the uncertainties. Neither of the estimated parameters converge to their actual values, however the controller is able to achieve slow state regulation. The parameter estimation errors, as pointed out in the proof of Theorem 1, are seen to be bounded. The control signal remains bounded as well.

For the choice of gains used for the simulation, the sufficient conditions stated in Theorem 1 are satisfied. To obtain the bounds of the perturbation parameter ε, the actuator magnitude limit is assumed as $U = 2$. The bounds obtained according to Theorem 2 are $\varepsilon_{**} = 0.0071, \varepsilon^{**} = 0.9383$. Therefore, the full-order nonlinear system is guaranteed to be stable for $0.0071 < \varepsilon < 0.9383$.

2.5 Three-Time-Scale Slow State Tracking with Uncertainties in Dynamics and Control Distribution: Spacecraft Attitude Control

[2] This section develops a three-time-scale slow state tracking controller by accounting for uncertainties and actuator dynamics. Although Sections 2.3 and 2.4 showed how uncertainties can be addressed for nonstandard systems using baseline controllers and online parameter estimators, the theory developed so far has a few limitations. First, the systems had only one slow state and one fast state. Second, actuator dynamics were not considered. Third, only the regulation problem of the slow state was studied. This section makes a number of improvements in terms of the capability of the theory. Systems with multiple slow and fast states are considered, and actuator dynamics are realistically accounted for in the design. A separate time-scale is assigned to the actuators, increasing the number of time-scales from two to three. Instead of the slow state regulation problem, the theory developed in this section considers the more general problem of slow state tracking. The theory is applicable to control the rotational motion of a generic nonlinear, nonstandard rigid spacecraft model with one major source of uncertainty: the inertias. For a spacecraft rotating in a orbit, it is difficult to obtain the moments and products of inertias accurately. Attitude parameters are the slow states of a spacecraft, whereas the angular velocities are fast. Attitude tracking with uncertain inertias can be thought of as a slow state tracking problem

[2] Section 2.5 of this dissertation is from Saha and Valasek [60], reprinted by permission of the American Institute of Aeronautics and Astronautics, Inc.

for a nonstandard multiple-time-scale system with parametric uncertainties. In the literature, there are some works on attitude control of spacecraft using time-scales, and some other works on adaptive control to account for model uncertainties, but not both. Shahravi and Azimi [2] developed a two-time-scale attitude and vibration controller for a deterministic spacecraft model. On the other hand, the works of Tandale and Valasek [58,59] accounted for uncertainties in inertias to design structured adaptive model inversion controllers, but time-scales in the dynamics were not considered. Attitude tracking using the benefits of geometric singular perturbation theory as well as handling parametric uncertainties has not been investigated yet.

The development shown here is from a recent work of Saha and Valasek [60]. A nonlinear multiple-time-scale slow state tracking control method is developed for a generic rigid spacecraft, realistically accounting for actuator dynamics and uncertainties in inertias. The control law can handle a total of three time-scales: the slowest time-scale of the attitudes, the second fastest time-scale of the angular velocities and the fastest time-scale of the actuators. To be able to apply the time-scale techniques for nonstandard systems to control the rotational dynamics of a spacecraft, the angular velocity dynamics must be modified to a form which does not have the uncertain inertia matrix multiplying the angular accelerations, and is linear in the uncertain parameters. In order to obtain such a form, a linearly overparameterized system is constructured using the inertia matrix itself and its inverse in Subsection 2.5.1. The final form derived in this Subsection has parametric uncertainties both in dynamics and in control distribution. The constant but unknown parameters are functions of the inertias. Using the best estimates of these parameters, a three-time-scale sequential controller is designed in Subsection 2.5.2. This controller guarantees the stability of the reduced subsystems. Subsection 2.5.3 uses the composite Lyapunov analysis to select update laws for the estimates of the uncertain parameters. This analysis also proves the ultimate boundedness of the tracking error, manifold error and parameter estimation error. Time-histories of states, controls and uncertain parameters corresponding to attitude tracking are presented in Subsection 2.5.4.

2.5.1 Linearly Overparameterized Three-Time-Scale Spacecraft Model

The rotational dynamics of a rigid spacecraft considered in this work are similar to the one in Tandale and Valasek [59] with a few modifications. The system is assumed to evolve in a total of three time-scales. The Modified Rodriguez Parameters (MRPs) are the slow states evolving in the slowest time-scale. The body-axis angular velocities evolve in the second fastest time-scale. The actuators exerting torque evolve in the fastest time-scale. To indicate the second fastest and the fastest time-scales, small positive perturbation parameters ε and ρ with $0 << \rho << \varepsilon << 1$ are introduced artificially in the model. In addition, actuator dynamics are included. The three-time-scale model is

$$\begin{aligned} \dot{\xi} &= T(\xi)\omega \\ \varepsilon \mathcal{I}\dot{\omega} &= -\omega^{\times}\mathcal{I}\omega + \delta \\ \rho\dot{\delta} &= f_{\delta}(\delta) + G_{\delta}(\delta)u. \end{aligned} \tag{2.80}$$

The 3×1 vector of MRPs is $\xi := \begin{bmatrix} \xi_1 & \xi_2 & \xi_3 \end{bmatrix}^T$. The 3×3 matrix T is $T(\xi) := \frac{1}{4}[(1 - \xi^T\xi)I_{3\times 3} + 2\xi^{\times} + 2\xi\xi^T]$ with $\xi^{\times} := \begin{bmatrix} 0 & -\xi_3 & \xi_2 \\ \xi_3 & 0 & -\xi_1 \\ -\xi_2 & \xi_1 & 0 \end{bmatrix}$ being a 3×3 skew-symmetric matrix representing vector cross-product. The 3×1 vector of angular velocities is $\omega := \begin{bmatrix} \omega_1 & \omega_2 & \omega_3 \end{bmatrix}^T$. $\mathcal{I} := \begin{bmatrix} \mathcal{I}_{11} & \mathcal{I}_{12} & \mathcal{I}_{13} \\ \mathcal{I}_{12} & \mathcal{I}_{22} & \mathcal{I}_{23} \\ \mathcal{I}_{13} & \mathcal{I}_{23} & \mathcal{I}_{33} \end{bmatrix}$ is the symmetric 3×3 matrix of constant but unknown inertias. This matrix is pre-multiplied by another 3×3 skew-symmetric matrix corresponding to cross-product, given by $\omega^{\times} := \begin{bmatrix} 0 & -\omega_3 & \omega_2 \\ \omega_3 & 0 & -\omega_1 \\ -\omega_2 & \omega_1 & 0 \end{bmatrix}$. The vectors $\delta = \begin{bmatrix} \delta_1 & \delta_2 & \delta_3 \end{bmatrix}^T$ and $u = \begin{bmatrix} u_1 & u_2 & u_3 \end{bmatrix}^T$ represent the actuators and the commanded torques respectively. The vector of functions $f_{\delta}(.)$ and

the matrix $G_\delta(.)$ represent the dependence of actuator dynamics on the actuators themselves and the commanded torques respectively. It can be seen in equation (2.80) that the angular accelerations $\dot{\omega}_i$ are nonlinear in the angular velocities ω_i due to the matrix product $\omega^\times \mathcal{I}\omega$. Therefore, the three-time-scale spacecraft model (2.80) is nonstandard.

The control objective is to drive the MRPs $\xi(t)$ to a smooth reference attitude trajectory $\xi_r(t)$. In a multiple-time-scale framework, this objective can be classified as slow state tracking. According to geometric singular perturbation theory, this can be achieved in the slowest time-scale, provided that the fast states and actuators can be stabilized onto suitable equilibrium manifolds in the faster time-scales. The theoretical developments in Sections 2.3 and 2.4 are based on a model linear in the uncertain parameters, and the parameters are estimated online using update laws based on the composite Lyapunov analysis. For the attitude tracking problem, the spacecraft model (2.80) is first represented as an overparameterized model, linear in the uncertain parameters, and subsequently the time-scale controller and parameter estimator are designed.

The angular accelerations in (2.80) can be written as

$$\begin{aligned} \varepsilon\dot{\omega} &= -\mathcal{I}^{-1}\omega^\times \mathcal{I}\omega + \mathcal{I}^{-1}\delta \\ &= -\mathcal{S}\omega^\times \mathcal{I}\omega + \mathcal{S}\delta \end{aligned} \tag{2.81}$$

where $\mathcal{S} = \Big[\mathcal{S}_{ij}\Big]_{3\times 3} := \mathcal{I}^{-1}$ is a 3×3 matrix of constant but unknown parameters. This matrix $\mathcal{S}$ can be thought of representing the uncertainty in control distribution multiplying the actuation vector δ. The uncertainty in the dynamics can be written as

$$-\mathcal{S}\omega^\times \mathcal{I}\omega = Bf(\omega) \tag{2.82}$$

where $f(\omega) := \begin{bmatrix} \omega_1^2 & \omega_2^2 & \omega_3^2 & \omega_1\omega_2 & \omega_2\omega_3 & \omega_3\omega_1 \end{bmatrix}^T$ is a 6×1 column vector of nonlinear functions of angular velocities $\omega_1, \omega_2, \omega_3$, and $B = \Big[B_{ij}\Big]_{3\times 6}$ is a 3×6 matrix of constant but unknown parameters in terms of the elements of the matrices $\mathcal{S}$ and $\mathcal{I}$. The individual elements of matrix B

are provided in Appendix A. Using (2.81) and (2.82), equation (2.80) can be written as

$$\begin{aligned} \dot{\xi} &= T(\xi)\omega \\ \varepsilon\dot{\omega} &= Bf(\omega) + \mathcal{S}\delta \\ \rho\dot{\delta} &= f_\delta(\delta) + G_\delta(\delta)u. \end{aligned} \tag{2.83}$$

The slow state vector ξ is to reach its reference ξ_r. The slow state error is defined as $e_\xi := \xi - \xi_r$. This can be achieved if the actuation vector δ can be stabilized on a suitable equilibrium manifold δ^0 in the fastest time-scale, and the fast state vector ω can be stabilized on a suitable equilibrium manifold ω^0 in the second fastest time-scale. Keeping this in mind, two more error vectors are defined as $e_\omega := \omega - \omega^0$ and $e_\delta := \delta - \delta^0$. The nonlinear state-space model (2.83) in the error coordinates is

$$\begin{aligned} \dot{e}_\xi &= T(\xi)(e_\omega + \omega^0) - \dot{\xi}_r \\ \varepsilon\dot{e}_\omega &= Bf(\omega) + \mathcal{S}(e_\delta + \delta^0) - \varepsilon\dot{\omega}^0 \\ \rho\dot{e}_\delta &= f_\delta(\delta) + G_\delta(\delta)u - \rho\dot{\delta}^0. \end{aligned} \tag{2.84}$$

A few assumptions are made to prove boundedness of errors later in this section. The inertias are unknown, but each of them are bounded between a maximum and a minimum. As a consequence, $B_{ij} \in [\underline{B}_{ij}, \bar{B}_{ij}]$ and $\mathcal{S}_{ij} \in [\underline{\mathcal{S}}_{ij}, \bar{\mathcal{S}}_{ij}]$ for every element B_{ij} and $\mathcal{S}_{ij}$ of the parameter matrices B and $\mathcal{S}$ respectively. Furthermore, there exist constants v_1, v_2 such that the maximum singular values of the matrices T and $\mathcal{S}$ satisfy $\bar{\sigma}(T) \leq v_1, \bar{\sigma}(\mathcal{S}) \leq v_2$.

2.5.2 Development of Control Law Using Reduced Subsystems

2.5.2.1 Selection of the Manifold of Fast States in the Slowest Time-Scale

The sequential controller is designed over three time-scales. In the slowest time-scale it is assumed that the fast states are already on their manifold ω^0, and therefore the error e_ω remains at zero. The manifold ω^0 is specified as an intermediate control variable such that the slow states ξ track their reference ξ_r, or equivalently the slow state tracking error e_ξ reaches zero. From the

full-order dynamics (2.84), the reduced subsystem in the slowest time-scale is extracted as

$$\dot{e}_\xi = T(\xi)\omega^0 - \dot{\xi}_r. \tag{2.85}$$

A positive-definite candidate Lyapunov function for the reduced slow subsystem is

$$V_1 = \frac{1}{2} e_\xi^T e_\xi. \tag{2.86}$$

Its time-derivative with respect to the slow time-scale t is

$$\dot{V}_1 = e_\xi^T \dot{e}_\xi. \tag{2.87}$$

Along the trajectories of the reduced slow subsystem (2.85), the time-derivative becomes

$$\dot{V}_1|_{(2.85)} = e_\xi^T (T(\xi)\omega^0 - \dot{\xi}_r). \tag{2.88}$$

If the manifold of the fast states is selected as

$$\omega^0 = T^{-1}(\xi)(\dot{\xi}_r - K_\xi e_\xi) \tag{2.89}$$

where K_ξ is a gain matrix, then the time-derivative of the Lyapunov function V_1 becomes

$$\dot{V}_1|_{(2.85)} = -e_\xi^T K_\xi e_\xi \tag{2.90}$$

which is negative-definite for any $K_\xi > 0$. Therefore, the equilibrium $e_\xi = 0$ of the reduced subsystem (2.85) is asymptotically stable.

2.5.2.2 *Selection of Actuator Manifold in the Second Fastest Time-Scale*

In the second fastest time-scale it is assumed that the actuators are already on their manifold δ^0; therefore, the error e_δ remains at zero. The manifold δ^0 is specified as an intermediate control variable such that the fast states ω reach their manifold ω^0, or equivalently the fast state error e_ω reaches zero. Let $\hat{B} := \left[\hat{B}_{ij}\right]_{3\times 6}$ and $\hat{S} := \left[\hat{S}_{ij}\right]_{3\times 3}$ represent the best estimates of the constant but unknown parameter matrices B and S respectively. Using these estimates and setting the perturbation parameter $\varepsilon = 0$, from the full-order dynamics (2.130) the reduced subsystem in the second fastest time-scale is extracted as

$$e'_\omega = \hat{B} f(\omega) + \hat{\mathcal{S}}\delta^0. \tag{2.91}$$

A positive-definite candidate Lyapunov function for this reduced subsystem is

$$V_2 = \frac{1}{2} e_\omega^T e_\omega. \tag{2.92}$$

Its time-derivative with respect to the time-scale $t_\varepsilon = \frac{t}{\varepsilon}$ is

$$V'_2 = e_\omega^T e'_\omega. \tag{2.93}$$

Along the trajectories of the reduced subsystem (2.91), the time-derivative becomes

$$V'_2|_{(2.91)} = e_\omega^T (\hat{B} f(\omega) + \hat{\mathcal{S}}\delta^0). \tag{2.94}$$

If the manifold of the fast actuators is selected as

$$\delta^0 = \hat{\mathcal{S}}^{-1}(-\hat{B} f(\omega) - K_\omega e_\omega) \tag{2.95}$$

where K_ω is a gain matrix, then the time-derivative of the Lyapunov function V_2 becomes

$$v_2'|_{(2.91)} = -e_\omega^T K_\omega e_\xi \tag{2.96}$$

which is negative-definite for any $K_\omega > 0$. Therefore, the equilibrium $e_\omega = 0$ of the reduced subsystem (2.91) is asymptotically stable.

2.5.2.3 Selection of Control in the Fastest Time-Scale

In the fastest time-scale the control u is designed such that the actuators δ reach their manifold δ^0, or equivalently the actuator error e_δ reaches zero. Setting $\rho = 0$, from the full-order dynamics (2.130), the reduced subsystem in the fastest time-scale is extracted as

$$\breve{e}_\delta = f_\delta(.) + G_\delta(.)u. \tag{2.97}$$

A positive-definite candidate Lyapunov function for this reduced subsystem is

$$V_3 = \frac{1}{2} e_\delta^T e_\delta. \tag{2.98}$$

Its time-derivative with respect to the time-scale $t_\rho = \frac{t}{\rho}$ is

$$\breve{V}_3 = e_\delta^T \breve{e}_\delta. \tag{2.99}$$

Along the trajectories of the reduced subsystem (2.97), the time-derivative becomes

$$\breve{V}_3|_{(2.97)} = e_\delta^T (f_\delta(.) + G_\delta(.)u). \tag{2.100}$$

If the control is selected as

$$u = G_\delta(.)^{-1}(-f_\delta(.) - K_\delta e_\delta) \tag{2.101}$$

where K_δ is a gain matrix, then the time-derivative of the Lyapunov function V_3 becomes

$$\overset{\vee}{V}_3|_{(2.97)} = -e_\delta^T K_\delta e_\delta \tag{2.102}$$

which is negative-definite for any $K_\delta > 0$. Therefore, the equilibrium $e_\delta = 0$ of the reduced subsystem (2.97) is asymptotically stable.

2.5.3 Stability Analysis of the Full-Order System: Selection of Parameter Update Laws and Bounds of Time-Scale Separation

For slow state regulation problem in presence of parametric uncertainties, Sections 2.3 and 2.4 used a composite Lyapunov function which was a weighted sum of the Lyapunov functions used for controller design and the Lyapunov functions to represent parameter estimator errors. In this Section, the parametric uncertainties are captured in matrices. Define parameter estimation error matrices $\tilde{B} = \left[\tilde{B}_{ij}\right]_{3\times 6} := B - \hat{B}$, $\tilde{\mathcal{S}} = \left[\tilde{S}_{ij}\right]_{3\times 3} := \mathcal{S} - \hat{\mathcal{S}}$. A candidate composite Lyapunov function for the full-order system (2.84) can be chosen as

$$V_c = \alpha_1 V_1 + \alpha_2 V_2 + \alpha_3 V_3 + \frac{1}{2}\alpha_4 tr(\tilde{B}^T \tilde{B}) + \frac{1}{2}\alpha_5 tr(\tilde{S}^T \tilde{S}) \tag{2.103}$$

where $\alpha_i > 0; i = 1, ..., 5$ represent the weights of the individual Lyapunov functions in the composite, and $tr(A)$ represents the trace of a matrix A. Suppose that $l_{ij}; i = 1, ..., m; j = 1, ..., n$ denotes the (i, j)-th element of an $(m \times n)$ matrix L. Then $tr[L^T L] = \sum_{i=1}^{m}\sum_{j=1}^{n} l_{ij}^2$. Therefore, the composite Lyapunov function (2.103) contains a weighted sum of squares of all the parameter estimation errors. To show the estimation errors explicitly, equation (2.103) can be written as

$$V_c = \alpha_1 V_1 + \alpha_2 V_2 + \alpha_3 V_3 + \frac{1}{2}\alpha_4 \sum_{i=1}^{3}\sum_{j=1}^{6} \tilde{B}_{ij}^2 + \frac{1}{2}\alpha_5 \sum_{i=1}^{3}\sum_{j=1}^{3} \tilde{\mathcal{S}}_{ij}^2. \tag{2.104}$$

The time-derivative of this function along the trajectories of the full-order system (2.84) is

$$\dot{V}_c = \alpha_1 \dot{V}_1|_{(2.84)} + \frac{\alpha_2}{\varepsilon} V_2'|_{(2.84)} + \frac{\alpha_3}{\rho} \breve{V}_3|_{(2.84)} + \frac{\alpha_4}{\varepsilon} \sum_{i=1}^{3} \sum_{j=1}^{6} \tilde{B}_{ij} \tilde{B}_{ij}' + \frac{\alpha_5}{\varepsilon} \sum_{i=1}^{3} \sum_{j=1}^{3} \tilde{\mathcal{S}}_{ij} \tilde{\mathcal{S}}_{ij}' \quad (2.105)$$

Introducing appropriate reduced subsystems, the time-derivative can be written as

$$\begin{aligned} \dot{V}_c = {} & \alpha_1 \dot{V}_1|_{(2.85)} + \frac{\alpha_2}{\varepsilon} V_2'|_{(2.91)} + \frac{\alpha_3}{\rho} \breve{V}_3|_{(2.97)} + \alpha_1 (\dot{V}_1|_{(2.84)} - \dot{V}_1|_{(2.85)}) + \frac{\alpha_2}{\varepsilon} (V_2'|_{(2.84)} - V_2'|_{(2.91)}) \\ & + \frac{\alpha_3}{\rho} (\breve{V}_3|_{(2.84)} - \breve{V}_3|_{(2.97)}) + \frac{\alpha_4}{\varepsilon} \sum_{i=1}^{3} \sum_{j=1}^{6} \tilde{B}_{ij} \tilde{B}_{ij}' + \frac{\alpha_5}{\varepsilon} \sum_{i=1}^{3} \sum_{j=1}^{3} \tilde{\mathcal{S}}_{ij} \tilde{\mathcal{S}}_{ij}' \end{aligned} \quad (2.106)$$

Making substitutions for the time-derivatives of individual Lyapunov functions along the trajectories of the reduced subsystems and the dynamics corresponding to the difference terms and simplifying, the time-derivative of the composite Lyapunov function becomes

$$\begin{aligned} \dot{V}_c = {} & -\alpha_1 e_\xi^T K_\xi e_\xi - \frac{\alpha_2}{\varepsilon} e_\omega^T K_\omega e_\omega - \frac{\alpha_3}{\rho} e_\delta^T K_\delta e_\delta + \alpha_1 e_\xi^T T(\xi) e_\omega + \frac{\alpha_2}{\varepsilon} e_\omega^T \mathcal{S} e_\delta - \alpha_2 e_\omega^T \dot{\omega}^0 \\ & - \alpha_3 e_\delta^T \dot{\delta}^0 + \frac{\alpha_4}{\varepsilon} \sum_{i=1}^{3} \sum_{j=1}^{6} (\frac{\alpha_2}{\alpha_4} e_{\omega_i} f_j(\omega) - \hat{B}_{ij}') \tilde{B}_{ij} + \frac{\alpha_5}{\varepsilon} \sum_{i=1}^{3} \sum_{j=1}^{3} (\frac{\alpha_2}{\alpha_5} e_{\omega_i} \delta_j^0 - \hat{\mathcal{S}}_{ij}') \tilde{\mathcal{S}}_{ij} \end{aligned} \quad (2.107)$$

where e_{ω_i} is the i^{th} element of the fast state vector e_ω, $f_j(\omega)$ is the j^{th} element of the vector of functions $f(\omega)$, and δ_0^j is the j^{th} element of the fast actuator manifold δ^0.

For slow state regulation of an uncertain two-time-scale system in Sections 2.3 and 2.4, the parameter update laws were selected so the parameter estimation error terms were eliminated from the $\dot{V}_c$ equation. However, for the current problem it is desired to keep parameter estimation error terms, and therefore update laws are chosen differently. In the work of Park *et. al.* [61], the adaptive laws were selected using sigma-modification. For sigma-modification, the parameter estimates tend to approach zero when the errors in the states become small. For this problem, should the parameters associated with control effectiveness become close to zero, the control law using inverses of the parameter estimate matrices will have numerical issues. Therefore, the parameter update laws are selected similar to some of the laws in the work of Dong and Kuhnert [62]. The

update laws are

$$\begin{aligned}\hat{B}'_{ij} &= \frac{\alpha_2}{\alpha_4} e_{\omega_i} f_j(\omega) - \frac{\theta_1}{\alpha_4}(\hat{B}_{ij} - B^0_{ij}) \\ \hat{\mathcal{S}}'_{ij} &= \frac{\alpha_2}{\alpha_5} e_{\omega_i} \delta^0_j - \frac{\theta_2}{\alpha_5}(\hat{\mathcal{S}}_{ij} - \mathcal{S}^0_{ij})\end{aligned} \tag{2.108}$$

where $\theta_1 > 0, \theta_2 > 0, B^0_{ij}, \mathcal{S}^0_{ij}$ are design variables. Part of each update law is to cancel the corresponding parameter estimation error term, and the remaining is to let the estimate settle to a suitably selected final value, following a first-order dynamics with a suitably chosen time-constant. With this selection of parameter update laws, the time-derivative (2.107) becomes

$$\begin{aligned}\dot{V}_c = &-\alpha_1 e_\xi^T K_\xi e_\xi - \frac{\alpha_2}{\varepsilon} e_\omega^T K_\omega e_\omega - \frac{\alpha_3}{\rho} e_\delta^T K_\delta e_\delta + \alpha_1 e_\xi^T T(\xi) e_\omega + \frac{\alpha_2}{\varepsilon} e_\omega^T \mathcal{S} e_\delta - \alpha_2 e_\omega^T \dot{\omega}^0 \\ &- \alpha_3 e_\delta^T \dot{\delta}^0 + \frac{\theta_1}{\varepsilon} \sum_{i=1}^{3} \sum_{j=1}^{6} (\hat{B}_{ij} - B^0_{ij}) \tilde{B}_{ij} + \frac{\theta_2}{\varepsilon} \sum_{i=1}^{3} \sum_{j=1}^{3} (\hat{\mathcal{S}}_{ij} - \mathcal{S}^0_{ij}) \tilde{\mathcal{S}}_{ij}.\end{aligned} \tag{2.109}$$

It is to be noted that that for any constant but unknown parameter p bounded as $\underline{p} \leq p \leq \bar{p}$, the expression $\tilde{p}(\hat{p} - p^0)$ can be bounded as follows:

$$\begin{aligned}\tilde{p}(\hat{p} - p^0) &= \tilde{p}(p - \tilde{p} - p^0) \\ &= \tilde{p}(p - p^0) - \tilde{p}^2 \\ &\leq \frac{1}{2}[\tilde{p}^2 + (p - p^0)^2] - \tilde{p}^2 \\ &= \frac{1}{2}(p - p^0)^2 - \frac{1}{2}\tilde{p}^2 \\ &\leq \frac{1}{2} \max_{\underline{p} \leq p \leq \bar{p}} (p - p^0)^2 - \frac{1}{2}\tilde{p}^2 \\ &= \frac{1}{2} p^+ - \frac{1}{2}\tilde{p}^2\end{aligned} \tag{2.110}$$

where $p^+ := \max_{\underline{p} \leq p \leq \bar{p}} (p - p^0)^2$. Using this result, the time-derivative (2.109) can be rewritten as the

following inequality:

$$\begin{aligned}\dot{V}_c \leq & -\alpha_1 e_\xi^T K_\xi e_\xi - \frac{\alpha_2}{\varepsilon} e_\omega^T K_\omega e_\omega - \frac{\alpha_3}{\rho} e_\delta^T K_\delta e_\delta - \frac{\theta_1}{2\varepsilon} \sum_{i=1}^{3}\sum_{j=1}^{6} \tilde{B}_{ij}^2 - \frac{\theta_2}{2\varepsilon} \sum_{i=1}^{3}\sum_{j=1}^{3} \tilde{\mathcal{S}}_{ij}^2 \\ & + \alpha_1 e_\xi^T T(\xi) e_\omega + \frac{\alpha_2}{\varepsilon} e_\omega^T \mathcal{S} e_\delta - \alpha_2 e_\omega^T \dot{\omega}^0 - \alpha_3 e_\delta^T \dot{\delta}^0 + \frac{\theta_1}{2\varepsilon} \sum_{i=1}^{3}\sum_{j=1}^{6} B_{ij}^+ + \frac{\theta_2}{2\varepsilon} \sum_{i=1}^{3}\sum_{j=1}^{3} \mathcal{S}_{ij}^+\end{aligned} \tag{2.111}$$

where

$$\begin{aligned} B_{ij}^+ &:= \max_{\underline{B}_{ij} \leq B_{ij} \leq \bar{B}_{ij}} (B_{ij} - B_{ij}^0)^2 \\ \mathcal{S}_{ij}^+ &:= \max_{\underline{\mathcal{S}}_{ij} \leq \mathcal{S}_{ij} \leq \bar{\mathcal{S}}_{ij}} (\mathcal{S}_{ij} - \mathcal{S}_{ij}^0)^2 \end{aligned} \tag{2.112}$$

Equation (2.111) has several terms for which the upper bounds are to be found. Some of these terms involve analytical expressions of manifolds and their time-derivatives. Given the design based on the reduced subsystems, using the exact expressions of the manifolds and their time-derivatives can make the stability analysis cumbersome. This has similarities with backstepping for nonlinear systems in strict-feedback form. In backstepping the states not to be tracked are specified as intermediate controls before the actual control is designed. A major limitation of backstepping is the 'explosion of terms' due to explicit differentiation of the intermediate controls. For sequential control of singularly perturbed systems, artificially equating the perturbation parameters to zero eliminates the time-derivatives of the manifolds and the 'explosion of terms' in the reduced-order subsystems. However, it is to be addressed in the composite Lyapunov analysis. A method to overcome the issue of explicit differentiation during backstepping is dynamic surface control developed in the work of Swaroop *et. al.* [63, 64]. This method uses first-order filters to replace the explcit evaluation of the derivatives of the intermediate controls. An adaptive version of this method can be found in Yip and Hedrick [65]. Applications of this method in robotics can be found in Park *et. al.* [61] and Cao *et. al.* [66]. For the current problem, additional first-order filters are not needed, but boundedness of tracking error is to be proven. One of the results used to prove the boundedness of tracking error for dynamic surface control is the extreme value theorem, which states that a continuous function in a compact set has a maximum. Using this result, inferences can

be drawn for some of the terms present in the time-derivative (2.111).

The combined dimension of the states and unknown parameters for this problem is $3 + 3 + 3 + 18 + 9 = 36$. Consider a compact set $Q_1 \in \mathbb{R}^{36}$, characterized by the composite Lyapunov function in (2.30) upper-bounded by $\bar{V}$; i.e. $V_c \leq \bar{V}$ for some $\bar{V} > 0$. Again, the combined dimension of the references and their time-derivatives of first and second orders is $3 + 3 + 3 = 9$. Consider a compact set $Q_2 \in \mathbb{R}^9$, characterized by $\|\xi_r\|_2^2 + \left\|\dot{\xi}_r\right\|_2^2 + \left\|\ddot{\xi}_r\right\|_2^2 \leq R^2$ for some $R > 0$. Then $Q := Q_1 \times Q_2$ is a compact set in $\mathbb{R}^{36+9} = \mathbb{R}^{45}$, and all the elements of the vectors $\dot{\omega}^0$ and $\dot{\delta}^0$ are continuous functions in the compact set Q. Therefore, each element of these vectors has a maximum, and consequently there exist constants M_1, M_2 such that $\left\|\dot{\omega}^0\right\|_\infty = M_1, \left\|\dot{\delta}^0\right\|_\infty = M_2$. Upper bounds of the cross-terms involving $\dot{\omega}^0$ and $\dot{\delta}^0$ present in the time-derivative (2.111) can now be found as follows.

$$\begin{aligned} -\alpha_2 e_\omega^T \dot{\omega}^0 &\leq \alpha_2 \|e_\omega\|_2 \left\|\dot{\omega}^0\right\|_2 \\ &\leq \alpha_2 \|e_\omega\|_2 \sqrt{3} \left\|\dot{\omega}^0\right\|_\infty \\ &= \alpha_2 \sqrt{3} M_1 \|e_\omega\|_2 \\ &= \alpha_2 \sqrt{3} M_1 \nu_1 \frac{1}{\nu_1} \|e_\omega\|_2 \\ &\leq \frac{1}{2} \alpha_2 \sqrt{3} M_1 (\nu_1^2 + \frac{1}{\nu_1^2} e_\omega^T e_\omega) \end{aligned} \tag{2.113}$$

The last step in (2.113) was obtained using the Young's inequality: $ab \leq \frac{1}{2}(a^2 + b^2)$. The constant ν_1 can be arbitrarily chosen. Similarly,

$$-\alpha_3 e_\delta^T \dot{\delta}^0 \leq \frac{1}{2} \alpha_3 \sqrt{3} M_2 (\nu_2^2 + \frac{1}{\nu_2^2} e_\delta^T e_\delta) \tag{2.114}$$

where the constant ν_2 can be arbitrarily chosen. The other cross-terms involving product of two

error vectors can be bounded as follows:

$$\begin{aligned}\alpha_1 e_\xi^T T(\xi) e_\omega &\leq \alpha_1 \left\|e_\xi\right\|_2 \left\|T(\xi)\right\|_2 \|e_\omega\|_2 \\ &\leq \alpha_1 \left\|e_\xi\right\|_2 v_1 \|e_\omega\|_2 \\ &\leq \frac{1}{2}\alpha_1 v_1 (e_\xi^T e_\xi + e_\omega^T e_\omega)\end{aligned} \tag{2.115}$$

Similarly,

$$\begin{aligned}\frac{\alpha_2}{\varepsilon} e_\omega^T \mathcal{S} e_\delta &\leq \frac{\alpha_2}{\varepsilon} \|e_\omega\|_2 \|\mathcal{S}\|_2 \|e_\delta\|_2 \\ &\leq \frac{\alpha_2}{\varepsilon} \|e_\omega\|_2 v_2 \|e_\delta\|_2 \\ &\leq \frac{1}{2}\frac{\alpha_2}{\varepsilon} v_2 (e_\omega^T e_\omega + e_\delta^T e_\delta)\end{aligned} \tag{2.116}$$

Using inequalities (2.113) - (2.116), the time-derivative of the composite Lyapunov function in (2.111) can be written as

$$\begin{aligned}\dot{V}_c \leq & -\alpha_1 e_\xi^T K_\xi e_\xi - \frac{\alpha_2}{\varepsilon} e_\omega^T K_\omega e_\omega - \frac{\alpha_3}{\rho} e_\delta^T K_\delta e_\delta - \frac{\theta_1}{2\varepsilon}\sum_{i=1}^{3}\sum_{j=1}^{6}\tilde{B}_{ij}^2 - \frac{\theta_2}{2\varepsilon}\sum_{i=1}^{3}\sum_{j=1}^{3}\tilde{\mathcal{S}}_{ij}^2 \\ & + \frac{\alpha_1 v_1}{2}(e_\xi^T e_\xi + e_\omega^T e_\omega) + \frac{\alpha_2 v_2}{2\varepsilon}(e_\omega^T e_\omega + e_\delta^T e_\delta) + \frac{\alpha_2\sqrt{3}M_1}{2}(\nu_1^2 + \frac{1}{\nu_1^2} e_\omega^T e_\omega) \\ & + \frac{\alpha_3 M_2\sqrt{3}}{2}(\nu_2^2 + \frac{1}{\nu_2^2} e_\delta^T e_\delta) + \frac{\theta_1}{2\varepsilon}\sum_{i=1}^{3}\sum_{j=1}^{6} B_{ij}^+ + \frac{\theta_2}{2\varepsilon}\sum_{i=1}^{3}\sum_{j=1}^{3}\mathcal{S}_{ij}^+.\end{aligned} \tag{2.117}$$

This can further be rewritten as

$$\begin{aligned}\dot{V}_c \leq & -\alpha_1 \lambda_{\min}(K_\xi) e_\xi^T e_\xi - \frac{\alpha_2}{\varepsilon}\lambda_{\min}(K_\omega) e_\omega^T e_\omega - \frac{\alpha_3}{\rho}\lambda_{\min}(K_\delta) e_\delta^T e_\delta - \frac{\theta_1}{2\varepsilon}\sum_{i=1}^{3}\sum_{j=1}^{6}\tilde{B}_{ij}^2 \\ & - \frac{\theta_2}{2\varepsilon}\sum_{i=1}^{3}\sum_{j=1}^{3}\tilde{\mathcal{S}}_{ij}^2 + \frac{\alpha_1 v_1}{2}(e_\xi^T e_\xi + e_\omega^T e_\omega) + \frac{\alpha_2 v_2}{2\varepsilon}(e_\omega^T e_\omega + e_\delta^T e_\delta) + \frac{\alpha_2\sqrt{3}M_1}{2}(\nu_1^2 + \frac{1}{\nu_1^2} e_\omega^T e_\omega) \\ & + \frac{\alpha_3 M_2\sqrt{3}}{2}(\nu_2^2 + \frac{1}{\nu_2^2} e_\delta^T e_\delta) + \frac{\theta_1}{2\varepsilon}\sum_{i=1}^{3}\sum_{j=1}^{6} B_{ij}^+ + \frac{\theta_2}{2\varepsilon}\sum_{i=1}^{3}\sum_{j=1}^{3}\mathcal{S}_{ij}^+\end{aligned} \tag{2.118}$$

where $\lambda_{\min}(A)$ represents the minimum eigenvalue of a matrix A. Grouping the quadratic and

other terms, the time-derivative becomes

$$\begin{aligned}\dot{V}_c &\leq -\beta_1 e_\xi^T e_\xi - \beta_2 e_\omega^T e_\omega - \beta_3 e_\delta^T e_\delta - \frac{\theta_1}{2\varepsilon}\sum_{i=1}^{3}\sum_{j=1}^{6}\tilde{B}_{ij}^2 - \frac{\theta_2}{2\varepsilon}\sum_{i=1}^{3}\sum_{j=1}^{3}\tilde{\mathcal{S}}_{ij}^2 + \mu \\ &\leq -\min(\beta_1,\beta_2,\beta_3,\frac{\theta_1}{2\varepsilon},\frac{\theta_2}{2\varepsilon})(e_\xi^T e_\xi + e_\omega^T e_\omega + e_\delta^T e_\delta + \sum_{i=1}^{3}\sum_{j=1}^{6}\tilde{B}_{ij}^2 + \sum_{i=1}^{3}\sum_{j=1}^{3}\tilde{\mathcal{S}}_{ij}^2) + \mu \\ &\leq -\frac{\min(\beta_1,\beta_2,\beta_3,\frac{\theta_1}{2\varepsilon},\frac{\theta_2}{2\varepsilon})}{\max(\frac{\alpha_1}{2},\frac{\alpha_2}{2},\frac{\alpha_3}{2},\frac{\alpha_4}{2},\frac{\alpha_5}{2})}V_c + \mu\end{aligned} \tag{2.119}$$

where

$$\begin{aligned}\beta_1 &:= \alpha_1\lambda_{\min}(K_\xi) - \frac{\alpha_1 v_1}{2} \\ \beta_2 &:= \frac{\alpha_2}{\varepsilon}\lambda_{\min}(K_\omega) - \frac{\alpha_1 v_1}{2} - \frac{\alpha_2 v_2}{2\varepsilon} - \frac{\alpha_2\sqrt{3}M_1}{2\nu_1^2} \\ \beta_3 &:= \frac{\alpha_3}{\rho}\lambda_{\min}(K_\delta) - \frac{\alpha_2 v_2}{2\varepsilon} - \frac{\alpha_3\sqrt{3}M_2}{2\nu_2^2} \\ \mu &:= \mu_1 + \frac{\mu_2}{\varepsilon}\end{aligned} \tag{2.120}$$

with

$$\begin{aligned}\mu_1 &:= \frac{\alpha_2 M_1\sqrt{3}}{2}\nu_1^2 + \frac{\alpha_3 M_2\sqrt{3}}{2}\nu_2^2 \\ \mu_2 &:= \frac{\theta_1}{2}\sum_{i=1}^{3}\sum_{j=1}^{6}B_{ij}^{+} + \frac{\theta_2}{2}\sum_{i=1}^{3}\sum_{j=1}^{3}\mathcal{S}_{ij}^{+}\end{aligned} \tag{2.121}$$

Inequality (2.119) indicates that the tracking error e_ξ, the manifold errors e_ω, e_δ and the parameter estimation errors $\tilde{B}_{ij}, \tilde{\mathcal{S}}_{ij}$ will be ultimately bounded. In order to find the bounds on the time-scale separation parameters ε and ρ guaranteeing ultimate boundedness, the following form of the inequality (2.119) is considered:

$$\dot{V}_c \leq -\eta\|e\|_2^2 + \mu \tag{2.122}$$

where

$$\begin{aligned}\eta &:= \min(\beta_1,\beta_2,\beta_3,\frac{\theta_1}{2\varepsilon},\frac{\theta_2}{2\varepsilon}) \\ e &:= \begin{bmatrix} e_\xi & e_\omega & e_\delta & \tilde{B}_{ij} & \tilde{S}_{lm}\end{bmatrix}; i=1,2,3; j=1,...,6; l=1,2,3; m=1,2,3\end{aligned} \tag{2.123}$$

It can be seen that e contains all the errors: the tracking error for the slow states ξ, the manifold error for the fast states ω and actuators δ, and the estimation errors for all parameters in the B and $\mathcal{S}$ matrices. Suppose that it is desired to keep the error vector e uniformly ultimately bounded within a ball of radius θ_r; i.e. $\dot{V}_c < 0$ on the boundary of the ball represented by $\|e\|_2 = \theta_r$. This is possible if $-\eta\theta_r^2 + \mu < 0$; i.e. if $\eta > \frac{\mu}{\theta_r^2}$. The inequality $\eta > \frac{\mu}{\theta_r^2}$ will be true if the following are true:

$$\beta_1 > \frac{\mu}{\theta_r^2}, \quad \beta_2 > \frac{\mu}{\theta_r^2}, \quad \beta_3 > \frac{\mu}{\theta_r^2}, \quad \frac{\theta_1}{2\varepsilon} > \frac{\mu}{\theta_r^2}, \quad \frac{\theta_2}{2\varepsilon} > \frac{\mu}{\theta_r^2}.$$

Making substitutions and simplifying, these five conditions lead to bounds of the time-scale separation parameters ε and ρ. The bound of ε is

$$\varepsilon_{**} < \varepsilon < \varepsilon^{**} \tag{2.124}$$

where $\varepsilon_{**} > 0$ is a suitably chosen small positive number, and

$$\varepsilon^{**} := \min\left(\frac{\theta_1\theta_r^2 - 2\mu_2}{2\mu_1}, \frac{\theta_2\theta_r^2 - 2\mu_2}{2\mu_1}, \frac{\alpha_2\lambda_{\min}(K_\omega) - \frac{\alpha_2 v_2}{2} - \frac{\mu_2}{\theta_r^2}}{\frac{\mu_1}{\theta_r^2} + \frac{\alpha_1 v_1}{2} + \frac{\alpha_2\sqrt{3}M_1}{2\nu_1^2}}\right). \tag{2.125}$$

The bound of ρ is

$$\rho_{**} < \rho < \rho^{**} \tag{2.126}$$

where $\rho_{**} := 0$ and

$$\rho^{**} := \frac{\alpha_3\lambda_{\min}(K_\delta)}{\left(\frac{\alpha_3\sqrt{3}M_2}{2\nu_2^2} + \frac{\mu_1}{\theta_r^2}\right) + \frac{1}{\varepsilon_{**}}\left(\frac{\alpha_2 v_2}{2} + \frac{\mu_2}{\theta_r^2}\right)}. \tag{2.127}$$

In addition, the gain matrix K_ξ should be chosen to ensure that

$$\lambda_{\min}(K_\xi) > \frac{1}{\alpha_1}\left[\frac{\alpha_1 v_1}{2} + \frac{1}{\theta_r^2}(\mu_1 + \frac{\mu_2}{\varepsilon^{**}})\right]. \tag{2.128}$$

2.5.4 Numerical Results

This subsection shows in simulation slow state tracking using the control and estimation laws developed in Subsections 2.5.2 - 2.5.3 on a nonlinear generic spacecraft model represented by (2.80). The actual inertias, initial conditions of the MRPs and angular velocities are the same as the ones in the work of Tandale and Valasek [59]. At time zero, the MRPs and angular velocities are at the initial condition $\xi(0) = \begin{bmatrix} 0.1 & 0.09 & 0.05 \end{bmatrix}^T$ and $\omega(0) = \begin{bmatrix} 0.09 & 0.07 & 0.08 \end{bmatrix}^T$ deg/s respectively. The actuators are assumed to be at zero initial condition in the beginning of the simulation. The actual inertias are $\mathcal{I} = \begin{bmatrix} 30 & 10 & 5 \\ 10 & 20 & 3 \\ 5 & 3 & 15 \end{bmatrix}$ kg-m^2 . The initial estimates of the inertias are assumed 20% below the actual values; i.e. to compute the initial estimates of the matrices B and $\mathcal{S}$, the initial estimates of inertias are selected as $\hat{I}(0) = \begin{bmatrix} 24 & 8 & 4 \\ 8 & 16 & 2.4 \\ 4 & 2.4 & 12 \end{bmatrix}$ kg-m^2 . Discussions on some commonly used torque actuators such as reaction wheels and control moment gyros can be found in the works of Vadali [67], Schaub and Junkins [68], and Hurtado [41]. A generic first-order actuator model is proposed in the work of Kristiansen and Hagen [69]. For the current simulation each actuator is assumed to be first-order with a time-constant of 0.1 sec. With these sets of numbers, two different rotational maneuvers are tracked using the control and estimation laws developed in Subsections 2.5.2 - 2.5.3.

2.5.4.1 Evaluation Maneuver I: Tracking a Set of Lightly Damped Sinusoidal Trajectories

This is an evaluation maneuver similar to the one used in Tandale and Valasek [59]. For this evaluation maneuver, the reference trajectories for the MRPs are

$$\xi_r(t) = e^{-kt} \begin{bmatrix} A_1 \sin(q_1 t) & A_2 \sin(q_2 t) & A_3 \sin(q_3 t) \end{bmatrix}^T$$

with $k = 0.01, A_i = 0.2; q_i = 0.5; i = 1, 2, 3$. The controller gain matrices are selected as $K_\xi = diag[1, 1, 1], K_\omega = diag[10, 10, 10], K_\delta = diag[10, 10, 10]$. For parameter estimation, the weights of individual Lyapunov functions in the composite are selected as $\alpha_2 = 10^{-10}, \alpha_4 = 1, \alpha_5 = 1$. The two gain factors θ_1 and θ_2 in the parameter estimation laws are chosen as $\theta_1 = 0.1, \theta_2 = 0.1$. The design variables B_{ij}^0 and $\mathcal{S}_{ij}^0$ are selected such that they correspond to the inertias being 5% above the actual inertias. The simulation is run for 100 sec.

Figures 2.5 - 2.7 show the time-histories of the states and the controls. It can be seen in Figure 2.5 that the MRPs reach their references about 5 seconds into the simulation, and tracks the references accurately for the remaining 95 seconds. Figure 2.6 shows that the angular velocities quickly reach and then stay on their manifolds. Figure 2.7 show that all the controls remain bounded. Figures 2.8 - 2.10 show the evolution of the estimates of all the uncertain parameters in the B and $\mathcal{S}$ matrices. It can be seen that the parameter estimates remain bounded. It is observed that the magnitude of estimation error significantly small for the elements of the $\hat{B}$ matrix. This is due to the fact that they are formed as products of the elements of the inertia matrix and its inverse. From figures 2.5 - 2.10 it can be concluded that the desired objective of slow state tracking is accomplished, and the tracking errors, manifold errors and parameter estimation errors remain bounded and small in magnitude.

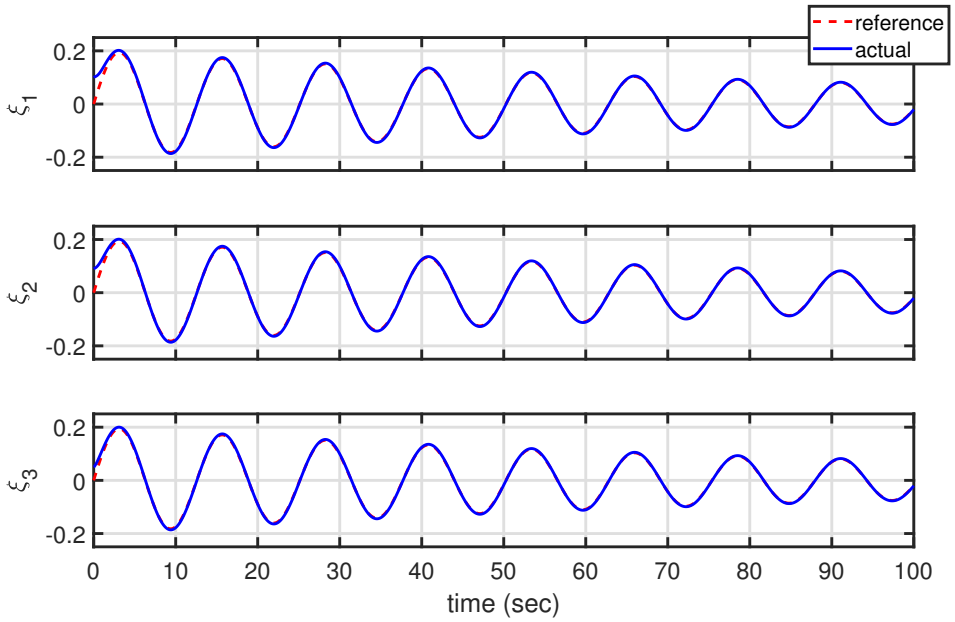

Figure 2.5: Modified Rodriguez Parameters for damped sinusoidal trajectory tracking; from Saha and Valasek [60], reprinted by permission of the American Institute of Aeronautics and Astronautics, Inc.

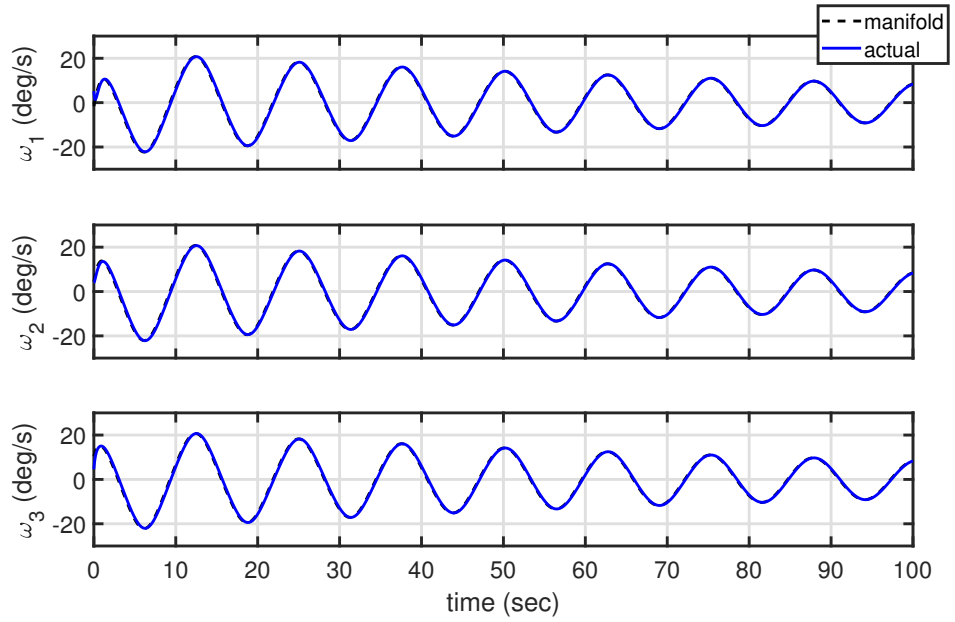

Figure 2.6: Angular velocities for damped sinusoidal trajectory tracking; from Saha and Valasek [60], reprinted by permission of the American Institute of Aeronautics and Astronautics, Inc.

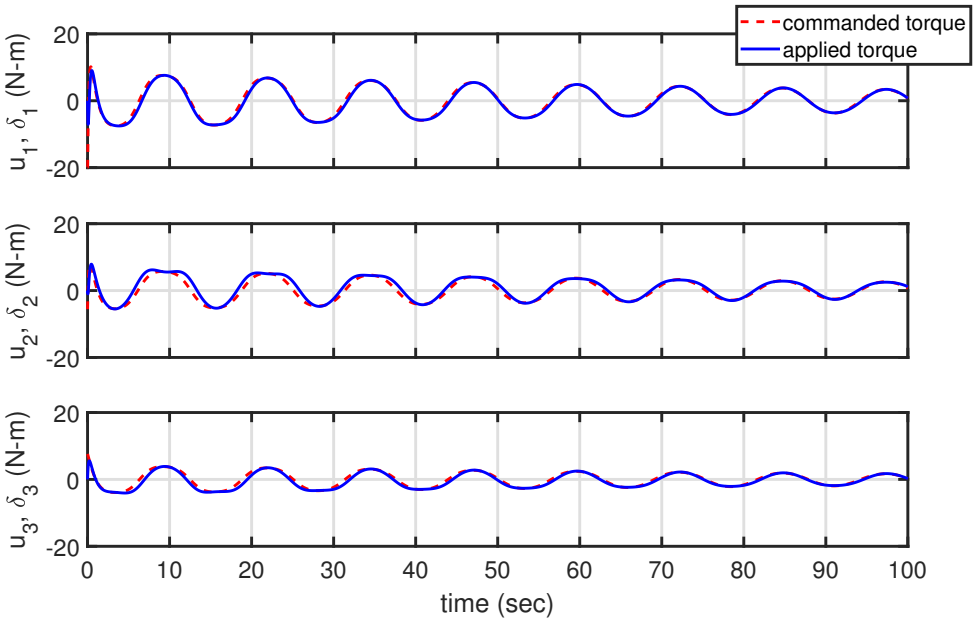

Figure 2.7: Control torques for damped sinusoidal trajectory tracking; from Saha and Valasek [60], reprinted by permission of the American Institute of Aeronautics and Astronautics, Inc.

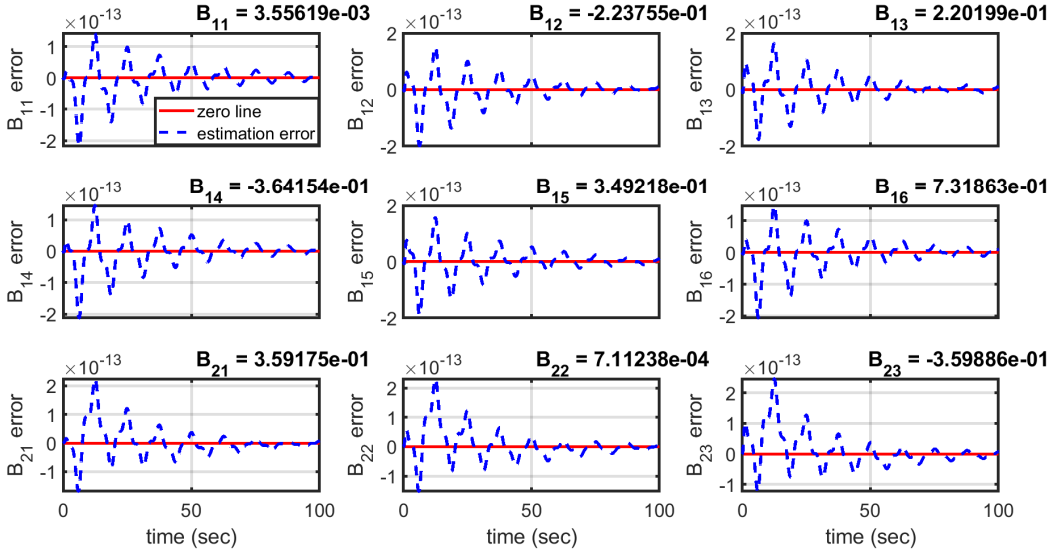

Figure 2.8: Uncertain parameters $B_{11} - B_{23}$ for damped sinusoidal trajectory tracking; from Saha and Valasek [60], reprinted by permission of the American Institute of Aeronautics and Astronautics, Inc.

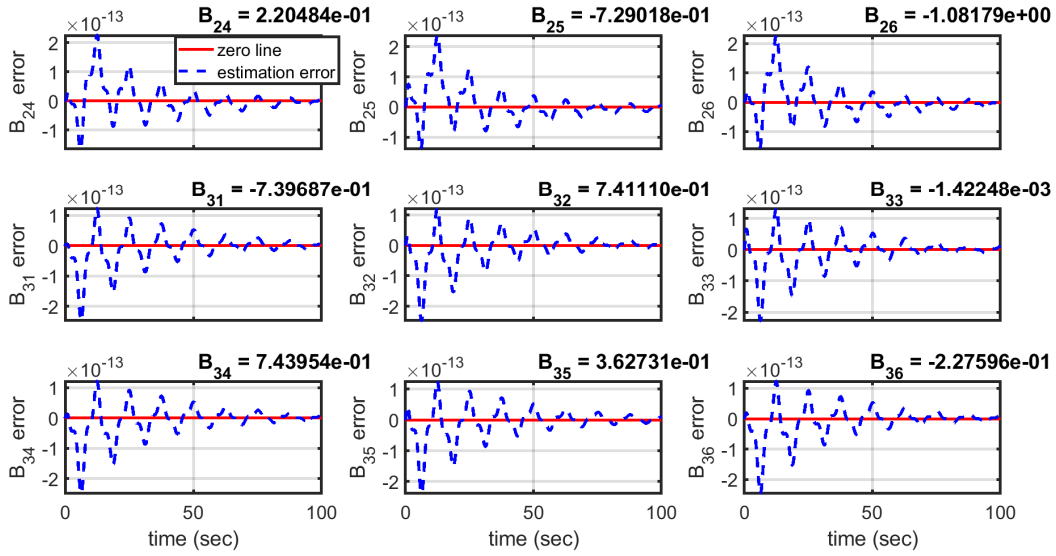

Figure 2.9: Uncertain parameters $B_{24} - B_{36}$ for damped sinusoidal trajectory tracking; from Saha and Valasek [60], reprinted by permission of the American Institute of Aeronautics and Astronautics, Inc.

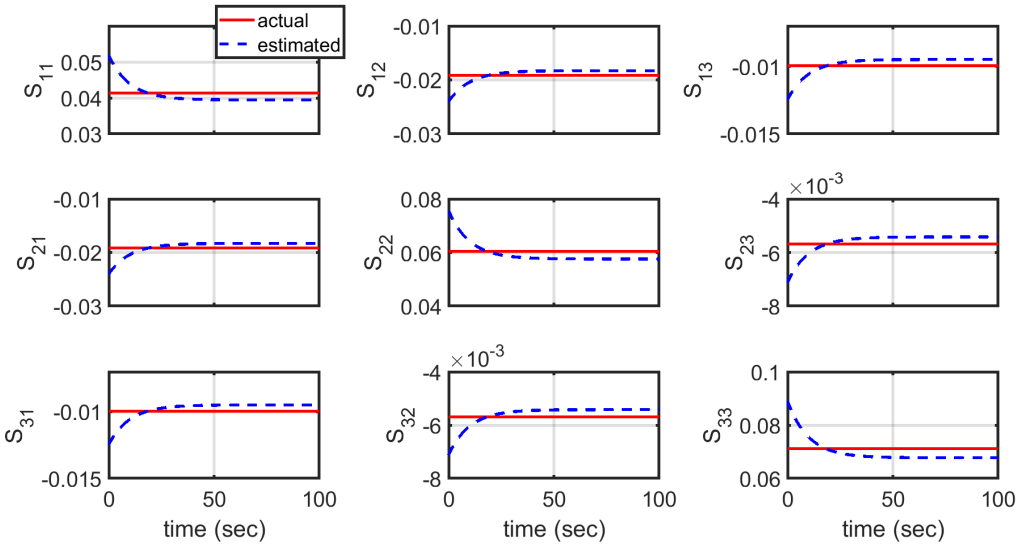

Figure 2.10: Uncertain parameters $\mathcal{S}_{11} - \mathcal{S}_{33}$ for damped sinusoidal trajectory tracking; from Saha and Valasek [60], reprinted by permission of the American Institute of Aeronautics and Astronautics, Inc.

2.5.4.2 *Evaluation Maneuver II: Three Euler Angle Rotations in a 3-2-1 Sequence*

For this evaluation maneuver, the reference trajectory is provided in terms of Euler angles, and converted to MRPs by a transformation using the Direction Cosine Matrix. It is desired that the spacecraft performs a 3-2-1 sequence of Euler angle rotations to point to a certain direction. It first changes heading by 120 degrees to the left in 10 seconds, then then pitches up by 60 degrees in 5 seconds, and finally banks to the left by 90 degrees in 7.5 seconds. For this The controller gain matrices are selected as $K_\xi = diag[5,5,5], K_\omega = diag[20,20,20], K_\delta = diag[5,5,5]$. For parameter estimation, the weights of individual Lyapunov functions in the composite are selected as $\alpha_2 = 10^{-10}, \alpha_4 = 1, \alpha_5 = 1$. The two gain factors θ_1 and θ_2 in the parameter estimation laws are chosen as $\theta_1 = 0.2, \theta_2 = 0.2$. The design variables B_{ij}^0 and $\mathcal{S}_{ij}^0$ are selected such that they correspond to the inertias being 5% above the actual inertias. The simulation is run for 30 sec.

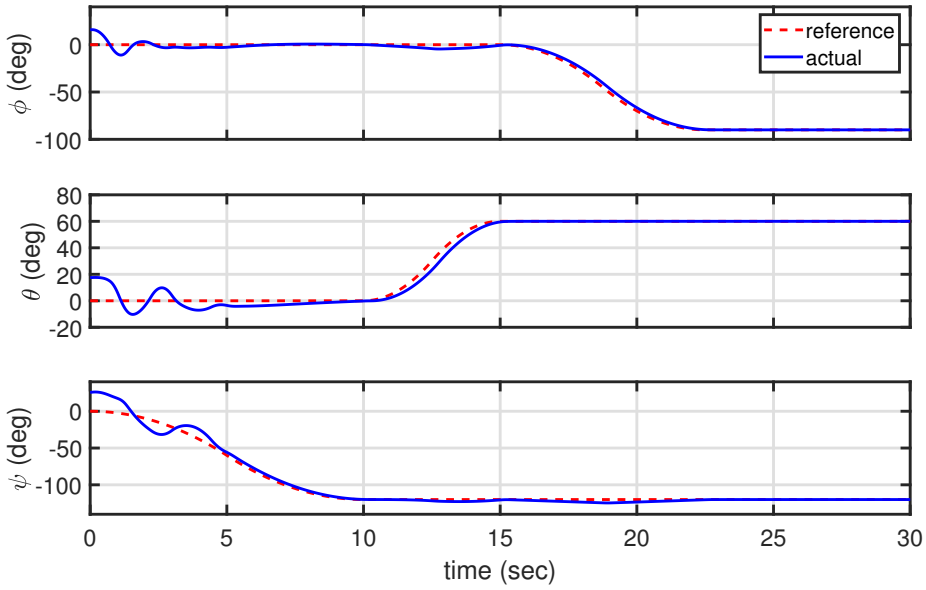

Figure 2.11: Euler angles for sequential Euler angle rotation: the bank angle ϕ, the pitch attitude angle θ, and the heading angle ψ; from Saha and Valasek [60], reprinted by permission of the American Institute of Aeronautics and Astronautics, Inc.

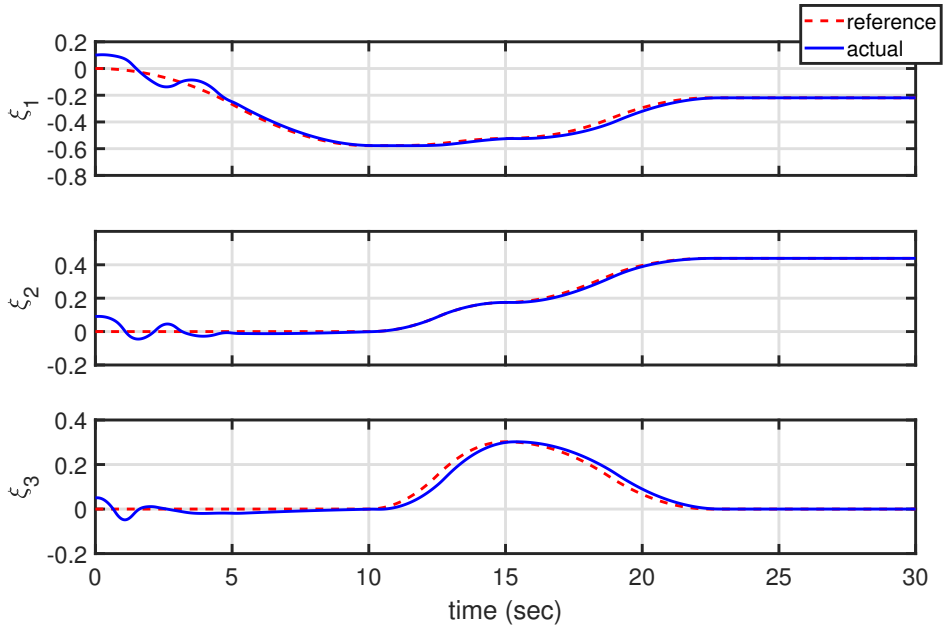

Figure 2.12: Modified Rodriguez Parameters for sequential Euler angle rotation; from Saha and Valasek [60], reprinted by permission of the American Institute of Aeronautics and Astronautics, Inc.

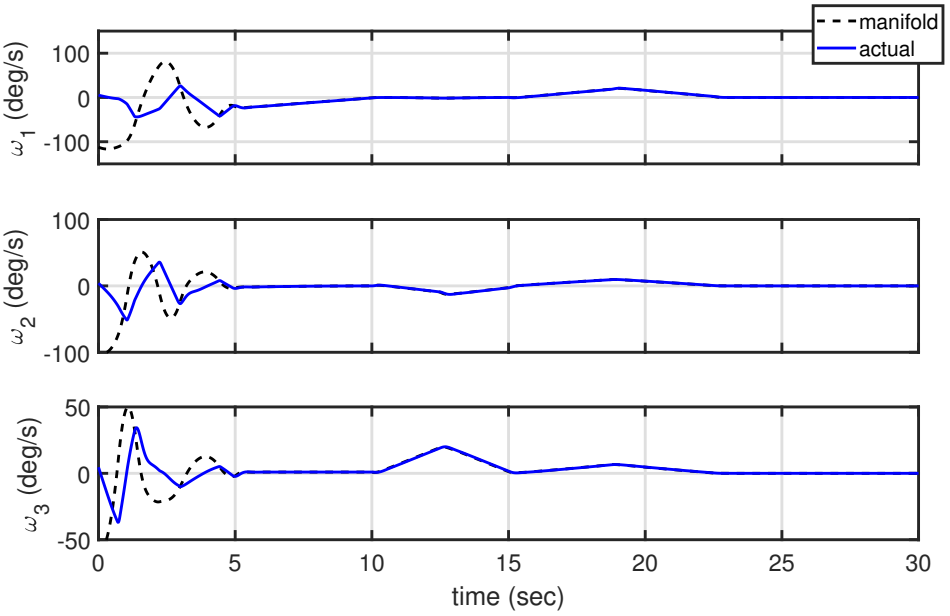

Figure 2.13: Angular velocities for sequential Euler angle rotation; from Saha and Valasek [60], reprinted by permission of the American Institute of Aeronautics and Astronautics, Inc.

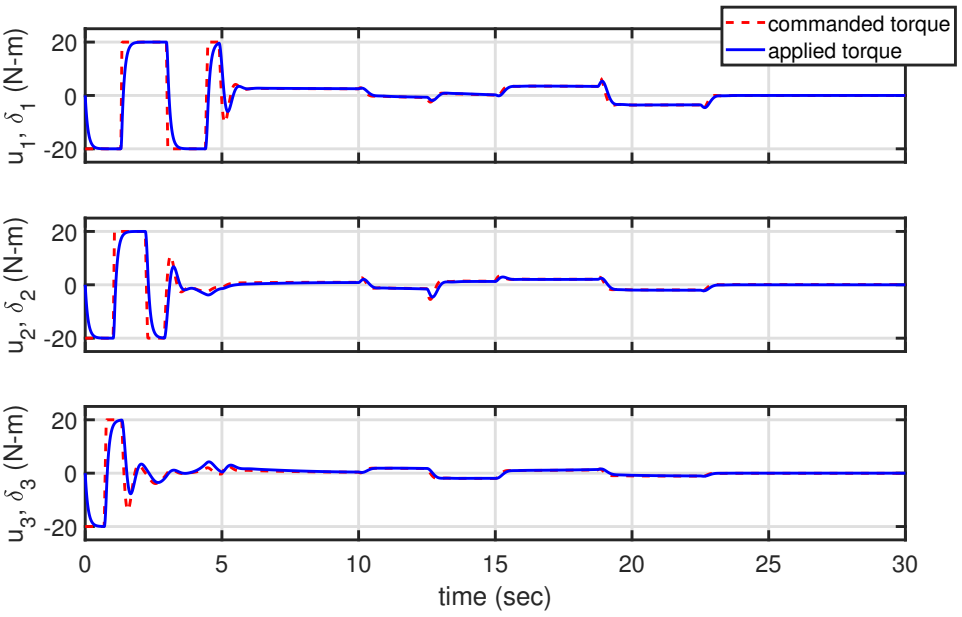

Figure 2.14: Control torques for sequential Euler angle rotation; from Saha and Valasek [60], reprinted by permission of the American Institute of Aeronautics and Astronautics, Inc.

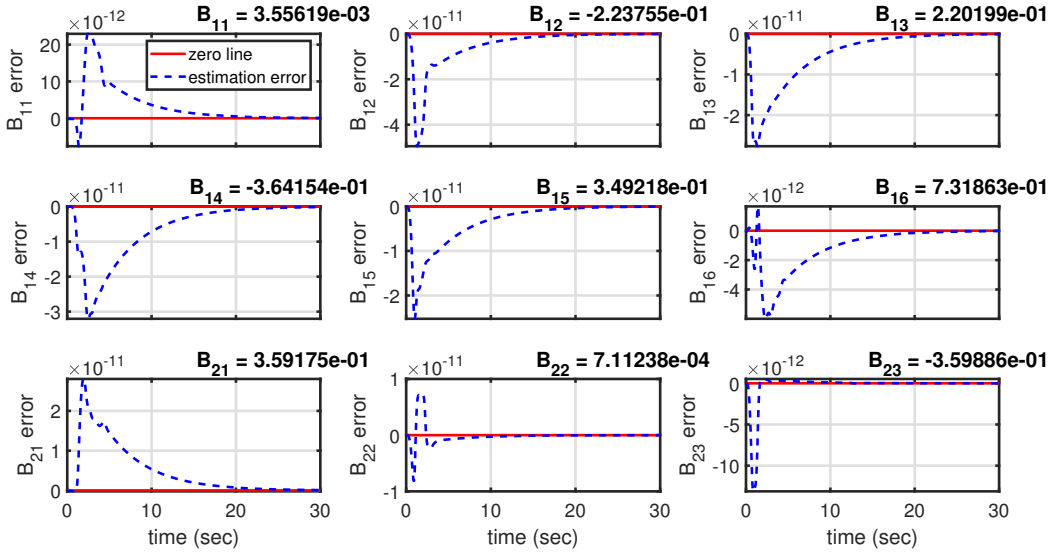

Figure 2.15: Uncertain parameters $B_{11} - B_{23}$ for sequential Euler angle rotation; from Saha and Valasek [60], reprinted by permission of the American Institute of Aeronautics and Astronautics, Inc.

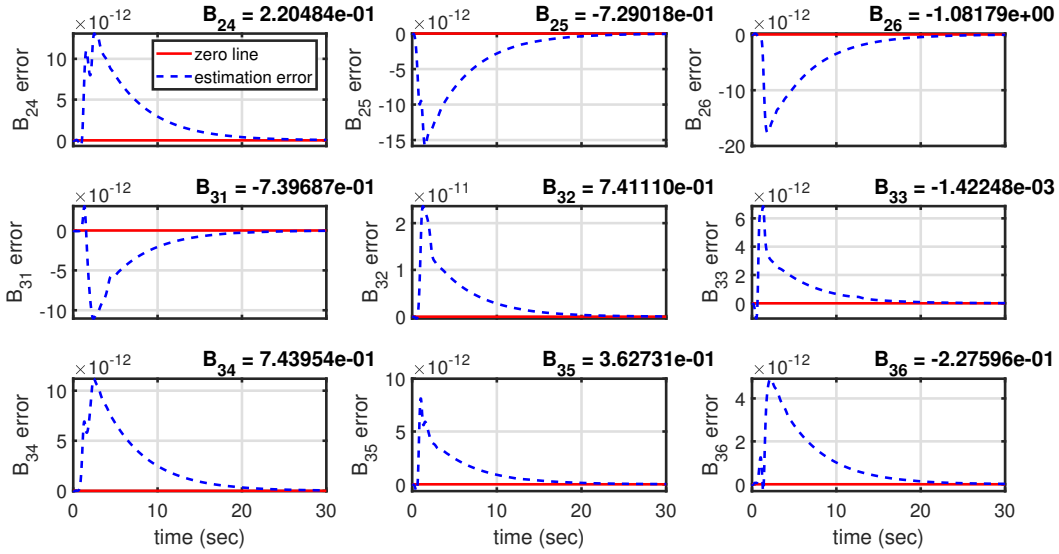

Figure 2.16: Uncertain parameters $B_{24} - B_{36}$ for sequential Euler angle rotation; from Saha and Valasek [60], reprinted by permission of the American Institute of Aeronautics and Astronautics, Inc.

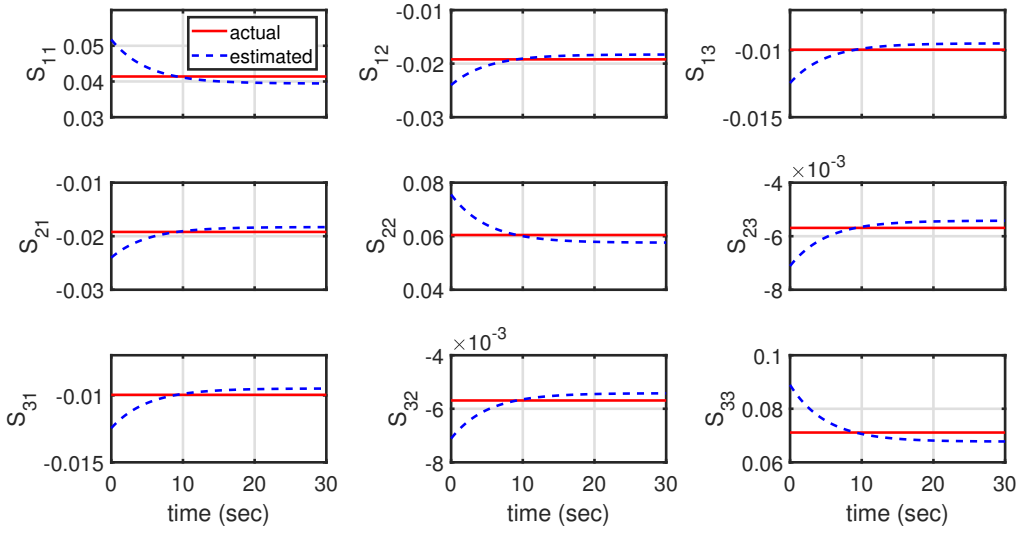

Figure 2.17: Uncertain parameters $\mathcal{S}_{11} - \mathcal{S}_{33}$ for sequential Euler angle rotation; from Saha and Valasek [60], reprinted by permission of the American Institute of Aeronautics and Astronautics, Inc.

Figures 2.11 shows the tracking of the Euler angles. It can be seen that the tracking is good after some initial tumbling motion due to the initial conditions being nonzero. A similar observation can be made from the tracking history of the equivalent MRPs in Figure 2.12. Figure 2.13 shows that the angular velocities reach their manifold within the first five seconds, and stay there for the rest of the simulation. The effect of initial conditions lead to saturation of the controls for the initial five seconds as seen in Figure 2.14. Thereafter the controls remain small in magnitude. Figures 2.15 - 2.17 show the evolution of the estimates of all the uncertain parameters in the B and $\mathcal{S}$ matrices. It can be seen that the parameter estimation errors remain bounded. Similar to the earlier evaluation maneuver, it is observed that the magnitude of estimation error significantly small for the elements of the $\hat{B}$ matrix. This is due to the fact that they are formed as products of the elements of the inertia matrix and its inverse. From figures 2.11 - 2.17 it can be concluded that the desired objective of slow state tracking is accomplished, and the tracking errors, manifold errors and parameter estimation errors remain bounded and small in magnitude.

Some insightful remarks can be made from a careful observation of the theory and the numerical results.

Remark 5. ***Choices of the gains in parameter update laws:*** *Part of the parameter update laws canceling the errors uses gains as small as* 10^{-10}*, whereas the other part corresponding to first-order dynamics uses gains of the order of* 10^{-1}*. Running a case of simulation with the first set of gains assigned a value of zero, there is no significant difference in the tracking and control torques. However, not all parameter errors in the B matrix show a diminishing trend with time; some increase over time although the magnitude remains small. This is expected as some of the errors are not canceled. It is recommended to use small positive gains instead of hard zeros.*

Remark 6. ***Robustness with respect to parametric uncertainties:*** *This simulation has been tried with initial estimates of the inertias anywhere between 50% below and 100% above the actual inertias, and the controller can still ensure good tracking. This shows that the gains are so selected that wide uncertainties in the parameters can be handled.*

Remark 7. ***Avoiding singularity with respect to control:*** *The unknown parameter matrix* $\mathcal{S}$

multiplies the actuator vector δ. It is important that the estimate matrix $\hat{\mathcal{S}}$ never becomes singular. This is ensured by adjusting the final estimates in the parameter update laws. In general, for any parameter multiplying a control or actuator signal, the estimate is prevented from becoming zero by setting a suitable final value in the parameter update law.

2.6 Four-Time-Scale Slow State Tracking with Uncertainties in the Evolution of States as Well as Actuators

This section extends the theory of slow state tracking to four-time-scales with slow and fast actuator dynamics and more generic forms of uncertainties. Section 2.5 developed the theory of slow state tracking for a three-time-scale system in the presence of uncertainties. While actuator dynamics were accounted for, all actuators were assumed to work in the fastest time-scale. This is a good assumption when only the rotational dynamics of a spacecraft are to be controlled. However, for a combined longitudinal and lateral/directional maneuver of an aircraft, it may be necessary to control both of the translational and the rotational dynamics at the same time. For example, for a turning maneuver of an aircraft, the velocity as well as the angles are to be controlled. The primary control for velocity is throttle, whereas the angles can be controlled using the aerodynamic control surfaces: elevator, aileron and rudder. Due to the slow engine dynamics, throttle is a slow actuator, whereas the aerodynamic actuators are fast. This leads to an interesting situation which involves time-scales in actuators, in addition to the time-scales in the system states. As a result, aircraft models can be thought of evolving in a total of four time-scales. Velocity, angle-of-attack, sideslip angle and the three Euler angles - bank angle, pitch attitude angle and heading angle - are the slow states evolving in the slowest time-scale. Throttle is the slow actuator evolving in the second slowest time-scale. Body-axis roll, pitch and yaw rates are the fast states evolving in the second fastest time-scale. Elevator, aileron and rudder are the fast actuators evolving in the fastest time-scale.

In some of the earlier works on multiple-time-scale aircraft flight control, velocity was not tracked; throttle was kept constant and not used as an automatic control [33]. As a consequence, the Mach number dropped from 0.3 to below 0.2 as the aircraft performed a 45 degree turn.

A later work of Saha *et. al.* [35] accounted for slow and fast actuator dynamics and designed a four-time-scale slow state tracking controller to reduce the loss of airspeed during turn. The method used in this work was an extension of the sequential control with slow and fast actuator dynamics developed in Narang-Siddarth and Valasek [11]. Similar to the first limitation pointed out in Subsection 2.2.4, this extension of sequential control also assumed the model to be deterministic. However, in practice, aircraft flight control laws should be able to handle these major sources of uncertainty: inertias, control derivatives and engine time-constant. It is difficult to estimate the inertias accurately using the inexpensive methods such as class-I methods. Typically, the aerodynamics are modeled using stability and control derivatives, and it is more difficult to obtain accurate estimates of the control derivatives. Additionally, for a modern fly-by-wire flight control architecture, the control derivatives play a more significant role than the stability and damping derivatives. Furthermore, the turbomachinery can be modeled as a first-order actuator with an uncertain time-constant. Handling these uncertainties needs the development of a new theory which deals with uncertainties in the dynamics and in the control distribution for both of the states and the actuators. This is the theory developed in this section.

The next few subsections describe the theory and numerical results of four-time-scale slow state tracking in the following order. Subsection 2.6.1 describes the class of systems for which the theory is to be developed. Development of the control law using reduced subsystems is in Subsection 2.6.2. Selection of parameter update laws, proof of boundedness of errors along with the bounds of time-scale separation are in Subsection 2.6.3. Subsection 2.6.4 shows the numerical results for an example four-time-scale system and a nonlinear six-degree-of-freedom generic F-16A.

2.6.1 The Class of Systems

The class of systems considered in this section is motivated by the one used for flight control design in Saha *et. al.* [35]. This class has a total of four time-scales: the slow states evolving in the slowest time-scale, the slow actuators evolving in the second slowest time-scale, the fast states evolving in the second fastest time-scale, and the fast actuators evolving in the fastest time-scale. All the states and actuators have uncertainties in their evolution. This class can potentially represent

a linearly overparameterized model of a nonlinear 6-DOF aircraft with uncertainties in the inertias, control derivatives and engine time-constant. The exact mathematical expressions of the vectors and matrices are provided in Appendix B.

The slow states to track are classified as kinetic and kinematic states. The kinetic slow states can be influenced directly by the both of the slow and the fast actuators. The kinematic slow states can be influenced directly by the fast states, but not by any actuator. The fast states can be influenced directly by the fast actuators, but not by the slow actuators. The slow and fast states, as well the the slow and fast actuators have parametric uncertainties in dynamics and in control distribution. Time-dependent and state-dependent static uncertainties are added in the dynamics of the slow and the fast states. These are the additive uncertainties. However, there is no uncertainty in the evolution of the kinematic slow states. The theory of slow state tracking control is developed on nonlinear state-space model

$$\begin{aligned}
\dot{x} &= B_{xx} f_{xx}(x,\xi) + B_{xz} F_{xz}(x,\xi) z + \gamma_x(t,x,\xi,z) + \Lambda_{x\delta_s} G_{x\delta_s}(x,\xi)\delta_s + \Lambda_{x\delta_f} G_{x\delta_f}(x,\xi)\delta_f \\
\dot{\xi} &= F_{\xi z}(x,\xi) z \\
\sigma\dot{\delta}_s &= B_{\delta_s} f_{\delta_s}(\delta_s) + \Lambda_{\delta_s u_s} G_{\delta_s u_s}(\delta_s) u_s \\
\varepsilon\dot{z} &= \sum_k B_z^k f_z^k(x,\xi,z) + \gamma_z(t,x,\xi,z) + \Lambda_{z\delta_f} G_{z\delta_f}(x,\xi)\delta_f \\
\rho\dot{\delta}_f &= B_{\delta_f} f_{\delta_f}(\delta_f) + \Lambda_{\delta_f u_f} G_{\delta_f u_f}(\delta_f) u_f.
\end{aligned} \tag{2.129}$$

Equation (2.129) represents a four-time-scale nonlinear nonstandard system with uncertainties. Here $x \in \mathbb{R}^n$ is the vector of n kinetic slow states, $\xi \in \mathbb{R}^m$ is the vector of m kinematic slow states, $z \in \mathbb{R}^m$ is the vector of m fast states, $\delta_s \in \mathbb{R}^n$ is the vector of n slow actuators, $\delta_f \in \mathbb{R}^m$ is the vector of m fast actuators. The perturbation parameters σ, ε and ρ satisfy $0 < \rho << \varepsilon << \sigma << 1$. The 'dot' represents time-derivative with respect to the slowest time-scale t. The second slowest time-scale is $t_\sigma = \frac{t}{\sigma}$; the second fastest time-scale is $t_\varepsilon = \frac{t}{\varepsilon}$, and the fastest time-scale is $t_\rho = \frac{t}{\rho}$.

The parametric uncertainties in the dynamics of the kinetic slow states x are captured in the constant but unknown matrices B_{xx} and B_{xz}. The parameter matrix B_{xz} is such that its largest

singular value satisfies $\bar{\sigma}(B_{xz}) \leq v_1$, where v_1 is a known constant. The vector of functions f_{xx} represents the dependence of the slow dynamics on the slow states, and the matrix F_{xz} represents the dependence of the slow dynamics on the fast states. Both f_{xx} and F_{xz} are assumed to consist of known, smooth functions. In addition, the matrix F_{xz} is such that its largest singular value satisfies $\bar{\sigma}(F_{xz}) \leq v_2$, where v_2 is a known constant. For the kinetic slow states, the parametric uncertainties in the control distribution corresponding to the slow and fast actuators are captured in the constant but unknown parameter matrices $\Lambda_{x\delta_s}$ and $\Lambda_{x\delta_f}$ respectively. The dependence of the slow dynamics on the slow and fast actuators are represented by the matrices $G_{x\delta_s}$ and $G_{x\delta_f}$ respectively. Both of these matrices consist of known, smooth functions, and the matrix $G_{x\delta_s}$ is nonsingular. The largest singular values of these matrices satisfy $\bar{\sigma}(\Lambda_{x\delta_s}) \leq v_3, \bar{\sigma}(G_{x\delta_s}) \leq v_4, \bar{\sigma}(\Lambda_{x\delta_f}) \leq v_5, \bar{\sigma}(G_{x\delta_s}) \leq v_6$ for some known constants v_3, v_4, v_5, v_6. The vector of functions $\gamma_x(t, x, \xi, z)$ represent the time-dependent and state-dependent uncertainties in slow dynamics. This is an additive uncertainty. It is known that the Euclidean norm of this vector satisfies

$$\left\|\gamma_x(t, x, \xi, z)\right\|_2 \leq \kappa_1 \|x\|_2 + \kappa_2 \|\xi\|_2 + \kappa_3 \|z\|_2$$

for some known constants $\kappa_1, \kappa_2, \kappa_3 \geq 0$. In addition to kinetic slow states x, the kinematic slow states ξ evolve in the slowest time-scale t. Their evolution depends solely on the fast state vector z through the influence matrix $F_{\xi z}$. This matrix is assumed nonsingular. It consists of known, smooth functions, and its largest singular value satisfies $\bar{\sigma}(F_{\xi z}) \leq v_7$ for some known constant v_7.

The fast dynamics have a combination of k constant but unknown parameter matrices B_z^k multiplied by known vectors of functions $f_z^k(.)$. The functions $f_z^k(.)$ represent the dependence of the fast dynamics on the slow and fast states. This vector is assumed to consist of known, smooth functions. The parametric uncertainties in the control distribution are captured in the constant but unknown matrix $\Lambda_{z\delta_f}$. The dependence of the fast dynamics on the fast actuators is represented by the matrix $G_{z\delta_f}$, which is assumed to be nonsingular and consisting of known, smooth functions. The largest singular values of these matrices satisfy $\bar{\sigma}(\Lambda_{z\delta_f}) \leq v_8, \bar{\sigma}(G_{z\delta_f}) \leq v_9$ for some known

constants v_8 and v_9. The vector of functions $\gamma_z(t, x, \xi, z)$ captures the time-dependent and state-dependent uncertainties in the fast dynamics. The Euclidean norm of this additive uncertainty satisfies

$$\left\|\gamma_z(t, x, \xi, z)\right\|_2 \leq \kappa_4\|x\|_2 + \kappa_5\|\xi\|_2 + \kappa_6\|z\|_2$$

for some known constants $\kappa_4, \kappa_5, \kappa_6 \geq 0$. The matrices $B_{\delta_s}, \Lambda_{\delta_s u_s}, B_{\delta_f}, \Lambda_{\delta_f u_f}$ represent constant but unknown parameters in the evolution of slow and fast actuators.

Each of the constant but unknown parameters in the parameter matrices are assumed to be within lower and upper bounds; i.e. $p_{ij} \in [\underline{p}_{ij}, \bar{p}_{ij}]$, where p_{ij} is any of the constant but unknown parameters. The vector of functions $f_{\delta_s}, f_{\delta_f}$ represent how the actuator rates depend on the current actuator deflections. The matrices $G_{\delta_s u_s}, G_{\delta_f u_f}$ represent how the actuator rates depend on the control commands u_s and u_f respectively. The matrices $G_{\delta_s u_s}$ and $G_{\delta_f u_f}$ are assumed nonsingular.

The control objective is to design the slow control vector u_s and the fast control vector u_f such that the kinetic slow state vector $x(t)$ tracks a twice differentiable reference trajectory $x_r(t)$, and the kinematic slow state vector $\xi(t)$ tracks a twice differentiable reference trajectory $\xi_r(t)$. In order to achieve this objective using the geometric singular perturbation approach, the fast states z need to be stabilized on a suitable manifold z^0, the slow actuators δ_s need to be stabilized on a suitable manifold δ_s^0, and the fast actuators need to be stabilized on a suitable manifold δ_f^0. Define error variables $e_x := x - x_r, e_\xi := \xi - \xi_r, e_z := z - z^0, e_{\delta_s} := \delta_s - \delta_s^0, e_{\delta_f} := \delta_f - \delta_f^0$. The tracking problem becomes an equivalent stabilization problem in the error coordinates. The full-order system (2.129) in the error co-ordinates become

$$\begin{aligned}
\dot{e}_x &= B_{xx}f_{xx} + B_{xz}F_{xz}(e_z + z^0) + \gamma_x + \Lambda_{x\delta_s}G_{x\delta_s}(e_{\delta_s} + \delta_s^0) + \Lambda_{x\delta_f}G_{x\delta_f}(e_{\delta_f} + \delta_f^0) - \dot{x}_r \\
\dot{e}_\xi &= F_{\xi z}(e_z + z^0) - \dot{\xi}_r \\
\sigma\dot{e}_{\delta_s} &= B_{\delta_s}f_{\delta_s} + \Lambda_{\delta_s u_s}G_{\delta_s u_s}u_s - \sigma\dot{\delta}_s^0 \\
\varepsilon\dot{e}_z &= \sum_k B_z^k f_z^k + \gamma_z + \Lambda_{z\delta_f}G_{z\delta_f}(e_{\delta_f} + \delta_f^0) - \varepsilon\dot{z}^0 \\
\rho\dot{e}_{\delta_f} &= B_{\delta_f}f_{\delta_f} + \Lambda_{\delta_f u_f}G_{\delta_f u_f}u_f - \rho\dot{\delta}_f^0.
\end{aligned} \tag{2.130}$$

The following subsections develop a four-time-scale control law based on lower-order reduced subsystems obtained from (2.130) and prove the boundedness of errors.

2.6.2 Development of Nominal Control Law Using Reduced Subsystems

This is done in four steps. A schematic of the steps is shown in Figure 2.18. The numbers 1, 2, 3, 4 on the schematic indicates the sequence in which the specific design variables are selected. The design steps are detailed below.

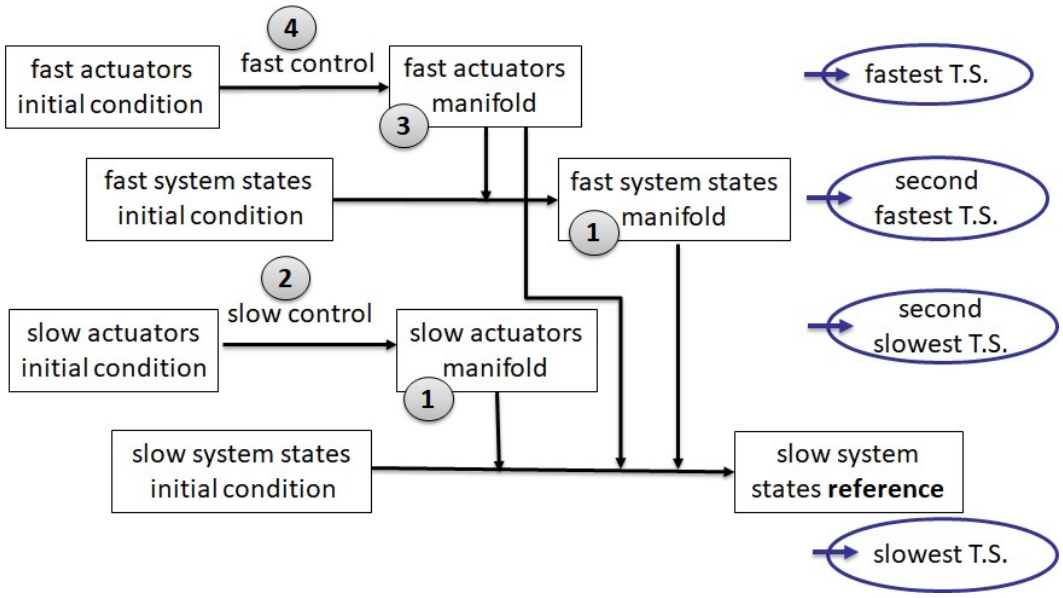

Figure 2.18: Steps of four-time-scale slow state tracking control design

2.6.2.1 Design of Manifold of Fast States and Slow Actuators in the Slowest Time-Scale

In the slowest time-scale t, it is assumed that the fast states are on their manifold z^0, the slow actuator is on its manifold δ_s^0, and the fast actuators are on a special case of their manifold $\delta_f^0|_{z^0}$. Mathematically this is obtained by artificially substituting $\sigma = \varepsilon = \rho = 0$, as a result of which the last three differential equations in (2.130), viz. the $\dot{e}_{\delta_s}$, $\dot{e}_z$, $\dot{e}_{\delta_f}$ equations reduce to algebraic

equations. This indicates that the fast states, the slow actuators and the fast actuators have already reached their manifolds and are no longer evolving independently. Only the slow state errors e_x and e_ξ evolve independently in this time-scale. The manifolds z^0 and δ_s^0 are selected such that the slow states reach their reference; that is, the slow state error vectors e_x and e_ξ go to zero. Moreover, to construct the reduced subsystem, the constant but unknown parameter matrices B_{xx}, B_{xz}, $\Lambda_{x\delta_s}$, $\Lambda_{x\delta_f}$ are replaced by their best estimates $\hat{B}_{xx}$, $\hat{B}_{xz}$, $\hat{\Lambda}_{x\delta_s}$, $\hat{\Lambda}_{x\delta_f}$ respectively, and the additive uncertainty γ_x is ignored. The reduced subsystem in the slowest time-scale is

$$\begin{aligned} \dot{e}_x &= \hat{B}_{xx} f_{xx} + \hat{B}_{xz} F_{xz} z^0 - \dot{x}_r + \hat{\Lambda}_{x\delta_s} G_{x\delta_s} \delta_s^0 + \hat{\Lambda}_{x\delta_f} G_{x\delta_f} \delta_f^0|_{z^0} \\ \dot{e}_\xi &= F_{\xi z} z^0 - \dot{\xi}_r. \end{aligned} \tag{2.131}$$

A positive-definite candidate Lyapunov function for subsystem (2.131) can be selected as

$$V_1 = \frac{1}{2} e_x^T e_x + \frac{1}{2} e_\xi^T e_\xi. \tag{2.132}$$

Its time-derivative with respect to the slowest time-scale t is

$$\dot{V}_1 = e_x^T \dot{e}_x + e_\xi^T \dot{e}_\xi. \tag{2.133}$$

Along the trajectories of subsystem (2.131), the time-derivative of the Lyapunov function V_1 is

$$\begin{aligned} \dot{V}_1|_{(2.131)} = {} & e_x^T (\hat{B}_{xx} f_{xx} + \hat{B}_{xz} F_{xz} z^0 + \hat{\Lambda}_{x\delta_s} G_{x\delta_s} \delta_s^0 + \hat{\Lambda}_{x\delta_f} G_{x\delta_f} \delta_f^0|_{z^0} - \dot{x}_r) \\ & + e_\xi^T (F_{\xi z} z^0 - \dot{\xi}_r). \end{aligned} \tag{2.134}$$

Suppose that the manifold of the fast states z^0 is selected as

$$z^0 = F_{\xi z}^{-1} (\dot{\xi}_r - K_\xi e_\xi). \tag{2.135}$$

and that the manifold of the slow actuators δ_s^0 is selected as

$$\delta_s^0 = G_{x\delta_s}^{-1}\hat{\Lambda}_{x_{\delta_s}}^{-1}(\dot{x}_r - \hat{B}_{xx}f_{xx} - \hat{B}_{xz}F_{xz}z^0 - \hat{\Lambda}_{x\delta_f}G_{x\delta_f}\delta_f^0|_{z^0} - K_x e_x) \tag{2.136}$$

where $\hat{\Lambda}_{x_{\delta_s}}$ is assumed nonsingular, and $\delta_f^0|_{z^0}$ is yet to be determined. For these choices, the time-derivative of the Lyapunov function V_1 for the reduced subsystem (2.131) becomes

$$\dot{V}_1|_{(2.131)} = -e_x^T K_x e_x - e_\xi^T K_\xi e_\xi. \tag{2.137}$$

This is negative-definite for any positive-definite K_x and K_ξ, indicating that the equilibrium $e_x = 0, e_\xi = 0$ of the reduced subsystem (2.131) is Lyapunov-stable. The use of kinetic and kinematic slow states in the control design enable sequential selections of the manifolds z^0 and δ_s^0.

2.6.2.2 Design of Slow Control in the Second Slowest Time-Scale

In the second slowest time-scale $t_\sigma = \frac{t}{\sigma}$, the slow controls u_s are designed such that the slow actuators δ_s reaches their manifold δ_s^0, and consequently slow actuator errors e_{δ_s} go to zero. Considering time-derivatives in the second slowest time-scale, and artifically substituting $\sigma = \varepsilon = \rho = 0$, the slow dynamics reduce to $\grave{e}_x = 0, \grave{e}_\xi = 0$, where where $\grave{e}$ is the derivative of e with respect to the second slowest time-scale $t_\sigma = \frac{t}{\sigma}$. This indicates that the slow state errors are 'frozen' at their initial conditions. Furthermore, the $\dot{e}_z$ and $\dot{e}_{\delta_f}$ differential equations in (2.130) reduce to algebraic equations, indicating that the fast actuators and fast states have settled on their manifolds, and are no longer evolving independently. Only the slow actuator errors are evolving independently in this time-scale. Replacing the unknown parameter matrices with their estimates, the reduced subsystem in the second slowest time-scale is

$$\grave{e}_{\delta_s} = \hat{B}_{\delta_s}f_{\delta_s} + \hat{\Lambda}_{\delta_s u_s}G_{\delta_s u_s}u_s. \tag{2.138}$$

A positive-definite candidate Lyapunov function for this subsystem can be selected as

$$V_2 = \frac{1}{2} e_{\delta_s}^T e_{\delta_s}. \tag{2.139}$$

Its time-derivative with respect to the second slowest time-scale is

$$\grave{V}_2 = e_{\delta_s}^T \grave{e}_{\delta_s}. \tag{2.140}$$

Along the trajectories of the reduced subsystem (2.138), the time-derivative is

$$\grave{V}_2|_{(2.138)} = e_{\delta_s}^T (\hat{B}_{\delta_s} f_{\delta_s} + \hat{\Lambda}_{\delta_s u_s} G_{\delta_s u_s} u_s). \tag{2.141}$$

If the vector of slow controls u_s is selected as

$$u_s = G_{\delta_s u_s}^{-1} \hat{\Lambda}_{\delta_s u_s}^{-1} (-\hat{B}_{\delta_s} f_{\delta_s} - K_{\delta_s} e_{\delta_s}) \tag{2.142}$$

then the derivative of the Lyapunov function V_2 with respect to the second slowest time-scale becomes

$$\grave{V}_2|_{(2.138)} = -e_{\delta_s}^T K_{\delta_s} e_{\delta_s} \tag{2.143}$$

which is negative-definite for any positive-definite K_{δ_s}. Thus the equilibrium $e_{\delta_s} = 0$ of the reduced subsystem (2.138) is Lyapunov-stable.

2.6.2.3 Design of Manifold of Fast Actuators in the Second Fastest Time-Scale

In the second fastest time-scale $t_\varepsilon = \frac{t}{\varepsilon}$, the manifold of the fast actuators δ_f^0 is selected such that the fast states z reach their manifold z^0, or equivalently the fast state error vector e_z become zero. Considering derivatives in the second slowest time-scale and artificially substituting $\sigma = \varepsilon = \rho = 0$, the slow state and slow actuator error dynamics become $e_x' = 0, e_\xi' = 0, e_{\delta_s}' = 0$, where 'prime' denotes differentiation with respect to the second fastest time-scale. This indicates that the

slow state and slow actuator errors are 'frozen' at their initial conditions in this time-scale. The $\dot{e}_{\delta_f}$ differential equation in (2.130) becomes a system of algebraic equations, indicating that the fast actuators have already reached their manifold, and are no longer evolving independently. Only the fast state error vector e_z evolves independently in this time-scale. Furthermore, to construct the reduced subsystem, the constant but unknown parameter matrices B_z^k and $\Lambda_{z\delta_f}$ are replaced by their estimates $\hat{B}_z^k$ and $\hat{\Lambda}_{z\delta_f}$ respectively. The additive uncertainty γ_z is ignored. The reduced subsystem in the second fastest time-scale is

$$e_z' = \sum_k \hat{B}_z^k f_z^k + \hat{\Lambda}_{z\delta_f} G_{z\delta_f} \delta_f^0 \tag{2.144}$$

A positive-definite candidate Lyapunov function for this subsystem is

$$V_3 = \frac{1}{2} e_z^T e_z. \tag{2.145}$$

Its time-derivative with respect to the time-scale t_z is

$$V_3' = e_z^T e_z'. \tag{2.146}$$

Along the trajectories of subsystem (2.144), the time-derivative is

$$V_3'|_{(2.144)} = e_z^T (\sum_k \hat{B}_z^k f_z^k + \hat{\Lambda}_{z\delta_f} G_{z\delta_f} \delta_f^0) \tag{2.147}$$

If the manifold of the fast actuators is selected as

$$\delta_f^0 = G_{z\delta_f}^{-1} \hat{\Lambda}_{z\delta_f}^{-1} (-\sum_k \hat{B}_z^k f_z^k - K_z e_z) \tag{2.148}$$

where $\hat{\Lambda}_{z_{\delta_f}}$ is assumed nonsingular, then the time-derivative of the Lyapunov function V_3 becomes

$$V_3'|_{(2.144)} = -e_z^T K_z e_z \tag{2.149}$$

which is negative-definite for any positive-definite K_z. This ensures that the equilibrium $e_z = 0$ of the reduced subsystem (2.144) is Lyapunov-stable.

By design of the fast actuator manifold δ_f^0, the special case $\delta_f^0|_{z^0}$ needed in the slowest time-scale can now be determined as

$$\delta_f^0|_{z^0} = -G_{z\delta_f}^{-1}\hat{\Lambda}_{z\delta_f}^{-1}\sum_k \hat{B}_z^k f_z^k(x,\xi,z^0). \tag{2.150}$$

This is to be used to design the manifold for the slow actuators δ_s^0 given by (4.84) in the slowest time-scale.

2.6.2.4 Design of Fast Control in the Fastest Time-Scale

In the fastest time-scale $t_\rho = \frac{t}{\rho}$, the fast controls u_f are selected such that the fast actuators δ_f reach their manifold δ_f^0, or equivalently fast actuator errors $e_{\delta_f} = \delta_f - \delta_f^0$ reach zero. Considering time-derivatives in the fastest time-scale and artificially substituting $\sigma = \varepsilon = \rho = 0$ in the full-order dynamics (2.130) lead to $\breve{e}_x = 0, \breve{\xi} = 0, \breve{\delta}_s = 0, \breve{z} = 0$, where $\breve{e}$ stands for derivative of e with respect to the fastest time-scale $t_\rho = \frac{t}{\rho}$. This means that the slow states, slow actuators and fast state errors are 'frozen' at their initial conditions in the fastest time-scale. Only the fast actuator errors are evolving according to

$$\breve{e}_{\delta_f} = \hat{B}_{\delta_f} f_{\delta_f} + \hat{\Lambda}_{\delta_f u_f} G_{\delta_f u_f} u_f. \tag{2.151}$$

A positive-definite candidate Lyapunov function for the subsystem (2.151) can be selected as

$$V_4 = \frac{1}{2} e_{\delta_f}^T e_{\delta_f}. \tag{2.152}$$

Its time-derivative with respect to the fast actuator time-scale is

$$\breve{V}_4 = e_{\delta_f}^T \breve{e}_{\delta_f}. \tag{2.153}$$

Along the trajectories of the reduced subsystem (2.151), the time-derivative becomes

$$\breve{V}_4|_{(2.151)} = e_{\delta_f}^T(\hat{B}_{\delta_f} f_{\delta_f} + \hat{\Lambda}_{\delta_f u_f} G_{\delta_f u_f} u_f). \tag{2.154}$$

If the fast actuator command vector u_f is selected as

$$u_f = G_{\delta_f u_f}^{-1} \hat{\Lambda}_{\delta_f u_f}^{-1}(-\hat{B}_{\delta_f} f_{\delta_f} - K_{\delta_f} e_{\delta_f}) \tag{2.155}$$

then the derivative of the Lyapunov function V_4 becomes

$$\breve{V}_4|_{(2.151)} = -e_{\delta_f}^T K_{\delta_f} e_{\delta_f} \tag{2.156}$$

which is negative-definite for any positive-definite K_{δ_f}. Thus the equilibrium $e_{\delta_f} = 0$ of the reduced subsystem (2.151) is Lyapunov-stable.

2.6.3 Stability Analysis of the Full-Order System: Selection of Parameter Update Laws and Bounds of Time-Scale Separation

Define parameter estimation error matrices $\tilde{B}_{xx} \coloneqq B_{xx} - \hat{B}_{xx}$, $\tilde{B}_{xz} \coloneqq B_{xz} - \hat{B}_{xz}$, $\tilde{\Lambda}_{x\delta_s} \coloneqq \Lambda_{x\delta_s} - \hat{\Lambda}_{x\delta_s}$, $\tilde{\Lambda}_{x\delta_f} \coloneqq \Lambda_{x\delta_f} - \hat{\Lambda}_{x\delta_f}$, $\tilde{B}_{\delta_s} \coloneqq B_{\delta_s} - \hat{B}_{\delta_s}$, $\tilde{\Lambda}_{\delta_s u_s} \coloneqq \Lambda_{\delta_s u_s} \hat{\Lambda}_{\delta_s u_s}$, $\tilde{B}_z^k \coloneqq B_z^k - \hat{B}_z^k$, $\tilde{\Lambda}_{z\delta_f} \coloneqq \Lambda_{z\delta_f} - \hat{\Lambda}_{z\delta_f}$, $\tilde{B}_{\delta_f} \coloneqq B_{\delta_f} - \hat{B}_{\delta_f}$, $\tilde{\Lambda}_{\delta_f u_f} \coloneqq \Lambda_{\delta_f u_f} - \hat{\Lambda}_{\delta_f u_f}$. A composite Lyapunov function for the full-order system (2.130) can be selected as

$$\begin{aligned} V_c = {} & \alpha_1 V_1 + \alpha_2 V_2 + \alpha_3 V_3 + \alpha_4 V_4 + \frac{1}{2}\alpha_5 tr[\tilde{B}_{xx}^T \tilde{B}_{xx}] + \frac{1}{2}\alpha_6 tr[\tilde{B}_{xz}^T \tilde{B}_{xz}] + \frac{1}{2}\alpha_7 tr[\tilde{\Lambda}_{x\delta_s}^T \tilde{\Lambda}_{x\delta_s}] \\ & + \frac{1}{2}\alpha_8 tr[\tilde{\Lambda}_{x\delta_f}^T \tilde{\Lambda}_{x\delta_f}] + \frac{1}{2}\alpha_9 tr[\tilde{B}_{\delta_s}^T \tilde{B}_{\delta_s}] + \frac{1}{2}\alpha_{10} tr[\tilde{\Lambda}_{\delta_s u_s}^T \tilde{\Lambda}_{\delta_s u_s}] + \frac{1}{2}\sum_k \alpha_{11k} tr[\tilde{B}_z^{k^T} \tilde{B}_z^k] \\ & + \frac{1}{2}\alpha_{12} tr[\tilde{\Lambda}_{z\delta_f}^T \tilde{\Lambda}_{z\delta_f}] + \frac{1}{2}\alpha_{13} tr[\tilde{B}_{\delta_f}^T \tilde{B}_{\delta_f}] + \frac{1}{2}\alpha_{14} tr[\tilde{\Lambda}_{\delta_f u_f}^T \tilde{\Lambda}_{\delta_f u_f}] \end{aligned} \tag{2.157}$$

where $\alpha_i > 0; i = 1, ..., 14$ represent the weights of the individual Lyapunov functions in the composite. Similar to the case of three-time-scale control, the composite Lyapunov function (2.157) contains a weighted sum of squares of all the parameter estimation errors. To show the

estimation errors explicitly, equation (2.157) can be written as

$$V_c = \alpha_1 V_1 + \alpha_2 V_2 + \alpha_3 V_3 + \alpha_4 V_4 + \frac{1}{2}\alpha_5 \sum_i \sum_j \tilde{b}^2_{xx_{ij}} + \frac{1}{2}\alpha_6 \sum_i \sum_j \tilde{b}^2_{xz_{ij}} + \frac{1}{2}\alpha_7 \sum_i \sum_j \tilde{\lambda}^2_{x\delta_{s_{ij}}}$$
$$+ \frac{1}{2}\alpha_8 \sum_i \sum_j \tilde{\lambda}^2_{x\delta_{f_{ij}}} + \frac{1}{2}\alpha_9 \sum_i \sum_j \tilde{b}^2_{\delta_{s_{ij}}} + \frac{1}{2}\alpha_{10} \sum_i \sum_j \tilde{\lambda}^2_{\delta_s u_{s_{ij}}} + \frac{1}{2}\sum_k \alpha_{11k} \sum_i \sum_j \tilde{b}^{k^2}_{z_{ij}}$$
$$+ \frac{1}{2}\alpha_{12} \sum_i \sum_j \tilde{\lambda}^2_{z\delta_{f_{ij}}} + \frac{1}{2}\alpha_{13} \sum_i \sum_j \tilde{b}^2_{\delta_{f_{ij}}} + \frac{1}{2}\alpha_{14} \sum_i \sum_j \tilde{\lambda}^2_{\delta_f u_{f_{ij}}}. \tag{2.158}$$

Along the trajectories of the full-order system (2.130), the time-derivative of the composite Lyapunov function (2.158) is

$$\dot{V}_c = \alpha_1 \dot{V}_1|_{(2.130)} + \frac{\alpha_2}{\sigma}\dot{V}_2|_{(2.130)} + \frac{\alpha_3}{\varepsilon}V_3'|_{(2.130)} + \frac{\alpha_4}{\rho}\breve{V}_4|_{(2.130)} + \sum_i \sum_j \alpha_5 \tilde{b}_{xx_{ij}} \dot{\tilde{b}}_{xx_{ij}}$$
$$+ \alpha_6 \sum_i \sum_j \tilde{b}_{xz_{ij}} \dot{\tilde{b}}_{xz_{ij}} + \alpha_7 \sum_i \sum_j \tilde{\lambda}_{x\delta_{s_{ij}}} \dot{\tilde{\lambda}}_{x\delta_{s_{ij}}} + \alpha_8 \sum_i \sum_j \tilde{\lambda}_{x\delta_{f_{ij}}} \dot{\tilde{\lambda}}_{x\delta_{f_{ij}}} + \frac{\alpha_9}{\sigma} \sum_i \sum_j \tilde{b}_{\delta_{s_{ij}}} \dot{\tilde{b}}_{\delta_{s_{ij}}}$$
$$+ \frac{\alpha_{10}}{\sigma} \sum_i \sum_j \tilde{\lambda}_{\delta_s u_{s_{ij}}} \dot{\tilde{\lambda}}_{\delta_s u_{s_{ij}}} + \frac{1}{\varepsilon} \sum_k \sum_i \sum_j \alpha_{11k} \tilde{b}^k_{z_{ij}} \tilde{b}^{k'}_{z_{ij}} + \frac{\alpha_{12}}{\varepsilon} \sum_i \sum_j \tilde{\lambda}_{z\delta_{f_{ij}}} \tilde{\lambda}'_{z\delta_{f_{ij}}})$$
$$+ \frac{\alpha_{13}}{\rho} \sum_i \sum_j \tilde{b}_{\delta_{f_{ij}}} \breve{\tilde{b}}_{\delta_{f_{ij}}} + \frac{\alpha_{14}}{\rho} \sum_i \sum_j \tilde{\lambda}_{\delta_f u_{f_{ij}}} \breve{\tilde{\lambda}}_{\delta_f u_{f_{ij}}}. \tag{2.159}$$

It can be seen in (2.159) that the time-derivatives of the parameter estimation errors are taken in the time-scale the parameters appear in the full-order dynamics (2.130). For example, the ones appearing in the evolution of the slow state are differentiated with respect to the slowest time-scale t; the ones appearing in the evolution of the slow actuator are differentiated with respect to the second slowest time-scale $t_\sigma = \frac{t}{\sigma}$, and so on. Adding and subtracting appropriate reduced subsystems for the derivatives of the Lyapunov functions used for controller design, and substituting the time-derivatives of the parameter estimation errors in terms of those of the

estimates, (2.159) reduces to

$$\begin{aligned}\dot{V}_c = {} & \alpha_1 \dot{V}_1|_{(2.131)} + \frac{\alpha_2}{\sigma}\grave{V}_2|_{(2.138)} + \frac{\alpha_3}{\varepsilon}V_3'|_{(2.144)} + \frac{\alpha_4}{\rho}\breve{V}_4|_{(2.151)} + \alpha_1(\dot{V}_1|_{(2.130)} - \dot{V}_1|_{(2.131)}) \\ & + \frac{\alpha_2}{\sigma}(\grave{V}_2|_{(2.130)} - \grave{V}_2|_{(2.138)}) + \frac{\alpha_3}{\varepsilon}(V_3'|_{(2.130)} - V_3'|_{(2.144)}) + \frac{\alpha_4}{\rho}(\breve{V}_4|_{(2.130)} - \breve{V}_4|_{(2.151)}) \\ & - \alpha_5 \sum_i \sum_j \tilde{b}_{xx_{ij}} \dot{\hat{b}}_{xx_{ij}} - \alpha_6 \sum_i \sum_j \tilde{b}_{xz_{ij}} \dot{\hat{b}}_{xz_{ij}} - \alpha_7 \sum_i \sum_j \tilde{\lambda}_{x\delta_{s_{ij}}} \dot{\hat{\lambda}}_{x\delta_{s_{ij}}} \\ & - \alpha_8 \sum_i \sum_j \tilde{\lambda}_{x\delta_{f_{ij}}} \dot{\hat{\lambda}}_{x\delta_{f_{ij}}} - \frac{\alpha_9}{\sigma} \sum_i \sum_j \tilde{b}_{\delta_{s_{ij}}} \grave{\hat{b}}_{\delta_{s_{ij}}} - \frac{\alpha_{10}}{\sigma} \sum_i \sum_j \tilde{\lambda}_{\delta_s u_{s_{ij}}} \grave{\hat{\lambda}}_{\delta_s u_{s_{ij}}} \\ & - \frac{1}{\varepsilon} \sum_k \alpha_{11k} \sum_i \sum_j \tilde{b}^k_{z_{ij}} \hat{b}^{k'}_{z_{ij}} - \frac{\alpha_{12}}{\varepsilon} \sum_i \sum_j \tilde{\lambda}_{z\delta_{f_{ij}}} \hat{\lambda}'_{z\delta_{f_{ij}}} - \frac{\alpha_{13}}{\rho} \sum_i \sum_j \tilde{b}_{\delta_{f_{ij}}} \breve{\hat{b}}_{\delta_{f_{ij}}} \\ & - \frac{\alpha_{14}}{\rho} \sum_i \sum_j \tilde{\lambda}_{\delta_f u_{f_{ij}}} \breve{\hat{\lambda}}_{\delta_f u_{f_{ij}}}.\end{aligned} \tag{2.160}$$

The expressions of $\dot{V}_1|_{(2.131)}, \grave{V}_2|_{(2.138)}, V_3'|_{(2.144)}, \breve{V}_4|_{(2.151)}$ are substituted using equations (2.137), (4.91), (2.149) and (2.156) respectively. The differences between full-order and reduced-order dynamics are

$$\begin{aligned}\dot{V}_1|_{(2.130)} - \dot{V}_1|_{(2.131)} &= e_x^T(\dot{e}_x|_{(2.130)} - \dot{e}_x|_{(2.131)}) + e_\xi^T(\dot{e}_\xi|_{(2.130)} - \dot{e}_\xi|_{(2.131)}) \\ \grave{V}_2|_{(2.130)} - \grave{V}_2|_{(2.138)} &= e_{\delta_s}^T(\grave{e}_{\delta_s}|_{(2.130)} - \grave{e}_{\delta_s}|_{(2.138)}) \\ V_3'|_{(2.130)} - V_3'|_{(2.144)} &= e_z^T(e_z'|_{(2.130)} - e_z'|_{(2.144)}) \\ \breve{V}_4|_{(2.130)} - \breve{V}_4|_{(2.151)} &= e_{\delta_f}^T(\breve{e}_{\delta_f}|_{(2.130)} - \breve{e}_{\delta_f}|_{(2.151)}).\end{aligned} \tag{2.161}$$

Substituting for all the dynamics terms from appropriate full and reduced systems and simplifying,

equation (2.160) becomes

$$\begin{aligned}
\dot{V}_c = &-\alpha_1(e_x^T K_x e_x + e_\xi^T K_\xi e_\xi) - \frac{\alpha_2}{\sigma} e_{\delta_s}^T K_{\delta_s} e_{\delta_s} - \frac{\alpha_3}{\varepsilon} e_z^T K_z e_z - \frac{\alpha_4}{\rho} e_{\delta_f}^T K_{\delta_f} e_{\delta_f} \\
&+ \alpha_1 e_x^T [B_{xz} F_{xz} e_z + \gamma_x + \Lambda_{x\delta_s} G_{x\delta_s} e_{\delta_s} + \Lambda_{x\delta_f} G_{x\delta_f} (e_{\delta_f} + \delta_f^0 - \delta_f^0|_{z^0})] + \alpha_1 e_\xi^T F_{\xi z} e_z \\
&+ \frac{\alpha_3}{\varepsilon} e_z^T (\gamma_z + \Lambda_{z\delta_f} G_{z\delta_f} e_{\delta_f}) - \alpha_2 e_{\delta_s}^T \dot{\delta}_s^0 - \alpha_3 e_z^T \dot{z}^0 - \alpha_4 e_{\delta_f}^T \dot{\delta}_f^0 \\
&+ \sum_i \sum_j \tilde{b}_{xx_{ij}} (\alpha_1 e_{x_i} f_{xx_j} - \alpha_5 \dot{\hat{b}}_{xx_{ij}}) + \sum_i \sum_j \tilde{b}_{xz_{ij}} (\alpha_1 (e_{x_i} (F_{xz} z^0)_j - \alpha_6 \dot{\hat{b}}_{xz_{ij}}) \\
&+ \sum_i \sum_j \tilde{\lambda}_{x\delta_{s_{ij}}} (\alpha_1 (e_{x_i} (G_{x\delta_s} \delta_s^0)_j - \alpha_7 \dot{\hat{\lambda}}_{x\delta_{s_{ij}}}) + \sum_i \sum_j \tilde{\lambda}_{x\delta_{f_{ij}}} (\alpha_1 (e_{x_i} (G_{x\delta_f} \delta_f^0|_{z^0})_j - \alpha_8 \dot{\hat{\lambda}}_{x\delta_{f_{ij}}}) \\
&+ \frac{1}{\sigma} \sum_i \sum_j \tilde{b}_{\delta_{s_{ij}}} (\alpha_2 e_{\delta_{s_i}} f_{\delta_{s_j}} - \alpha_9 \dot{\hat{b}}_{\delta_{s_{ij}}}) + \frac{1}{\sigma} \sum_i \sum_j \tilde{\lambda}_{\delta_s u_{s_{ij}}} (\alpha_2 e_{\delta_{s_i}} (G_{\delta_s u_s} u_s)_j - \alpha_{10} \dot{\hat{\lambda}}_{\delta_s u_{s_{ij}}}) \\
&+ \frac{1}{\varepsilon} \sum_k \sum_i \sum_j \tilde{b}_{z_{ij}}^k (\alpha_3 e_{z_i} f_{z_j}^k - \alpha_{11k} \hat{b}_{z_{ij}}^{k\prime}) + \frac{1}{\varepsilon} \sum_i \sum_j \tilde{\lambda}_{z\delta_{f_{ij}}} (\alpha_3 e_{z_i} (G_{z_{\delta_f}} \delta_f^0)_j - \alpha_{12} \hat{\lambda}'_{z\delta_{f_{ij}}}) \\
&+ \frac{1}{\rho} \sum_i \sum_j \tilde{b}_{\delta_{f_{ij}}} (\alpha_4 e_{\delta_{f_i}} f_{\delta_{f_j}} - \alpha_{13} \ddot{\hat{b}}_{\delta_{f_{ij}}}) + \frac{1}{\rho} \sum_i \sum_j \tilde{\lambda}_{\delta_f u_{f_{ij}}} (\alpha_4 e_{\delta_{f_i}} (G_{\delta_f u_f} u_f)_j - \alpha_{14} \ddot{\hat{\lambda}}_{\delta_f u_{f_{ij}}}).
\end{aligned} \tag{2.162}$$

In order to retain parameter estimation error terms instead of canceling them altogether, the parameter update laws are selected in a way similar to Subsection 2.5.3. The update laws are

$$\begin{aligned}
\dot{\hat{b}}_{xx_{ij}} &= \frac{\alpha_1}{\alpha_5} e_{x_i} f_{xx_j} - \frac{\theta_1}{\alpha_5} (\hat{b}_{xx_{ij}} - b_{xx_{ij}}^0) \\
\dot{\hat{b}}_{xz_{ij}} &= \frac{\alpha_1}{\alpha_6} e_{x_i} (F_{xz} z^0)_j - \frac{\theta_2}{\alpha_6} (\hat{b}_{xz_{ij}} - b_{xz_{ij}}^0) \\
\dot{\hat{\lambda}}_{x\delta_{s_{ij}}} &= \frac{\alpha_1}{\alpha_7} e_{x_i} (G_{x\delta_s} \delta_s^0)_j - \frac{\theta_3}{\alpha_7} (\hat{\lambda}_{x\delta_{s_{ij}}} - \lambda_{x\delta_{s_{ij}}}^0) \\
\dot{\hat{\lambda}}_{x\delta_{f_{ij}}} &= \frac{\alpha_1}{\alpha_8} e_{x_i} (G_{x\delta_f} \delta_f^0|_{z^0})_j - \frac{\theta_4}{\alpha_8} (\hat{\lambda}_{x\delta_{f_{ij}}} - \lambda_{x\delta_{f_{ij}}}^0)
\end{aligned} \tag{2.163}$$

$$\begin{aligned}
\dot{\hat{b}}_{\delta_{s_{ij}}} &= \frac{\alpha_2}{\alpha_9} e_{\delta_{s_i}} f_{\delta_{s_j}} - \frac{\theta_5}{\alpha_9} (\hat{b}_{\delta_{s_{ij}}} - b_{\delta_{s_{ij}}}^0) \\
\dot{\hat{\lambda}}_{\delta_s u_{s_{ij}}} &= \frac{\alpha_2}{\alpha_{10}} e_{\delta_{s_i}} (G_{\delta_s u_s} u_s)_j - \frac{\theta_6}{\alpha_{10}} (\hat{\lambda}_{\delta_s u_{s_{ij}}} - \lambda_{\delta_s u_{s_{ij}}}^0)
\end{aligned} \tag{2.164}$$

$$\begin{aligned}
\hat{b}_{z_{ij}}^{k\prime} &= \frac{\alpha_3}{\alpha_{11k}} e_{z_i} f_{z_j}^k - \frac{\theta_7}{\alpha_{11k}} (\hat{b}_{z_{ij}}^k - b_{z_{ij}}^{k^0}) \\
\hat{\lambda}'_{z\delta_{f_{ij}}} &= \frac{\alpha_3}{\alpha_{12}} e_{z_i} (G_{z\delta_f} \delta_f^0)_j - \frac{\theta_8}{\alpha_{12}} (\hat{\lambda}_{z\delta_{f_{ij}}} - \lambda_{z\delta_{f_{ij}}}^0)
\end{aligned} \tag{2.165}$$

$$\begin{aligned}
\dot{\hat{b}}_{\delta_{f_{ij}}} &= \frac{\alpha_4}{\alpha_{13}} e_{\delta_{f_i}} f_{\delta_{f_j}} - \frac{\theta_9}{\alpha_{13}} (\hat{b}_{\delta_{f_{ij}}} - b^0_{\delta_{f_{ij}}}) \\
\dot{\hat{\lambda}}_{\delta_f u_{f_{ij}}} &= \frac{\alpha_4}{\alpha_{14}} e_{\delta_{f_i}} (G_{\delta_f u_f} u_f)_j - \frac{\theta_{10}}{\alpha_{14}} (\hat{\lambda}_{\delta_f u_{f_{ij}}} - \lambda^0_{\delta_f u_{f_{ij}}})
\end{aligned} \tag{2.166}$$

In the update laws (2.163) - (2.166), x_i denotes the i-th element of the column vector x, and the following are design variables: $\theta_i > 0, i = 1, ..., 10$; $b^0_{xx_{ij}}, b^0_{xz_{ij}}, \lambda^0_{x\delta_{sij}}, \lambda^0_{x\delta_{f_{ij}}}, b^0_{\delta_{sij}}, \lambda^0_{\delta_s u_{sij}}, b^{k^0}_{z_{ij}}, \lambda^0_{z\delta_{f_{ij}}}$, $b^0_{\delta_{f_{ij}}}, \lambda^0_{\delta_f u_{f_{ij}}}$. With these parameter update laws, the time-derivative (2.162) becomes

$$\begin{aligned}
\dot{V}_c = &-\alpha_1 (e_x^T K_x e_x + e_\xi^T K_\xi e_\xi) - \frac{\alpha_2}{\sigma} e^T_{\delta_s} K_{\delta_s} e_{\delta_s} - \frac{\alpha_3}{\varepsilon} e_z^T K_z e_z - \frac{\alpha_4}{\rho} e^T_{\delta_f} K_{\delta_f} e_{\delta_f} \\
&+ \alpha_1 e_x^T [B_{xz} F_{xz} e_z + \gamma_x + \Lambda_{x\delta_s} G_{x\delta_s} e_{\delta_s} + \Lambda_{x\delta_f} G_{x\delta_f} (e_{\delta_f} + \delta^0_f - \delta^0_f|_{z^0})] + \alpha_1 e_\xi^T F_{\xi z} e_z \\
&+ \frac{\alpha_3}{\varepsilon} e_z^T (\gamma_z + \Lambda_{z\delta_f} G_{z\delta_f} e_{\delta_f}) - \alpha_2 e^T_{\delta_s} \dot{\delta}^0_s - \alpha_3 e_z^T \dot{z}^0 - \alpha_4 e^T_{\delta_f} \dot{\delta}^0_f \\
&+ \theta_1 \sum_i \sum_j \tilde{b}_{xx_{ij}} (\hat{b}_{xx_{ij}} - b^0_{xx_{ij}}) + \theta_2 \sum_i \sum_j \tilde{b}_{xz_{ij}} (\hat{b}_{xz_{ij}} - b^0_{xz_{ij}}) \\
&+ \theta_3 \sum_i \sum_j \tilde{\lambda}_{x\delta_{sij}} (\hat{\lambda}_{x\delta_{sij}} - \lambda^0_{x\delta_{sij}}) + \theta_4 \sum_i \sum_j \tilde{\lambda}_{x\delta_{f_{ij}}} (\hat{\lambda}_{x\delta_{f_{ij}}} - \lambda^0_{x\delta_{f_{ij}}}) \\
&+ \frac{\theta_5}{\sigma} \sum_i \sum_j \tilde{b}_{\delta_{sij}} (\hat{b}_{\delta_{sij}} - b^0_{\delta_{sij}}) + \frac{\theta_6}{\sigma} \sum_i \sum_j \tilde{\lambda}_{\delta_s u_{sij}} (\hat{\lambda}_{\delta_s u_{sij}} - \lambda^0_{\delta_s u_{sij}}) \\
&+ \frac{\theta_7}{\varepsilon} \sum_k \sum_i \sum_j \tilde{b}^k_{z_{ij}} (\hat{b}^k_{z_{ij}} - b^{k^0}_{z_{ij}}) + \frac{\theta_8}{\varepsilon} \sum_i \sum_j \tilde{\lambda}_{z\delta_{f_{ij}}} (\hat{\lambda}_{z\delta_{f_{ij}}} - \lambda^0_{z\delta_{f_{ij}}}) \\
&+ \frac{\theta_9}{\rho} \sum_i \sum_j \tilde{b}_{\delta_{f_{ij}}} (\hat{b}_{\delta_{f_{ij}}} - b^0_{\delta_{f_{ij}}}) + \frac{\theta_{10}}{\rho} \sum_i \sum_j \tilde{\lambda}_{\delta_f u_{f_{ij}}} (\hat{\lambda}_{\delta_f u_{f_{ij}}} - \lambda^0_{\delta_f u_{f_{ij}}}).
\end{aligned} \tag{2.167}$$

At this point, a result is used similar to Subsection 2.5.3 to simplify the time-derivative (2.167). For any constant but unknown parameter p bounded as $\underline{p} \leq p \leq \bar{p}$, the expression $\tilde{p}(\hat{p} - p^0) = \tilde{p}(p - \tilde{p} - p^0) = \tilde{p}(p - p^0) - \tilde{p}^2 \leq \frac{1}{2}[\tilde{p}^2 + (p - p^0)^2] - \tilde{p}^2 \leq \frac{1}{2} \max_{\underline{p} \leq p \leq \bar{p}} (p - p^0)^2 - \frac{1}{2}\tilde{p}^2 = \frac{1}{2} p^+ - \frac{1}{2}\tilde{p}^2$,

where $p^+ = \max_{\underline{p} \le p \le \bar{p}} (p - p^0)^2$. Therefore, (2.167) can be upper-bounded as

$$\begin{aligned}
\dot{V}_c \le & -\alpha_1 (e_x^T K_x e_x + e_\xi^T K_\xi e_\xi) - \frac{\alpha_2}{\sigma} e_{\delta_s}^T K_{\delta_s} e_{\delta_s} - \frac{\alpha_3}{\varepsilon} e_z^T K_z e_z - \frac{\alpha_4}{\rho} e_{\delta_f}^T K_{\delta_f} e_{\delta_f} \\
& + \alpha_1 e_x^T [B_{xz} F_{xz} e_z + \gamma_x + \Lambda_{x\delta_s} G_{x\delta_s} e_{\delta_s} + \Lambda_{x\delta_f} G_{x\delta_f} (e_{\delta_f} + \delta_f^0 - \delta_f^0|_{z^0})] + \alpha_1 e_\xi^T F_{\xi z} e_z \\
& + \frac{\alpha_3}{\varepsilon} e_z^T (\gamma_z + \Lambda_{z\delta_f} G_{z\delta_f} e_{\delta_f}) - \alpha_2 e_{\delta_s}^T \dot{\delta}_s^0 - \alpha_3 e_z^T \dot{z}^0 - \alpha_4 e_{\delta_f}^T \dot{\delta}_f^0 \\
& - \frac{\theta_1}{2} \sum_i \sum_j \tilde{b}_{xx_{ij}}^2 - \frac{\theta_2}{2} \sum_i \sum_j \tilde{b}_{xz_{ij}}^2 - \frac{\theta_3}{2} \sum_i \sum_j \tilde{\lambda}_{x\delta_{s_{ij}}}^2 - \frac{\theta_4}{2} \sum_i \sum_j \tilde{\lambda}_{x\delta_{f_{ij}}}^2 \\
& - \frac{\theta_5}{2\sigma} \sum_i \sum_j \tilde{b}_{\delta_{s_{ij}}}^2 - \frac{\theta_6}{2\sigma} \sum_i \sum_j \tilde{\lambda}_{\delta_s u_{s_{ij}}}^2 - \frac{\theta_7}{2\varepsilon} \sum_k \sum_i \sum_j \tilde{b}_{z_{ij}}^{k^2} \\
& - \frac{\theta_8}{2\varepsilon} \sum_i \sum_j \tilde{\lambda}_{z\delta_{f_{ij}}}^2 - \frac{\theta_9}{2\rho} \sum_i \sum_j \tilde{b}_{\delta_{f_{ij}}}^2 - \frac{\theta_{10}}{2\rho} \sum_i \sum_j \tilde{\lambda}_{\delta_f u_{f_{ij}}}^2 + \mu_0.
\end{aligned} \tag{2.168}$$

where

$$\begin{aligned}
\mu_0 := & \frac{\theta_1}{2} \sum_i \sum_j b_{xx_{ij}}^+ + \frac{\theta_2}{2} \sum_i \sum_j b_{xz_{ij}}^+ + \frac{\theta_3}{2} \sum_i \sum_j \lambda_{x\delta_{s_{ij}}}^+ + \frac{\theta_4}{2} \sum_i \sum_j \lambda_{x\delta_{f_{ij}}}^+ \\
& + \frac{\theta_5}{2\sigma} \sum_i \sum_j b_{\delta_{s_{ij}}}^+ + \frac{\theta_6}{2\sigma} \sum_i \sum_j \lambda_{\delta_s u_{s_{ij}}}^+ + \frac{\theta_7}{2\varepsilon} \sum_k \sum_i \sum_j b_{z_{ij}}^{k^+} \\
& + \frac{\theta_8}{2\varepsilon} \sum_i \sum_j \lambda_{z\delta_{f_{ij}}}^+ + \frac{\theta_9}{2\rho} \sum_i \sum_j b_{\delta_{f_{ij}}}^+ + \frac{\theta_{10}}{2\rho} \sum_i \sum_j \lambda_{\delta_f u_{f_{ij}}}^+.
\end{aligned} \tag{2.169}$$

Equation (2.168) has several terms for which the upper bounds are to be found. Similar to Subsection 2.5.3, this is done by invoking the notion of compact sets. Let N_1 denote the combined dimension of the states and the unknown parameters. Consider a compact set $Q_1 \in \mathbb{R}^{N_1}$, in which the composite Lyapunov function (2.157) is upper-bounded by $\bar{V}$; i.e. $V_c \le \bar{V}$ for some $\bar{V} > 0$. Let N_2 denote the combined dimension of the references and their time-derivatives of first and second orders. Consider a compact set $Q_2 \in \mathbb{R}^{N_2}$, characterized by $\|x_r\|_2^2 + \|\dot{x}_r\|_2^2 + \|\ddot{x}_r\|_2^2 + \|\xi_r\|_2^2 + \left\|\dot{\xi}_r\right\|_2^2 + \left\|\ddot{\xi}_r\right\|_2^2 \le R^2$ for some $R > 0$. Then $Q := Q_1 \times Q_2$ is a compact set in $\mathbb{R}^{N_1+N_2}$, and all the elements of the vectors $z^0, \delta_f^0 - \delta_f^0|_{z^0}, \dot{\delta}_s^0, \dot{z}^0, \dot{\delta}_f^0$ are continuous functions in the compact set Q. Therefore, each element of these vectors has a maximum, and consequently

there exist constants M_1, M_2, M_3, M_4, M_5 such that $\left\|z^0\right\|_\infty = M_1, \left\|\delta_f^0 - \delta_f^0|_{z^0}\right\|_\infty = M_2, \left\|\dot{\delta}_s^0\right\|_\infty = M_3, \left\|\dot{z}^0\right\|_\infty = M_4, \left\|\dot{\delta}_f^0\right\|_\infty = M_5$ Upper bounds of the cross-terms present in the time-derivative (2.162) can now be found as follows. One of the cross-terms can be bounded as

$$\begin{aligned}
\alpha_1 e_x^T B_{xz} F_{xz} e_z &= \alpha_1 (B_{xz}^T e_x)^T (F_{xz} e_z) \\
&\leq \alpha_1 \left\| B_{xz}^T e_x \right\|_2 \|F_{xz} e_z\|_2 \\
&\leq \alpha_1 \left\| B_{xz}^T \right\|_2 \|e_x\|_2 \|F_{xz}\|_2 \|e_z\|_2 \\
&= \alpha_1 \bar{\sigma}(B_{xz}^T) \|e_x\|_2 \, \bar{\sigma}(F_{xz}) \|e_z\|_2 \\
&\leq \alpha_1 v_1 \|e_x\|_2 \, v_2 \|e_z\|_2 \\
&\leq \frac{1}{2} \alpha_1 v_1 v_2 (e_x^T e_x + e_z^T e_z).
\end{aligned} \tag{2.170}$$

The results used in order to obtain the final form of (2.170) are (i) Cauchy-Schwarz inequality: $u^T v \leq \|u\|_2 \|v\|_2$, (ii) property of induced norm of matrices: $\|Ax\| \leq \|A\| \|x\|$, (iii) induced 2-norm being the same as the largest singular value, (iv) Young's inequality: $ab \leq \frac{1}{2}(a^2 + b^2)$. Similarly, another one of the cross-terms can be bounded as follows:

$$\begin{aligned}
\alpha_1 e_x^T \gamma_x &\leq \alpha_1 \|e_x\|_2 \|\gamma_x\|_2 \\
&\leq \alpha_1 \|e_x\|_2 \, (\kappa_1 \|x\|_2 + \kappa_2 \|\xi\|_2 + \kappa_3 \|z\|_2).
\end{aligned} \tag{2.171}$$

Writing $x = e_x + x_r, \xi = e_\xi + \xi_r, z = e_z + z^0$ and using the triangle inequality of vector norms $\|u + v\|_2 \leq \|u\|_2 + \|v\|_2$, (2.171) becomes

$$\begin{aligned}
\alpha_1 e_x^T \gamma_x \leq \alpha_1 \|e_x\|_2 \, (&\kappa_1 \|e_x\|_2 + \kappa_1 \|x_r\|_2 + \kappa_2 \left\|e_\xi\right\|_2 + \kappa_2 \|\xi_r\|_2 \\
&+ \kappa_3 \|e_z\|_2 + \kappa_3 \left\|z^0\right\|_2).
\end{aligned} \tag{2.172}$$

The vector norms satisfy $\|x\|_\infty \leq \|x\|_2 \leq \sqrt{dim(x)} \|x\|_\infty$, where $dim(x)$ indicates the dimension of the vector x. Using this, $\left\|z^0\right\|_2 \leq \sqrt{m} \left\|z^0\right\|_\infty = \sqrt{m} M_1$. For the references, $\|x_r\|_2 \leq R, \|\xi_r\|_2 \leq$

R. Using these results and Young's inequality,

$$\begin{aligned}\alpha_1 e_x^T \gamma_x \leq \frac{1}{2}\alpha_1(2\kappa_1+\kappa_2+\kappa_3)e_x^T e_x + \frac{1}{2}\alpha_1\kappa_2 e_\xi^T e_\xi \\ + \frac{1}{2}\alpha_1\kappa_3 e_z^T e_z + \alpha_1(\kappa_1 R+\kappa_2 R+\kappa_3 M_1\sqrt{m})\|e_x\|_2 .\end{aligned} \tag{2.173}$$

Proceeding in this manner, the other cross-terms can be bounded as shown below.

$$\begin{aligned}\alpha_1 e_x^T \Lambda_{x\delta_s} G_{x\delta_s} e_{\delta_s} &\leq \frac{1}{2}\alpha_1 v_3 v_4 (e_x^T e_x + e_{\delta_s}^T e_{\delta_s}) \\ \alpha_1 e_x^T \Lambda_{x\delta_f} G_{x\delta_f}(e_{\delta_f}+\delta_f^0-\delta_f^0|_{z^0}) &\leq \frac{1}{2}\alpha_1 v_5 v_6 (e_x^T e_x + e_{\delta_f}^T e_{\delta_f}) + \alpha_1 v_5 v_6\sqrt{m}M_2\|e_x\|_2 \\ \alpha_1 e_\xi^T F_{\xi z} e_z &\leq \frac{1}{2}\alpha_1 v_7 (e_\xi^T e_\xi + e_z^T e_z) \\ \frac{\alpha_3}{\varepsilon} e_z^T \gamma_z &\leq \frac{\alpha_3\kappa_4}{2\varepsilon} e_x^T e_x + \frac{\alpha_3\kappa_5}{2\varepsilon} e_\xi^T e_\xi + \frac{\alpha_3}{2\varepsilon}(\kappa_4+\kappa_5 \\ &\quad + 2\kappa_6) e_z^T e_z + \frac{\alpha_3}{\varepsilon}(\kappa_4 R+\kappa_5 R+\kappa_6 M_1\sqrt{m})\|e_z\|_2 \\ \frac{\alpha_3}{\varepsilon} e_z^T \Lambda_{z\delta_f} G_{z\delta_f} e_{\delta_f} &\leq \frac{\alpha_3}{2\varepsilon} v_8 v_9 (e_z^T e_z + e_{\delta_f}^T e_{\delta_f} \\ -\alpha_2 e_{\delta_s}^T \dot{\delta}_s^0 &\leq \alpha_2 M_3\sqrt{n}\|e_{\delta_s}\|_2 \\ -\alpha_3 e_z^T \dot{z}^0 &\leq \alpha_3 M_4\sqrt{m}\|z\|_2 \\ -\alpha_4 e_{\delta_f}^T \dot{\delta}_f^0 &\leq \alpha_4 M_5\sqrt{m}\left\|e_{\delta_f}\right\|_2\end{aligned} \tag{2.174}$$

Substituting inequalities (2.170), (2.173), (2.174) in the time-derivative of the composite Lyapunov function (2.168) leads to a group of terms quadratic in the state errors and parameter errors, and another group of terms linear in the norms of the state errors. Using Young's inequality, the group of linear terms can be upper-bounded as

$$\begin{aligned}\|e_x\|_2 &\leq \frac{1}{2}(\nu_1^2 + \frac{1}{\nu_1^2} e_x^T e_x) \\ \|e_{\delta_s}\|_2 &\leq \frac{1}{2}(\nu_2^2 + \frac{1}{\nu_2^2} e_{\delta_s}^T e_{\delta_s}) \\ \|e_z\|_2 &\leq \frac{1}{2}(\nu_3^2 + \frac{1}{\nu_3^2} e_z^T e_z) \\ \left\|e_{\delta_f}\right\|_2 &\leq \frac{1}{2}(\nu_4^2 + \frac{1}{\nu_4^2} e_{\delta_f}^T e_{\delta_f})\end{aligned} \tag{2.175}$$

where constants $\nu_1, \nu_2, \nu_3, \nu_4$ can be arbitrarily chosen. Using (2.170), (2.173), (2.174), (2.175) and properties of quadratic forms related to eigenvalues of matrices, the time-derivative of the composite Lyapunov function (2.168) reduces to the following:

$$\begin{aligned}\dot{V}_c \leq & -\beta_1 e_x^T e_x - \beta_2 e_\xi^T e_\xi - \beta_3 e_{\delta_s}^T e_{\delta_s} - \beta_4 e_z^T e_z - \beta_5 e_{\delta_f}^T e_{\delta_f} \\ & - \frac{\theta_1}{2}\sum_j \tilde{b}_{xx_{ij}}^2 - \frac{\theta_2}{2}\sum_i\sum_j \tilde{b}_{xz_{ij}}^2 - \frac{\theta_3}{2}\sum_i\sum_j \tilde{\lambda}_{x\delta_{s_{ij}}}^2 - \frac{\theta_4}{2}\sum_i\sum_j \tilde{\lambda}_{x\delta_{f_{ij}}}^2 \\ & - \frac{\theta_5}{2\sigma}\sum_i\sum_j \tilde{b}_{\delta_{s_{ij}}}^2 - \frac{\theta_6}{2\sigma}\sum_i\sum_j \tilde{\lambda}_{\delta_s u_{s_{ij}}}^2 - \frac{\theta_7}{2\varepsilon}\sum_k\sum_i\sum_j \tilde{b}_{z_{ij}}^{k^2} \\ & - \frac{\theta_8}{2\varepsilon}\sum_i\sum_j \tilde{\lambda}_{z\delta_{f_{ij}}}^2 - \frac{\theta_9}{2\rho}\sum_i\sum_j \tilde{b}_{\delta_{f_{ij}}}^2 - \frac{\theta_{10}}{2\rho}\sum_i\sum_j \tilde{\lambda}_{\delta_f u_{f_{ij}}}^2 + \mu\end{aligned} \tag{2.176}$$

where $\beta_i; i = 1, 2, 3, 4, 5$ are given by

$$\begin{aligned}\beta_1 &:= \frac{1}{2}\alpha_1(2\lambda_{min}(K_x) - (2\kappa_1 + \kappa_2 + \kappa_3) - v_1 v_2 - \frac{\kappa_1 R + \kappa_2 R + \kappa_3 M_1\sqrt{m}}{\nu_1^2} - v_3 v_4 - v_5 v_6 \\ &\quad - \frac{v_5 v_6 M_2\sqrt{m}}{\nu_1^2}) - \frac{\alpha_3\kappa_4}{2\varepsilon} := \alpha_1\lambda_{min}(K_x) - \bar{\beta}_1 - \frac{\alpha_3 k_4}{2\varepsilon} \\ \beta_2 &:= \frac{\alpha_1}{2}(2\lambda_{min}(K_\xi) - \kappa_2 - v_7) - \frac{\alpha_3\kappa_5}{2\varepsilon} \\ \beta_3 &:= \frac{1}{2}(2\frac{\alpha_2}{\sigma}\lambda_{min}(K_{\delta_s}) - \alpha_1 v_3 v_4 - \frac{\alpha_2 M_3\sqrt{n}}{\nu_2^2}) := \frac{\alpha_2}{\sigma}\lambda_{min}(K_{\delta_s}) - \bar{\beta}_3 \\ \beta_4 &:= \frac{1}{2}\frac{\alpha_3}{\varepsilon}(2\lambda_{min}(K_z) - (\kappa_4 + \kappa_5 + 2\kappa_6) - \frac{\kappa_4 R + \kappa_5 R + \kappa_6 M_1\sqrt{m}}{\nu_3^2} - v_8 v_9 - \frac{M_4\sqrt{m}}{\nu_3^2}) \\ &\quad - \frac{\alpha_1}{2}(v_1 v_2 + \kappa_3 + v_7) \\ &\quad := \frac{\alpha_3}{\varepsilon}(\lambda_{min}(K_z) - \beta_{41}) - \beta_{42} \\ \beta_5 &:= \frac{1}{2}(2\frac{\alpha_4}{\rho}\lambda_{min}(K_{\delta_f}) - \frac{\alpha_4 M_5\sqrt{m}}{\nu_4^2} - \alpha_1 v_5 v_6 - \frac{\alpha_3}{\varepsilon}v_8 v_9) := \frac{\alpha_4}{\rho}\lambda_{min}(K_{\delta_f}) - \bar{\beta}_5 - \frac{\alpha_3 v_8 v_9}{\varepsilon}\end{aligned} \tag{2.177}$$

and the factor μ is given by

$$\begin{aligned}\mu := \mu_0 + \frac{1}{2}[&\alpha_1(\kappa_1 R + \kappa_2 R + \kappa_3 M_1\sqrt{m})\nu_1^2 + \alpha_1 v_5 v_6 M_2\sqrt{m}\nu_1^2 + \frac{\alpha_3}{\varepsilon}(\kappa_4 R + \kappa_5 R \\ &+ \kappa_6 M_1\sqrt{m})\nu_3^2 + \alpha_2 M_3\sqrt{n}\nu_2^2 + \alpha_3 M_4\sqrt{m}\nu_3^2 + \alpha_4 M_5\sqrt{m}\nu_4^2\end{aligned} \tag{2.178}$$

with μ_0 given by equation (2.169). Note that μ can be written in the form

$$\mu = \mu_1 + \frac{\mu_2}{\sigma} + \frac{\mu_3}{\varepsilon} + \frac{\mu_4}{\rho} \tag{2.179}$$

where $\mu_i, i = 1, 2, 3, 4$ are constants. Furthermore, define the following:

$$\begin{aligned} \eta &:= \min\{\beta_1, \beta_2, \beta_3, \beta_4, \beta_5, \frac{\theta_1}{2}, \frac{\theta_2}{2}, \frac{\theta_3}{2}, \frac{\theta_4}{2}, \frac{\theta_5}{2\sigma}.\frac{\theta_6}{2\sigma}, \frac{\theta_7}{2\varepsilon}, \frac{\theta_8}{2\varepsilon}, \frac{\theta_9}{2\rho}, \frac{\theta_{10}}{2\rho}\} \\ \bar{\eta} &:= \frac{1}{2}\max\{\alpha_1, ..., \alpha_{10}, \alpha_{11k}, \alpha_{12}, ..., \alpha_{14}\} \end{aligned} \tag{2.180}$$

In addition, consider e to be the vector formed by stacking up in one column all the errors: tracking errors for the slow states, deviation from equilibrium manifolds of fast states and actuators, and all parameter estimation errors. The inequality (4.115) can be expressed as

$$\begin{aligned} \dot{V}_c &\leq -\eta\|e\|_2^2 + \mu \\ &\leq -\frac{\eta}{\bar{\eta}}V_c + \mu \end{aligned} \tag{2.181}$$

Inequality (2.181) shows that $\dot{V}_c$ is negative outside the compact set $\|e\|_2 > \sqrt{\frac{\mu}{\eta}}$, therefore, the errors will be uniformly ultimately bounded within $0 \leq \|e\|_2 \leq \sqrt{\frac{\mu}{\eta}}$. Suppose that it is desired to keep the error vector e ultimately bounded within a ball of radius θ_r; i.e. $\dot{V}_c < 0$ on the boundary of the ball represented by $\|e\|_2 = \theta_r$. This is possible if $-\eta\theta_r^2 + \mu < 0$; i.e. if

$$\eta > \frac{\mu}{\theta_r^2}. \tag{2.182}$$

This is equivalent to saying that every element in the set

$$\mathcal{A} := \{\beta_1, \beta_2, \beta_3, \beta_4, \beta_5, \frac{\theta_1}{2}, \frac{\theta_2}{2}, \frac{\theta_3}{2}, \frac{\theta_4}{2}, \frac{\theta_5}{2\sigma}.\frac{\theta_6}{2\sigma}, \frac{\theta_7}{2\varepsilon}, \frac{\theta_8}{2\varepsilon}, \frac{\theta_9}{2\rho}, \frac{\theta_{10}}{2\rho}\}$$

is greater than $\frac{\mu}{\theta_r^2}$. Therefore, *if the gains and other design variables are chosen such that every element in the set $\mathcal{A}$ exceeds $\frac{\mu}{\theta_r^2}$ for some $\sigma, \varepsilon, \rho > 0$, then $\sigma_{**}, \sigma^{**}, \varepsilon_{**}, \varepsilon^{**}, \rho_{**}, \rho^{**}$ are the lower*

and upper bounds of the time-scale separation parameters within which condition (2.182) holds, resulting in ultimate boundedness of tracking errors, manifold errors and parameter estimation errors.

Remark 8. *Condition (2.182) leads to a set of coupled inequalities involving $\sigma, \varepsilon, \rho$. For a nonstandard system with a form similar to (2.129) but no uncertainties in actuator dynamics, these inequalities can be decoupled and results in the following bounds. The bound of ε is $\varepsilon_{**} < \varepsilon < \varepsilon^{**}$ where*

$$\varepsilon_{**} := \max_{j=1,2,3,4} \{ \frac{2\mu_3}{\theta_j \theta_r^2 - 2\mu_1} \} \tag{2.183}$$

and

$$\varepsilon^{**} := \min(\min_{k=7,8} \{ \frac{\theta_r^2 \theta_k - 2\mu_2}{2\mu_1} \}, \frac{\alpha_3 (\lambda_{min}(K_z) - \beta_{41}) - \frac{\mu_2}{\theta_r^2}}{\frac{\mu_1}{\theta_r^2} + \beta_{42}}). \tag{2.184}$$

The bounds of σ and ρ are

$$0 < \sigma < \sigma^{**} := \frac{\alpha_2 \lambda_{\min}(K_{\delta_s})}{\frac{\mu_1}{\theta_r^2} + \bar{\beta}_3 + \frac{\mu_2}{\theta_r^2 \varepsilon^{**}}} \tag{2.185}$$

$$0 < \rho < \rho^* := \frac{\alpha_4 \lambda_{min}(K_{\delta_f})}{\frac{\mu_1}{\theta_r^2} + \bar{\beta}_5 + (\frac{\mu_2}{\theta_r^2} + \alpha_3 \upsilon_8 \upsilon_9) \frac{1}{\varepsilon^{**}}} \tag{2.186}$$

In addition, the following are sufficient conditions on the gain matrices K_x and K_ξ:

$$\lambda_{min}(K_x) > \frac{1}{\alpha_1} (\frac{\mu_1}{\theta_r^2} + \bar{\beta}_1 + \frac{\alpha_3 \kappa_4}{2\varepsilon_{**}} + \frac{\mu_2}{\delta^2 \varepsilon_{**}}) \tag{2.187}$$

$$\lambda_{min}(K_\xi) > \frac{1}{\alpha_1} (\frac{\mu_1}{\theta_r^2} + \frac{\alpha_1 \kappa_2 + \alpha_1 \upsilon_7}{2} + \frac{\alpha_3 \kappa_5}{2\varepsilon_{**}} + \frac{\mu_2}{\delta^2 \varepsilon_{**}}) \tag{2.188}$$

2.6.4 Numerical Results

This subsection shows slow state tracking using the control and estimation laws developed in Subsection 2.6.2 - 2.6.3 on an example fifth-order system as well as on a nonlinear 6-DOF generic F-16A, which is commanded to perform two different combined longitudinal and lateral/directional maneuvers.

2.6.4.1 An Example Fifth-Order System

Consider a nonlinear, nonstandard four-time-scale system with two slow states, one fast states, one slow actuator and one fast actuator. In total, the system has five state variables: three system states and two actuators. Suppose that the full-order dynamics are

$$\begin{aligned}
\dot{x} &= p_1(1+x^3\xi^2) + p_2(e^{-x^2}\sin\xi)z + \gamma_x(.) + p_3(1+\cos^2 x)\delta_s + p_4(1+\sin^2\xi)\delta_f \\
\dot{\xi} &= (1+cos^2\xi)z \\
\sigma\dot{\delta}_s &= p_5\delta_s + p_6 u_s \\
\varepsilon\dot{z} &= p_7 + p_8 xz + p_9\xi^2 e^{-z} + \gamma_z(.) + p_{10}(1+\sin^2 xcos^2\xi)\delta_f \\
\rho\dot{\delta}_f &= p_{11}\delta_f + p_{12}u_f.
\end{aligned} \tag{2.189}$$

The parametric uncertainties in the dynamics of the slow and fast states are reflected in the constant but unknown parameters $p_1, p_2, p_3, p_4, p_7, p_8, p_9, p_{10}$. For this model, both of the slow and the fast actuators are assumed first-order with constant but unknown time-constants, reflected in the parameters p_5, p_6, p_{11}, p_{12}. The actual values of the constant but unknown parameters are $B_{xx} = p_1 = 0.1$, $B_{xz} = p_2 = 0.1$, $\Lambda_{x\delta_s} = p_3 = 1$, $\Lambda_{x\delta_f} = p_4 = 0.1$, $B_{\delta_s} = p_5 = -1$, $\Lambda_{\delta_s u_s} = p_6 = 1$ $B_z^1 = p_7 = -0.1$, $B_z^2 = p_8 = 0.1$, $B_z^3 = p_9 = 0.1$, $\Lambda_{z\delta_f} = p_{10} = 1$, $B_{\delta_f} = p_{11} = -1$, $\Lambda_{\delta_f u_f} = p_{12} = 1$. The additive uncertainties are assumed as follows:

$$\begin{aligned}
\gamma_x(t,x,\xi,z) &= 0.01(x+0.1\xi+0.1z)sin(t) \\
\gamma_z(t,x,\xi,z) &= 0.01(x+0.1\xi+0.1z)cos(t)
\end{aligned} \tag{2.190}$$

The slow states are at initial conditions $x(0) = 0.5, \xi(0) = -0.1$. The slow actuator, fast state and fast actuator are at zero initial conditions. The slow state tracking controller is to track sinusoidal trajectories with different amplitudes, frequencies and initial phases for the slow states $x(t)$ and $\xi(t)$. The references are $x_r(t) = 0.5\sin(\frac{2\pi}{4}t - \frac{\pi}{2})$ and $\xi_r(t) = 0.1\sin(\frac{2\pi}{2}t + \frac{\pi}{2})$. The time-scale separation parameters are assumed to be $\sigma = 0.1, \varepsilon = 0.01, \rho = 0.001$.

Given the dynamics (2.189), the known functions are as follows:

$$
\begin{aligned}
f_{xx}(x,\xi) &= 1 + x^3\xi^2 \\
F_{xz}(x,\xi) &= e^{-x^2} sin(\xi) \\
G_{x\delta_s}(x,\xi) &= 1 + cos^2(x) \\
G_{x\delta_f}(x,\xi) &= 1 + sin^2(\xi) \\
F_{\xi z}(x,\xi) &= 1 + cos^2(\xi) \\
f_{\delta_s}(\delta_s) &= \delta_s \\
G_{\delta_s u_s} &= 1 \\
f_z^1(x,\xi,z) &= 1 \\
f_z^2(x,\xi,z) &= xz \\
f_z^3(x,\xi,z) &= \xi^2 e^{-z} \\
G_{z\delta_f} &= 1 + sin^2(x)cos^2(\xi) \\
f_{\delta_f}(\delta_f) &= \delta_f \\
G_{\delta_f u_f} &= 1
\end{aligned}
\tag{2.191}
$$

Although the slow and fast states have nonlinear dynamics, for purposes of visualization the actuators are linear, first-order with the fast actuator 100 times faster than the slow actuator. Actuator time-constants are assumed unknown for control synthesis. The controller gains are selected as $K_x = 10, K_\xi = 5, K_{\delta_s} = 0.5, K_z = 10, K_{\delta_f} = 0.5$. In the composite Lyapunov function, the weights of the individual Lyapunov functions are selected as $\alpha_1 = 0.01, \alpha_2 = 0.01, \alpha_3 = 0.01, \alpha_4 = 0.01, \alpha_5 = 1, \alpha_6 = 1, \alpha_7 = 1, \alpha_8 = 1, \alpha_9 = 1, \alpha_{10} = 1, \alpha_{11}^1 = 1, \alpha_{11}^2 = 1, \alpha_{11}^3 = 1, \alpha_{12} = 1, \alpha_{13} = 1, \alpha_{14} = 1$. The initial estimates of the constant but unknown parameters are assumed to be $\hat{p}_1(0) = -0.5, \hat{p}_2(0) = -0.5, \hat{p}_3(0) = 0.5, \hat{p}_4(0) = -0.5, \hat{p}_5(0) = 0.5, \hat{p}_6(0) = 0.5, \hat{p}_7(0) = 0.5, \hat{p}_8(0) = 0.5, \hat{p}_9(0) = -0.5, \hat{p}_{10}(0) = 0.5, \hat{p}_{11}(0) = -0.5, \hat{p}_{12}(0) = 0.5$. The gains in the parameter estimator are chosen to be $\theta_1 = 1, \theta_2 = 1, \theta_3 = 1, \theta_4 = 1, \theta_5 =$

$0.1, \theta_6 = 0.1, \theta_7 = 0.01, \theta_8 = 0.01, \theta_9 = 0.001, \theta_{10} = 0.001$. The free design variables in the parameter estimator are chosen to be $p_1^0 = 0.2, p_2^0 = 0.2, p_3^0 = 0.9, p_4^0 = 0.2, p_5^0 = -1.1, p_6^0 = 1.2, p_7^0 = -0.3, p_8^0 = 0.2, p_9^0 = 0.2, p_{10}^0 = 1.2, p_{11}^0 = -0.8, p_{12}^0 = 1.1$.

Figures 2.19 - 2.22 show the time-histories of the states, controls and the uncertain parameters for a time span of eight seconds. Good tracking for both of the kinetic and kinematic states can be seen in Figure 2.19, as both are able to reach and stay close to their reference trajectories. The fast state reaches its manifold quickly and stays very close to its manifold throughout the simulation. Figure 2.20 shows that both of the slow and the fast controls remain bounded and diminish in less than one second. The slow actuator follows the control command with a small time-delay. The fast actuator, which was assumed 100 times faster than the slow actuator, is seen to respond very quickly to the change in control command. Figures 2.21-2.22 show that estimation errors for all parameters remain small and bounded. Figures 2.19 and 2.21-2.22 together demonstrate that the objective of slow state tracking is accomplished even though the estimated parameters do not necessarily converge to the actual parameters.

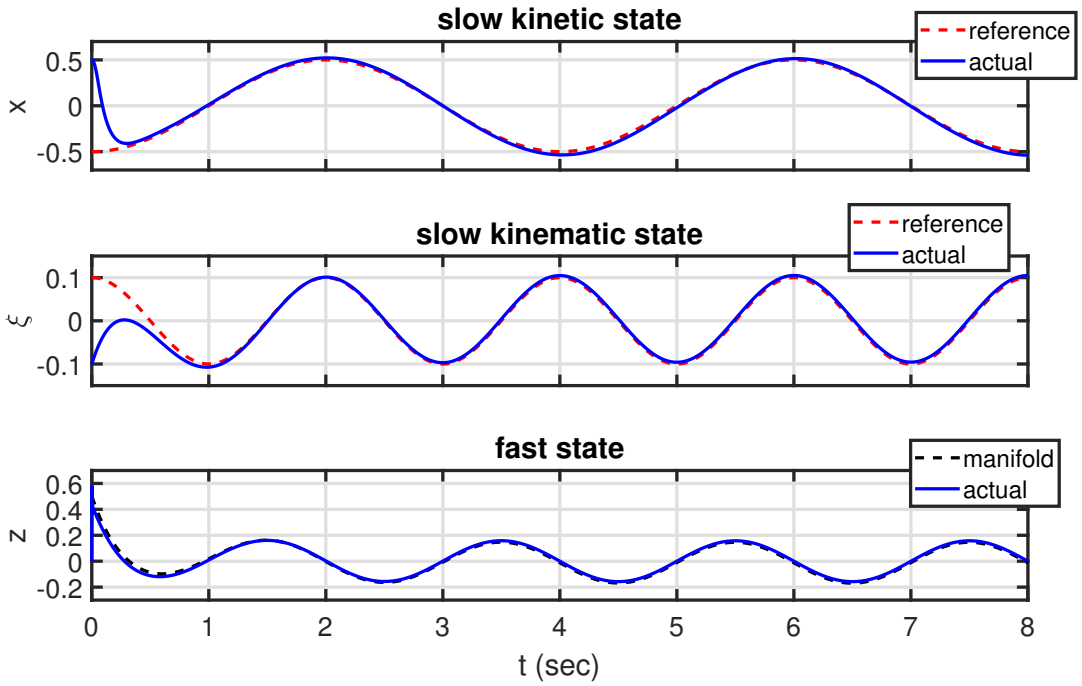

Figure 2.19: Trajectories of slow and fast states for four-time-scale example (2.189)

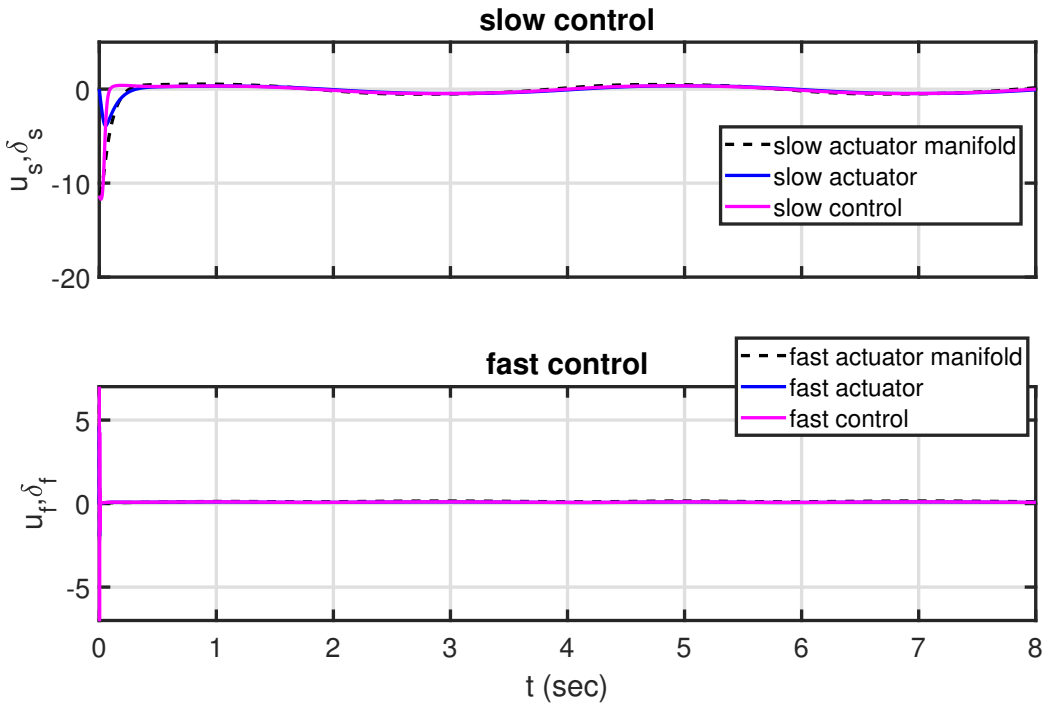

Figure 2.20: The slow and fast controls for four-time-scale example (2.189)

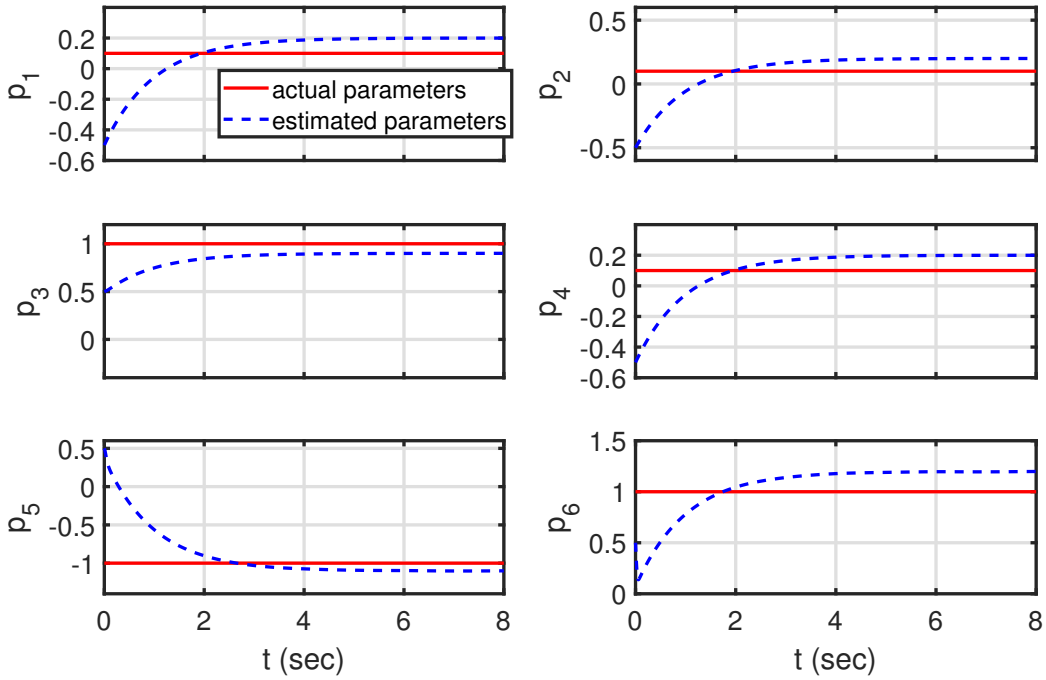

Figure 2.21: The uncertain parameters $p_1 - p_6$ for four-time-scale example (2.189)

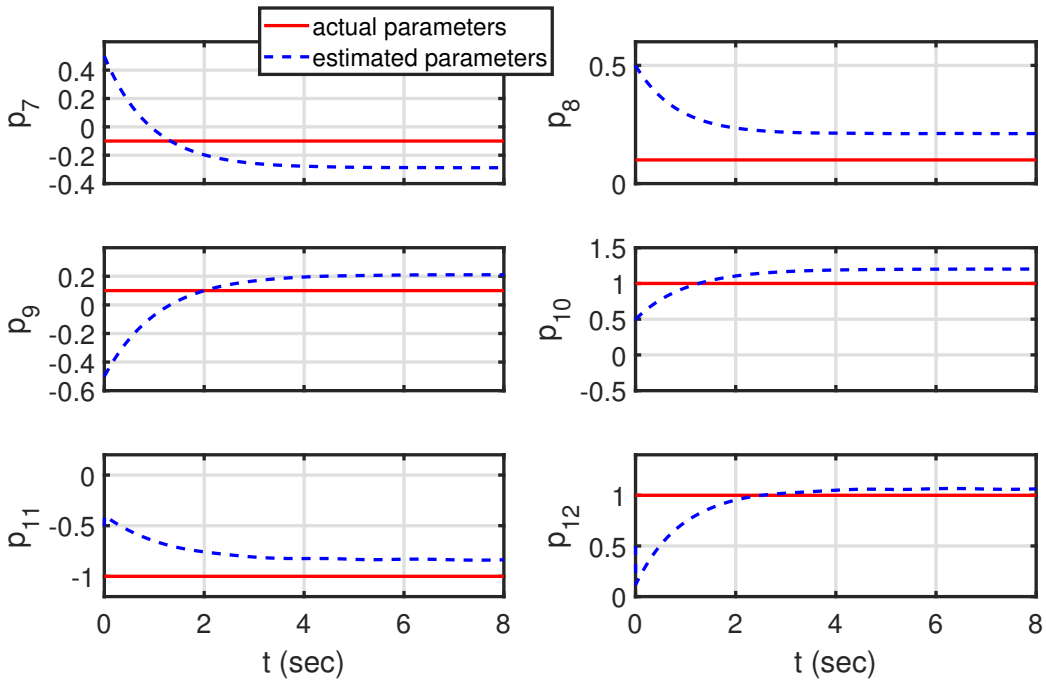

Figure 2.22: The uncertain parameters $p_7 - p_{12}$ for four-time-scale example (2.189)

2.6.4.2 *Aircraft Evaluation Maneuver I: Sequential 90 Degree Left and Right Turn Maneuver of a Generic F-16A*

Slow state tracking using the four-time-scale control and parameter estimation laws is shown in simulation on a nonlinear 6-DOF generic F-16A commanded to perform two different evaluation maneuvers. The first evaluation maneuver is from a previous work of Valasek [36]. For this evaluation maneuver, the generic F-16A is initially at trim in straight and level flight with a velocity of 800 ft/s at an altitude of 15,000 ft. The trim angle-of-attack and elevator deflection are 0.9 deg and -1.6 deg respectively. The thrust at trim is 3265.0 lbf, which is 18.34% of the maximum military thrust of 17,800 lbf. To ensure straight and level flight, the pitch attitude angle at trim is the same as the trim angle-of-attack. All other angles, rates and control surface deflections are zero at trim. The aircraft is commanded to perform a 90 deg left turn followed by a 90 deg right turn. The heading angle is desired to change by 90 deg in 10 seconds for each turn. Bank angle and pitch attitude angle associated with each turn are commanded to reach a maximum from zero, and

then come back to zero as the turn is complete. The maximum bank angle and pitch attitude angle associated with each turn are 75 deg and 15 deg respectively. Velocity is commanded to be close to its trim value of 800 ft/s throughout the maneuver.

The uncertainties are assumed as follows. The initial estimate of each of the inertias I_{xx}, I_{yy}, I_{zz}, I_{xz} is assumed 15% below its actual value. The initial estimate of each of the control derivatives $C_{x_{\delta_e}}, C_{y_{\delta_a}}, C_{y_{\delta_r}}, C_{z_{\delta_e}}, C_{m_{\delta_e}}, C_{l_{\delta_a}}, C_{l_{\delta_r}}, C_{n_{\delta_a}}, C_{n_{\delta_r}}$ is assumed 20% below its actual value. The engine time-constant is assumed 25% above its actual value. No uncertainty is assumed for the stability derivatives and the time-constants of the elevator, aileron and rudder.

The controller gains are selected as $K_x = 10$, $K_\xi = diag[1.2, 1.2, 1]$, $K_{\delta_s} = 0.02$, $K_z = diag[100, 100, 100]$, $K_{\delta_f} = diag[0.5, 2, 0.05]$. To design the parameter estimator, gains are selected as $\alpha_1 = 10^{-13}, \alpha_2 = 10^{-14}, \alpha_3 = 10^{-15}, \alpha_8 = 1, \alpha_9 = 1, \alpha_{10} = 1, , \alpha_{111} = 1, \alpha_{112} = 1, \alpha_{12} = 1, \theta_i = 0.1; i = 4, 5, 6, 7, 8$. The design variables corresponding to the final value of the estimates in the parameter update laws are chosen such that the inertias, control derivatives and engine time-constant are 5% above the actual values. The simulation is run for 80 sec.

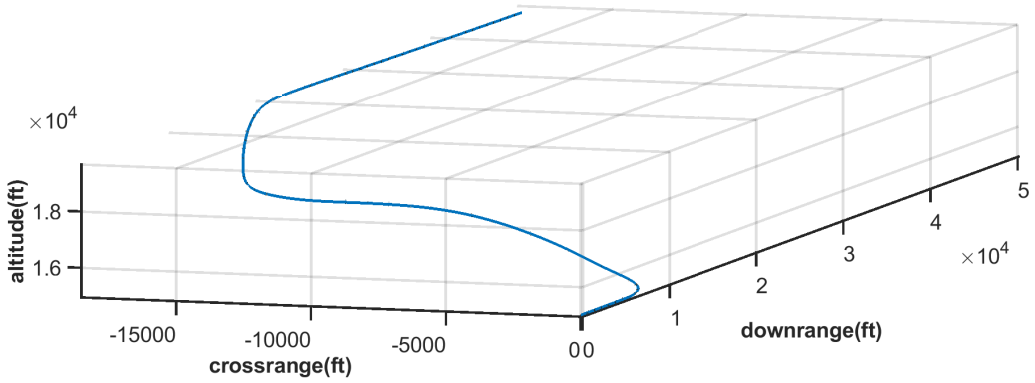

Figure 2.23: Trajectory of the generic F-16A during left and right turn

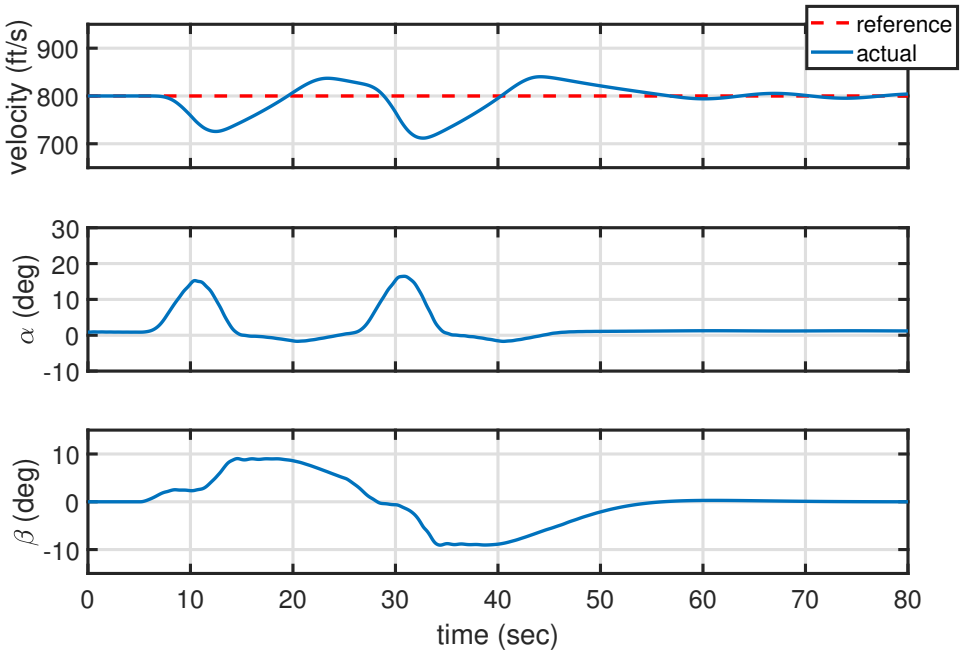

Figure 2.24: Velocity, angle-of-attack and sideslip angle during left and right turn

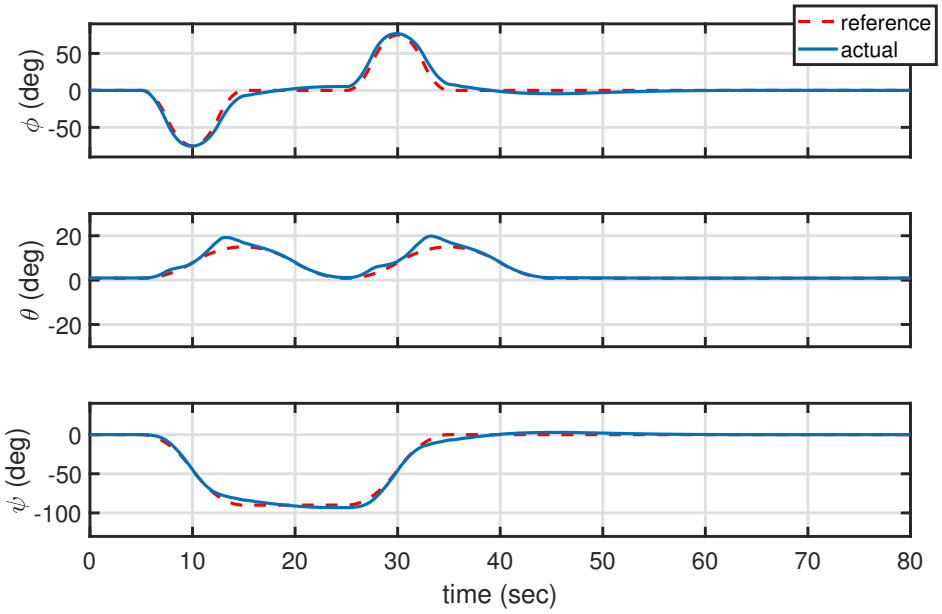

Figure 2.25: Bank angle, pitch attitude angle and heading angle during left and right turn

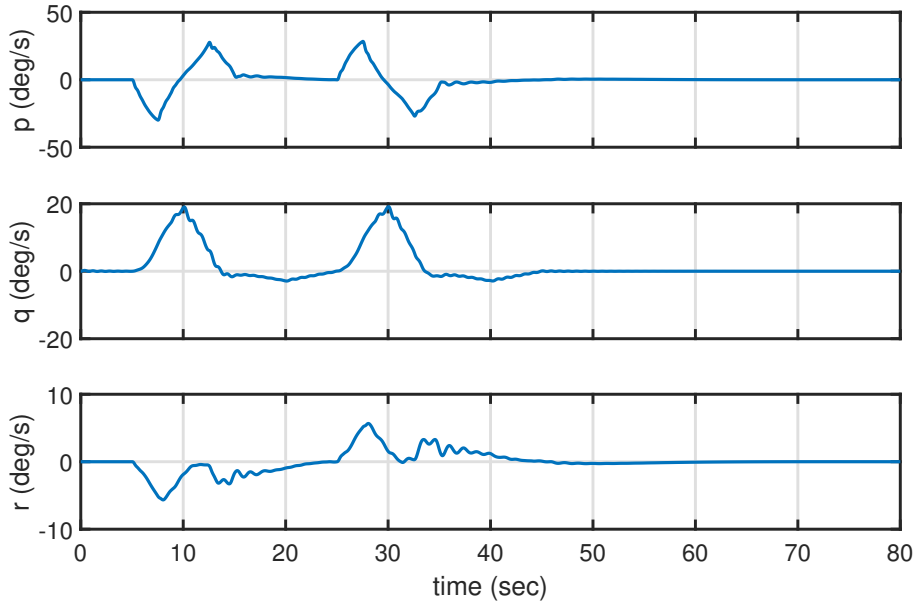

Figure 2.26: Body-axis roll, pitch and yaw rates during left and right turn

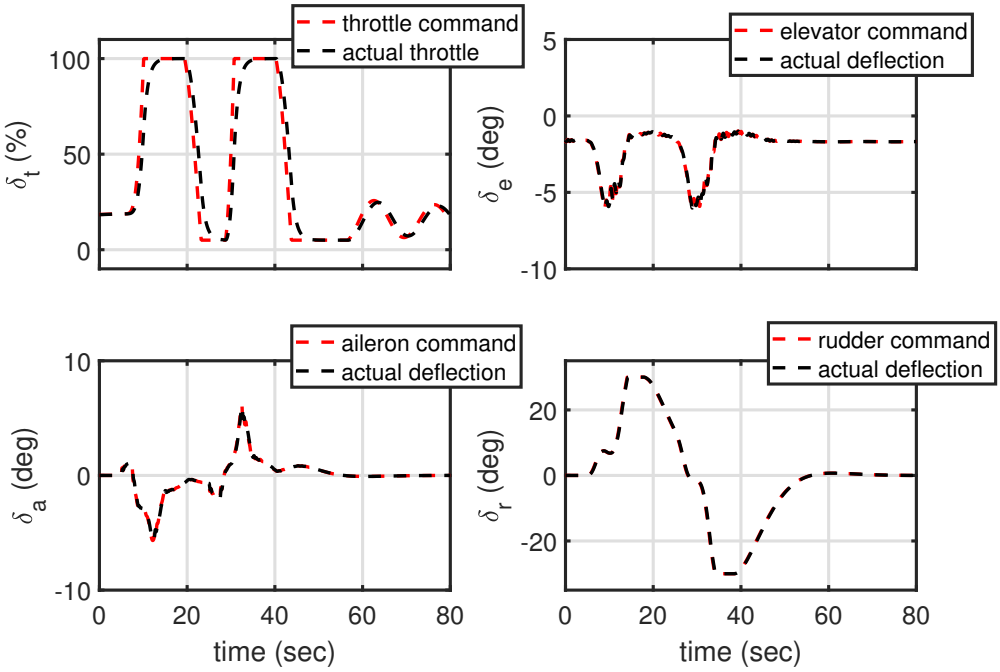

Figure 2.27: Throttle, elevator, aileron and rudder deflections during left and right turn

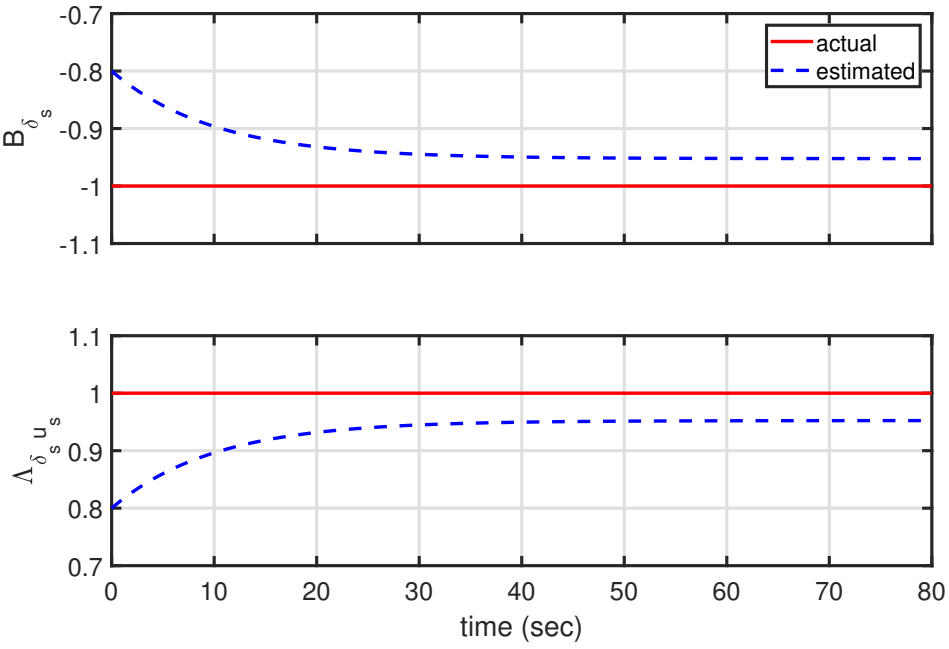

Figure 2.28: Uncertain parameters B_{δ_s} and $\Lambda_{\delta_s u_s}$ during left and right turn

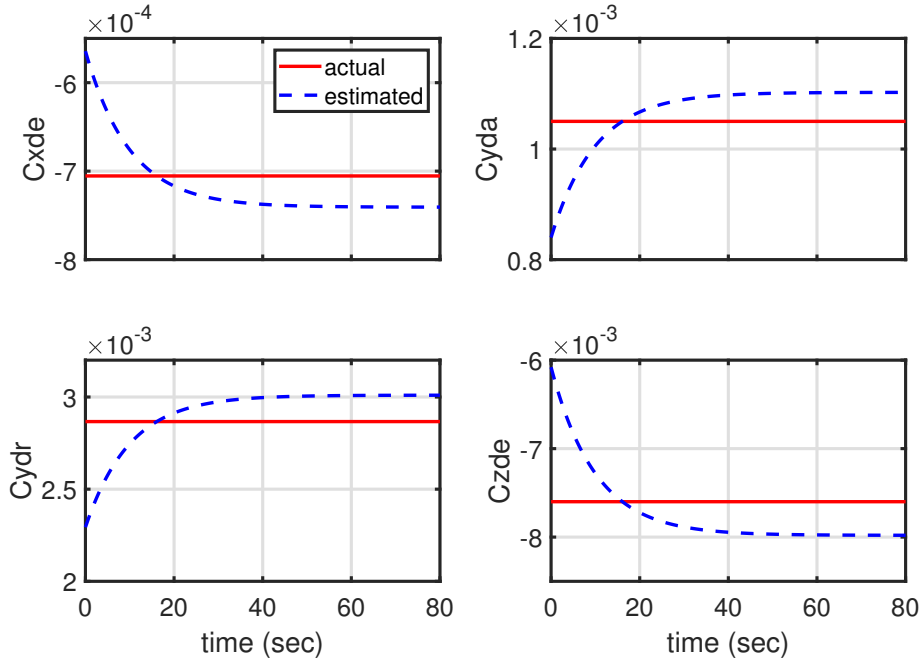

Figure 2.29: Uncertain parameters $C_{x_{\delta_e}}, C_{y_{\delta_a}}, C_{y_{\delta_r}}, C_{z_{\delta_e}}$ during left and right turn

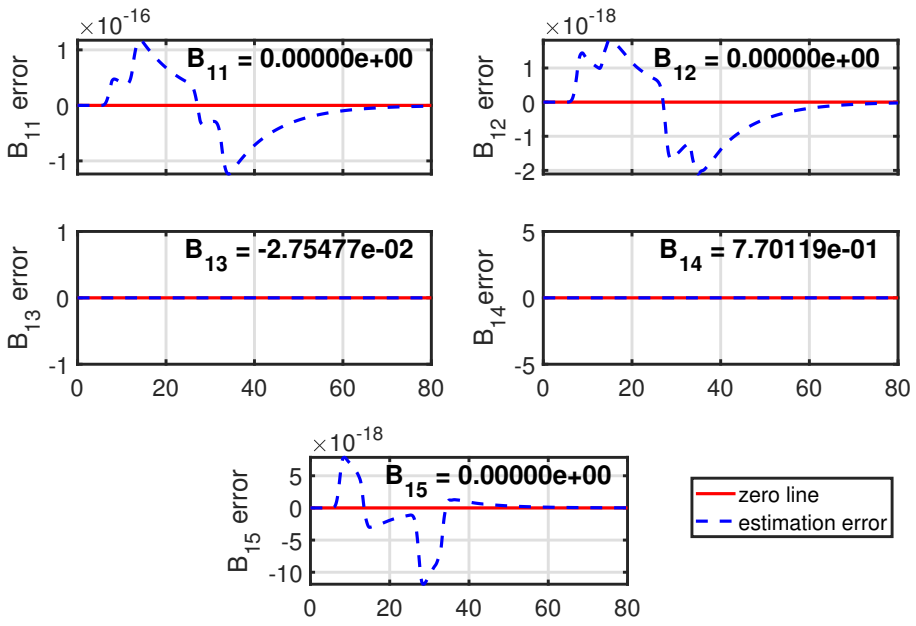

Figure 2.30: Uncertain parameters $B_{11} - B_{15}$ during left and right turn; the x-axis of each graph representing time in seconds

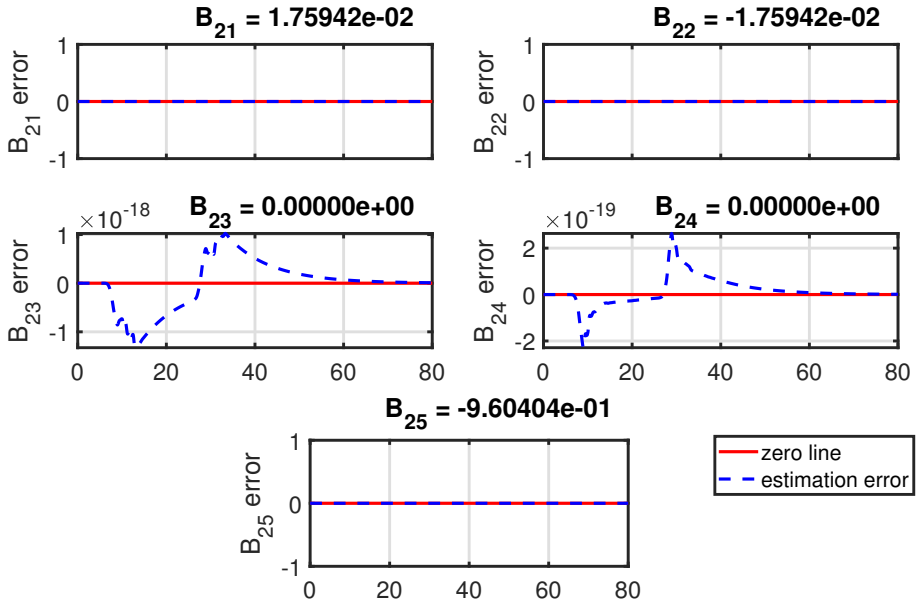

Figure 2.31: Uncertain parameters $B_{21} - B_{25}$ during left and right turn; the x-axis of each graph representing time in seconds

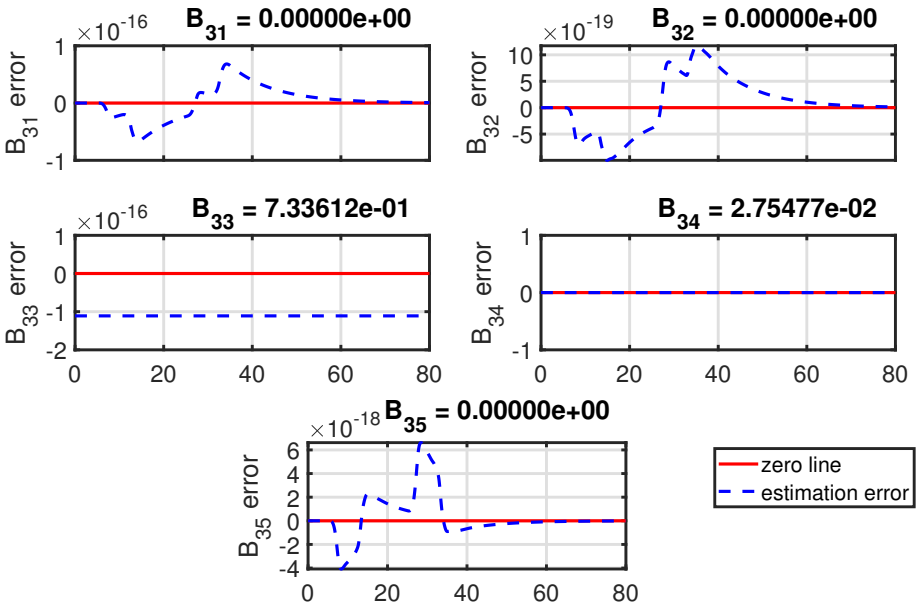

Figure 2.32: Uncertain parameters $B_{31} - B_{35}$ during left and right turn; the x-axis of each graph representing time in seconds

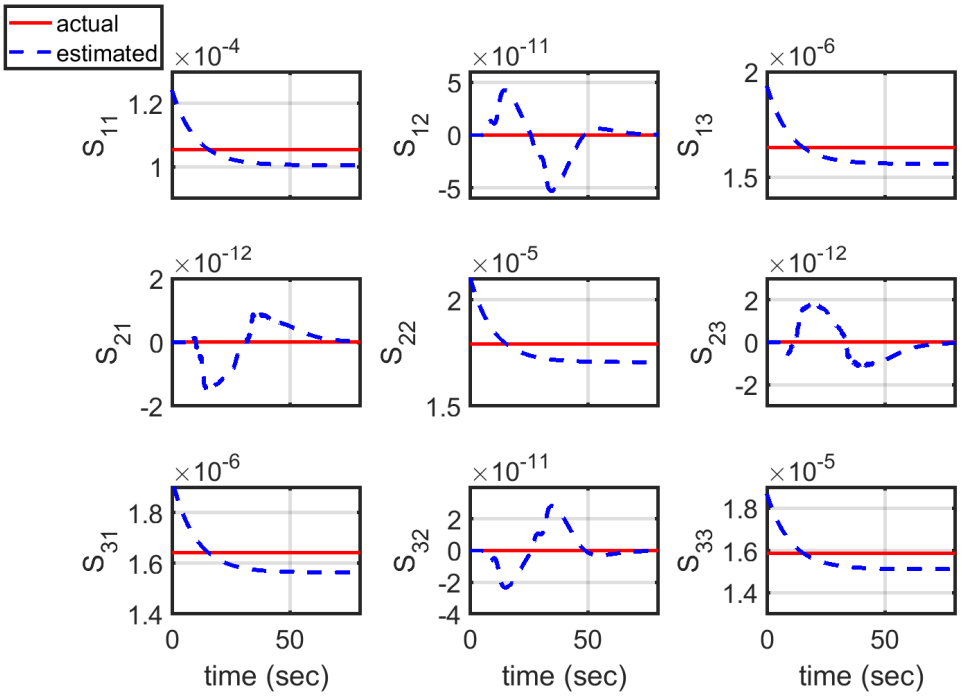

Figure 2.33: Uncertain parameters $S_{31} - S_{33}$ during left and right turn

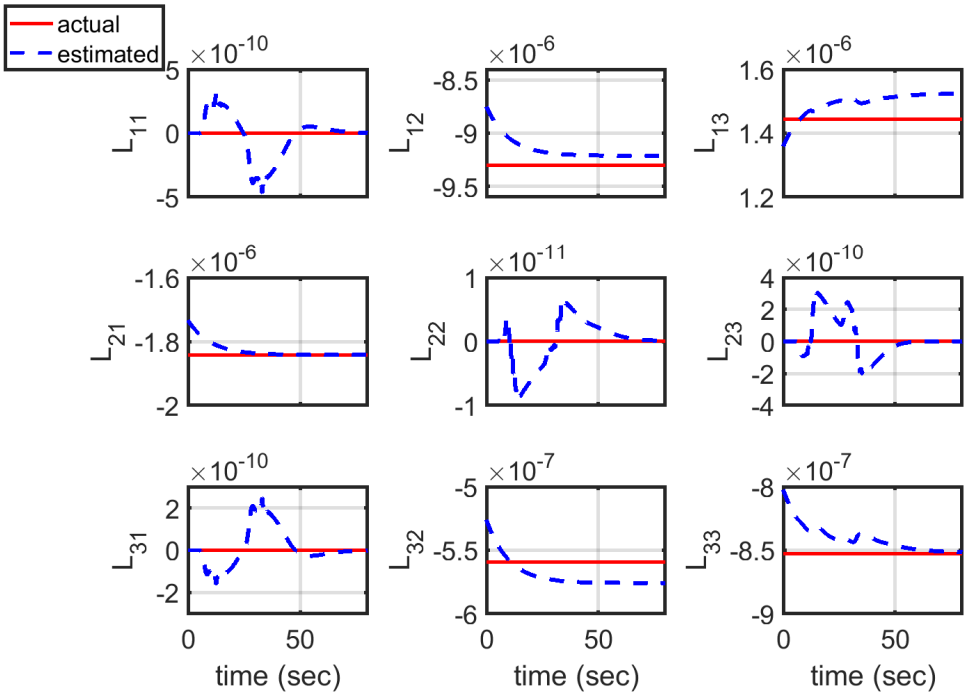

Figure 2.34: Uncertain parameters $L_{11} - L_{33}$ during left and right turn

Figures 2.23 - 2.27 shows the time-history of the aircraft states and controls. Figure 2.23 shows the aircraft performing a 90 deg left turn followed by a 90 deg right turn. Figure 2.24 shows that the loss of airspeed during the maneuver is within 100 ft/s. The lost airspeed is recovered as soon as each turn is complete. Figure 2.25 show that kinematic angles are well-tracked. Figure 2.27 shows that the throttle goes from trim to full once each turn is initiated, and back to lower values once each turn is complete. Because of the slow engine dynamics, the actual throttle follows the commanded throttle with a time-delay. In contrast, the aerodynamic controls are seen respond much faster to a change in the control commands. It can be seen from Figures 2.25, 2.26 and 2.27 that the angle-of-attack, sideslip angle and body-axis rates are bounded, and that the control surface deflections are within acceptable limits.

Figures 2.28 - 2.34 show the evolutions of the uncertain parameters. It can be seen that the parameter estimation errors remain bounded. Specifically, for the B matrix which is obtained by multiplying inertia matrix with its inverse, the estimation errors are significantly small in

magnitude. Overall, Figures 2.23 - 2.34 show a successful slow state tracking maneuver with bounded and small parameter estimation errors.

2.6.4.3 Aircraft Evaluation Maneuver II: A Turn Maneuver Performed in an Engineering Flight Simulator

The second evaluation maneuver was generated by flying an F-16A in the XPlane 10 engineering flight simulator in the Vehicle Systems & Control Laboratory. For this maneuver, the generic F-16A is initially at trim in straight and level flight with a velocity of 500 knots, i.e. 843.9 ft/s at an altitude of 15,000 ft. The trim angle-of-attack and elevator deflection are 0.6 deg and -1.5 deg respectively. The thrust at trim is 3630.3 lbf, which is 20.4% of the maximum military thrust of 17,800 lbf. The pitch attitude angle at trim is the same as the trim angle-of-attack so the flight path angle is zero. The initial heading angle of the aircraft is 100 deg. All other angles, rates and control surface deflections are zero at trim. In flight simulator the aircraft is commanded to perform a left turn changing its heading angle to about 80 deg and then a right turn to change the heading to about 110 deg. Each heading change is commanded to occur over a time span of 5 sec. The maximum bank angle and pitch attitude angle are within 60 deg and 10 deg respectively. The velocity stays within 50 ft/s of the trim value throughout the maneuver. Uncertainties are assumed exactly the same as the ones for the previous evaluation maneuver.

To simulate this maneuver The controller gains are selected as $K_x = 5$, $K_\xi = diag[2, 4, 2]$, $K_{\delta_s} = 1$, $K_z = diag[15, 15, 15]$, $K_{\delta_f} = diag[1, 1, 1]$. To design the parameter estimator, gains are chosen as $\alpha_1 = 10^{-13}, \alpha_2 = 10^{-14}, \alpha_3 = 10^{-15}, \alpha_8 = 1, \alpha_9 = 1, \alpha_{10} = 1, , \alpha_{111} = 1, \alpha_{112} = 1, \alpha_{12} = 1, \theta_i = 0.5; i = 4, 5, 6, 7, 8$. The design variables corresponding to the final value of the estimates in the parameter update laws are chosen such that the inertias, control derivatives and engine time-constant are 5% above the actual values. The simulation is run for 22 sec.

Figures 2.35 - 2.39 shows the time-history of the aircraft states and controls during the maneuver. Figure 2.35 shows a left turn causing the heading angle to decrease to 80 degrees, followed by a right turn causing the heading angle to increase to 110 degrees. Figure 2.36 shows that the actual velocity is very close the reference throughout the maneuver. Figure 2.37 show that kinematic

angles are well-tracked. Figure 2.39 shows the throttle responding to the change in command with a small time-delay due to the slow engine dynamics, whereas the aerodynamic controls respond much faster to any change in command. It can be seen from Figures 2.37, 2.38 and 2.39 that the angle-of-attack, sideslip angle and body-axis rates are bounded, and that the control surface deflections are within acceptable limits.

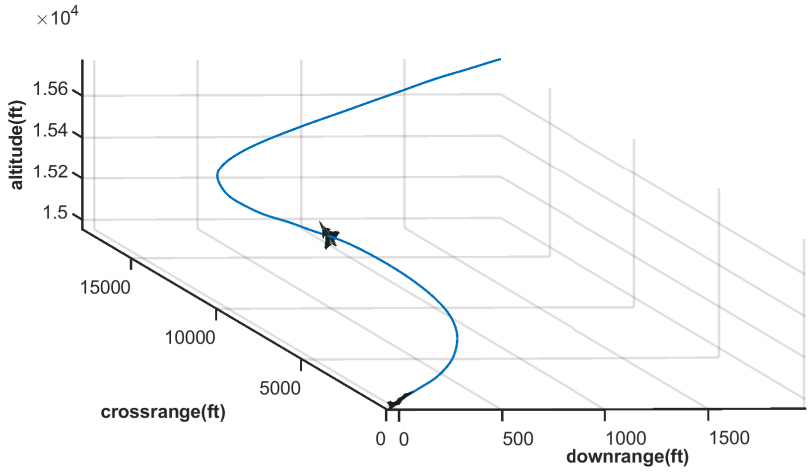

Figure 2.35: Trajectory of the generic F-16A during the flight simulator maneuver

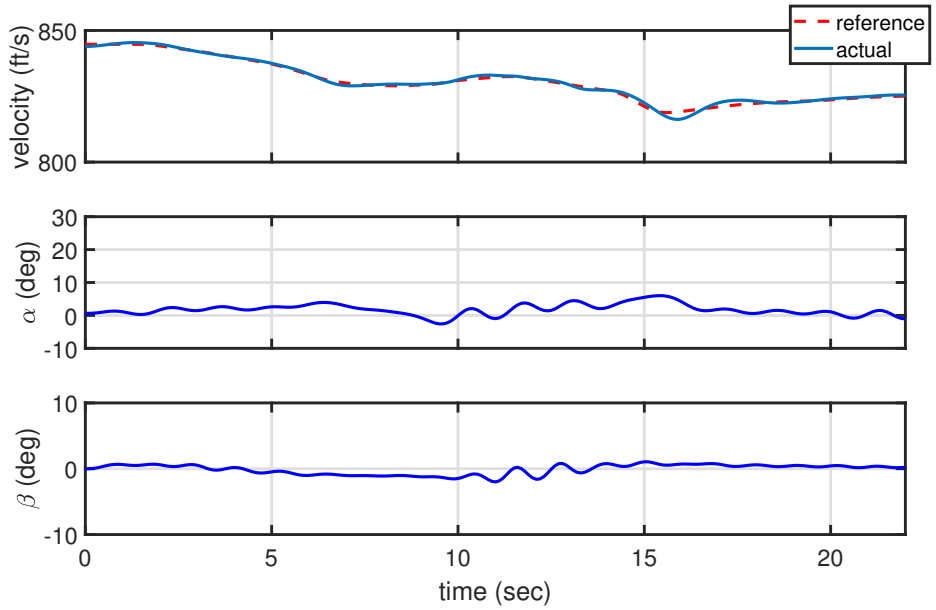

Figure 2.36: Velocity, angle-of-attack and sideslip angle during the flight simulator maneuver

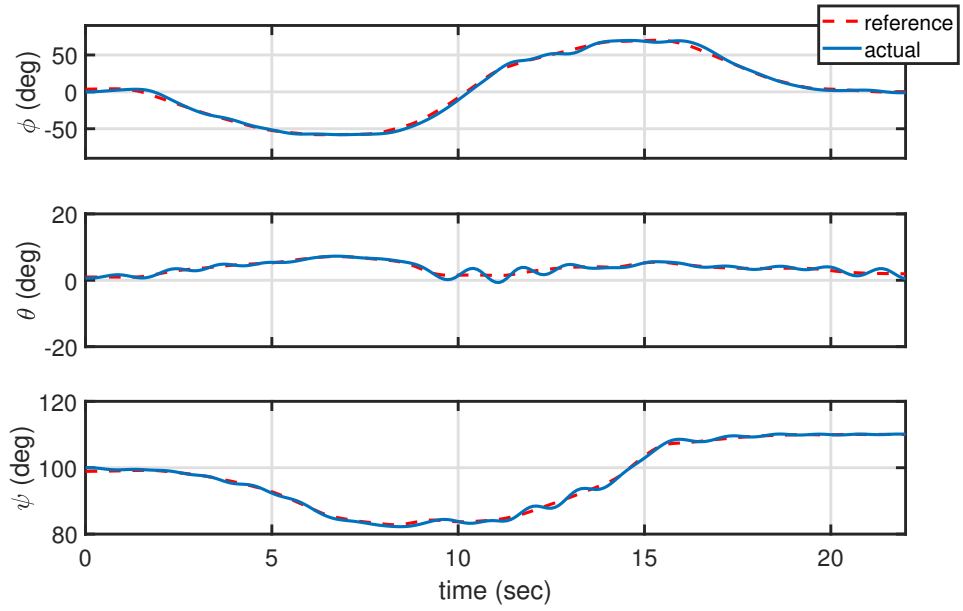

Figure 2.37: Bank angle, pitch attitude angle and heading angle during the flight simulator maneuver

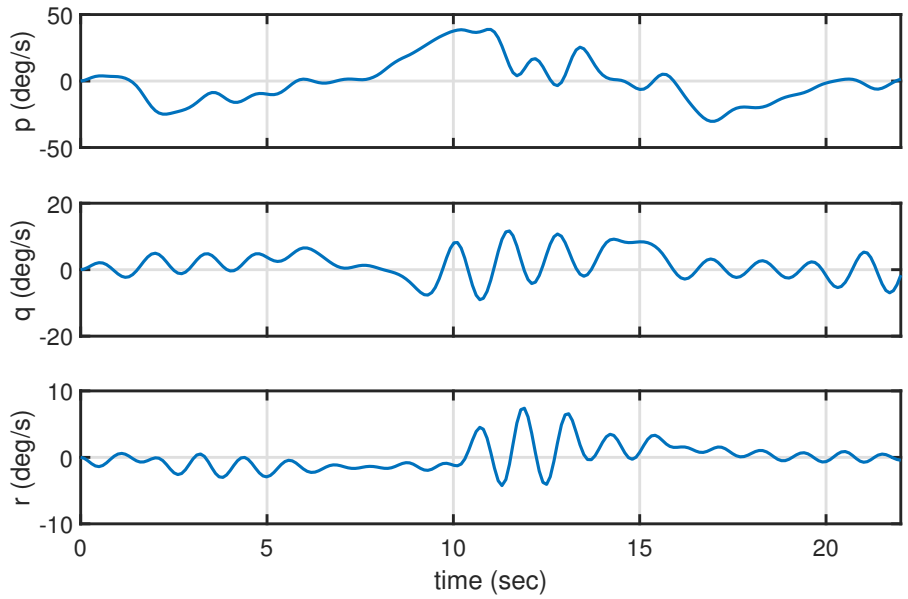

Figure 2.38: Body-axis roll, pitch and yaw rates during the flight simulator maneuver

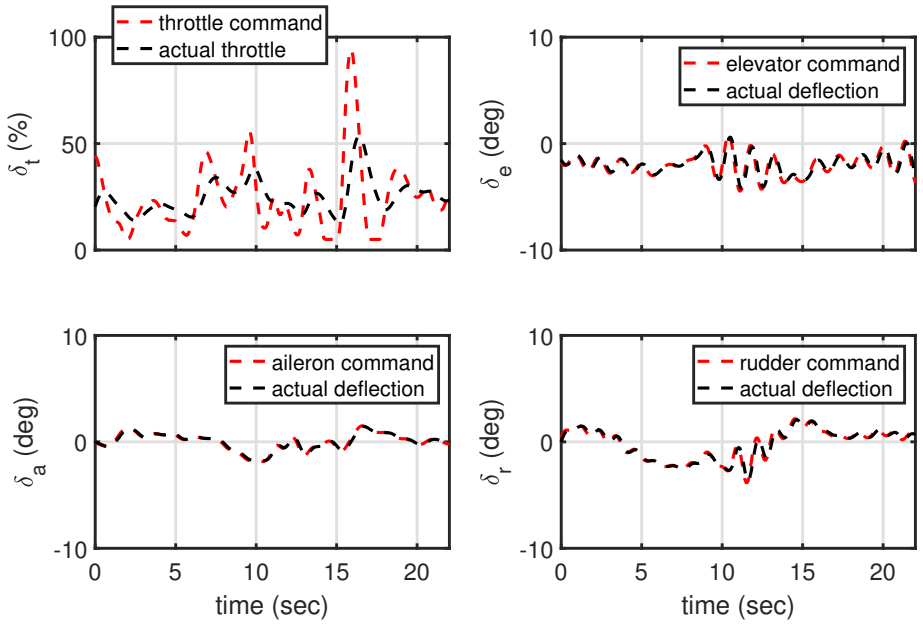

Figure 2.39: Throttle, elevator, aileron and rudder deflections during the flight simulator maneuver

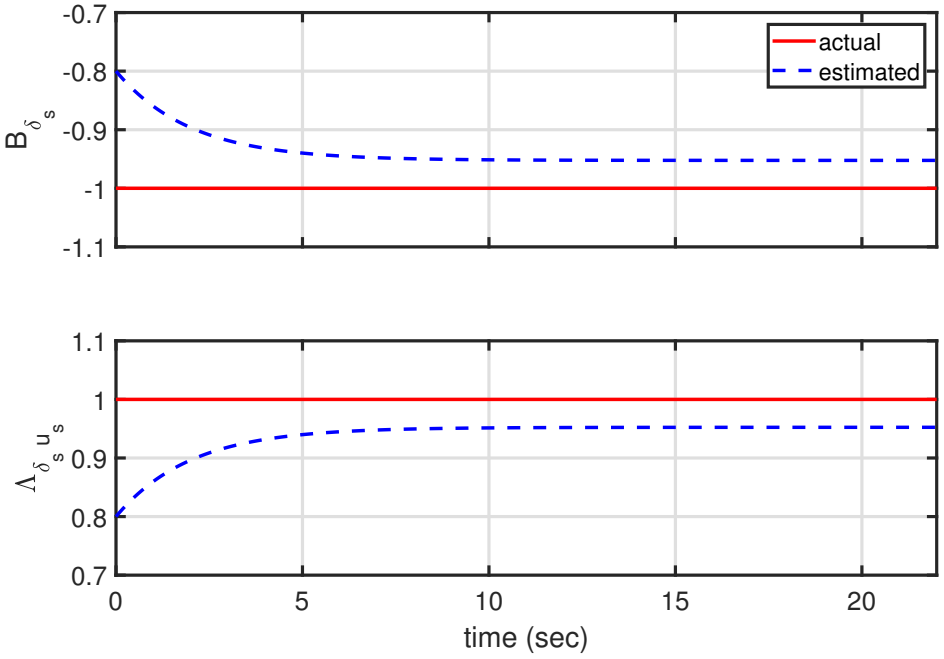

Figure 2.40: Uncertain parameters B_{δ_s} and $\Lambda_{\delta_s u_s}$ during the flight simulator maneuver

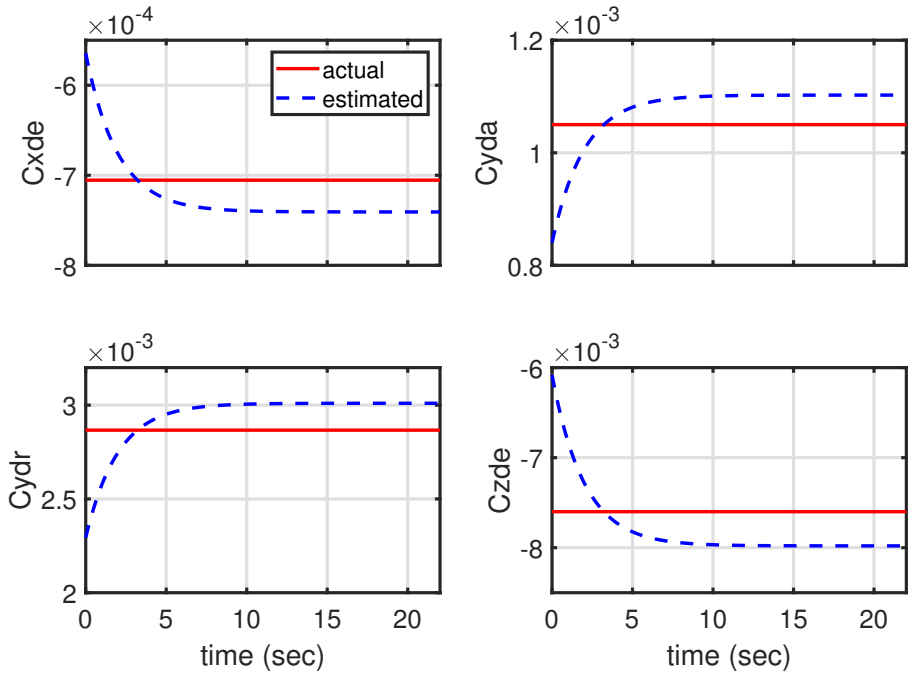

Figure 2.41: Uncertain parameters $C_{x_{\delta_e}}, C_{y_{\delta_a}}, C_{y_{\delta_r}}, C_{z_{\delta_e}}$ during the flight simulator maneuver

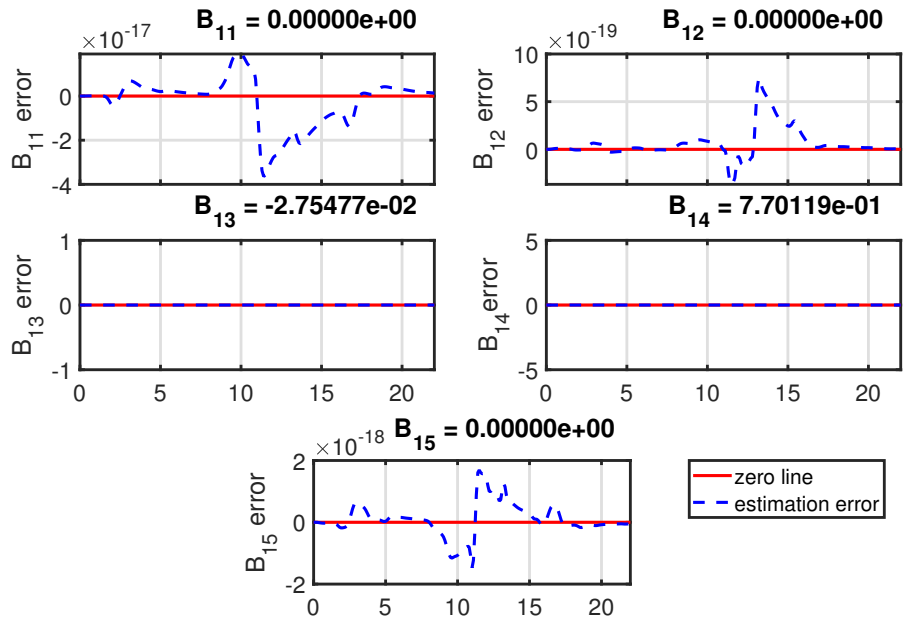

Figure 2.42: Uncertain parameters $B_{11} - B_{15}$ during the flight simulator maneuver; the x-axis of each graph representing time in seconds

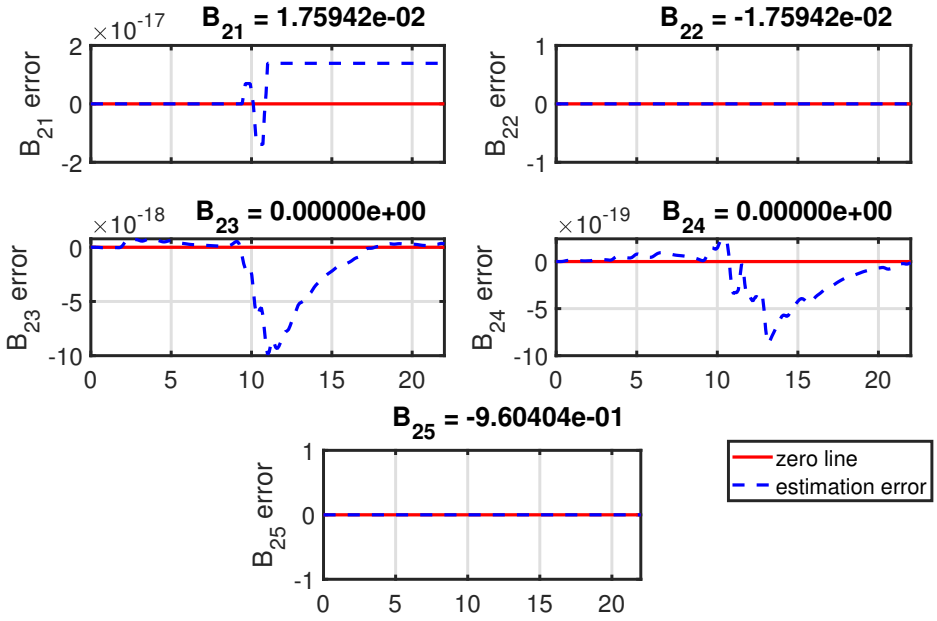

Figure 2.43: Uncertain parameters $B_{21} - B_{25}$ during the flight simulator maneuver; the x-axis of each graph representing time in seconds

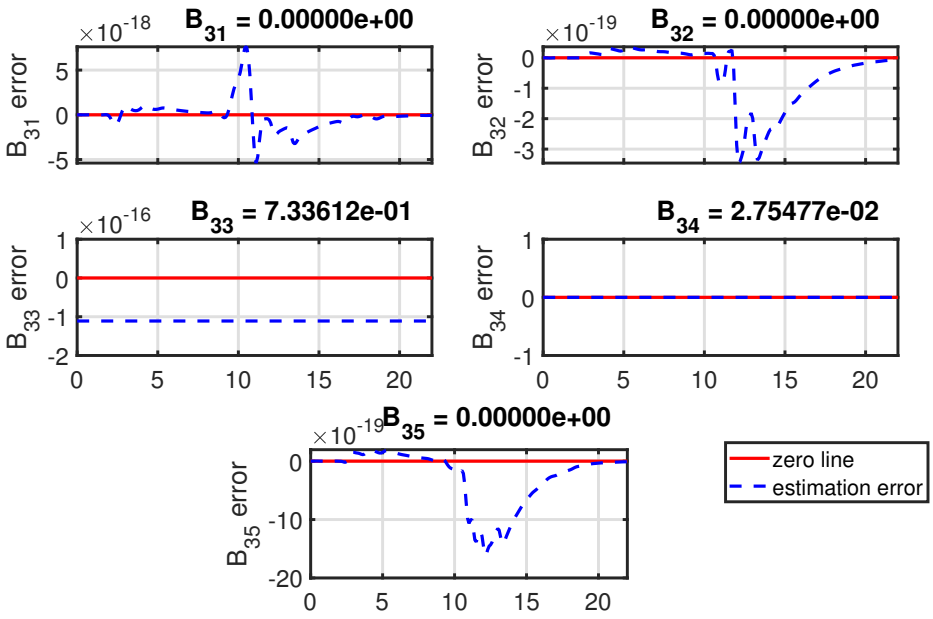

Figure 2.44: Uncertain parameters $B_{31} - B_{35}$ during the flight simulator maneuver; the x-axis of each graph representing time in seconds

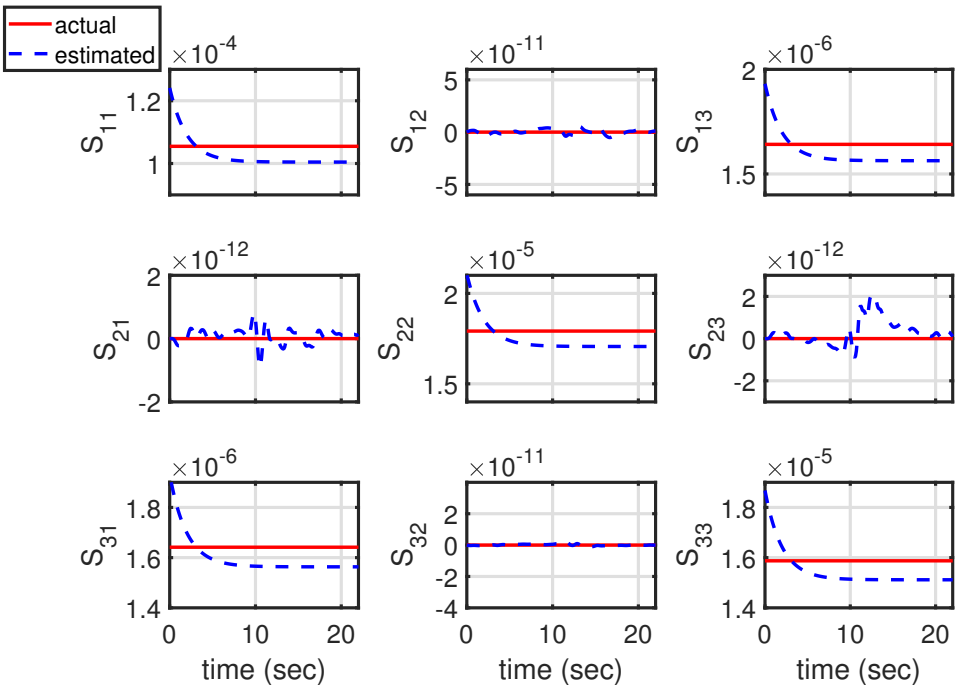

Figure 2.45: Uncertain parameters $S_{31} - S_{33}$ during the flight simulator maneuver

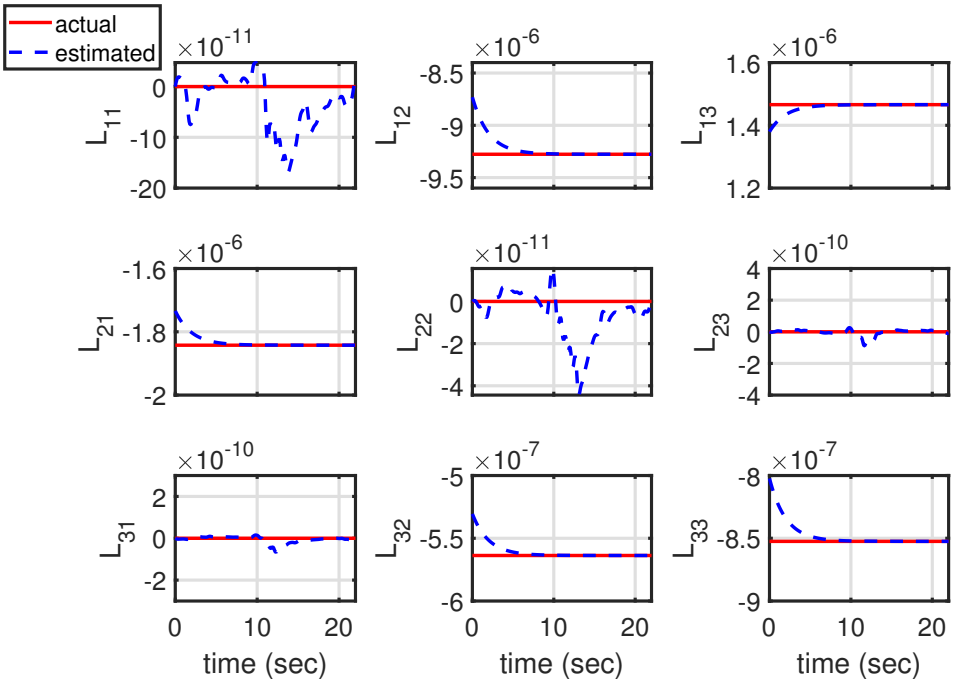

Figure 2.46: Uncertain parameters $L_{11} - L_{33}$ during the flight simulator maneuver

Figures 2.40 - 2.46 show the evolutions of the uncertain parameters. It can be seen that the parameter estimation errors remain bounded. Specifically, for the B matrix which is obtained by multiplying inertia matrix with its inverse, the estimation errors are significantly small in magnitude. Similar to the previous aircraft turn maneuver, Figures 2.35 - 2.46 show a successful slow state tracking maneuver with bounded and small parameter estimation errors.

2.7 Concluding Remarks for the Chapter

This chapter investigated and developed a theory of slow state tracking for finite-dimensional, nonlinear, nonstandard multiple-time-scale systems with uncertainties in model structure and parameters. The control objective of slow state tracking was accomplished using a sequential controller using the best estimates of the unknown parameters and an online parameter estimator updating the estimates. Spacecraft attitude control and aircraft turn maneuvers were demonstrated as examples.

The theory developed in this chapter significantly increased the capability of slow state tracking

control design for nonstandard systems. The theory accounted for parametric uncertainties in the dynamics as well as in the control distribution of all of the following: slow states, slow actuators, fast states and fast actuators. In addition, additive uncertainties in the evolution of slow and fast states were also accounted for. The development realistically accounted for slow and fast actuator dynamics instead of assuming all actuators to be infinitely fast, or adding actuator dynamics only in simulation. All these aspects together were applicable to aerospace applications such as aircraft and spacecraft with multiple time-scales and uncertainties.

The development was simplified by utilizing the fact that kinematic states do not have any uncertainty in their evolution. Therefore, kinetic and kinematic slow states were considered separately. In addition to how uncertainty was handled, this consideration resulted in decoupled selections of the manifolds of the fast states and slow actuators in the slowest time-scale. For slow state tracking of an aircraft, the selection of velocity and kinematic angles as states to be tracked was a direct consequence of this consideration.

Using composite Lyapunov analysis, it was proved that the tracking error of the slow states, the manifold error of the fast states and actuators, and the estimation error of the unknown parameters remain ultimately bounded. To ensure ultimate boundedness, this method established new bounds of the time-scale separation parameters: $\sigma_{**}, \sigma^{**}, \varepsilon_{**}, \varepsilon^{**}, \rho_{**}, \rho^{**}$. The explicit differentiations of the manifolds was cumbersome for the classes of systems considered as three-time-scale and four-time-scale. The use of compact sets and extreme value theorem helped avoid the explicit differentiation and simplified the boundedness proof.

While this method considered actuator dynamics and thereby actuator rate limits, magnitude limits of actuators were not realistically accounted for in the control design. The control signals were kept within acceptable limits implicitly with gains. However, for some maneuvers such as the sequential Euler angle rotation of spacecraft or the 90 degree left and right turn of aircraft, it was seen that some or all of the controls were saturated for a while. An improved version of the theory is needed to handle actuator magnitude limits realistically in the design.

Uncertainties were assumed in the deterministic sense instead of stochastic. While parametric

uncertainties could be taken care of, handling certain types of disturbances such as gust and turbulence in aircraft requires an improved version of the theory with stochastic uncertainties. A major challenge to overcome is to rigorously prove stability using stochastic Lyapunov functions.

This method relied on several parameter estimate matrices being invertible, especially the ones appearing in the control distribution. A way to ensure invertibility was to wisely choose the initial conditions and design parameters corresponding to final values of the estimates. An updated version of the theory is needed to realistically account for singularities in control distribution.

3. SIMULTANEOUS SLOW AND FAST STATE TRACKING IN THE PRESENCE OF UNCERTAINTIES AND ACTUATOR DYNAMICS WITH FULL-STATE FEEDBACK

3.1 Introduction

This chapter addresses the second objective of simultaneous slow and fast tracking for uncertain nonlinear, nonstandard multiple-time-scale systems using full-state feedback. In contrast to slow state tracking, the fast states need to reach their reference trajectory instead of any suitable equilibrium manifold, so the method of sequential control for slow state tracking cannot be applied directly. Simultaneous slow and fast tracking was previously accomplished using a two-stage design [11]. While the two-stage design ensured closed-loop stability, it did not consider two very important aspects: (i) slow and fast actuator dynamics, and (ii) uncertainties.

To show a clear distinction between the two-stage design approach and the new sequential approach developed in this work, the control law development for simultaneous slow and fast tracking of a deterministic two-time-scale aircraft model is reviewed in Section 3.2. Section 3.3 shows the new approach which includes actuator dynamics and uncertainties. The addition of slow and fast actuator dynamics increases the number of time-scales from two to four. In addition, the control problem is formulated in a way that makes it convenient to use an approach similar to the sequential approach for slow state tracking developed in Section 2.6. Concluding remarks are in Section 3.4.

3.2 Review of the Earlier Two-Stage Design: Climb and Roll Maneuver of a Nonlinear Six-Degree-of-Freedom Aircraft

[1] A control law for simultaneous slow and fast state tracking of a generic nonlinear nonstandard two-time-scale system along with stability guarantees was developed in Narang-Siddarth and Valasek [11]. The authors implemented the control law on a nonlinear 6-DOF generic F/A-18A aircraft

[1] Section 3.2 of this dissertation is from Saha and Valasek [37], reprinted by permission of the American Institute of Aeronautics and Astronautics, Inc.

commanded to perform a climb and roll maneuver. For this maneuver, the velocity was not tracked, and the throttle was kept constant. Only the three aerodynamic controls were used to track sideslip angle and body-axis roll and pitch rates. It was seen from the simulation that the aircraft lost almost half of its airspeed during climb. A later work of Saha and Valasek [37] followed the theory of two-stage design but made some important modifications. This work introduced tracking of velocity and used throttle as an automatic control to reduce the loss of airspeed. This is the work detailed in Subsections 3.2.1 - 3.2.3. Subsection 3.2.4 explains the limitations of this approach and establishes the need for a new theory.

3.2.1 Two-Time-Scale Aircraft Model

The 6-DOF model has a total of 12 states. The system has more states than controls, so for developing the control law four states are chosen for tracking. Velocity and sideslip angle are the slow states to be tracked. The fast ones to be tracked are the body-axis roll and pitch rates. The dynamics of the four states to be tracked can be written in the following form:

$$\begin{bmatrix} \dot{v}_A \\ \dot{\beta} \\ \varepsilon\dot{p} \\ \varepsilon\dot{q} \end{bmatrix} = J(.)_{4\times1} + K(.)_{4\times4} \begin{bmatrix} \delta_t \\ \delta_e \\ \delta_a \\ \delta_r \end{bmatrix} \tag{3.1}$$

where the vector J and the matrix K are functions of states and system parameters. These functions are derived from the equations of motion in Appendix B. The factor ε is introduced artificially in front of the time-derivatives of the body-axis roll rate p and pitch rate q to indicate that they are the fast states.

3.2.2 Development of Control Law Using Reduced Subsystems

The control is to be designed such that the states v_A, β, p, q track their references v_{A_r}, β_r, p_r, q_r respectively. The tracking problem is converted to an equivalent stabilization problem in terms

of the error coordinates

$$\begin{aligned} e_{v_A} &:= v_A - v_{A_r} \\ e_\beta &:= \beta - \beta_r \\ e_p &:= p - p_r \\ e_q &:= q - q_r \end{aligned} \tag{3.2}$$

where all the errors should go to zero. The error dynamics are

$$\begin{bmatrix} \dot{e}_{v_A} \\ \dot{e}_\beta \\ \varepsilon\dot{e}_p \\ \varepsilon\dot{e}_q \end{bmatrix} = \begin{bmatrix} J_1(.) - \dot{V}_{A_r} \\ J_2(.) - \dot{\beta}_r \\ J_3(.) - \varepsilon\dot{p}_r \\ J_4(.) - \varepsilon\dot{q}_r \end{bmatrix} + K \begin{bmatrix} \delta_t \\ \delta_e \\ \delta_a \\ \delta_r \end{bmatrix} \tag{3.3}$$

According to the two-stage design approach, the control vector is the sum of two components:

$$\begin{bmatrix} \delta_t \\ \delta_e \\ \delta_a \\ \delta_r \end{bmatrix} = \begin{bmatrix} \delta_t^0 \\ \delta_e^0 \\ \delta_a^0 \\ \delta_r^0 \end{bmatrix} + \begin{bmatrix} \Delta\delta_t \\ \Delta\delta_e \\ \Delta\delta_a \\ \Delta\delta_r \end{bmatrix} \tag{3.4}$$

The first component is the effective control vector in the slow time-scale. The second component is the additional control which is present in the fast time-scale only. These two components are designed in the following two steps.

3.2.2.1 Step I: Design of One Component of Control in the Slow Time-Scale

In the slow time-scale the slow state errors *go to zero*. The fast state errors are assumed to have gone to zero already; they are required to *stay at zero*. This is achieved by considering the reduced

slow subsystem. Setting $\varepsilon = 0$ in (3.3), the reduced slow subsystem is

$$\begin{bmatrix} \dot{e}_{v_A} \\ \dot{e}_\beta \\ 0 \\ 0 \end{bmatrix} = \begin{bmatrix} J_1(.) - \dot{v}_{A_r} \\ J_2(.) - \dot{\beta}_r \\ J_3(.) \\ J_4(.) \end{bmatrix} + K \begin{bmatrix} \delta_t^0 \\ \delta_e^0 \\ \delta_a^0 \\ \delta_r^0 \end{bmatrix} \tag{3.5}$$

If the component of the control vector in the slow time-scale is designed as

$$\begin{bmatrix} \delta_t^0 \\ \delta_e^0 \\ \delta_a^0 \\ \delta_r^0 \end{bmatrix} = K^{-1}(- \begin{bmatrix} J_1(.) - \dot{v}_{A_r} \\ J_2(.) - \dot{\beta}_r \\ J_3(.) \\ J_4(.) \end{bmatrix} - \begin{bmatrix} a_{v_A} & 0 & 0 & 0 \\ 0 & a_\beta & 0 & 0 \\ 0 & 0 & a_p & 0 \\ 0 & 0 & 0 & a_q \end{bmatrix} \begin{bmatrix} e_{v_A} \\ e_\beta \\ e_p \\ e_q \end{bmatrix}) \tag{3.6}$$

then the closed-loop reduced slow subsystem becomes

$$\begin{aligned} \dot{e}_{v_A} &= -a_{v_A} e_{v_A} \\ \dot{e}_\beta &= -a_\beta e_\beta \\ 0 &= -a_p e_p \\ 0 &= -a_q e_q \end{aligned} \tag{3.7}$$

The gains are to be selected now such that the slow state errors e_{v_A} and e_β *reach zero* and the fast state errors e_p and e_q *stay at zero*. According to equation (3.7) the gains a_{v_A} and a_β need to be positive for closed-loop stability. Their values are to be selected to obtain the desired speed of response for velocity and sideslip angle. Moreover, an inspection of equation (3.7) reveals that The gains a_p and a_q at this point can be arbitrary non-zero numbers so the errors e_p, e_q stay identically at zero. The signs of the gains a_p, a_q will be specified in step II.

3.2.2.2 *Step II: Design of the Second Component of Control in the Fast Time-Scale*

In the fast time-scale the slow state errors are frozen at their initial values, and the fast state errors go to zero. This is achieved by considering the reduced fast subsystem. The full system in the fast time scale $\tau = \frac{t}{\varepsilon}$ is

$$\begin{bmatrix} e'_{v_A} \\ e'_{\beta} \\ e'_{p} \\ e'_{q} \end{bmatrix} = \begin{bmatrix} \varepsilon(J_1(.) - \dot{v}_{A_r}) \\ \varepsilon(J_2(.) - \dot{\beta}_r) \\ J_3(.) - p'_r \\ J_4(.) - q'_r \end{bmatrix} + \begin{bmatrix} \varepsilon K_{11} & \varepsilon K_{12} & \varepsilon K_{13} & \varepsilon K_{14} \\ \varepsilon K_{21} & \varepsilon K_{22} & \varepsilon K_{23} & \varepsilon K_{24} \\ K_{31} & K_{32} & K_{33} & K_{34} \\ K_{41} & K_{42} & K_{43} & K_{44} \end{bmatrix} \begin{bmatrix} \delta_t^0 + \Delta\delta_t \\ \delta_e^0 + \Delta\delta_e \\ \delta_a^0 + \Delta\delta_a \\ \delta_r^0 + \Delta\delta_r \end{bmatrix} \tag{3.8}$$

Setting $\varepsilon = 0$ in (3.8), the reduced fast subsystem is

$$\begin{bmatrix} e'_{v_A} \\ e'_{\beta} \\ e'_{p} \\ e'_{q} \end{bmatrix} = \begin{bmatrix} 0 \\ 0 \\ J_3(.) - p'_r \\ J_4(.) - q'_r \end{bmatrix} + \begin{bmatrix} 0 & 0 & 0 & 0 \\ 0 & 0 & 0 & 0 \\ K_{31} & K_{32} & K_{33} & K_{34} \\ K_{41} & K_{42} & K_{43} & K_{44} \end{bmatrix} \begin{bmatrix} \delta_t^0 + \Delta\delta_t \\ \delta_e^0 + \Delta\delta_e \\ \delta_a^0 + \Delta\delta_a \\ \delta_r^0 + \Delta\delta_r \end{bmatrix} \tag{3.9}$$

From (3.9) the fast state error dynamics can be isolated as

$$\begin{bmatrix} e'_{p} \\ e'_{q} \end{bmatrix} = \begin{bmatrix} J_3(.) - p'_r \\ J_4(.) - q'_r \end{bmatrix} + \begin{bmatrix} K_{31} & K_{32} & K_{33} & K_{34} \\ K_{41} & K_{42} & K_{43} & K_{44} \end{bmatrix} \begin{bmatrix} \delta_t^0 \\ \delta_e^0 \\ \delta_a^0 \\ \delta_r^0 \end{bmatrix} + \begin{bmatrix} K_{31} & K_{32} & K_{33} & K_{34} \\ K_{41} & K_{42} & K_{43} & K_{44} \end{bmatrix} \begin{bmatrix} \Delta\delta_t \\ \Delta\delta_e \\ \Delta\delta_a \\ \Delta\delta_r \end{bmatrix} \tag{3.10}$$

By the choice of the control vector in the slow time-scale as in equation (3.6)

$$\begin{bmatrix} K_{31} & K_{32} & K_{33} & K_{34} \\ K_{41} & K_{42} & K_{43} & K_{44} \end{bmatrix} \begin{bmatrix} \delta_t^0 \\ \delta_e^0 \\ \delta_a^0 \\ \delta_r^0 \end{bmatrix} = - \begin{bmatrix} J_3(.) + a_p e_p \\ J_4(.) + a_q e_q \end{bmatrix} \tag{3.11}$$

Therefore, the fast dynamics simplify to

$$\begin{bmatrix} e'_p \\ e'_q \end{bmatrix} = - \begin{bmatrix} p'_r \\ q'_r \end{bmatrix} - \begin{bmatrix} a_p e_p \\ a_q e_q \end{bmatrix} + \begin{bmatrix} K_{31} & K_{32} & K_{33} & K_{34} \\ K_{41} & K_{42} & K_{43} & K_{44} \end{bmatrix} \begin{bmatrix} \Delta\delta_t \\ \Delta\delta_e \\ \Delta\delta_a \\ \Delta\delta_r \end{bmatrix} \tag{3.12}$$

If the additional component of the control in the fast time-scale is selected as

$$\begin{bmatrix} \Delta\delta_t \\ \Delta\delta_e \\ \Delta\delta_a \\ \Delta\delta_r \end{bmatrix} = K^{-1} \begin{bmatrix} 0 \\ 0 \\ p'_r \\ q'_r \end{bmatrix} \tag{3.13}$$

then the closed-loop reduced fast subsystem becomes

$$\begin{aligned} e'_{v_A} &= 0 \\ e'_\beta &= 0 \\ e'_p &= -a_p e_p \\ e'_q &= -a_q e_q \end{aligned} \tag{3.14}$$

According to equation (3.14) the gains a_p, a_q must be positive for closed-loop stability. Their values are to be selected to have the desired speed of response at which the fast state errors should go to zero.

Looking at the two components of the control vector designed according to equations (3.6) and (3.13), the overall control law can be written as

$$\begin{bmatrix} \delta_t \\ \delta_e \\ \delta_a \\ \delta_r \end{bmatrix} = K^{-1}(-J + \begin{bmatrix} \dot{v}_{A_r} \\ \dot{\beta}_r \\ p'_r \\ q'_r \end{bmatrix} - \begin{bmatrix} a_{v_A} & 0 & 0 & 0 \\ 0 & a_\beta & 0 & 0 \\ 0 & 0 & a_p & 0 \\ 0 & 0 & 0 & a_q \end{bmatrix} \begin{bmatrix} v_A - v_{A_r} \\ \beta - \beta_r \\ p - p_r \\ q - q_r \end{bmatrix}) \tag{3.15}$$

where the gains a_{v_A} and a_β are to be selected to obtain the desired slow state error dynamics in the slow time-scale, and a_p and a_q are to be selected to obtain the desired fast state error dynamics in the fast time-scale. All four of these gains must be positive to ensure closed-loop stability.

3.2.2.3 Adding Actuator Dynamics in Simulation

It is to be noted here that the control law development assumed all actuators to be infinitely fast. However, different actuators of an aircraft respond at different rates. For this problem actuator dynamics is included in simulation. To include actuator dynamics, all four actuators are modeled as first order systems with known time-constants. As a result the control law computes the *commanded* actuator positions:

$$\begin{bmatrix} \delta_{t_c} \\ \delta_{e_c} \\ \delta_{a_c} \\ \delta_{r_c} \end{bmatrix} = K^{-1}(-J + \begin{bmatrix} \dot{V}_{A_r} \\ \dot{\beta}_r \\ p'_r \\ q'_r \end{bmatrix} - \begin{bmatrix} a_{v_A} & 0 & 0 & 0 \\ 0 & a_\beta & 0 & 0 \\ 0 & 0 & a_p & 0 \\ 0 & 0 & 0 & a_q \end{bmatrix} \begin{bmatrix} v_A - v_{A_r} \\ \beta - \beta_r \\ p - p_r \\ q - q_r \end{bmatrix}) \tag{3.16}$$

The *actual* actuator positions are obtained from the commanded positions as

$$\begin{aligned}
\dot{\delta}_t &= -\frac{1}{T_{eng}}\delta_t + \frac{1}{T_{eng}}\delta_{t_c} \\
\dot{\delta}_e &= -\frac{1}{T_{elev}}\delta_e + \frac{1}{T_{elev}}\delta_{e_c} \\
\dot{\delta}_a &= -\frac{1}{T_{ail}}\delta_a + \frac{1}{T_{ail}}\delta_{a_c} \\
\dot{\delta}_r &= -\frac{1}{T_{rud}}\delta_r + \frac{1}{T_{rud}}\delta_{r_c}
\end{aligned} \tag{3.17}$$

where $T_{eng}, T_{el}, T_{ail}, T_{rud}$ are the time-constants of the engine, elevator, aileron and rudder respectively.

3.2.3 Numerical Results

This subsection shows in simulation simultaneous slow and fast state tracking for a nonlinear 6-DOF generic F-16A using the controller designed in Subsection 3.2.2. The evaluation maneuver consists of the generic F-16 starting at steady level trim with a velocity of 800 ft/s at an altitude of 15,000 ft. The trim angle-of-attack and elevator deflection are 0.9 deg and -1.6 deg respectively. The thrust at trim is 3265.0 lbf, which is 18.34% of the maximum military thrust of 17,800 lbf. All other angles, rates and control surface deflections are zero at trim. A climb is commanded at a pitch rate of 15 deg/s followed by a roll at a rate of 20 deg/s while maintaining zero sideslip angle and velocity 800 ft/s. The reference pitch rate increases smoothly from zero to 15 deg/s, then goes back to zero and reaches -15 deg/s before becoming zero again. Similarly the commanded roll rate goes from zero to 20 deg/s, then decreases to zero, reaches -20 deg/s, and finally becomes zero again.

Ref. [37] shows three cases of simulation: (i) using constant throttle, (ii) using throttle as an automatic control, using military thrust, (iii) using throttle as an automatic control, using afterburner thrust level. The second case is presented in this Subsection. The selected closed-loop gains are $a_{v_A} = 0.75$, $a_\beta = 1$, $a_p = 15$, $a_q = 15$. The gains are selected such that the time-scale separation between the slow state and fast state error dynamics is maintained. Furthermore, the

time-constant of the engine is taken as $T_{eng} = 1$ sec. The time-constants of the other control surfaces are $T_{elev} = T_{ail} = T_{rud} = 0.1$ sec.

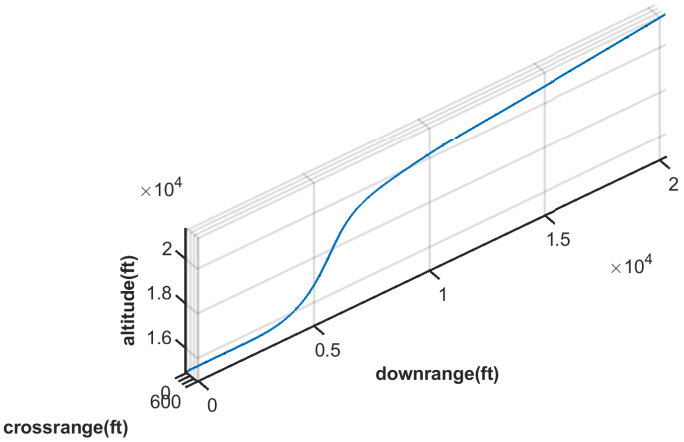

Figure 3.1: Trajectory of the generic F-16A during climb and roll maneuver using the earlier two-stage design method; from Saha and Valasek [37], reprinted by permission of the American Institute of Aeronautics and Astronautics, Inc.

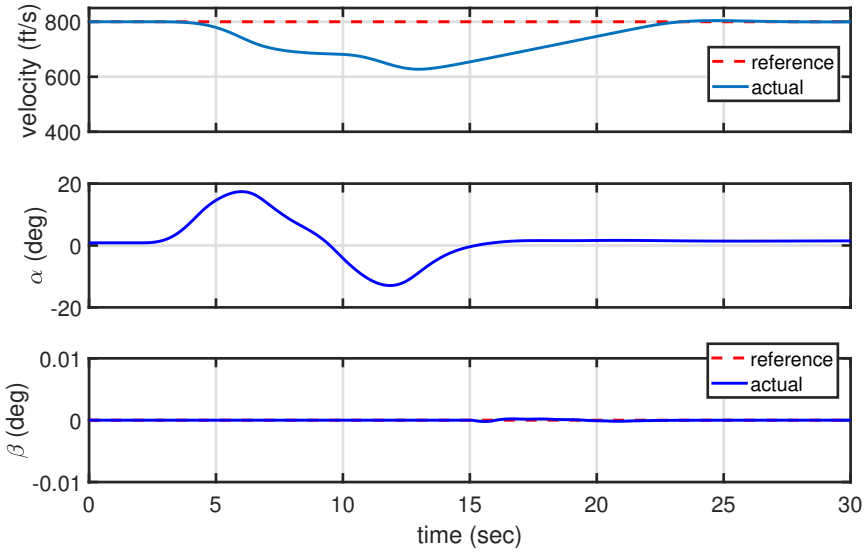

Figure 3.2: Velocity, angle-of-attack and sideslip angle during climb and roll maneuver using the earlier two-stage design method; from Saha and Valasek [37], reprinted by permission of the American Institute of Aeronautics and Astronautics, Inc.

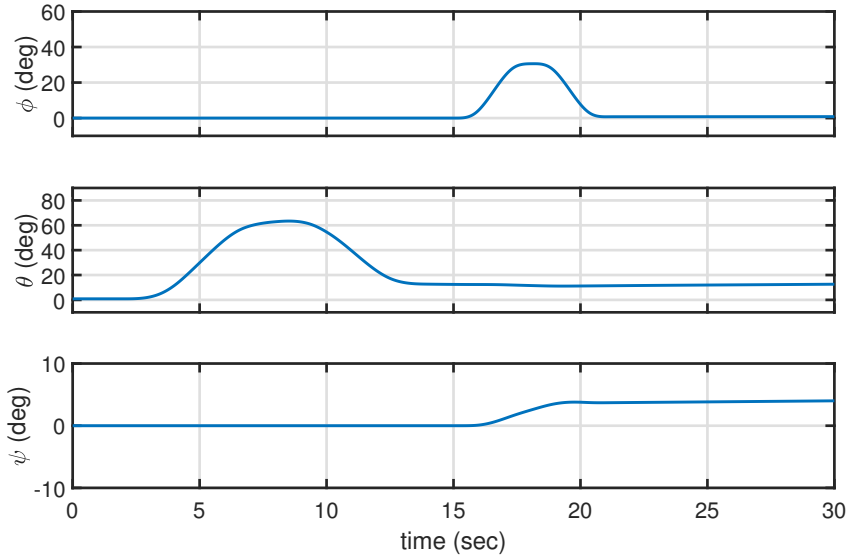

Figure 3.3: Bank angle, pitch attitude angle and heading angle during during climb and roll maneuver using the earlier two-stage design method; from Saha and Valasek [37], reprinted by permission of the American Institute of Aeronautics and Astronautics, Inc.

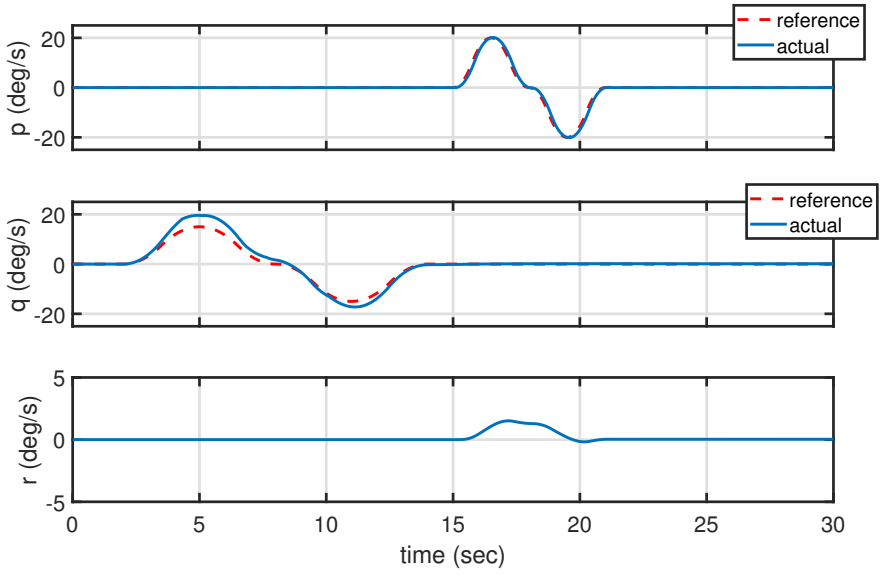

Figure 3.4: Body-axis roll, pitch and yaw rates during climb and roll maneuver using the earlier two-stage design method; from Saha and Valasek [37], reprinted by permission of the American Institute of Aeronautics and Astronautics, Inc.

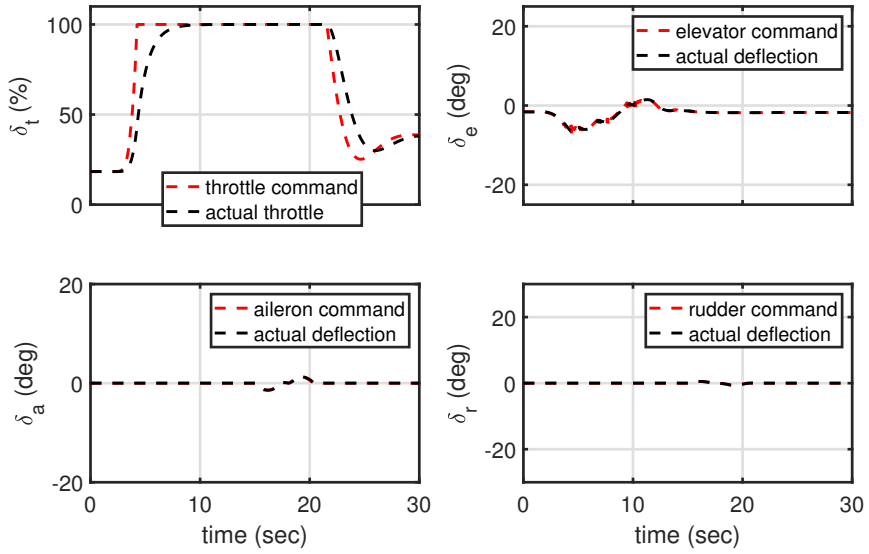

Figure 3.5: Throttle, elevator, aileron and rudder deflections during during climb and roll maneuver using the earlier two-stage design method; from Saha and Valasek [37], reprinted by permission of the American Institute of Aeronautics and Astronautics, Inc.

Figures 3.1 - 3.5 show the time-histories. Figure 3.2 shows that the loss of airspeed for this case stays within 200 ft/s during the climb. The 25% loss of airspeed is still better than loss of half the airspeed when using constant throttle [37]. Furthermore, Ref. [37] also demonstrates that the deceleration can be reduced using afterburner thrust. From Figure 3.2 it can also be seen that the velocity comes back and stays close to the trim value of 800 ft/s after the climb. This is a consequence of using throttle as an automatic control. From Figures 3.2 and 3.4 it is seen that the other three commanded states - sideslip angle, body-axis roll rate and pitch rate - are tracked well. In addition, it can be seen from 3.1 the aircraft climbs about 700 ft during the maneuver. All the states and controls remain bounded.

3.2.4 Limitations of the Two-Stage Design Approach

A close review of the control law development in Subsection 3.2.2 shows a few limitations.

1. The two-stage design approach does not account for actuator dynamics. For this problem, actuator dynamics were included only in simulation. However, a more rigorous design

methodology should realistically account for actuator dynamics in the synthesis. Aircraft have both slow and fast actuators so more than one additional time-scales are needed to accommodate the actuators. It is not straightforward to add actuator time-scales to the two-stage design method, so a new theory is needed.

2. The two stage-design approach relies on the assumption of a deterministic model and full-state feedback. Due to imperfections in models of practical systems, a new theory is needed to address uncertainties. Moreover, it may not always be possible to measure all the states so a new theory of output feedback is needed.

The rest of this chapter develops the theory of simultaneous slow and fast state tracking, considering actuator dynamics and uncertainties, using full-state feedback. The development is similar to the four-time-scale slow state tracking control design in Section 2.6. Tracking control with output feedback will be the focus of Chapter 4.

3.3 Four-Time-Scale Slow and Fast State Tracking with Uncertainties

This section develops a new sequential approach to track simultaneously the slow and the fast states of a four-time-scale nonlinear nonstandard system with actuator dynamics and uncertainties. The class of systems considered in this section is similar to the one in Section 2.6 with a few major modifications. It is assumed that the system has n slow states, n slow actuators, m fast states and m fast actuators. Thus the number of slow states is equal to the number of slow actuators, and the number of fast states is equal to the number of fast actuators. However, unlike slow state tracking the slow states are not divided as kinetic and kinematic. All the slow states are kinetic slow states and can be influenced directly by both slow and fast actuators. In contrast, the fast states can be influenced only by the fast actuators. The types of uncertainties are similar to slow state tracking.

The class of systems is

$$\begin{aligned}
\dot{x} &= B_x f_x(x,z) + \gamma_x(t,x,z) + \Lambda_{x\delta_s} G_{x\delta_s}(x)\delta_s + \Lambda_{x\delta_f} G_{x\delta_f}(x)\delta_f \\
\sigma\dot{\delta}_s &= B_{\delta_s} f_{\delta_s}(\delta_s) + \Lambda_{\delta_s u_s} G_{\delta_s u_s}(\delta_s) u_s \\
\varepsilon\dot{z} &= \sum_k B_z^k f_z^k(x,z) + \gamma_z(t,x,z) + \Lambda_{z\delta_f} G_{z\delta_f}(x)\delta_f \\
\rho\dot{\delta}_f &= B_{\delta_f} f_{\delta_f}(\delta_f) + \Lambda_{\delta_f u_f} G_{\delta_f u_f}(\delta_f) u_f.
\end{aligned} \tag{3.18}$$

Equation (3.18) represents a four-time-scale nonlinear nonstandard system with uncertainties. Here $x \in \mathbb{R}^n$ is the vector of n slow states, $z \in \mathbb{R}^m$ is the vector of m fast states, $\delta_s \in \mathbb{R}^n$ is the vector of n slow actuators, $\delta_f \in \mathbb{R}^m$ is the vector of m fast actuators. The perturbation parameters σ, ε and ρ satisfy $0 < \rho << \varepsilon << \sigma << 1$.

The parametric uncertainties in the evolution of the kinetic slow states x are captured in the constant but unknown matrix B_x. The known vector of smooth functions $f(x,z)$ represents the dependence of the slow dynamics on the slow and fast states. For the slow states, the parametric uncertainties in the control distribution corresponding to the slow and fast actuators are captured in the constant but unknown parameter matrices $\Lambda_{x\delta_s}$ and $\Lambda_{x\delta_f}$ respectively. The dependence of the slow dynamics on the slow and fast actuators are represented by the matrices $G_{x\delta_s}$ and $G_{x\delta_f}$ respectively. Both of these matrices consist of known, smooth functions, and the matrix $G_{x\delta_s}$ is nonsingular. The largest singular values of these matrices satisfy $\bar{\sigma}(\Lambda_{x\delta_s}) \leq v_1, \bar{\sigma}(G_{x\delta_s}) \leq v_2, \bar{\sigma}(\Lambda_{x\delta_f}) \leq v_3, \bar{\sigma}(G_{x\delta_s}) \leq v_4$ for some known constants v_1, v_2, v_3, v_4. The vector of functions $\gamma_x(t,x,z)$ represent the time-dependent and state-dependent uncertainties in slow dynamics. This is an additive uncertainty, and he Euclidean norm of this vector satisfies $\left\|\gamma_z(t,x,z)\right\|_2 \leq \kappa_1\|x\|_2 + \kappa_2\|z\|_2$ for some known constants $\kappa_1, \kappa_2 \geq 0$.

The fast dynamics have a combination of k constant but unknown parameter matrices B_z^k multiplied by known vectors of functions $f_z^k(.)$. The functions $f_z^k(.)$ represent the dependence of the fast dynamics on the slow and fast states. This vector is assumed to consist of known, smooth functions. The parametric uncertainties in the control distribution are captured in the constant but

unknown matrix $\Lambda_{z\delta_f}$. The dependence of the fast dynamics on the fast actuators is represented by the matrix $G_{z\delta_f}$, which is assumed to be nonsingular and consisting of known, smooth functions. The largest singular values of these matrices satisfy $\bar{\sigma}(\Lambda_{z\delta_f}) \leq v_5, \bar{\sigma}(G_{z\delta_f}) \leq v_6$ for some known constants v_5 and v_6. The vector of functions $\gamma_z(t, x, z)$ captures the time-dependent and state-dependent uncertainties in the fast dynamics. This is another additive uncertainty, and the Euclidean norm of this uncertainty satisfies $\left\|\gamma_x(t, x, z)\right\|_2 \leq \kappa_3\|x\|_2 + \kappa_4\|z\|_2$ for some known constants $\kappa_3, \kappa_4 \geq 0$. The matrices $B_{\delta_s}, \Lambda_{\delta_s u_s}, B_{\delta_f}, \Lambda_{\delta_f u_f}$ represent the constant but unknown parameters in the evolution of slow and fast actuators.

Each of the constant but unknown parameters in the parameter matrices is assumed to be within lower and upper bounds; i.e. $p_{ij} \in [\underline{p}_{ij}, \bar{p}_{ij}]$, where p_{ij} is any of the constant but unknown parameters. The vector of functions $f_{\delta_s}, f_{\delta_f}$ represent how the actuator rates depend on the current actuator deflections. The matrices $G_{\delta_s u_s}, G_{\delta_f u_f}$ represent how the actuator rates depend on the control commands u_s and u_f respectively. The matrices $G_{\delta_s u_s}$ and $G_{\delta_f u_f}$ are assumed to be nonsingular.

The control objective is to design the slow control vector u_s and the fast control vector u_f such that the slow state vector $x(t)$ tracks a twice differentiable reference trajectory $x_r(t)$, and the fast state vector $z(t)$ tracks a twice differentiable reference trajectory $z_r(t)$. In order to achieve this objective using the geometric singular perturbation approach, the slow actuators δ_s need to be stabilized on a suitable manifold δ_s^0, and the fast actuators need to be stabilized on a suitable manifold δ_f^0. Define error variables $e_x := x - x_r, e_z := z - z_r, e_{\delta_s} := \delta_s - \delta_s^0, e_{\delta_f} := \delta_f - \delta_f^0$. The tracking problem becomes an equivalent stabilization problem in the error coordinates. The full-order system (3.18) in the error co-ordinates become

$$\begin{aligned}
\dot{e}_x &= B_x f_x + \gamma_x + \Lambda_{x\delta_s} G_{x\delta_s}(e_{\delta_s} + \delta_s^0) + \Lambda_{x\delta_f} G_{x\delta_f}(e_{\delta_f} + \delta_f^0) - \dot{x}_r \\
\sigma\dot{e}_{\delta_s} &= B_{\delta_s} f_{\delta_s} + \Lambda_{\delta_s u_s} G_{\delta_s u_s} u_s - \sigma\dot{\delta}_s^0 \\
\varepsilon\dot{e}_z &= \sum_k B_z^k f_z^k + \gamma_z + \Lambda_{z\delta_f} G_{z\delta_f}(e_{\delta_f} + \delta_f^0) - \varepsilon\dot{z}_r \\
\rho\dot{e}_{\delta_f} &= B_{\delta_f} f_{\delta_f} + \Lambda_{\delta_f u_f} G_{\delta_f u_f} u_f - \rho\dot{\delta}_f^0.
\end{aligned} \tag{3.19}$$

The following Subsections develop a four-time-scale control law based on the lower-order reduced subsystems obtained from (3.19) and prove the boundedness of tracking error.

3.3.1 Development of Nominal Control Law Using Reduced Subsystems

This is done in four steps. A schematic of the steps is shown in Figure 3.6. The numbers 1, 2, 3, 4 on the schematic indicates the sequence in which the specific design variables are selected. The design steps are detailed below.

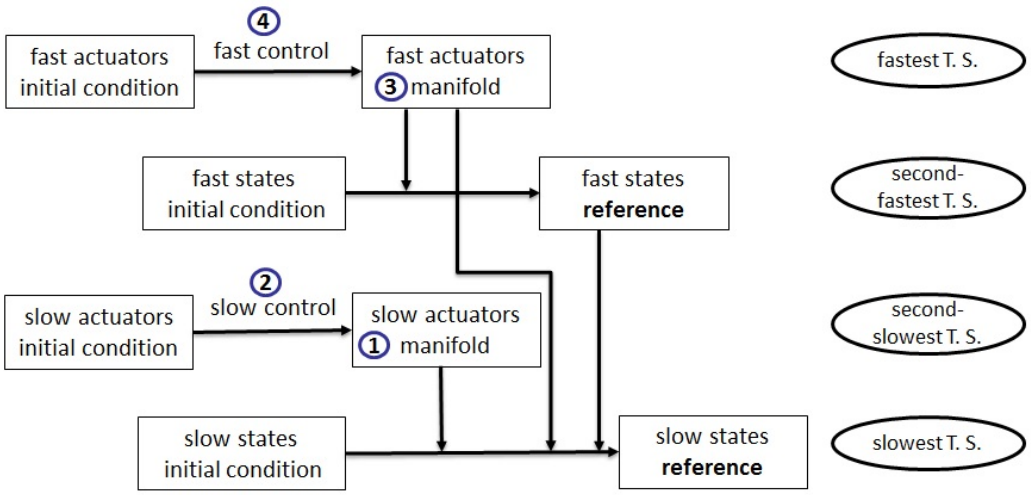

Figure 3.6: Steps of four-time-scale slow state tracking control design

3.3.1.1 Design of Manifold of Slow Actuators in the Slowest Time-Scale

In the slowest time-scale t, it is assumed that the slow actuators are on their manifold δ_s^0. The fast states have already reached their reference z_r, so the fast actuators are on a special case of their manifold $\delta_f^0|_{z_r}$. Mathematically this is obtained by artificially substituting $\sigma = \varepsilon = \rho = 0$, as a result of which the last three differential equations in (3.19), viz. the $\dot{e}_{\delta_s}$, $\dot{e}_z$, $\dot{e}_{\delta_f}$ equations reduce to algebraic equations. This indicates that the fast states have already reached the reference.

Moreover, the slow actuators and the fast actuators have already reached their manifolds; they are no longer evolving independently. Only the slow state errors e_x evolve independently in this time-scale. The slow actuator manifold δ_s^0 is selected such that the slow states reach their reference; that is, the slow state error vector e_x goes to zero. Moreover, to construct the reduced subsystem, the constant but unknown parameter matrices B_x, $\Lambda_{x\delta_s}$, $\Lambda_{x\delta_f}$ are replaced by their best estimates $\hat{B}_x$, $\hat{\Lambda}_{x\delta_s}$, $\hat{\Lambda}_{x\delta_f}$ respectively, and the additive uncertainty γ_x is ignored. The reduced subsystem in the slowest time-scale is

$$\dot{e}_x = \hat{B}_x f_x + \hat{\Lambda}_{x\delta_s} G_{x\delta_s} \delta_s^0 + \hat{\Lambda}_{x\delta_f} G_{x\delta_f} \delta_f^0|_{z_r} - \dot{x}_r. \tag{3.20}$$

A positive-definite candidate Lyapunov function for subsystem (3.20) can be selected as

$$V_1 = \frac{1}{2} e_x^T e_x. \tag{3.21}$$

Its time-derivative with respect to the slowest time-scale t is

$$\dot{V}_1 = e_x^T \dot{e}_x. \tag{3.22}$$

Along the trajectories of subsystem (3.20), the time-derivative of the Lyapunov function V_1 is

$$\dot{V}_1|_{(3.20)} = e_x^T (\hat{B}_x f_x + \hat{\Lambda}_{x\delta_s} G_{x\delta_s} \delta_s^0 + \hat{\Lambda}_{x\delta_f} G_{x\delta_f} \delta_f^0|_{z_r} - \dot{x}_r). \tag{3.23}$$

Suppose that the manifold of the slow actuators δ_s^0 is selected as

$$\delta_s^0 = G_{x\delta_s}^{-1} \hat{\Lambda}_{x_{\delta_s}}^{-1} (\dot{x}_r - \hat{B}_x f_x - \hat{\Lambda}_{x\delta_f} G_{x\delta_f} \delta_f^0|_{z_r} - K_x e_x) \tag{3.24}$$

where $\hat{\Lambda}_{x_{\delta_s}}$ is assumed nonsingular, and $\delta_f^0|_{z_r}$ is yet to be determined. For these choices, the

time-derivative of the Lyapunov function V_1 for the reduced subsystem (3.20) becomes

$$\dot{V}_1|_{(3.20)} = -e_x^T K_x e_x. \tag{3.25}$$

This is negative-definite for any positive-definite K_x, indicating that the equilibrium $e_x = 0$ of the reduced subsystem (3.20) is Lyapunov-stable.

3.3.1.2 Design of Slow Control in the Second Slowest Time-Scale

In the second slowest time-scale $t_\sigma = \frac{t}{\sigma}$, the slow controls u_s are designed such that the slow actuators δ_s reaches their manifold δ_s^0, and consequently slow actuator errors e_{δ_s} go to zero. Considering time-derivatives in the second slowest time-scale, and artifically substituting $\sigma = \varepsilon = \rho = 0$, the slow dynamics reduce to $\grave{e}_x = 0, \grave{e}_\xi = 0$, where where $\grave{e}$ is the derivative of e with respect to the second slowest time-scale $t_\sigma = \frac{t}{\sigma}$. This indicates that the slow state errors are 'frozen' at their initial conditions. Furthermore, the $\dot{e}_z$ and $\dot{e}_{\delta_f}$ differential equations in (3.19) reduce to algebraic equations, indicating that the fast actuators have settled on their manifold, and that fast states have settled on their reference. They and are no longer evolving independently. Only the slow actuator errors are evolving independently in this time-scale. Replacing the unknown parameter matrices with their estimates, the reduced subsystem in the second slowest time-scale is

$$\grave{e}_{\delta_s} = \hat{B}_{\delta_s} f_{\delta_s} + \hat{\Lambda}_{\delta_s u_s} G_{\delta_s u_s} u_s. \tag{3.26}$$

A positive-definite candidate Lyapunov function for this subsystem can be selected as

$$V_2 = \frac{1}{2} e_{\delta_s}^T e_{\delta_s}. \tag{3.27}$$

Its time-derivative with respect to the second slowest time-scale is

$$\grave{V}_2 = e_{\delta_s}^T \grave{e}_{\delta_s}. \tag{3.28}$$

Along the trajectories of the reduced subsystem (3.26), the time-derivative is

$$\dot{V}_2|_{(3.26)} = e_{\delta_s}^T(\hat{B}_{\delta_s} f_{\delta_s} + \hat{\Lambda}_{\delta_s u_s} G_{\delta_s u_s} u_s). \tag{3.29}$$

If the vector of slow controls u_s is selected as

$$u_s = G_{\delta_s u_s}^{-1} \hat{\Lambda}_{\delta_s u_s}^{-1}(-\hat{B}_{\delta_s} f_{\delta_s} - K_{\delta_s} e_{\delta_s}) \tag{3.30}$$

then the derivative of the Lyapunov function V_2 with respect to the second slowest time-scale becomes

$$\dot{V}_2|_{(3.26)} = -e_{\delta_s}^T K_{\delta_s} e_{\delta_s} \tag{3.31}$$

which is negative-definite for any positive-definite K_{δ_s}. Thus the equilibrium $e_{\delta_s} = 0$ of the reduced subsystem (3.26) is Lyapunov-stable.

3.3.1.3 Design of Manifold of Fast Actuators in the Second Fastest Time-Scale

In the second fastest time-scale $t_\varepsilon = \frac{t}{\varepsilon}$, the manifold of the fast actuators δ_f^0 is selected such that the fast states z reach their reference z_r, or equivalently the fast state error vector e_z become zero. Considering derivatives in the second slowest time-scale and artificially substituting $\sigma = \varepsilon = \rho = 0$, the slow state and slow actuator error dynamics become $e_x' = 0, e_\xi' = 0, e_{\delta_s}' = 0$, where 'prime' denotes differentiation with respect to the second fastest time-scale. This indicates that the slow state and slow actuator errors are 'frozen' at their initial conditions in this time-scale. The $\dot{e}_{\delta_f}$ differential equation in (3.19) becomes a system of algebraic equations, indicating that the fast actuators have already reached their manifold, and are no longer evolving independently. Only the fast state error vector e_z evolves independently in this time-scale. Furthermore, to construct the reduced subsystem, the constant but unknown parameter matrices B_z^k and $\Lambda_{z\delta_f}$ are replaced by their estimates $\hat{B}_z^k$ and $\hat{\Lambda}_{z\delta_f}$ respectively. The additive uncertainty γ_z is ignored. The reduced

subsystem in the second fastest time-scale is

$$e_z' = \sum_k \hat{B}_z^k f_z^k + \hat{\Lambda}_{z\delta_f} G_{z\delta_f} \delta_f^0 - z_r' \tag{3.32}$$

A positive-definite candidate Lyapunov function for this subsystem is

$$V_3 = \frac{1}{2} e_z^T e_z. \tag{3.33}$$

Its time-derivative with respect to the time-scale t_z is

$$V_3' = e_z^T e_z'. \tag{3.34}$$

Along the trajectories of subsystem (3.32), the time-derivative is

$$V_3'|_{(3.32)} = e_z^T (\sum_k \hat{B}_z^k f_z^k + \hat{\Lambda}_{z\delta_f} G_{z\delta_f} \delta_f^0 - z_r') \tag{3.35}$$

If the manifold of the fast actuators is selected as

$$\delta_f^0 = G_{z\delta_f}^{-1} \hat{\Lambda}_{z\delta_f}^{-1} (z_r' - \sum_k \hat{B}_z^k f_z^k - K_z e_z) \tag{3.36}$$

where $\hat{\Lambda}_{z\delta_f}$ is assumed nonsingular, then the time-derivative of the Lyapunov function V_3 becomes

$$V_3'|_{(3.32)} = -e_z^T K_z e_z \tag{3.37}$$

which is negative-definite for any positive-definite K_z. This ensures that the equilibrium $e_z = 0$ of the reduced subsystem (3.32) is Lyapunov-stable.

By design of the fast actuator manifold δ_f^0, the special case $\delta_f^0|_{z_r}$ needed in the slowest time-scale

can now be determined as

$$\delta_f^0|_{z_r} = -G_{z\delta_f}^{-1}\hat{\Lambda}_{z\delta_f}^{-1}\sum_k \hat{B}_z^k f_z^k(x, z_r). \tag{3.38}$$

This is to be used to design the manifold for the slow actuators δ_s^0 given by (4.120) in the slowest time-scale.

3.3.1.4 Design of Fast Control in the Fastest Time-Scale

In the fastest time-scale $t_\rho = \frac{t}{\rho}$, the fast controls u_f are selected such that the fast actuators δ_f reach their manifold δ_f^0, or equivalently fast actuator errors $e_{\delta_f} = \delta_f - \delta_f^0$ reach zero. Considering time-derivatives in the fastest time-scale and artificially substituting $\sigma = \varepsilon = \rho = 0$ in the full-order dynamics (3.19) lead to $\breve{e}_x = 0, \breve{\xi} = 0, \breve{\delta}_s = 0, \breve{z} = 0$, where $\breve{e}$ stands for derivative of e with respect to the fastest time-scale $t_\rho = \frac{t}{\rho}$. This means that the slow states, slow actuators and fast state errors are 'frozen' at their initial conditions in the fastest time-scale. Only the fast actuator errors are evolving according to

$$\breve{e}_{\delta_f} = \hat{B}_{\delta_f} f_{\delta_f} + \hat{\Lambda}_{\delta_f u_f} G_{\delta_f u_f} u_f. \tag{3.39}$$

A positive-definite and decrescent Lyapunov function for the subsystem (3.39) can be selected as

$$V_4 = \frac{1}{2} e_{\delta_f}^T e_{\delta_f}. \tag{3.40}$$

Its time-derivative with respect to the fast actuator time-scale is

$$\breve{V}_4 = e_{\delta_f}^T \breve{e}_{\delta_f}. \tag{3.41}$$

Along the trajectories of the reduced subsystem (3.39), the time-derivative becomes

$$\breve{V}_4|_{(3.39)} = e_{\delta_f}^T (\hat{B}_{\delta_f} f_{\delta_f} + \hat{\Lambda}_{\delta_f u_f} G_{\delta_f u_f} u_f). \tag{3.42}$$

If the fast actuator command vector u_f is selected as

$$u_f = G_{\delta_f u_f}^{-1} \hat{\Lambda}_{\delta_f u_f}^{-1} (-\hat{B}_{\delta_f} f_{\delta_f} - K_{\delta_f} e_{\delta_f}) \tag{3.43}$$

then the derivative of the Lyapunov function V_4 becomes

$$\breve{V}_4|_{(3.39)} = -e_{\delta_f}^T K_{\delta_f} e_{\delta_f} \tag{3.44}$$

which is negative-definite for any positive-definite K_{δ_f}. Thus the equilibrium $e_{\delta_f} = 0$ of the reduced subsystem (3.39) is Lyapunov-stable.

3.3.2 Stability Analysis of the Full-Order System: Selection of Parameter Update Laws and Bounds of Time-Scale Separation

Define parameter estimation error matrices

$$\begin{aligned}
\tilde{B}_x &\coloneqq B_x - \hat{B}_x \\
\tilde{\Lambda}_{x\delta_s} &\coloneqq \Lambda_{x\delta_s} - \hat{\Lambda}_{x\delta_s} \\
\tilde{\Lambda}_{x\delta_f} &\coloneqq \Lambda_{x\delta_f} - \hat{\Lambda}_{x\delta_f}, \\
\tilde{B}_{\delta_s} &\coloneqq B_{\delta_s} - \hat{B}_{\delta_s} \\
\tilde{\Lambda}_{\delta_s u_s} &\coloneqq \Lambda_{\delta_s u_s} \hat{\Lambda}_{\delta_s u_s} \\
\tilde{B}_z^k &\coloneqq B_z^k - \hat{B}_z^k \\
\tilde{\Lambda}_{z\delta_f} &\coloneqq \Lambda_{z\delta_f} - \hat{\Lambda}_{z\delta_f} \\
\tilde{B}_{\delta_f} &\coloneqq B_{\delta_f} - \hat{B}_{\delta_f} \\
\tilde{\Lambda}_{\delta_f u_f} &\coloneqq \Lambda_{\delta_f u_f} - \hat{\Lambda}_{\delta_f u_f}.
\end{aligned} \tag{3.45}$$

A composite Lyapunov function for the full-order system (3.19) can be selected as

$$\begin{aligned} V_c = {} & \alpha_1 V_1 + \alpha_2 V_2 + \alpha_3 V_3 + \alpha_4 V_4 + \frac{1}{2}\alpha_5 tr[\tilde{B}_x^T \tilde{B}_x] + \frac{1}{2}\alpha_6 tr[\tilde{\Lambda}_{x\delta_s}^T \tilde{\Lambda}_{x\delta_s}] \\ & + \frac{1}{2}\alpha_7 tr[\tilde{\Lambda}_{x\delta_f}^T \tilde{\Lambda}_{x\delta_f}] + \frac{1}{2}\alpha_8 tr[\tilde{B}_{\delta_s}^T \tilde{B}_{\delta_s}] + \frac{1}{2}\alpha_9 tr[\tilde{\Lambda}_{\delta_s u_s}^T \tilde{\Lambda}_{\delta_s u_s}] + \frac{1}{2}\sum_k \alpha_{10k} tr[\tilde{B}_z^{k^T} \tilde{B}_z^k] \\ & + \frac{1}{2}\alpha_{11} tr[\tilde{\Lambda}_{z\delta_f}^T \tilde{\Lambda}_{z\delta_f}] + \frac{1}{2}\alpha_{12} tr[\tilde{B}_{\delta_f}^T \tilde{B}_{\delta_f}] + \frac{1}{2}\alpha_{13} tr[\tilde{\Lambda}_{\delta_f u_f}^T \tilde{\Lambda}_{\delta_f u_f}] \end{aligned} \tag{3.46}$$

where $\alpha_i > 0; i = 1, ..., 13$ represent the weights of the individual Lyapunov functions in the composite. The composite Lyapunov function (2.157) contains a weighted sum of squares of all the parameter estimation errors. To show the estimation errors explicitly, equation (3.46) can be written as

$$\begin{aligned} V_c = {} & \alpha_1 V_1 + \alpha_2 V_2 + \alpha_3 V_3 + \alpha_4 V_4 + \frac{1}{2}\alpha_5 \sum_i \sum_j \tilde{b}_{x_{ij}}^2 + \frac{1}{2}\alpha_6 \sum_i \sum_j \tilde{\lambda}_{x\delta_{s_{ij}}}^2 \\ & + \frac{1}{2}\alpha_7 \sum_i \sum_j \tilde{\lambda}_{x\delta_{f_{ij}}}^2 + \frac{1}{2}\alpha_8 \sum_i \sum_j \tilde{b}_{\delta_{s_{ij}}}^2 + \frac{1}{2}\alpha_9 \sum_i \sum_j \tilde{\lambda}_{\delta_s u_{s_{ij}}}^2 + \frac{1}{2}\sum_k \alpha_{10k} \sum_i \sum_j \tilde{b}_{z_{ij}}^{k^2} \\ & + \frac{1}{2}\alpha_{11} \sum_i \sum_j \tilde{\lambda}_{z\delta_{f_{ij}}}^2 + \frac{1}{2}\alpha_{12} \sum_i \sum_j \tilde{b}_{\delta_{f_{ij}}}^2 + \frac{1}{2}\alpha_{13} \sum_i \sum_j \tilde{\lambda}_{\delta_f u_{f_{ij}}}^2. \end{aligned} \tag{3.47}$$

Along the trajectories of the full-order system (3.19), the time-derivative of the composite Lyapunov function (3.47) is

$$\begin{aligned} \dot{V}_c = {} & \alpha_1 \dot{V}_1|_{(3.19)} + \frac{\alpha_2}{\sigma}\dot{V}_2|_{(3.19)} + \frac{\alpha_3}{\varepsilon}V_3'|_{(3.19)} + \frac{\alpha_4}{\rho}\breve{V}_4|_{(3.19)} + \alpha_5 \sum_i \sum_j \tilde{b}_{x_{ij}} \dot{\tilde{b}}_{x_{ij}} \\ & + \alpha_6 \sum_i \sum_j \tilde{\lambda}_{x\delta_{s_{ij}}} \dot{\tilde{\lambda}}_{x\delta_{s_{ij}}} + \alpha_7 \sum_i \sum_j \tilde{\lambda}_{x\delta_{f_{ij}}} \dot{\tilde{\lambda}}_{x\delta_{f_{ij}}} + \frac{\alpha_8}{\sigma} \sum_i \sum_j \tilde{b}_{\delta_{s_{ij}}} \breve{\tilde{b}}_{\delta_{s_{ij}}} \\ & + \frac{\alpha_9}{\sigma} \sum_i \sum_j \tilde{\lambda}_{\delta_s u_{s_{ij}}} \breve{\tilde{\lambda}}_{\delta_s u_{s_{ij}}} + \frac{1}{\varepsilon}\sum_k \alpha_{10k} \tilde{b}_{z_{ij}}^k \tilde{b}_{z_{ij}}^{k'} + \frac{\alpha_{11}}{\varepsilon} \sum_i \sum_j \tilde{\lambda}_{z\delta_{f_{ij}}} \tilde{\lambda}'_{z\delta_{f_{ij}}}) \\ & + \frac{\alpha_{12}}{\rho} \sum_i \sum_j \tilde{b}_{\delta_{f_{ij}}} \breve{\tilde{b}}_{\delta_{f_{ij}}} + \frac{\alpha_{13}}{\rho} \sum_i \sum_j \tilde{\lambda}_{\delta_f u_{f_{ij}}} \breve{\tilde{\lambda}}_{\delta_f u_{f_{ij}}}. \end{aligned} \tag{3.48}$$

It can be seen in (3.48) that the time-derivatives of the parameter estimation errors are taken in the time-scale the parameters appear in the full-order dynamics (3.19). For example, the ones

appearing in the evolution of the slow state are differentiated with respect to the slowest time-scale t; the ones appearing in the evolution of the slow actuator are differentiated with respect to the second slowest time-scale $t_\sigma = \frac{t}{\sigma}$, and so on. Adding and subtracting appropriate reduced subsystems for the derivatives of the Lyapunov functions used for controller design, and substituting the time-derivatives of the parameter estimation errors in terms of those of the estimates, (3.48) reduces to

$$\begin{aligned}
\dot{V}_c = {} & \alpha_1 \dot{V}_1|_{(3.20)} + \frac{\alpha_2}{\sigma}\grave{V}_2|_{(3.26)} + \frac{\alpha_3}{\varepsilon}V_3'|_{(3.32)} + \frac{\alpha_4}{\rho}\breve{V}_4|_{(3.39)} + \alpha_1(\dot{V}_1|_{(3.19)} - \dot{V}_1|_{(3.20)}) \\
& + \frac{\alpha_2}{\sigma}(\grave{V}_2|_{(3.19)} - \grave{V}_2|_{(3.26)}) + \frac{\alpha_3}{\varepsilon}(V_3'|_{(3.19)} - V_3'|_{(3.32)}) + \frac{\alpha_4}{\rho}(\breve{V}_4|_{(3.19)} - \breve{V}_4|_{(3.39)}) \\
& - \alpha_5 \sum_i \sum_j \tilde{b}_{x_{ij}} \dot{\hat{b}}_{x_{ij}} - \alpha_6 \sum_i \sum_j \tilde{\lambda}_{x\delta_{s_{ij}}} \dot{\hat{\lambda}}_{x\delta_{s_{ij}}} - \alpha_7 \sum_i \sum_j \tilde{\lambda}_{x\delta_{f_{ij}}} \dot{\hat{\lambda}}_{x\delta_{f_{ij}}} \\
& - \frac{\alpha_8}{\sigma} \sum_i \sum_j \tilde{b}_{\delta_{s_{ij}}} \grave{\hat{b}}_{\delta_{s_{ij}}} - \frac{\alpha_9}{\sigma} \sum_i \sum_j \tilde{\lambda}_{\delta_s u_{s_{ij}}} \grave{\hat{\lambda}}_{\delta_s u_{s_{ij}}} - \frac{1}{\varepsilon} \sum_k \alpha_{10k} \sum_i \sum_j \tilde{b}^k_{z_{ij}} \hat{b}^{k'}_{z_{ij}} \\
& - \frac{\alpha_{11}}{\varepsilon} \sum_i \sum_j \tilde{\lambda}_{z\delta_{f_{ij}}} \hat{\lambda}'_{z\delta_{f_{ij}}} - \frac{\alpha_{12}}{\rho} \sum_i \sum_j \tilde{b}_{\delta_{f_{ij}}} \breve{\hat{b}}_{\delta_{f_{ij}}} - \frac{\alpha_{13}}{\rho} \sum_i \sum_j \tilde{\lambda}_{\delta_f u_{f_{ij}}} \breve{\hat{\lambda}}_{\delta_f u_{f_{ij}}}.
\end{aligned} \tag{3.49}$$

The expressions of $\dot{V}_1|_{(3.20)}, \grave{V}_2|_{(3.26)}, V_3'|_{(3.32)}, \breve{V}_4|_{(3.39)}$ are substituted using equations (3.25), (3.31), (3.37) and (3.44) respectively. The differences between full-order and reduced-order dynamics are

$$\begin{aligned}
\dot{V}_1|_{(3.19)} - \dot{V}_1|_{(3.20)} &= e_x^T(\dot{e}_x|_{(3.19)} - \dot{e}_x|_{(3.20)}) \\
\grave{V}_2|_{(3.19)} - \grave{V}_2|_{(3.26)} &= e_{\delta_s}^T(\grave{e}_{\delta_s}|_{(3.19)} - \grave{e}_{\delta_s}|_{(3.26)}) \\
V_3'|_{(3.19)} - V_3'|_{(3.32)} &= e_z^T(e_z'|_{(3.19)} - e_z'|_{(3.32)}) \\
\breve{V}_4|_{(3.19)} - \breve{V}_4|_{(3.39)} &= e_{\delta_f}^T(\breve{e}_{\delta_f}|_{(3.19)} - \breve{e}_{\delta_f}|_{(3.39)}).
\end{aligned} \tag{3.50}$$

Substituting for all the dynamics terms from appropriate full and reduced systems and simplifying,

equation (3.49) becomes

$$\begin{aligned}
\dot{V}_c = &-\alpha_1 e_x^T K_x e_x - \frac{\alpha_2}{\sigma} e_{\delta_s}^T K_{\delta_s} e_{\delta_s} - \frac{\alpha_3}{\varepsilon} e_z^T K_z e_z - \frac{\alpha_4}{\rho} e_{\delta_f}^T K_{\delta_f} e_{\delta_f} \\
&+ \alpha_1 e_x^T [\gamma_x + \Lambda_{x\delta_s} G_{x\delta_s} e_{\delta_s} + \Lambda_{x\delta_f} G_{x\delta_f} (e_{\delta_f} + \delta_f^0 - \delta_f^0|_{z_r})] \\
&+ \frac{\alpha_3}{\varepsilon} e_z^T (\gamma_z + \Lambda_{z\delta_f} G_{z\delta_f} e_{\delta_f}) - \alpha_2 e_{\delta_s}^T \dot{\delta}_s^0 - \alpha_4 e_{\delta_f}^T \dot{\delta}_f^0 + \sum_i \sum_j \tilde{b}_{x_{ij}} (\alpha_1 e_{x_i} f_{x_j} - \alpha_5 \dot{\hat{b}}_{xx_{ij}}) \\
&+ \sum_i \sum_j \tilde{\lambda}_{x\delta_{s_{ij}}} (\alpha_1 (e_{x_i} (G_{x\delta_s} \delta_s^0)_j - \alpha_6 \dot{\hat{\lambda}}_{x\delta_{s_{ij}}}) + \sum_i \sum_j \tilde{\lambda}_{x\delta_{f_{ij}}} (\alpha_1 (e_{x_i} (G_{x\delta_f} \delta_f^0|_{z_r})_j - \alpha_7 \dot{\hat{\lambda}}_{x\delta_{f_{ij}}}) \\
&+ \frac{1}{\sigma} \sum_i \sum_j \tilde{b}_{\delta_{s_{ij}}} (\alpha_2 e_{\delta_{s_i}} f_{\delta_{s_j}} - \alpha_8 \dot{\hat{b}}_{\delta_{s_{ij}}}) + \frac{1}{\sigma} \sum_i \sum_j \tilde{\lambda}_{\delta_s u_{s_{ij}}} (\alpha_2 e_{\delta_{s_i}} (G_{\delta_s u_s} u_s)_j - \alpha_9 \dot{\hat{\lambda}}_{\delta_s u_{s_{ij}}}) \\
&+ \frac{1}{\varepsilon} \sum_k \sum_i \sum_j \tilde{b}_{z_{ij}}^k (\alpha_3 e_{z_i} f_{z_j}^k - \alpha_{10k} \hat{b}_{z_{ij}}^{k\prime}) + \frac{1}{\varepsilon} \sum_i \sum_j \tilde{\lambda}_{z\delta_{f_{ij}}} (\alpha_3 e_{z_i} (G_{z_{\delta_f}} \delta_f^0)_j - \alpha_{11} \hat{\lambda}'_{z\delta_{f_{ij}}}) \\
&+ \frac{1}{\rho} \sum_i \sum_j \tilde{b}_{\delta_{f_{ij}}} (\alpha_4 e_{\delta_{f_i}} f_{\delta_{f_j}} - \alpha_{12} \breve{\hat{b}}_{\delta_{f_{ij}}}) + \frac{1}{\rho} \sum_i \sum_j \tilde{\lambda}_{\delta_f u_{f_{ij}}} (\alpha_4 e_{\delta_{f_i}} (G_{\delta_f u_f} u_f)_j - \alpha_{13} \breve{\hat{\lambda}}_{\delta_f u_{f_{ij}}}).
\end{aligned} \tag{3.51}$$

In order to retain parameter estimation error terms instead of canceling them altogether, the parameter update laws are selected in a way similar to Sections 2.5 - 2.6. The update laws are

$$\begin{aligned}
\dot{\hat{b}}_{x_{ij}} &= \frac{\alpha_1}{\alpha_5} e_{x_i} f_{x_j} - \frac{\theta_1}{\alpha_5} (\hat{b}_{x_{ij}} - b_{x_{ij}}^0) \\
\dot{\hat{\lambda}}_{x\delta_{s_{ij}}} &= \frac{\alpha_1}{\alpha_6} e_{x_i} (G_{x\delta_s} \delta_s^0)_j - \frac{\theta_2}{\alpha_6} (\hat{\lambda}_{x\delta_{s_{ij}}} - \lambda_{x\delta_{s_{ij}}}^0) \\
\dot{\hat{\lambda}}_{x\delta_{f_{ij}}} &= \frac{\alpha_1}{\alpha_7} e_{x_i} (G_{x\delta_f} \delta_f^0|_{z_r})_j - \frac{\theta_3}{\alpha_7} (\hat{\lambda}_{x\delta_{f_{ij}}} - \lambda_{x\delta_{f_{ij}}}^0)
\end{aligned} \tag{3.52}$$

$$\begin{aligned}
\dot{\hat{b}}_{\delta_{s_{ij}}} &= \frac{\alpha_2}{\alpha_8} e_{\delta_{s_i}} f_{\delta_{s_j}} - \frac{\theta_4}{\alpha_8} (\hat{b}_{\delta_{s_{ij}}} - b_{\delta_{s_{ij}}}^0) \\
\dot{\hat{\lambda}}_{\delta_s u_{s_{ij}}} &= \frac{\alpha_2}{\alpha_9} e_{\delta_{s_i}} (G_{\delta_s u_s} u_s)_j - \frac{\theta_5}{\alpha_9} (\hat{\lambda}_{\delta_s u_{s_{ij}}} - \lambda_{\delta_s u_{s_{ij}}}^0)
\end{aligned} \tag{3.53}$$

$$\begin{aligned}
\hat{b}_{z_{ij}}^{k\prime} &= \frac{\alpha_3}{\alpha_{10k}} e_{z_i} f_{z_j}^k - \frac{\theta_6}{\alpha_{10k}} (\hat{b}_{z_{ij}}^k - b_{z_{ij}}^{k^0}) \\
\hat{\lambda}'_{z\delta_{f_{ij}}} &= \frac{\alpha_3}{\alpha_{11}} e_{z_i} (G_{z\delta_f} \delta_f^0)_j - \frac{\theta_7}{\alpha_{11}} (\hat{\lambda}_{z\delta_{f_{ij}}} - \lambda_{z\delta_{f_{ij}}}^0)
\end{aligned} \tag{3.54}$$

$$
\begin{aligned}
\dot{\hat{b}}_{\delta_{f_{ij}}} &= \frac{\alpha_4}{\alpha_{12}} e_{\delta_{f_i}} f_{\delta_{f_j}} - \frac{\theta_8}{\alpha_{12}} (\hat{b}_{\delta_{f_{ij}}} - b^0_{\delta_{f_{ij}}}) \\
\dot{\hat{\lambda}}_{\delta_f u_{f_{ij}}} &= \frac{\alpha_4}{\alpha_{13}} e_{\delta_{f_i}} (G_{\delta_f u_f} u_f)_j - \frac{\theta_9}{\alpha_{13}} (\hat{\lambda}_{\delta_f u_{f_{ij}}} - \lambda^0_{\delta_f u_{f_{ij}}})
\end{aligned}
\tag{3.55}
$$

In the update laws (4.126) - (4.129), x_i denotes the i-th element of the column vector x, and the following are design variables: $\theta_i > 0, i = 1, ..., 9$; $b^0_{x_{ij}}, \lambda^0_{x\delta_{sij}}, \lambda^0_{x\delta_{f_{ij}}}, b^0_{\delta_{sij}}, \lambda^0_{\delta_s u_{sij}}, b^{k^0}_{z_{ij}}, \lambda^0_{z\delta_{f_{ij}}}$, $b^0_{\delta_{f_{ij}}}, \lambda^0_{\delta_f u_{f_{ij}}}$. With these parameter update laws, the time-derivative (3.51) becomes

$$
\begin{aligned}
\dot{V}_c = & -\alpha_1 e_x^T K_x e_x - \frac{\alpha_2}{\sigma} e_{\delta_s}^T K_{\delta_s} e_{\delta_s} - \frac{\alpha_3}{\varepsilon} e_z^T K_z e_z - \frac{\alpha_4}{\rho} e_{\delta_f}^T K_{\delta_f} e_{\delta_f} \\
& + \alpha_1 e_x^T [\gamma_x + \Lambda_{x\delta_s} G_{x\delta_s} e_{\delta_s} + \Lambda_{x\delta_f} G_{x\delta_f} (e_{\delta_f} + \delta^0_f - \delta^0_f|_{z_r})] \\
& + \frac{\alpha_3}{\varepsilon} e_z^T (\gamma_z + \Lambda_{z\delta_f} G_{z\delta_f} e_{\delta_f}) - \alpha_2 e_{\delta_s}^T \dot{\delta}^0_s - \alpha_4 e_{\delta_f}^T \dot{\delta}^0_f + \theta_1 \sum_i \sum_j \tilde{b}_{x_{ij}} (\hat{b}_{x_{ij}} - b^0_{x_{ij}}) \\
& + \theta_2 \sum_i \sum_j \tilde{\lambda}_{x\delta_{sij}} (\hat{\lambda}_{x\delta_{sij}} - \lambda^0_{x\delta_{sij}}) + \theta_3 \sum_i \sum_j \tilde{\lambda}_{x\delta_{f_{ij}}} (\hat{\lambda}_{x\delta_{f_{ij}}} - \lambda^0_{x\delta_{f_{ij}}}) \\
& + \frac{\theta_4}{\sigma} \sum_i \sum_j \tilde{b}_{\delta_{sij}} (\hat{b}_{\delta_{sij}} - b^0_{\delta_{sij}}) + \frac{\theta_5}{\sigma} \sum_i \sum_j \tilde{\lambda}_{\delta_s u_{sij}} (\hat{\lambda}_{\delta_s u_{sij}} - \lambda^0_{\delta_s u_{sij}}) \\
& + \frac{\theta_6}{\varepsilon} \sum_k \sum_i \sum_j \tilde{b}^k_{z_{ij}} (\hat{b}^k_{z_{ij}} - b^{k^0}_{z_{ij}}) + \frac{\theta_7}{\varepsilon} \sum_i \sum_j \tilde{\lambda}_{z\delta_{f_{ij}}} (\hat{\lambda}_{z\delta_{f_{ij}}} - \lambda^0_{z\delta_{f_{ij}}}) \\
& + \frac{\theta_8}{\rho} \sum_i \sum_j \tilde{b}_{\delta_{f_{ij}}} (\hat{b}_{\delta_{f_{ij}}} - b^0_{\delta_{f_{ij}}}) + \frac{\theta_9}{\rho} \sum_i \sum_j \tilde{\lambda}_{\delta_f u_{f_{ij}}} (\hat{\lambda}_{\delta_f u_{f_{ij}}} - \lambda^0_{\delta_f u_{f_{ij}}}).
\end{aligned}
\tag{3.56}
$$

For any constant but unknown parameter p bounded as $\underline{p} \leq p \leq \bar{p}$, the expression $\tilde{p}(\hat{p} - p^0) = \tilde{p}(p - \tilde{p} - p^0) = \tilde{p}(p - p^0) - \tilde{p}^2 \leq \frac{1}{2}[\tilde{p}^2 + (p - p^0)^2] - \tilde{p}^2 \leq \frac{1}{2} \max_{\underline{p} \leq p \leq \bar{p}} (p - p^0)^2 - \frac{1}{2}\tilde{p}^2 = \frac{1}{2} p^+ - \frac{1}{2}\tilde{p}^2$,

where $p^+ = \max_{\underline{p} \le p \le \bar{p}} (p - p^0)^2$. Therefore, (3.56) can be upper-bounded as

$$\begin{aligned}
\dot{V}_c \le & -\alpha_1 e_x^T K_x e_x - \frac{\alpha_2}{\sigma} e_{\delta_s}^T K_{\delta_s} e_{\delta_s} - \frac{\alpha_3}{\varepsilon} e_z^T K_z e_z - \frac{\alpha_4}{\rho} e_{\delta_f}^T K_{\delta_f} e_{\delta_f} \\
& + \alpha_1 e_x^T [\gamma_x + \Lambda_{x\delta_s} G_{x\delta_s} e_{\delta_s} + \Lambda_{x\delta_f} G_{x\delta_f} (e_{\delta_f} + \delta_f^0 - \delta_f^0|_{z_r})] \\
& + \frac{\alpha_3}{\varepsilon} e_z^T (\gamma_z + \Lambda_{z\delta_f} G_{z\delta_f} e_{\delta_f}) - \alpha_2 e_{\delta_s}^T \dot{\delta}_s^0 - \alpha_4 e_{\delta_f}^T \dot{\delta}_f^0 \\
& - \frac{\theta_1}{2} \sum_i \sum_j \tilde{b}_{x_{ij}}^2 - \frac{\theta_2}{2} \sum_i \sum_j \tilde{\lambda}_{x\delta_{s_{ij}}}^2 - \frac{\theta_3}{2} \sum_i \sum_j \tilde{\lambda}_{x\delta_{f_{ij}}}^2 \\
& - \frac{\theta_4}{2\sigma} \sum_i \sum_j \tilde{b}_{\delta_{s_{ij}}}^2 - \frac{\theta_5}{2\sigma} \sum_i \sum_j \tilde{\lambda}_{\delta_s u_{s_{ij}}}^2 - \frac{\theta_6}{2\varepsilon} \sum_k \sum_i \sum_j \tilde{b}_{z_{ij}}^{k^2} \\
& - \frac{\theta_7}{2\varepsilon} \sum_i \sum_j \tilde{\lambda}_{z\delta_{f_{ij}}}^2 - \frac{\theta_8}{2\rho} \sum_i \sum_j \tilde{b}_{\delta_{f_{ij}}}^2 - \frac{\theta_9}{2\rho} \sum_i \sum_j \tilde{\lambda}_{\delta_f u_{f_{ij}}}^2 + \mu_0.
\end{aligned} \tag{3.57}$$

where

$$\begin{aligned}
\mu_0 := & \frac{\theta_1}{2} \sum_i \sum_j b_{x_{ij}}^+ + \frac{\theta_2}{2} \sum_i \sum_j \lambda_{x\delta_{s_{ij}}}^+ + \frac{\theta_3}{2} \sum_i \sum_j \lambda_{x\delta_{f_{ij}}}^+ \\
& + \frac{\theta_4}{2\sigma} \sum_i \sum_j b_{\delta_{s_{ij}}}^+ + \frac{\theta_5}{2\sigma} \sum_i \sum_j \lambda_{\delta_s u_{s_{ij}}}^+ + \frac{\theta_6}{2\varepsilon} \sum_k \sum_i \sum_j b_{z_{ij}}^{k^+} \\
& + \frac{\theta_7}{2\varepsilon} \sum_i \sum_j \lambda_{z\delta_{f_{ij}}}^+ + \frac{\theta_8}{2\rho} \sum_i \sum_j b_{\delta_{f_{ij}}}^+ + \frac{\theta_9}{2\rho} \sum_i \sum_j \lambda_{\delta_f u_{f_{ij}}}^+.
\end{aligned} \tag{3.58}$$

Equation (3.57) has several terms for which the upper bounds are to be found. Similar to Sections 2.5 - 2.6, this is done by invoking the notion of compact sets. Let N_1 denote the combined dimension of the states and the unknown parameters. Consider a compact set $Q_1 \in \mathbb{R}^{N_1}$, such that the composite Lyapunov function (3.46) everywhere in Q_1 is upper-bounded by $\bar{V}$; i.e. $V_c \le \bar{V}$ for some $\bar{V} > 0$. Let N_2 denote the combined dimension of the references and their time-derivatives of first and second orders. Consider a compact set $Q_2 \in \mathbb{R}^{N_2}$, characterized by $\|x_r\|_2^2 + \|\dot{x}_r\|_2^2 + \|\ddot{x}_r\|_2^2 + \|z_r\|_2^2 + \|\dot{z}_r\|_2^2 + \|\ddot{z}_r\|_2^2 \le R^2$ for some $R > 0$. Then $Q := Q_1 \times Q_2$ is a compact set in $\mathbb{R}^{N_1+N_2}$, and all the elements of the vectors $z^0, \delta_f^0 - \delta_f^0|_{z_r}, \dot{\delta}_s^0, \dot{z}^0, \dot{\delta}_f^0$ are continuous functions in the compact set Q. Therefore, each element of these vectors has a maximum, and consequently there exist constants M_1, M_2, M_3 such that $\left\|\delta_f^0 - \delta_f^0|_{z_r}\right\|_\infty = M_1, \left\|\dot{\delta}_s^0\right\|_\infty = M_2, \left\|\dot{\delta}_f^0\right\|_\infty = M_3$. At this point, upper bounds of the cross-terms can be found similar to Section 2.6, and the final form of

the time-derivative of the composite Lyapunov function becomes

$$\begin{aligned}\dot{V}_c \leq & -\beta_1 e_x^T e_x - \beta_2 e_{\delta_s}^T e_{\delta_s} - \beta_3 e_z^T e_z - \beta_4 e_{\delta_f}^T e_{\delta_f} \\ & - \frac{\theta_1}{2}\sum_j \tilde{b}_{x_{ij}}^2 - \frac{\theta_2}{2}\sum_i\sum_j \tilde{\lambda}_{x\delta_{sij}}^2 - \frac{\theta_3}{2}\sum_i\sum_j \tilde{\lambda}_{x\delta_{f_{ij}}}^2 \\ & - \frac{\theta_4}{2\sigma}\sum_i\sum_j \tilde{b}_{\delta_{sij}}^2 - \frac{\theta_5}{2\sigma}\sum_i\sum_j \tilde{\lambda}_{\delta_s u_{sij}}^2 - \frac{\theta_6}{2\varepsilon}\sum_k\sum_i\sum_j \tilde{b}_{z_{ij}}^{k^2} \\ & - \frac{\theta_7}{2\varepsilon}\sum_i\sum_j \tilde{\lambda}_{z\delta_{f_{ij}}}^2 - \frac{\theta_8}{2\rho}\sum_i\sum_j \tilde{b}_{\delta_{f_{ij}}}^2 - \frac{\theta_9}{2\rho}\sum_i\sum_j \tilde{\lambda}_{\delta_f u_{f_{ij}}}^2 + \mu\end{aligned} \tag{3.59}$$

where $\beta_i; i = 1, 2, 3, 4$ and μ are functions of known constants, controller and parameter estimator gains, and the time-scale separation parameters $\sigma, \varepsilon, \rho$. Similar to Section 2.6, the gains and other design variables can be chosen such that the errors will be ultimately bounded within some lower and upper bounds of the time-scale separation parameters.

Remark 9. *If the actuators are assumed free of uncertainty, closed-form solutions for the bounds of $\sigma, \varepsilon, \rho$ can be obtained similar to Section 2.6.*

3.3.3 Numerical Results: Climb and Roll Maneuver of a Generic F-16A Using the Sequential Approach

This subsection shows in simulation simultaneous slow and fast state tracking using the new sequential approach for a nonlinear six-degree-of-freedom aircraft. The new sets of control and parameter update laws are implemented on a nonlinear 6-DOF generic F-16A commanded to perform the same climb and roll maneuver as the one for the earlier two-stage design. The differences between the previous simulation and the current simulation are as follows:

1. To be consistent with the new theory, yaw rate is commanded instead of sideslip angle. As a result velocity is the slow state to be tracked, and the body-axis roll, pitch and yaw rates are the fast states to be tracked. Zero commanded yaw rate is considered as an equivalent of zero sideslip angle.

2. Actuator dynamics are included in the design synthesis.

3. Model uncertainties are accounted for. The inertias, control derivatives and the engine time-constant are assumed constant but unknown.

At time zero the generic F-16A is at steady level trim with a velocity of 800 ft/s at an altitude of 15,000 ft. The trim angle-of-attack and elevator deflection are 0.9 deg and -1.6 deg respectively. The thrust at trim is 3265.0 lbf, which is 18.34% of the maximum military thrust of 17,800 lbf. All other angles, rates and control surface deflections are zero at trim. A climb is commanded at a pitch rate of 15 deg/s followed by a roll at a rate of 20 deg/s while maintaining zero yaw rate and velocity 800 ft/s. The reference pitch rate increases smoothly from zero to 15 deg/s, then goes back to zero and reaches -15 deg/s before becoming zero again. Similarly, the commanded roll rate goes from zero to 20 deg/s, then decreases to zero, reaches -20 deg/s, and finally becomes zero again.

The uncertainties are assumed as follows. The initial estimate of each inertia $I_{xx}, I_{yy}, I_{zz}, I_{xz}$ is assumed 15% below its actual value. The initial estimate of each of the control derivatives $C_{x_{\delta_e}}, C_{y_{\delta_a}}, C_{y_{\delta_r}}, C_{z_{\delta_e}}, C_{m_{\delta_e}}, C_{l_{\delta_a}}, C_{l_{\delta_r}}, C_{n_{\delta_a}}, C_{n_{\delta_r}}$ is assumed 50% below its actual value. The engine time-constant is assumed 25% above its actual value. No uncertainty is assumed for the stability derivatives as well as the time-constants of the elevator, aileron and rudder.

The controller gains are selected such that the matrices $K_x, K_{\delta_s}, K_z, K_{\delta_f}$ are positive-definite. They are chosen as $K_x = 100$, $K_{\delta_s} = 0.005$, $K_z = diag[500, 1000, 500]$, $K_{\delta_f} = diag[1, 1, 1]$. To design the parameter estimator, gains are selected as $\alpha_1 = 10^{-13}, \alpha_2 = 10^{-14}, \alpha_3 = 10^{-15}, \alpha_7 = 1, \alpha_8 = 1, \alpha_9 = 1, , \alpha_{101} = 1, \alpha_{102} = 1, \alpha_{11} = 1, \theta_i = 0.5; i = 3, 4, 5, 6, 7$. The design variables corresponding to the final value of the estimates in the parameter update laws are chosen such that the inertias, control derivatives and engine time-constant are 5% above the actual values. The simulation is run for 40 sec.

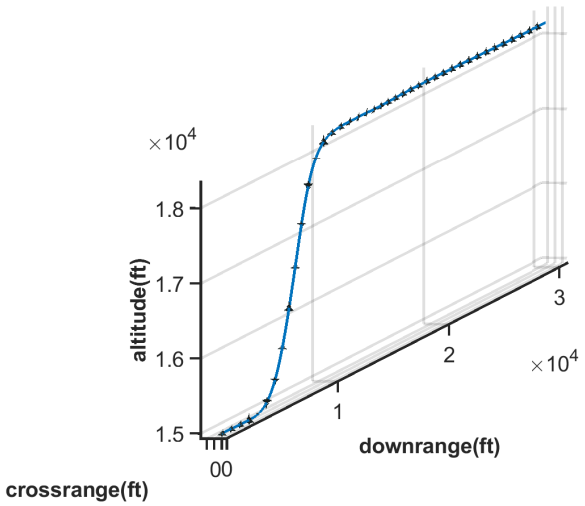

Figure 3.7: Trajectory of the generic F-16A during the climb and roll maneuver

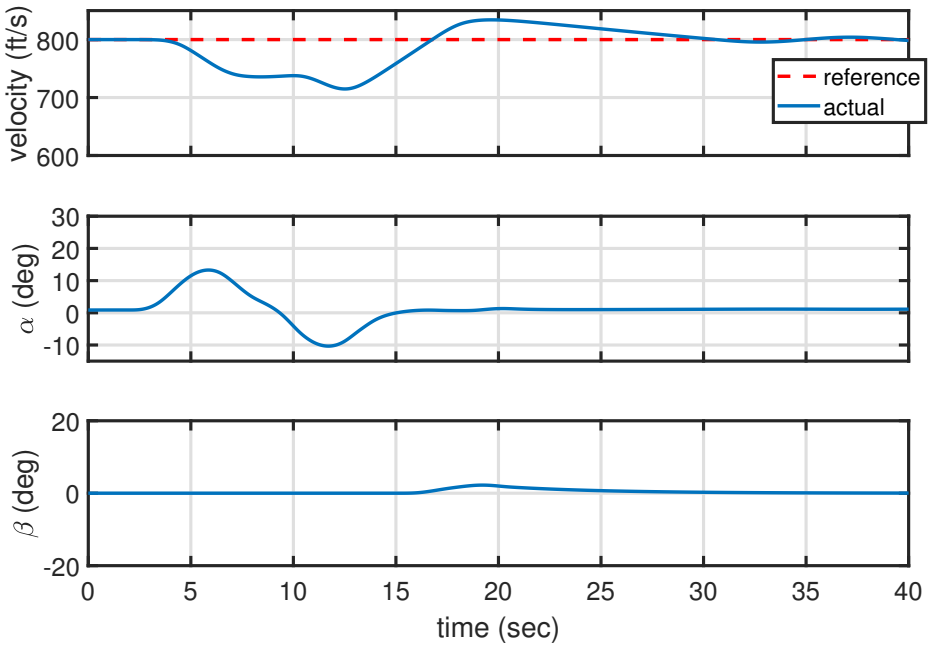

Figure 3.8: Velocity, angle-of-attack and sideslip angle during the climb and roll maneuver

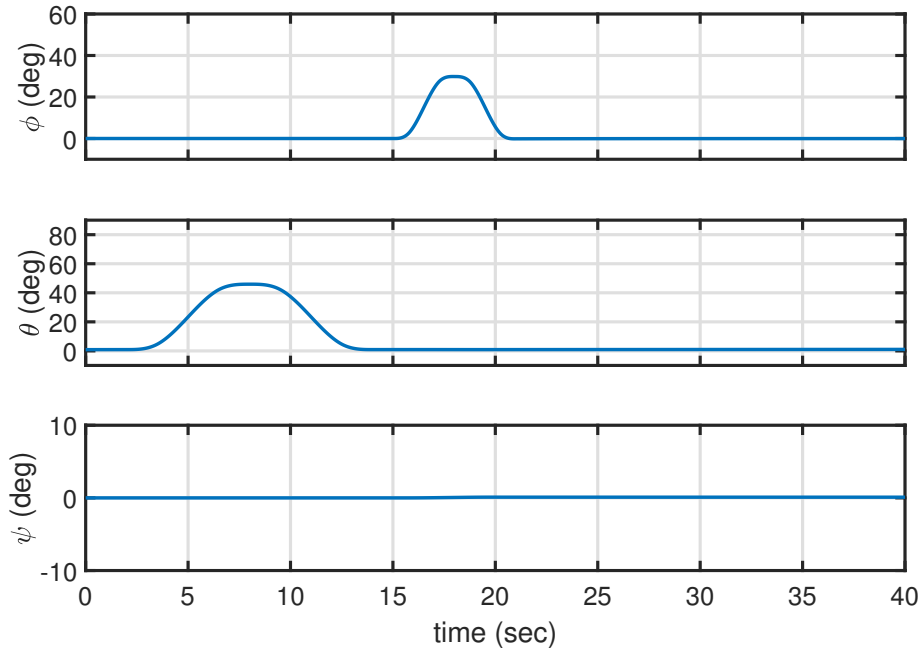

Figure 3.9: Bank angle, pitch attitude angle and heading angle during the climb and roll maneuver

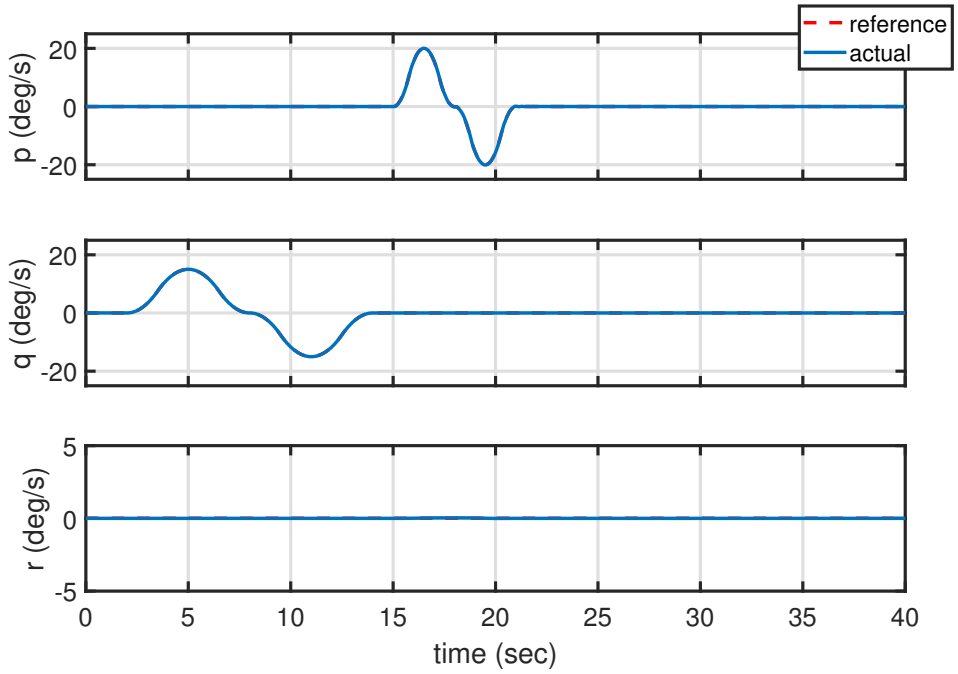

Figure 3.10: Body-axis roll, pitch and yaw rates during the climb and roll maneuver

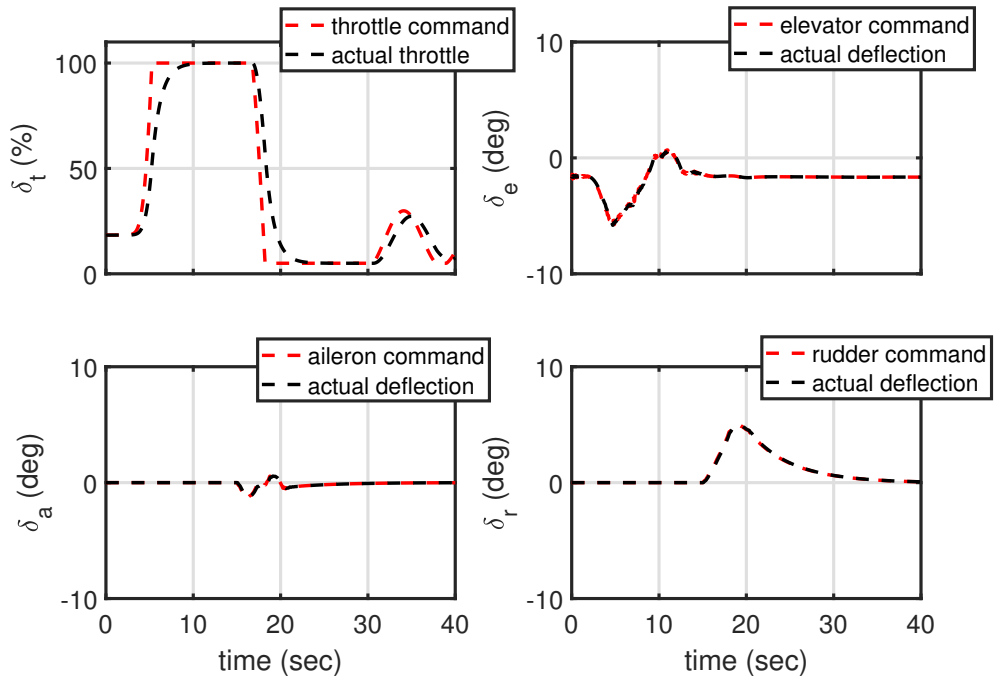

Figure 3.11: Throttle, elevator, aileron and rudder deflections during the climb and roll maneuver

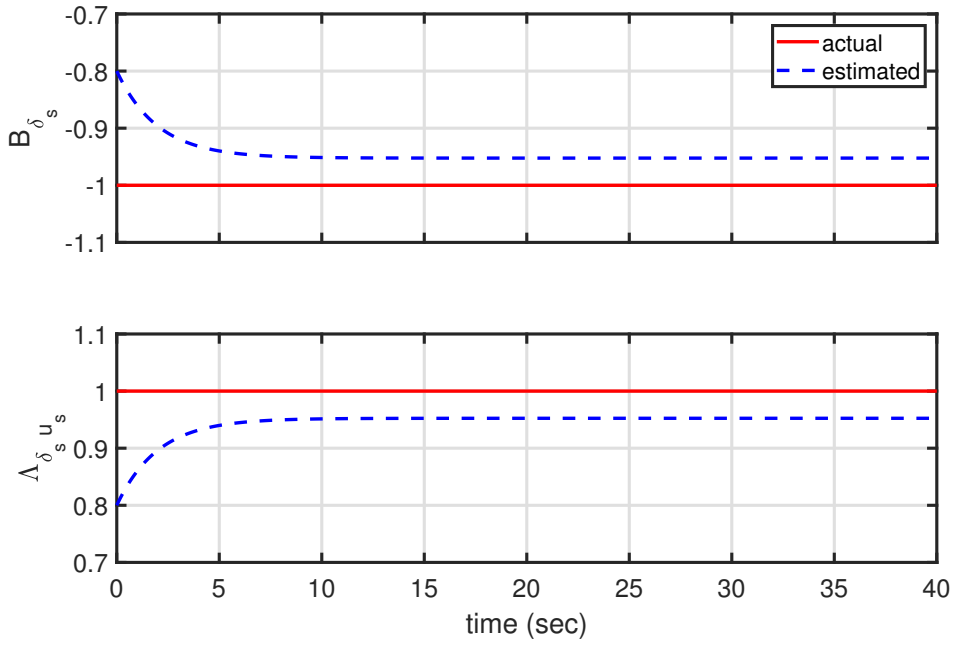

Figure 3.12: Uncertain parameters B_{δ_s} and $\Lambda_{\delta_s u_s}$ during the climb and roll maneuver

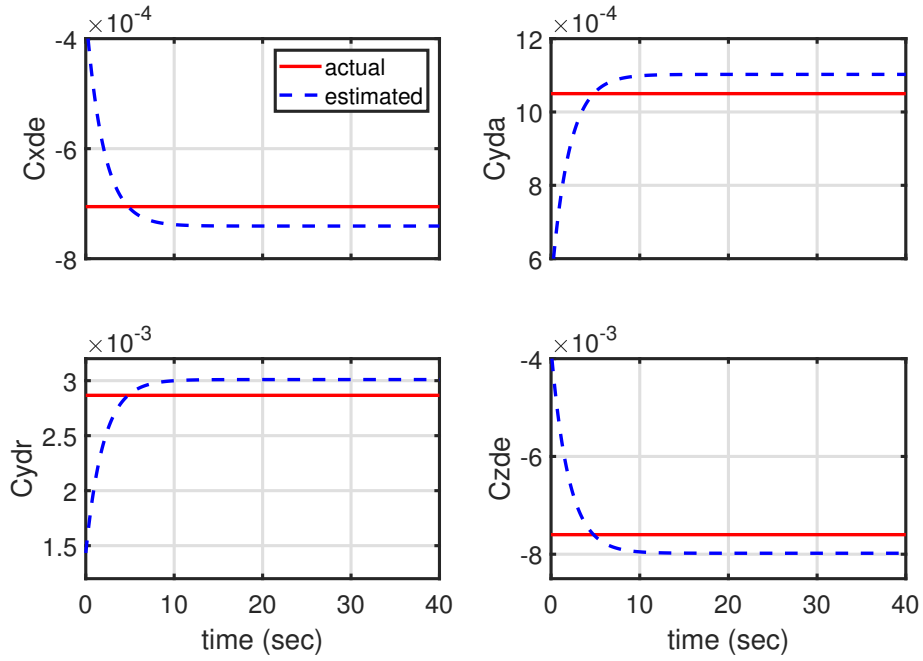

Figure 3.13: Uncertain parameters $C_{x_{\delta_e}}, C_{y_{\delta_a}}, C_{y_{\delta_r}}, C_{z_{\delta_e}}$ during the climb and roll maneuver

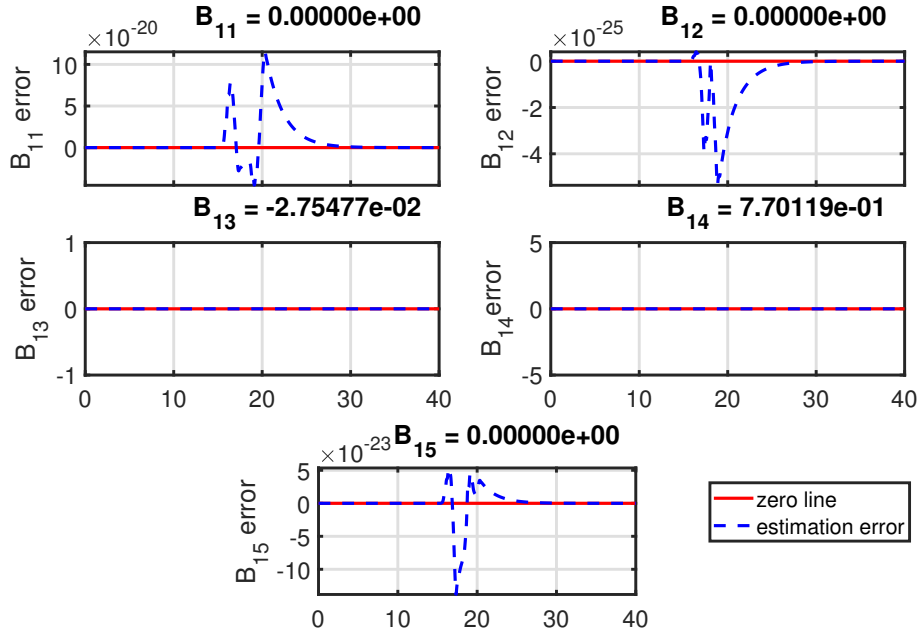

Figure 3.14: Uncertain parameters $B_{11} - B_{15}$ during the climb and roll maneuver; the x-axis of each graph representing time in seconds

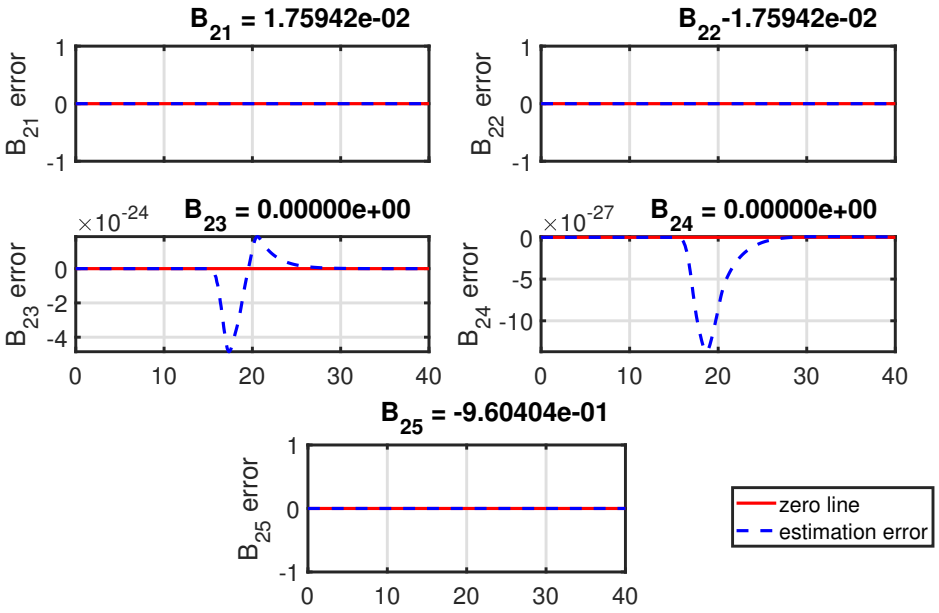

Figure 3.15: Uncertain parameters $B_{21} - B_{25}$ during the climb and roll maneuver; the x-axis of each graph representing time in seconds

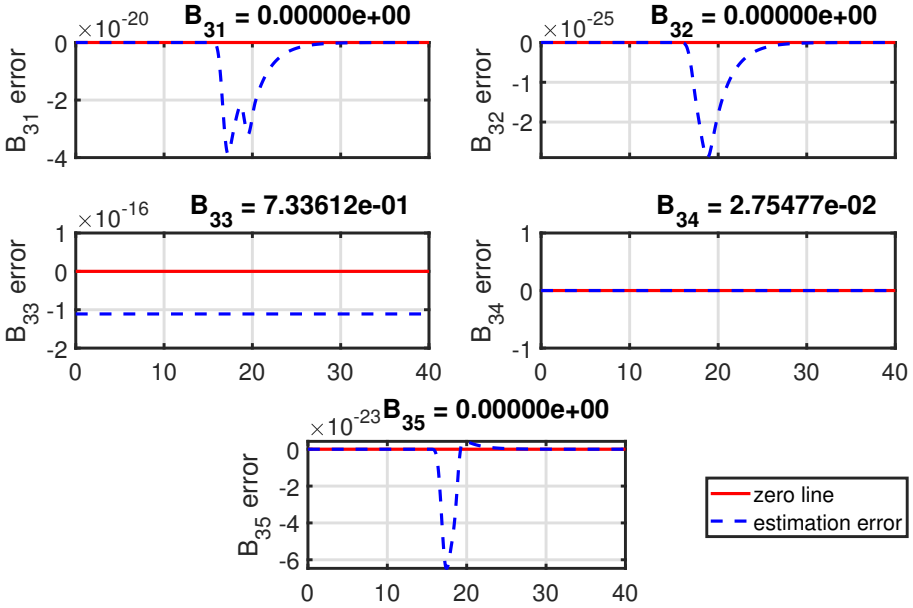

Figure 3.16: Uncertain parameters $B_{31} - B_{35}$ during the climb and roll maneuver; the x-axis of each graph representing time in seconds

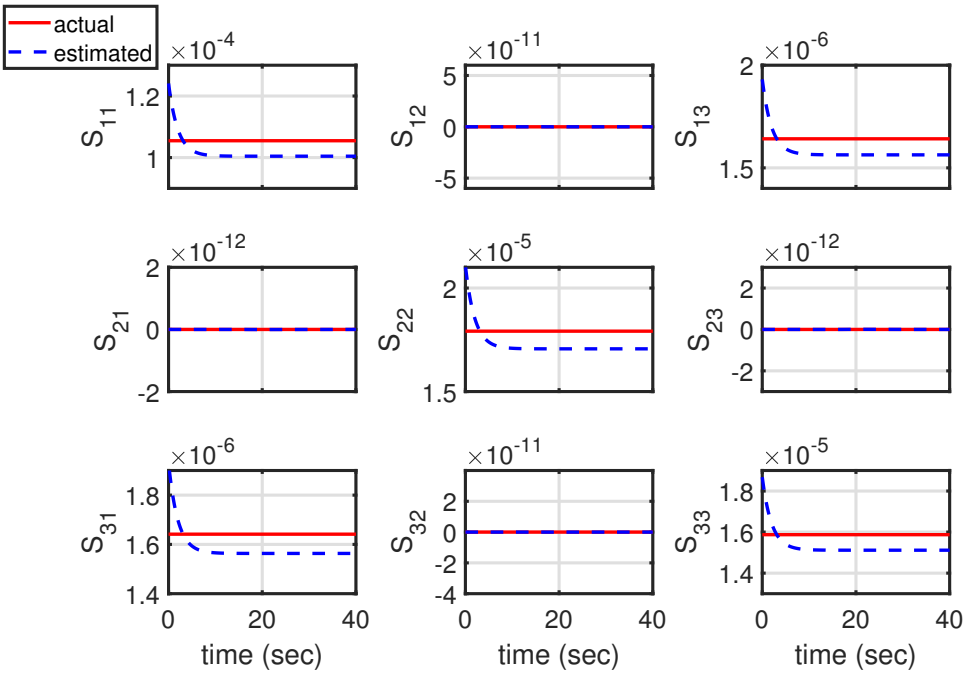

Figure 3.17: Uncertain parameters $S_{31} - S_{33}$ during the climb and roll maneuver

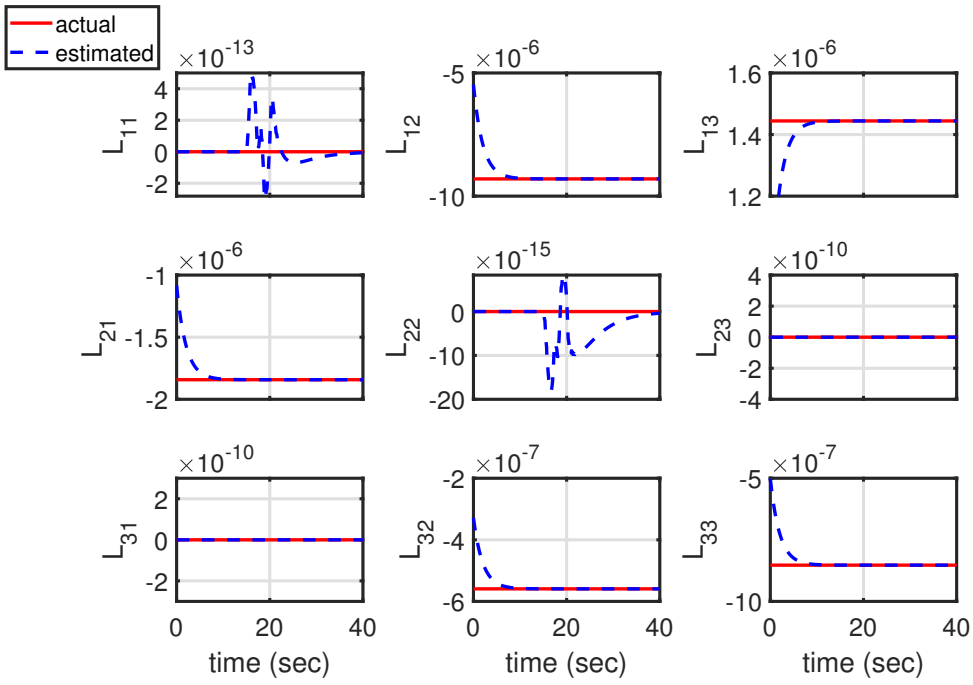

Figure 3.18: Uncertain parameters $L_{11} - L_{33}$ during the climb and roll maneuver

Figures 3.7 - 3.11 show the time-histories of the states and controls during the climb and roll maneuver. An improvement in velocity profile compared to the earlier two stage design can be observed in Figure 3.8. The loss of airspeed is within 10% compared to 25% in the earlier design. Good tracking of the body-axis roll, pitch and yaw rates can be observed in Figure 3.10. The tracking errors for the rates are seen to be are almost zero at all times. All the other states and the controls remain bounded and within acceptable limits.

Figures 3.12 - 3.18 show the time-histories of the uncertain parameters for the climb and roll maneuver. Similar to the slow state tracking maneuvers, it can be observed that the parameter estimation errors remain bounded and small.

3.4 Concluding Remarks for the Chapter

This chapter investigated and developed a novel approach of simultaneous slow and fast state tracking for finite-dimensional, nonlinear, nonstandard multiple-time-scale systems with actuator dynamics and uncertainties in model structure and parameters. This was accomplished using a controller using the estimates of the parameters, and a parameter estimator updating them online. A nonlinear 6-DOF aircraft simulation demonstrated the effectiveness of the new control synthesis method and showed the improvements over the previous two-stage design method.

For simultaneous slow and fast state tracking for nonstandard systems, the theory developed in this chapter made a transition from the earlier two-stage approach to the new sequential approach. Unlike the two-stage approach, the sequential approach was able to account for uncertainties and actuator dynamics. Parametric uncertainties in the evolutions of the slow states, slow actuators, fast states, fast actuators, and additive uncertainties in the evolutions of slow and fast states were accounted for. In addition, the development realistically accounted for slow and fast actuator dynamics instead of assuming all actuators to be infinitely fast, or adding actuator dynamics only in simulation.

Using composite Lyapunov analysis, it was rigorously proved that the tracking error of the slow states, the manifold error of the fast states and actuators, and the estimation error of the unknown parameters remain ultimately bounded. To ensure ultimate boundedness, this method

established new bounds of the time-scale separation parameters: $\sigma_{**}, \sigma^{**}, \varepsilon_{**}, \varepsilon^{**}, \rho_{**}, \rho^{**}$. The explicit differentiations of the manifolds was cumbersome for the classes of systems considered as three-time-scale and four-time-scale. The use of compact sets and extreme value theorem helped avoid the explicit differentiation and simplified the boundedness proof.

While this method considered actuator dynamics and thereby actuator rate limits, magnitude limits of actuators were not realistically accounted for in the control design. The control signals were kept within acceptable limits implicitly with gains. In the simulation the throttle was kept at 100% whenever the computed value was 100% or more. An improved version of the theory is needed to handle actuator magnitude limits realistically in the design.

Uncertainties were assumed in the deterministic sense instead of stochastic. While parametric uncertainties and modeling errors could be taken care of, handling certain types of disturbances such as gust and turbulence in aircraft requires an improved version of the theory with stochastic uncertainties. A major challenge to overcome is to rigorously prove stability using stochastic Lyapunov functions.

This method relied on several parameter estimate matrices being invertible, especially the ones appearing in the control distribution. A way to ensure invertibility was to wisely choose the initial conditions and design parameters corresponding to final values of the estimates. An updated version of the theory is needed to realistically account for singularities in control distribution.

4. STATE TRACKING IN THE PRESENCE OF UNCERTAINTIES AND ACTUATOR DYNAMICS WITH OUTPUT FEEDBACK

4.1 Introduction

This chapter addresses the third objective of developing a theory of output feedback for state tracking of nonlinear, nonstandard multiple-time-scale systems with actuator dynamics and uncertainties. To reach the end goal, output feedback design using state observers for deterministic systems is considered first. Section 4.2 covers the theory of output feedback design for slow state regulation of a two-time-scale system where the reduced subsystems are linear, but the nonlinearity appears in the full-order system. It is seen that a knowledge of the upper bound of the nonlinearity is utilized to provide sufficient conditions to select the gains. For different cases of measurement, Lyapunov-based observer designs are investigated. This section also produces a new bound ε^{***} of the time-scale separation parameter ε within which stability of the full-order system is guaranteed under output feedback. This is numerically compared with ε^{*}, the bound for full-state feedback. Subsequently, a more general class of four-time-scale systems is considered for output feedback design in Sections 4.3 and 4.4. This class is assumed to have multiplicative and additive uncertainties similar to the cases of full-state feedback, with the modification that the kinetic slow states are divided into measured and unmeasured states. Using composite Lyapunov analysis, update laws for both of the unknown parameters and unmeasured states are selected, and bounds of time-scale separation $\sigma_{***}, \sigma^{***}, \varepsilon_{***}, \varepsilon^{***}, \rho_{***}, \rho^{***}$ are established to guarantee ultimate boundedness of tracking error, manifold error, parameter estimation error, and state observation error. The theory is demonstrated in simulation on a nonlinear 6-DOF generic F-16A commanded to perform large-amplitude combined longitudinal and lateral/directional maneuvers. Section 4.5 lists the concluding remarks for this chapter.

4.2 Slow State Regulation of a Deterministic Two-Time-Scale System Using Output Feedback with Lyapunov-Based Controller and Observer

It was discussed in Chapter 1 that most of the works in the literature on observer design of multiple-time-scale systems assumed the system dynamics to be linear or linearized. For a nonlinear two-time-scale spring-mass-damper with one slow and one fast states, both of the controller and the observer were designed in two time-scales [51]. This observer-based feedback design was an extension of the method of sequential control developed earlier with the assumption of full-state feedback [11]. The Lyapunov design of observers in two time-scales led to guaranteed stability of the corresponding reduced subsystems. A total of six cases - two different cases of dynamics and three difference cases of measurement - were described, and results were presented for four of them. The cases of dynamics were (a) high damping and (b) high stiffness. The cases of measurement were (a) only the slow state measured, (b) only the fast state measured, (c) a linear combination of the states measured. While this paper demonstrated how the sequential control can be extended to observer-based feedback, the stability of the full-order nonlinear system including the controller and the observer in the loop was not investigated. For one of the four cases in this paper, the procedure was extended further to a nonlinear spring-mass-damper with multiple slow and fast states [52]. This work showed an approach to analyze closed-loop stability of the full-order system by using an extension of the composite Lyapunov analysis. The composite Lyapunov function for the full-order system was a linear combinations of the individual Lyapunov functions used to design the controller and the state observer.

While the previous works of the authors [51, 52] addressed the controller and observer design using reduced subsystems in two time-scales, a few issues have not been investigated yet. One of the previous works [52] established an acceptable range of the time-scale separation parameter graphically by plotting the eigenvalues of a matrix. Moreover, there was no guideline on acceptable ranges of gains to obtain a suitable bound of time-scale separation. A more rigorous analytical treatment of the composite Lyapunov analysis is needed for output feedback. In addition, the model used in this work [52] is such that the nonlinearity is present in the reduced subsystems.

This nonlinearity can be canceled in part by the controller design. However, the analysis becomes more challenging when the nonlinearity is present in the full-order dynamics but is not captured in the reduced subsystems. The cases of high damping in the authors' another previous work [51] fall under this category, and the stability analysis for them is yet to be investigated. Furthermore, how the different cases of measurement alter the bounds of stability is yet to be investigated. This Section develops the theory for output feedback for a class of nonlinear nonstandard two-time-scale systems similar to the high damping model [51] with a more generic form of the nonlinearity. The theory takes care of the nonlinearity present in the full-order system but not captured in reduced subsystems. All the three cases of measurement mentioned in the authors' previous work [51] are considered to develop the theory. An extension of the composite Lyapunov analysis includes both controller and observer for stability of the full-order nonlinear system in closed-loop. For different cases of measurement, the analysis produces guidelines to choose the gains as well as the bound ε^{***}, which is the upper bound of the time-scale separation parameter ε to ensure global asymptotic stability of the full-order system.

This section uses a nonlinear state-space model similar to the spring-mass-damper with high damping used in the authors' previous work [51], but considers a more generic form of the nonlinearity. The following class of systems is investigated in this paper:

$$\begin{aligned} \dot{x} &= z \\ \varepsilon \dot{z} &= -\varepsilon f(x,z)z - pz + u. \end{aligned} \tag{4.1}$$

The quantities in model (4.1) are as follows: x is the displacement, z is the velocity, ε satisfying $0 < \varepsilon << 1$ is the perturbation parameter, $f(x,z)$ can be any nonlinear function of x and z satisfying $0 \leq f(x,z) \leq \theta_f$ where θ_f is a specified upper bound, $p > 0$ is a known constant parameter, and u is the control force. The presence of ε with the time derivative of the state z indicates that the velocity z is the fast state, whereas displacement x is the slow state. The nonlinearity $f(x,z)z$ being multiplied by ε means that this is present in the full-order dynamics, but will not show up in the reduced-order dynamics obtained by the substitution $\varepsilon = 0$.

4.2.1 Development of Control Law Using Reduced Subsystems

It is desired for the control to drive the slow state x from its initial condition $x(0)$ to the origin. The fast state z has an initial condition $z(0)$, but does not have any specified reference. According to the singular perturbation theory, the control u must be able to stabilize z about any suitable manifold z^0 in the fast time-scale, such that the slow state x can be regulated in the slow time-scale. The method of sequential control [11] was developed to accomplish this objective. However, the method assumes full-state feedback. In case all the states are not explicitly measurable, one way to design output feedback control is to use a state observer to feed estimates of the unmeasured states to the controller. Since the system under study is nonlinear, and the controller and observer designs are likely to be coupled, a new theory needs to be developed in order to establish the closed-loop stability under observer-based feedback. To be able to compare the existing full-state feedback design and the new observer-based feedback design, this Section first addresses the design of the full-state feedback controller. Subsequently the observer-based feedback design is discussed, and it includes three cases of measurement: (a) only the slow state is measured, (b) only the fast state is measured, (c) a linear combination of the slow and the fast states is measured.

The method of sequential control involves the design of the manifold and control to ensure the Lyapunov-stability of the reduced subsystems and composite Lyapunov analysis to establish the Lyapunov-stability of the full-order system. In this paper composite Lyapunov analysis for full-state feedback is performed so the result can be compared with that for output feedback. The controller design using reduced subsystems involves two steps.

4.2.1.1 Design of Manifold in the Slow Time-Scale

The first step is the design of the manifold such that the reduced slow subsystem is stabilized about the origin. Substituting $\varepsilon = 0$ in the full-order dynamics (4.1) the reduced slow subsystem is

$$\begin{aligned} \dot{x} &= z^0 \\ 0 &= -pz^0 + u^0 \end{aligned} \tag{4.2}$$

where z^0 is the manifold of the fast state to be designed, and u^0 is the effective control in the slow time-scale. A positive-definite slow Lyapunov function and its derivative with respect to the slow time-scale t are

$$\begin{aligned} V_{s_c} &= \frac{1}{2}x^2 \\ \dot{V}_{s_c} &= x\dot{x}. \end{aligned} \tag{4.3}$$

Let $f(.)|_{(i)}$ denote the value of the function $f(.)$ for system denoted by equation (i). For the reduced slow subsystem (4.2) the time-derivative of the slow Lyapunov function becomes

$$\dot{V}_{s_c}|_{(4.2)} = x\dot{x}|_{(4.2)} = xz^0. \tag{4.4}$$

Choose the manifold as

$$z^0 = -k_1 x \tag{4.5}$$

where $k_1 > 0$ is a gain, such that the time-derivative of the Lyapunov function

$$\dot{V}_{s_c}|_{(4.2)} = -k_1 x^2 \tag{4.6}$$

is negative-definite. Thus the equilibrium $x = 0$ of the reduced slow subsystem is Lyapunov-stable.

4.2.1.2 Design of the Control in the Fast Time-Scale

The second step is to design the control u such that the reduced fast subsystem is stabilized about the manifold z^0 selected in the first step. Construct the fast time-scale $\tau = \frac{t}{\varepsilon}$. In this time-scale, the full-order system (4.1) becomes

$$\begin{aligned} x' &= \varepsilon z \\ z' &= -\varepsilon f(x,z)z - pz + u. \end{aligned} \tag{4.7}$$

The 'prime' denotes differentiation with respect to the fast time-scale τ. Set $\varepsilon = 0$ in (4.7) to obtain the reduced fast subsystem

$$\begin{aligned} x' &= 0 \\ z' &= -pz + u. \end{aligned} \tag{4.8}$$

A positive-definite fast Lyapunov function and its derivative with respect to the fast time-scale τ are

$$\begin{aligned} V_{f_c} &= \frac{1}{2}(z - z^0)^2 \\ V'_{f_c} &= (z - z^0)(z' - z^{0\prime}). \end{aligned} \tag{4.9}$$

For the reduced fast subsystem (4.8), the time-derivative becomes

$$\begin{aligned} V'_{f_c}|_{(4.8)} &= (z - z^0)(z'|_{(4.8)} - z^{0\prime}|_{(4.8)}) \\ &= (z - z^0)(z'|_{(4.8)} + k_1 x'|_{(4.8)}) = (z + k_1 x)(-pz + u). \end{aligned} \tag{4.10}$$

Design the control as

$$u = pz - k_2(z - z^0) = -k_1 k_2 x - (k_2 - p)z \tag{4.11}$$

where $k_2 > 0$ is another gain, such that the time-derivative

$$V'_{f_c}|_{(4.8)} = -k_2(z - z^0)^2 \tag{4.12}$$

is negative-definite. Thus the equilibrium $z = z^0$ of the reduced fast subsystem is Lyapunov-stable.

4.2.1.3 The Bound of Time-Scale Separation ε^* for Comparison

It is important to note that although the control is designed using the reduced subsystems given by (4.2) and (4.8), the control is to be implemented on the full-order system given by (4.1) or equivalently by (4.7). It is also important to note that the full-order system is nonlinear, while the reduced subsystems are linear. The difference between the full-order and reduced-order dynamics and the proof that the control law works on the full-order system up to a certain stability bound are addressed in this Subsubsection.

The composite Lyapunov analysis [10] accounts for the difference between full-order and reduced-order dynamics. This analysis starts with selecting a composite Lyapunov function for the full-order nonlinear system, and yields an upper bound ε^* of the perturbation parameter ε, up to which the control law ensures stability of the full-order system. A candidate composite Lyapunov function for the full-order system is

$$V_{c_{fs}} = w_1 V_{s_c} + w_2 V_{f_c}. \tag{4.13}$$

This function is positive-definite and radially unbounded for any $w_1, w_2 > 0$. The factors $w_1, w_2 > 0$ are gains signifying the contributions of the individual Lyapunov functions to the composite. The following theorem gives the bound of the time-scale separation parameter ε for stability of the full-order system under full-state feedback.

Theorem 3. *Suppose that the gains $k_1 > 0, w_1 > 0, w_2 > 0$ can be chosen such that the following inequalities hold:*

$$\begin{aligned} k_1 &< \frac{4w_1}{w_2\theta_f} \\ (w_2k_1^2 + w_1)^2 &- w_2^2k_1^3\theta_f > 0 \end{aligned} \tag{4.14}$$

where θ_f is the upper bound of the nonlinear function $f(x,z)$. Then the full-order system (4.1) (or equivalently (4.7)) under the full-state feedback control law (4.11) is globally asymptotically stable, and equivalently $z \to z^0$ and $x \to 0$ as $t \to \infty$ from any set of initial conditions $z(0), x(0)$ for $0 < \varepsilon < \varepsilon^*$, where

$$\varepsilon^* = \frac{k_1k_2w_2(4w_1 - w_2k_1\theta_f)}{(w_2k_1^2 + w_1)^2 - w_2^2k_1^3\theta_f}. \tag{4.15}$$

Proof. The time-derivative of the composite Lyapunov function (4.13) for the full-order system (4.1) (equivalently (4.7)) is

$$\dot{V}_{c_{fs}} = w_1\dot{V}_{s_c}|_{(4.1)} + \frac{w_2}{\varepsilon}V'_{f_c}|_{(4.7)}. \tag{4.16}$$

Adding and subtracting the time-derivatives of Lyapunov functions for appropriate reduced subsystems, the time-derivative of the composite Lyapunov function for the full-order system

becomes

$$\dot{V}_{c_{fs}} = w_1 \dot{V}_{s_c}|_{(4.2)} + \frac{w_2}{\varepsilon} V'_{f_c}|_{(4.8)} + w_1(\dot{V}_{s_c}|_{(4.1)} - \dot{V}_{s_c}|_{(4.2)}) + \frac{w_2}{\varepsilon}(V'_{f_c}|_{(4.7)} - V'_{f_c}|_{(4.8)}). \quad (4.17)$$

The first two terms in the right-hand side of equation (4.17) correspond to the reduced-order dynamics. The third and the fourth terms correspond to the difference between the full-order and the reduced-order dynamics. Making appropriate substitutions for the time-derivatives of the Lyapunov functions, equation (4.17) becomes

$$\begin{aligned} \dot{V}_{c_{fs}} = & -w_1 k_1 x^2 - \frac{w_2}{\varepsilon} k_2 (z - z^0)^2 + w_1 x(\dot{x}|_{(4.1)} - \dot{x}|_{(4.2)}) \\ & + \frac{w_2}{\varepsilon}(z - z^0)[(z'|_{(4.7)} - z'|_{(4.8)}) + k_1(x'|_{(4.7)} - x'|_{(4.8)})]. \end{aligned} \quad (4.18)$$

Substituting for all the relevant dynamics terms, the time-derivative of the composite Lyapunov function reduces to

$$\dot{V}_{c_{fs}} = -w_1 k_1 x^2 - \frac{w_2}{\varepsilon} k_2 (z - z^0)^2 + w_1 x(z - z^0) + \frac{w_2}{\varepsilon}(z - z^0)[-\varepsilon f(x, z) z + k_1 \varepsilon z]. \quad (4.19)$$

Rewriting $z(z - z^0) = (z - z^0 + z^0)(z - z^0) = (z - z^0 - k_1 x)(z - z^0) = (z - z^0)^2 - k_1 x(z - z^0)$, equation (4.19) can be written in the following form:

$$\dot{V}_{c_{fs}} = -\begin{bmatrix} x & z - z^0 \end{bmatrix} \begin{bmatrix} w_1 k_1 & \frac{1}{2}(w_2 k_1^2 - w_1) \\ \frac{1}{2}(w_2 k_1^2 - w_1) & w_2(\frac{k_2}{\varepsilon} - k_1) \end{bmatrix} \begin{bmatrix} x \\ z - z^0 \end{bmatrix} - w_2 f(x, z) z(z - z^0). \quad (4.20)$$

The non-quadratic term $-w_2 f(x, z) z(z - z^0)$ appears due to the nonlinearity being present in the

full-order system but not in the reduced subsystems. This term can be re-written as

$$\begin{aligned} -w_2 f(x,z) z(z-z^0) &= -w_2 f(x,z)[(z-\frac{z^0}{2})^2 - \frac{{z^0}^2}{4}] \\ &= -w_2 f(x,z)(z-\frac{z^0}{2})^2 + \frac{w_2}{4} k_1^2 x^2 f(x,z) \\ &\leq \frac{w_2}{4} k_1^2 x^2 f(x,z) \leq \frac{w_2}{4} k_1^2 x^2 \theta_f \end{aligned} \tag{4.21}$$

where $0 \leq f(x,z) \leq \theta_f$ has been utilized. Using inequality (4.21), equation (4.20) reduces to the following inequality:

$$\dot{V}_{c_{fs}} \leq -\begin{bmatrix} x & z-z^0 \end{bmatrix} \begin{bmatrix} w_1 k_1 - \frac{w_2}{4} k_1^2 \theta_f & \frac{1}{2}(w_2 k_1^2 - w_1) \\ \frac{1}{2}(w_2 k_1^2 - w_1) & w_2(\frac{k_2}{\varepsilon} - k_1) \end{bmatrix} \begin{bmatrix} x \\ z-z^0 \end{bmatrix}. \tag{4.22}$$

Let $\mathbb{K}_{2\times 2} := \begin{bmatrix} w_1 k_1 - \frac{w_2}{4} k_1^2 \theta_f & \frac{1}{2}(w_2 k_1^2 - w_1) \\ \frac{1}{2}(w_2 k_1^2 - w_1) & w_2(\frac{k_2}{\varepsilon} - k_1) \end{bmatrix}$ and $\mathbf{X}_{2\times 1} := \begin{bmatrix} x \\ z-z^0 \end{bmatrix}$ such that the time-derivative of the composite Lyapunov function can be expressed as

$$\dot{V}_{c_{fs}} \leq -\mathbf{X}^T \mathbb{K} \mathbf{X}. \tag{4.23}$$

If $\mathbb{K}$ is positive-definite, the time-derivative of the composite Lyapunov function is negative-definite everywhere in the state-space, and thus the origin of the full-order system (4.1) is guaranteed to be globally asymptotically stable. $\mathbb{K}_{2\times 2}$ is positive-definite if its 1×1 and 2×2 Leading Principal Minors (LPMs) are positive. The 1×1 LPM of $\mathbb{K}$ is $(w_1 k_1 - \frac{w_2}{4} k_1^2 \theta_f)$. This is positive if the first sufficient condition in (4.14) holds; that is, if $k_1 < \frac{4w_1}{w_2 \theta_f}$. The 2×2 LPM of $\mathbb{K}$ is $(w_1 k_1 - \frac{w_2}{4} k_1^2 \theta_f) w_2(\frac{k_2}{\varepsilon} - k_1) - \frac{1}{4}(w_2 k_1^2 - w_1)^2$. Solving for ε, the 2×2 LPM of $\mathbb{K}$ is positive if

$$\varepsilon < \frac{k_1 k_2 w_2 (4w_1 - w_2 k_1 \theta_f)}{(w_2 k_1^2 + w_1)^2 - w_2^2 k_1^3 \theta_f}. \tag{4.24}$$

Inequality (4.24) gives an upper bound of the perturbation parameter ε. If the first sufficient condition in (4.14) holds, the numerator of the upper bound will be positive. If the second sufficient

condition in (4.14) holds, the denominator of the upper bound will be positive. Therefore, if both of the sufficient conditions in (4.14) hold, the full-order system (4.1) under full-state feedback is globally asymptotically stable, and so $z(t) \to z^0$ and $x(t) \to 0$ as $t \to \infty$ from any set of initial conditions $z(0), x(0)$ for $0 < \varepsilon < \varepsilon^*$ where ε^* is the upper bound given by $\varepsilon^* = \frac{k_1 k_2 w_2 (4w_1 - w_2 k_1 \theta_f)}{(w_2 k_1^2 + w_1)^2 - w_2^2 k_1^3 \theta_f}$. This completes the proof. □

4.2.2 Design of Observer and the New Bound of Time-Scale Separation ε^{***}

For the two-time-scale system (4.1), the unavailability of full-state feedback means that the measurement can be either the slow state x, or the fast state z, or a combination of x and z. In this paper, state observer design is considered for three cases: (a) only the slow state is measured; that is, the output equation is $y = x$, (b) only the fast state is measured; that is, the output equation is $y = z$, (c) a linear combination of the slow and the fast states is measured; that is, the output equation is $y = c_1 x + c_2 z$, where c_1 and c_2 are nonzero constants. The following three Subsubsections develop the theory of observer design and stability analysis under output feedback for the cases of measurement described above.

4.2.2.1 Slow State Measured

The full-order system with the state and output equations in the slow time-scale is

$$\begin{aligned} \dot{x} &= z \\ \varepsilon \dot{z} &= -\varepsilon f(x,z) z - pz + \bar{u} \\ y &= x. \end{aligned} \tag{4.25}$$

In the fast time-scale $\tau = \frac{t}{\varepsilon}$, the full-order system is

$$\begin{aligned} x' &= \varepsilon z \\ z' &= -\varepsilon f(x,z) z - pz + \bar{u} \\ y &= x. \end{aligned} \tag{4.26}$$

The output feedback control is denoted $\bar{u}$ to distinguish it from the full-state feedback control u. Since the slow state x is measured but the fast state z is not, the control law is modified from the full-state version u given by (4.11) to

$$\bar{u} = -k_1 k_2 x - (k_2 - p)\hat{z} \tag{4.27}$$

with the fast state z replaced by its estimate $\hat{z}$. The manifold is $z^0 = -k_1 x$, same as the one for full-state feedback. The state z evolves in the fast time-scale. Consequently, a *fast* observer needs to be designed to make the estimate $\hat{z}$ converge to z in the fast time-scale. The fast observer is designed based on the reduced fast subsystem

$$\begin{aligned} x' &= 0 \\ z' &= -pz + \bar{u} \\ y &= x. \end{aligned} \tag{4.28}$$

Assume the fast observer dynamics to be a function of the observed fast state, control and output, of the form

$$\hat{z}' = \phi(\hat{z}, \bar{u}, y). \tag{4.29}$$

A positive-definite fast observer Lyapunov function and its derivative with respect to the fast time-scale τ are

$$\begin{aligned} V_{f_o} &= \frac{1}{2}(z - \hat{z})^2 \\ V'_{f_o} &= (z - \hat{z})(z' - \hat{z}'). \end{aligned} \tag{4.30}$$

For the reduced fast subsystem (4.28) the time-derivative becomes

$$\begin{aligned} V'_{f_o}|_{(4.28)} &= (z - \hat{z})(z'|_{(4.28)} - \hat{z}'|_{(4.29)}) \\ &= (z - \hat{z})(-pz + \bar{u} - \phi(.)). \end{aligned} \tag{4.31}$$

Choose fast observer dynamics

$$\phi(.) = \bar{u} - p\hat{z} \tag{4.32}$$

such that the time-derivative of the fast observer Lyapunov function becomes

$$V'_{f_o}|_{(4.28)} = -p(z - \hat{z})^2 \tag{4.33}$$

which is negative-definite since $p > 0$. Thus the fast observer is Lyapunov-stable and makes the observed fast state $\hat{z}$ converge to the actual fast state z evolving according to the reduced fast dynamics (4.28).

An extension of the composite Lyapunov analysis is performed to account for the difference between the full-order and the reduced-order dynamics with the observer included. Similar to the analysis for full-state feedback, the objective here is to find an upper bound ε^{***} of the perturbation parameter ε such that the full-order system is Lyapunov-stable. A candidate composite Lyapunov function for the full-order system is

$$V_{c_{ob}} = \alpha_1 V_{s_c} + \alpha_2 V_{f_c} + \alpha_3 V_{f_o}. \tag{4.34}$$

This function is a weighted sum of the two Lyapunov functions used for the controller design and one Lyapunov function used for the observer design. The gains $\alpha_1, \alpha_2, \alpha_3$ represent the weights of the individual Lyapunov functions in the composite. The composite Lyapunov function is positive-definite and radially unbounded for any $\alpha_1, \alpha_2, \alpha_3 > 0$. The following theorem gives the bound of ε for which the full-order system (4.25) is guaranteed to be globally asymptotically stable.

Theorem 4. *Suppose that the gains* $k_1 > 0, k_2 > 0, \alpha_1 > 0, \alpha_2 > 0, \alpha_3 > 0$ *can be selected such*

that the following inequalities hold:

$$\begin{aligned} &\alpha_1 k_1 - \frac{1}{2}|\alpha_2 k_1^2 - \alpha_1| - \frac{1}{4}\alpha_2 k_1^2 \theta_f - \frac{1}{2}\alpha_3 \theta_f (k_1^2 + k_1) > 0 \\ &k_2 > \frac{p}{3} \\ &2\alpha_3 p > \alpha_2 |k_2 - p| \end{aligned} \tag{4.35}$$

then the full-order system (4.25) or equivalently (4.26) under the control law (4.27) and the state observation law (4.32) is globally asymptotically stable, or equivalently $\hat{z} \to z$, $z \to z^0$, $x \to 0$ *as* $t \to \infty$ *from any set of initial conditions* $\hat{z}(0), z(0), x(0)$ *for* $0 < \varepsilon < \varepsilon^{***}$ *where* $\varepsilon^{***} = \min(\varepsilon_1^{***}, \varepsilon_2^{***})$ *with*

$$\begin{aligned} \varepsilon_1^{***} &= \frac{\alpha_2(2k_2 - |k_2 - p|)}{2\alpha_2 k_1 + |\alpha_2 k_1^2 - \alpha_1| + \alpha_3 \theta_f (k_1 + 1)} \\ \varepsilon_2^{***} &= \frac{2\alpha_3 p - \alpha_2 |k_2 - p|}{\alpha_3 \theta_f} \end{aligned} \tag{4.36}$$

Proof. The time-derivative of the composite Lyapunov function (4.34) for the full-order system is

$$\dot{V}_{c_{ob}} = \alpha_1 \dot{V}_{s_c}|_{(4.25)} + \frac{\alpha_2}{\varepsilon} V'_{f_c}|_{(4.26)} + \frac{\alpha_3}{\varepsilon} V'_{f_o}|_{(4.26)}. \tag{4.37}$$

Adding and subtracting the time-derivatives of the appropriate Lyapunov functions for the appropriate reduced subsystems, the time-derivative of the composite Lyapunov function becomes

$$\begin{aligned} \dot{V}_{c_{ob}} = \alpha_1 \dot{V}_{s_c}|_{(4.2)} + \frac{\alpha_2}{\varepsilon} V'_{f_c}|_{(4.8)} + \frac{\alpha_3}{\varepsilon} V'_{f_o}|_{(4.28)} + \alpha_1 (\dot{V}_{s_c}|_{(4.25)} - \dot{V}_{s_c}|_{(4.2)}) \\ + \frac{\alpha_2}{\varepsilon}(V'_{f_c}|_{(4.26)} - V'_{f_c}|_{(4.8)}) + \frac{\alpha_3}{\varepsilon}(V'_{f_o}|_{(4.26)} - V'_{f_o}|_{(4.28)}). \end{aligned} \tag{4.38}$$

The first two terms on the right-hand side of equation (4.38) correspond to the two reduced subsystems used for controller design. The third term corresponds to reduced subsystem used for observer design. The next three terms correspond to the difference between the full-order and the reduced-order dynamics. Substituting for appropriate Lyapunov functions and their derivatives

for the corresponding reduced subsystems leads to

$$\begin{aligned}\dot{V}_{c_{ob}} = -\alpha_1 k_1 x^2 - \frac{\alpha_2}{\varepsilon} k_2 (z - z^0)^2 - \frac{\alpha_3}{\varepsilon} p (z - \hat{z})^2 + \alpha_1 x (\dot{x}|_{(4.25)} - \dot{x}|_{(4.2)}) \\ + \frac{\alpha_2}{\varepsilon} (z - z^0)[(z'|_{(4.26)} - z'|_{(4.8)}) - (z^{0\prime}|_{(4.26)} - z^{0\prime}|_{(4.8)})]. \\ + \frac{\alpha_3}{\varepsilon} (z - \hat{z})[(z'|_{(4.26)} - z'|_{(4.28)}) - (\hat{z}'|_{(4.26)} - \hat{z}'|_{(4.28)})]\end{aligned} \tag{4.39}$$

Substituting for all the dynamics terms,

$$\begin{aligned}\dot{V}_{c_{ob}} = -\alpha_1 k_1 x^2 - \frac{\alpha_2}{\varepsilon} k_2 (z - z^0)^2 - \frac{\alpha_3}{\varepsilon} p (z - \hat{z})^2 + \alpha_1 x (z - z^0) \\ + \frac{\alpha_2}{\varepsilon} (z - z^0)[(-\varepsilon f(x, z) z + \bar{u} - u) + k_1 \varepsilon z] + \frac{\alpha_3}{\varepsilon} (z - \hat{z})[-\varepsilon f(x, z) z].\end{aligned} \tag{4.40}$$

Using equations (4.11) and (4.27), the difference between the output feedback control $\bar{u}$ and the full-state feedback control u can be expressed as

$$\bar{u} - u = (k_2 - p)(z - \hat{z}). \tag{4.41}$$

Using equation (4.41) and expressing $z(z - z^0) = (z - z^0)^2 - k_1 x (z - z^0)$, equation (4.40) becomes

$$\begin{aligned}\dot{V}_{c_{ob}} = -\alpha_1 k_1 x^2 - \alpha_2 (\frac{k_2}{\varepsilon} - k_1)(z - z^0)^2 - \frac{\alpha_3}{\varepsilon} p (z - \hat{z})^2 - (\alpha_2 k_1^2 - \alpha_1) x (z - z^0) \\ + \frac{\alpha_2 (k_2 - p)}{\varepsilon} (z - z^0)(z - \hat{z}) - \alpha_2 z (z - z^0) f(x, z) - \alpha_3 z (z - \hat{z}) f(x, z).\end{aligned} \tag{4.42}$$

Using completion of squares, bounds of several terms present in (4.42) can be found as follows:

$$-(\alpha_2 k_1^2 - \alpha_1) x (z - z^0) \leq \frac{1}{2} |\alpha_2 k_1^2 - \alpha_1| [x^2 + (z - z^0)^2] \tag{4.43}$$

$$\frac{\alpha_2 (k_2 - p)}{\varepsilon} (z - z^0)(z - \hat{z}) \leq \frac{\alpha_2 |k_2 - p|}{2\varepsilon} [(z - z^0)^2 + (z - \hat{z})^2] \tag{4.44}$$

$$-\alpha_2 z (z - z^0) f(x, z) \leq \frac{1}{4} \alpha_2 k_1^2 x^2 \theta_f \tag{4.45}$$

similar to the bound (4.21) obtained in the proof of Theorem 3.

$$
\begin{aligned}
-\alpha_3 z(z-\hat{z})f(x,z) &\leq \frac{\alpha_3}{2}[z^2+(z-\hat{z})^2]f(x,z) \\
&\leq \frac{\alpha_3}{2}[(z-z^0+z^0)^2+(z-\hat{z})^2]\theta_f \\
&= \frac{\alpha_3}{2}[(z-z^0)^2-2k_1x(z-z^0)+k_1^2x^2+(z-\hat{z})^2]\theta_f \\
&\leq \frac{\alpha_3}{2}[(z-z^0)^2+k_1(x^2+(z-z^0)^2)+k_1^2x^2+(z-\hat{z})^2]\theta_f \\
&= \frac{\alpha_3}{2}[(k_1^2+k_1)x^2+(k_1+1)(z-z^0)^2+(z-\hat{z})^2]\theta_f
\end{aligned} \tag{4.46}
$$

Substituting the upper bounds (4.43)-(4.46) in (4.42), the time-derivative of the composite Lyapunov function can be written as

$$
\dot{V}_{c_{ob}} \leq -\bar{\mathbf{X}}^T\bar{\mathbb{K}}\bar{\mathbf{X}} \tag{4.47}
$$

where $\bar{\mathbf{X}} = \begin{bmatrix} x \\ z-z^0 \\ z-\hat{z} \end{bmatrix}$ and $\bar{\mathbb{K}} = \begin{bmatrix} k_{11} & 0 & 0 \\ 0 & k_{22} & 0 \\ 0 & 0 & k_{33} \end{bmatrix}$, with the diagonal elements k_{11}, k_{22}, k_{33} given by

$$
\begin{aligned}
k_{11} &= \alpha_1 k_1 - \frac{1}{2}|\alpha_2 k_1^2 - \alpha_1| - \frac{1}{4}\alpha_2 k_1^2\theta_f - \frac{1}{2}\alpha_3\theta_f(k_1^2+k_1) \\
k_{22} &= \alpha_2(\frac{k_2}{\varepsilon}-k_1) - \frac{1}{2}|\alpha_2 k_1^2-\alpha_1| - \frac{1}{2\varepsilon}\alpha_2|k_2-p| - \frac{\alpha_3\theta_f}{2}(k_1+1) \\
k_{33} &= \frac{\alpha_3}{\varepsilon}p - \frac{\alpha_2|k_2-p|}{2\varepsilon} - \frac{\alpha_3\theta_f}{2}.
\end{aligned} \tag{4.48}
$$

If all the diagonal elements of the matrix $\bar{\mathbb{K}}$ are positive, the time-derivative of the composite Lyapunov function will be negative-definite everywhere in the state-space, and hence the full-order system will be globally asymptotically stable. The element k_{11} is positive if the first sufficient condition in (4.35) holds. The element k_{22} is positive if $\varepsilon < \varepsilon_1^{***}$, where ε_1^{***} is given by (4.36). This bound is positive if the second sufficient condition in (4.35) holds. The element k_{33} is positive if $\varepsilon < \varepsilon_2^{***}$ where ε_2^{***} is given by (4.36). This bound is positive if the third sufficient condition in (4.35) holds. Therefore, if all the three sufficient conditions in (4.35) hold, the full-order system under output feedback is globally asymptotically stable for $0 < \varepsilon < \varepsilon^{***}$ where

$\varepsilon^{***} = min(\varepsilon_1^{***}, \varepsilon_2^{***})$. This completes the proof.

□

4.2.2.2 Fast State Measured

The full-order system with the state and output equations in the slow time-scale is

$$\begin{aligned} \dot{x} &= z \\ \varepsilon \dot{z} &= -\varepsilon f(x,z)z - pz + \bar{u} \\ y &= z \end{aligned} \tag{4.49}$$

In the fast time-scale, the full-order system is

$$\begin{aligned} x' &= \varepsilon z \\ z' &= -\varepsilon f(x,z)z - pz + \bar{u} \\ y &= z \end{aligned} \tag{4.50}$$

The slow state x is not measured; it is to be estimated. The slow state evolves in the slow time-scale. In the fast time-scale, it does not vary much from its initial condition; however, the initial condition is not known directly from measurement. As a result, the slow state needs to be estimated in both the fast and the slow time-scales. Therefore, both fast and slow observers are needed. The fast observer should be designed based on the reduced fast subsystem

$$\begin{aligned} x' &= 0 \\ z' &= -pz + \bar{u} \\ y &= z \end{aligned} \tag{4.51}$$

Since the reduced subsystem is linear, it can be expressed in the form

$$\begin{bmatrix} x' \\ z' \end{bmatrix} = A \begin{bmatrix} x \\ z \end{bmatrix} + B\bar{u}$$
$$y = Cx \tag{4.52}$$

where $A = \begin{bmatrix} 0 & 0 \\ 0 & -p \end{bmatrix}$, $B = \begin{bmatrix} 0 \\ 1 \end{bmatrix}$, $C = \begin{bmatrix} 0 & 1 \end{bmatrix}$. The observability matrix for this system is

$$\mathbb{O} = \begin{bmatrix} C \\ CA \end{bmatrix} = \begin{bmatrix} 0 & 1 \\ 0 & -p \end{bmatrix} \tag{4.53}$$

The observability matrix is rank-deficient, so the system is not observable. Since the fast state z is measured, it can be concluded that the unobservable state is the slow state x. Therefore, the observer design based on reduced subsystems does not work when only the fast state is measured. This case will not be investigated any further.

4.2.2.3 A Linear Combination of Slow and Fast States Measured

For this case the full-order system in the slow time-scale is

$$\begin{aligned} \dot{x} &= z \\ \varepsilon\dot{z} &= -\varepsilon f(x,z)z - pz + \bar{u} \\ y &= c_1 x + c_2 z. \end{aligned} \tag{4.54}$$

In the fast time-scale the full-order system is

$$\begin{aligned} x' &= \varepsilon z \\ z' &= -\varepsilon f(x,z)z - pz + \bar{u} \\ y &= c_1 x + c_2 z. \end{aligned} \tag{4.55}$$

Since none of the states x and z are directly measured, the control law is modified from its full-state version (4.11) to

$$\bar{u} = -k_1 k_2 \hat{x} - (k_2 - p)\hat{z} \tag{4.56}$$

where $\hat{x}$ and $\hat{z}$ are the estimates of the states. An observer evolving in the fast time-scale is needed for the fast state z. For the slow state x, an observer evolving in the slow time-scale can work. In the fast time-scale, the slow state x remains close to its initial condition; however, the initial condition is not captured explicitly in the measurement. Therefore, both slow and fast observers are needed. The fast observer needs to estimate both x and z, while the slow observer needs to estimate only x.

The slow observer is designed using the reduced slow subsystem

$$\begin{aligned} \dot{x} &= \bar{z}^0 \\ 0 &= -\bar{z}^0 + \bar{u}^0 \\ \bar{y} &= c_1 x + c_2 \bar{z}^0. \end{aligned} \tag{4.57}$$

with the effective control in the slow time-scale $\bar{u}^0 = -k_1\hat{x}$. Furthermore, instead of the actual manifold $z^0 = -k_1 x$, an approximation of the manifold $\bar{z}^0 = -k_1\hat{x}$ is used in the reduced slow subsystem. Assume the slow observer dynamics to be a function of the observed slow state $\hat{x}$, the effective control $\bar{u}^0$ and the effective output $\bar{y}$ as

$$\dot{\hat{x}} = \psi(\hat{x}, \bar{u}^0, \bar{y}) \tag{4.58}$$

where $\psi(.)$ is to be chosen such that the observed slow state $\hat{x}$ converges to the actual slow state x. The slow observer Lyapunov function and its derivative with respect to the slow time-scale t are

$$\begin{aligned} V_{s_o} &= \frac{1}{2}(x - \hat{x})^2 \\ \dot{V}_{s_o} &= (x - \hat{x})(\dot{x} - \dot{\hat{x}}). \end{aligned} \tag{4.59}$$

For the reduced slow subsystem (4.57) the time-derivative becomes

$$\begin{aligned}\dot{V}_{s_o}|_{(4.57)} &= (x-\hat{x})(\dot{x}|_{(4.57)} - \dot{\hat{x}}|_{(4.57)}) \\ &= (x-\hat{x})(z^0 - \psi(\hat{x}, \bar{u}^0, \bar{y})).\end{aligned} \tag{4.60}$$

Select the slow observer dynamics

$$\psi(.) = l_1\bar{y} - (k_1(1-l_1c_2) + l_1c_1)\hat{x} \tag{4.61}$$

where l_1 is the slow observer gain. By this choice the time-derivative of the slow observer Lyapunov function for the reduced slow subsystem is

$$\dot{V}_{s_o}|_{(4.57)} = -l_1c_1(x-\hat{x})^2 \tag{4.62}$$

For any choice of the slow observer gain l_1 such that $l_1c_1 > 0$, the slow observer is Lyapunov-stable.

The fast observer is designed using the reduced fast subsystem

$$\begin{aligned}x' &= 0 \\ z' &= -pz + \bar{u} \\ y &= c_1x + c_2z.\end{aligned} \tag{4.63}$$

Assume the fast observer dynamics to be functions of the estimated states $\hat{x}, \hat{z}$, control $\bar{u}$ and output y as

$$\begin{aligned}\hat{x}' &= \phi_1(\hat{x}, \hat{z}, \bar{u}, y) \\ \hat{z}' &= \phi_2(\hat{x}, \hat{z}, \bar{u}, y)\end{aligned} \tag{4.64}$$

where the functions $\phi_1(.)$ and $\phi_2(.)$ are to be chosen such that the estimated states $\hat{x}, \hat{z}$ converge to the actual states x, z in the fast time-scale. A positive-definite fast observer Lyapunov function

and its derivative with respect to the fast time-scale τ are

$$\begin{aligned} V_{f_o} &= \frac{1}{2}(x-\hat{x})^2 + \frac{1}{2}(z-\hat{z})^2 \\ V'_{f_o} &= (x-\hat{x})(x'-\hat{x}') + (z-\hat{z})(z'-\hat{z}'). \end{aligned} \tag{4.65}$$

For the reduced fast subsystem (4.63), the time-derivative becomes

$$\begin{aligned} V'_{f_o}|_{(4.63)} &= (x-\hat{x})(x'|_{(4.63)} - \hat{x}'|_{(4.63)}) + (z-\hat{z})(z'|_{(4.63)} - \hat{z}'|_{(4.63)}) \\ &= -(x-\hat{x})\phi_1(.) + (z-\hat{z})(-pz + \bar{u} - \phi_2(.)). \end{aligned} \tag{4.66}$$

Select the fast observer dynamics as

$$\begin{aligned} \phi_1(.) &= l_2(y - c_1\hat{x} - c_2\hat{z}) \\ \phi_2(.) &= \bar{u} - \frac{l_2 c_2}{c_1}y + l_2 c_2 \hat{x} + (\frac{l_2 c_2^2}{c_1} - p)\hat{z} \end{aligned} \tag{4.67}$$

where l_2 is the fast observer gain. By this choice the time derivative of fast observer Lyapunov function is

$$V'_{f_o}|_{(4.63)} = -l_2 c_1 (x-\hat{x})^2 + (\frac{l_2 c_2^2}{c_1} - p)(z-\hat{z})^2 \tag{4.68}$$

For any choice of l_2 that satisfies the inequalities $l_2 c_1 > 0, l_2 < \frac{p c_1}{c_2^2}$, the fast observer is stable in the sense of Lyapunov.

An extension of the composite Lyapunov analysis [10] is developed to account for the difference between the full-order and the reduced-order dynamics with the observers included. Similar to the case of slow state measured, the objective here is to find out an upper bound ε^{***} of the perturbation parameter ε such that the full-order nonlinear system with the controller and the observer in the loop is Lyapunov-stable. A candidate composite Lyapunov function for the full-order system (4.54) is

$$V_{c_{ob}} = \beta_1 V_{s_c} + \beta_2 V_{f_c} + \beta_3 V_{s_o} + \beta_4 V_{f_o} \tag{4.69}$$

The composite Lyapunov function is a weighted sum of the two Lyapunov functions used for

controller design and the two used for observer design. This function is positive-definite and radially unbounded for any $\beta_1, \beta_2, \beta_3, \beta_4 > 0$. The gains $\beta_i; i = 1, 2, 3, 4$ represent the weights of individual Lyapunov functions in the composite. The following theorem gives the bound of ε for the full-order system (4.54) to be globally asymptotically stable.

Theorem 5. *Suppose that the gains* $k_1 > 0, k_2 > 0, \beta_1 > 0, \beta_2 > 0, \beta_3 > 0, \beta_4 > 0$ *and* l_1, l_2 *satisfying* $l_1 c_1 > 0, l_2 c_1 > 0, l_2 < \frac{p c_2}{c_1^2}$ *can be selected such that the following inequalities hold:*

$$\begin{aligned}
&\beta_1 k_1 - \frac{1}{2}|\beta_2 k_1^2 - \beta_1| - \frac{1}{2}\beta_4 k_1 - \frac{1}{4}\beta_2 k_1^2 \theta_f - \frac{1}{2}\beta_4 \theta_f (k_1^2 + k_1) > 0 \\
&2k_2 - k_1 k_2 - |k_2 - p| > 0 \\
&2\beta_4 l_2 c_1 - \beta_2 k_1 k_2 > 0 \\
&\beta_3 |1 - l_1 c_2| + \beta_4 (1 + k_1) - 2\beta_3 l_1 c_1 - 2\beta_3 (1 - l_1 c_2) k_1 > 0 \\
&2\beta_4 (p - \frac{l_2 c_2^2}{c_1}) > \beta_2 |k_2 - p|
\end{aligned} \tag{4.70}$$

Then the full-order system (4.54) or equivalently (4.55) under the control law (4.56) and the observation laws (4.61), (4.67) is globally asymptotically stable, or equivalently $\hat{z} \to z, \hat{x} \to x, z \to z^0, x \to 0$ *as* $t \to \infty$ *from any set of initial conditions* $\hat{z}(0), \hat{x}(0), z(0), x(0)$ *for* $0 < \varepsilon < \varepsilon^{***}$ *where* $\varepsilon^{***} = min(\varepsilon_1^{***}, \varepsilon_2^{***}, \varepsilon_3^{***})$ *with*

$$\begin{aligned}
\varepsilon_1^{***} &= \frac{\beta_2 (2k_2 - k_1 k_2 - |k_2 - p|)}{2\beta_2 k_1 + |\beta_2 k_1^2 - \beta_1| + \beta_3 |1 - l_1 c_2| + \beta_4 (1 + \theta_f (k_1 + 1))} \\
\varepsilon_2^{***} &= \frac{2\beta_4 l_2 c_1 - \beta_2 k_1 k_2}{\beta_3 |1 - l_1 c_2| + \beta_4 (1 + k_1) - 2\beta_3 l_1 c_1 - 2\beta_3 (1 - l_1 c_2) k_1} \\
\varepsilon_3^{***} &= \frac{2\beta_4 (p - \frac{l_2 c_2^2}{c_1}) - \beta_2 |k_2 - p|}{\beta_4 \theta_f}
\end{aligned} \tag{4.71}$$

Proof. The proof of this Theorem is very similar to the one of Theorem 4. An outline of the proof is presented.The time-derivative of the composite Lyapunov function (4.69) for the full-order system (4.54) or equivalently (4.55) is

$$\dot{V}_{c_{ob}} = \beta_1 \dot{V}_{s_c}|_{(4.54)} + \frac{\beta_2}{\varepsilon} V'_{f_c}|_{(4.55)} + \beta_3 \dot{V}_{s_o}|_{(4.54)} + \frac{\beta_4}{\varepsilon} V'_{f_o}|_{(4.55)}. \tag{4.72}$$

Adding and subtracting the time-derivatives of the Lyapunov functions for the appropriate reduced subsystems,

$$\begin{aligned}\dot{V}_{c_{ob}} = \beta_1 \dot{V}_{s_c}|_{(4.57)} + \frac{\beta_2}{\varepsilon} V'_{f_c}|_{(4.63)} + \beta_3 \dot{V}_{s_o}|_{(4.57)} + \frac{\beta_4}{\varepsilon} V'_{f_o}|_{(4.63)} \\ + \beta_1(\dot{V}_{s_c}|_{(4.54)} - \dot{V}_{s_c}|_{(4.57)}) + \frac{\beta_2}{\varepsilon}(V'_{f_c}|_{(4.55)} - V'_{f_c}|_{(4.63)}) \\ + \beta_3(\dot{V}_{s_o}|_{(4.54)} - \dot{V}_{s_o}|_{(4.57)}) + \frac{\beta_4}{\varepsilon}(V'_{f_o}|_{(4.55)} - V'_{f_o}|_{(4.63)}).\end{aligned} \tag{4.73}$$

Substituting for the Lyapunov functions and their time-derivatives, expressing the difference between the output feedback control $\bar{u}$ and the full-state feedback control u as $\bar{u} - u = k_1 k_2(x - \hat{x}) + (k_2 - p)(z - \hat{z})$ and the difference between the actual manifold z^0 and its approximation $\bar{z}^0$ as $z^0 - \bar{z}^0 = -k_1(x - \hat{x})$ and simplifying, the time-derivative of the composite Lyapunov function becomes

$$\begin{aligned}\dot{V}_{c_{ob}} = &-\beta_1 k_1 x^2 - \beta_2(\frac{k_2}{\varepsilon} - k_1)(z - z^0)^2 - (\beta_3 l_1 + \frac{\beta_4 l_2}{\varepsilon} c_1 + \beta_3(1 - l_1 c_2)k_1)(x - \hat{x})^2 \\ &- \frac{\beta_4}{\varepsilon}(p - \frac{l_2 c_2^2}{c_1})(z - \hat{z})^2 - (\beta_2 k_1^2 - \beta_1)x(z - z^0) - \beta_4 k_1 x(x - \hat{x}) \\ &+ (\frac{\beta_2 k_1 k_2}{\varepsilon} + \beta_3(1 - l_1 c_2) + \beta_4)(x - \hat{x})(z - z^0) + \beta_2 \frac{k_2 - p}{\varepsilon}(z - z^0)(z - \hat{z}) \\ &- \beta_2 z(z - z^0) f(x, z) - \beta_4 z(z - \hat{z}) f(x, z).\end{aligned} \tag{4.74}$$

Similar to the proof of Theorem 4, completion of squares can be used to find upper bounds of the cross-terms involving $x(z - z^0), x(x - \hat{x}), (x - \hat{x})(z - z^0), (z - z^0)(z - \hat{z})$ and the terms involving the nonlinearity $f(x, z)$. Substituting all the upper bounds, the time-derivative of the composite Lyapunov function becomes the following inequality:

$$\dot{V}_{c_{ob}} \leq -\breve{\mathbf{X}}^T M \breve{\mathbf{X}} \tag{4.75}$$

where $\breve{\mathbf{X}} = \begin{bmatrix} x \\ z - z^0 \\ x - \hat{x} \\ z - \hat{z} \end{bmatrix}$ and $M = \begin{bmatrix} m_{11} & 0 & 0 & 0 \\ 0 & m_{22} & 0 & 0 \\ 0 & 0 & m_{33} & 0 \\ 0 & 0 & 0 & m_{44} \end{bmatrix}$ with

$$
\begin{aligned}
m_{11} =& \beta_1 k_1 - \frac{1}{2}|\beta_2 k_1^2 - \beta_1| - \frac{1}{2}\beta_4 k_1 - \frac{1}{4}\beta_2 k_1^2 \theta_f - \frac{1}{2}\beta_4 \theta_f (k_1^2 + k_1) \\
m_{22} =& \beta_2 (\frac{k_2}{\varepsilon} - k_1) - \frac{1}{2}|\beta_2 k_1^2 - \beta_1| - \frac{1}{2}(\frac{\beta_2 k_1 k_2}{\varepsilon} + \beta_3 |1 - l_1 c_2| + \beta_4) - \beta_2 \frac{|k_2 - p|}{2\varepsilon} \\
& - \beta_4 \frac{\theta_f}{2}(k_1 + 1) \\
m_{33} =& (\beta_3 l_1 + \frac{\beta_4 l_2}{\varepsilon}) c_1 + \beta_3 (1 - l_1 c_2) k_1 - \frac{1}{2}\beta_4 k_1 - \frac{1}{2}(\frac{\beta_2 k_1 k_2}{\varepsilon} + \beta_3 |1 - l_1 c_2| + \beta_4) \\
m_{44} =& \frac{\beta_4}{\varepsilon}(p - \frac{l_2 c_2^2}{c_1}) - \beta_2 \frac{|k_2 - p|}{2\varepsilon} - \beta_4 \frac{\theta_f}{2}
\end{aligned}
\tag{4.76}
$$

If all the diagonal elements of the matrix M are positive, the time-derivative of the composite Lyapunov function is negative-definite everywhere in the state-space, and therefore the full-order system is globally asymptotically stable. The element m_{11} is positive if the first sufficient condition in (4.70) is met. The element $m_{22} > 0$ if $\varepsilon < \varepsilon_1^{***}$ specified in (4.71). The second sufficient condition in (4.70) ensures that ε_1^{***} is positive. The element $m_{33} > 0$ if $\varepsilon < \varepsilon_2^{***}$ specified in (4.71). The third and the fourth sufficient conditions in (4.70) ensure that ε_2^{***} is positive. The element $m_{44} > 0$ if $\varepsilon < \varepsilon_3^{***}$ specified in (4.71). The fifth sufficient condition in (4.70) ensures that ε_3^{***} is positive. Therefore, if all five of the sufficient conditions in (4.70) are satisfied, global asymptotic stability is guaranteed for $0 < \varepsilon < \varepsilon^{***} = min(\varepsilon_1^{***}, \varepsilon_2^{***}, \varepsilon_3^{***})$. This completes the proof. □

4.2.3 Numerical Results

This section compares the performances of the full-state feedback and output feedback controllers in simulation as well as the stability bounds within which the controllers are guaranteed to ensure closed-loop stability. For simulation, the time-scale separation parameter ε is assumed to be 0.01. The initial conditions are $x(0) = 3, z(0) = 0$. The constant parameter is $p = 0.8$, and the

nonlinear function multiplying ε in the fast dynamics is $f(x,z) = \theta_f e^{-z^2} sin^2(x)$ with its upper bound $\theta_f = 1$. The controller gains are chosen as $k_1 = 1, k_2 = 1$. Figures 4.1a and 4.2a show the states and controls under the action of full-state feedback. It can be seen in figure 4.1a that the slow state remains almost constant at its initial condition, while the fast state converges to its manifold in the fast time-scale. Figure 4.2a show that the slow state converges to zero in the slow time-scale, while the fast state stays on its manifold. Figures 4.1b and 4.2b show the time-histories of the states and control in the fast and slow time-scales respectively for the case of only the slow state being measured. For this case, the initial estimate of the fast state is $\hat{z}(0) = 5$. Figure 4.1b shows that in the fast time-scale the estimate of the fast state converges to the actual fast state, and that the fast state converges to its manifold $z^0 = -k_1 x = -x$. Since the slow state x is almost constant at $x(0) = 3$, the fast state reaches and stays close to -3. Figure 4.2b shows that the slow state x goes to zero in the slow time-scale, and that the fast state stays on its manifold $z^0 = -k_1 x = -x$. In summary, the observed fast state reaches the actual fast state which in turn reaches its manifold, and the slow state reaches its desired value of zero. Similar to the previous case, it can be seen from the plots that the output feedback controller leads to state trajectories similar to the full-state feedback controller once the observed fast state $\hat{z}$ converges to the actual fast state z.

For the case of output feedback with a linear combination of slow and fast states measured, the initial estimate of the slow state is $\hat{x}(0) = -5$ and that of the fast state is $\hat{z}(0) = 5$. The coefficients c_1 and c_2 in the output equation are $c_1 = 1, c_2 = 1$. The observer gains are selected as $l_1 = 1, l_2 = 0.6$. Figures 4.3b and 4.4b show the time-histories of the states and control in the fast and slow time-scales respectively. Figure 4.3b shows that the fast observer makes both the slow and fast state estimates converge to the actual states, while the controller makes the fast state converge to its manifold. Figure 4.4b shows that the slow observer ensuring the slow state estimate remaining close to the actual slow state, which evolves from its initial condition to zero. It is also seen in Figure 4.4b that the fast state stays on its manifold. Similar to the previous case, it can be seen from the plots that the output feedback controller leads to state trajectories similar to the full-state feedback controller once the observed states $\hat{x}, \hat{z}$ converge to the actual states x, z.

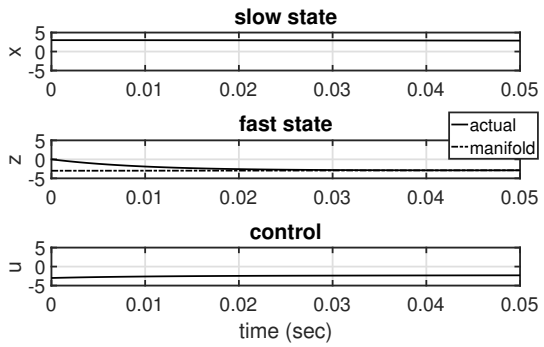

(a) full-state feedback

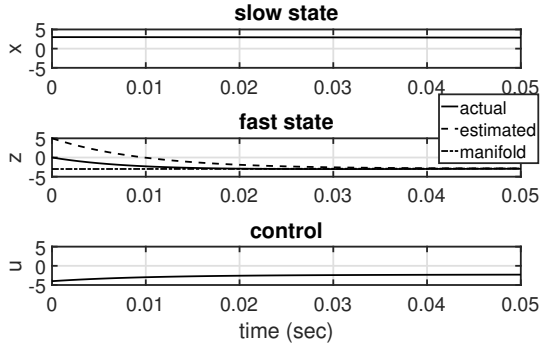

(b) output feedback, slow state measured

Figure 4.1: Comparison in the fast time-scale between full-state feedback and output feedback with slow state measured

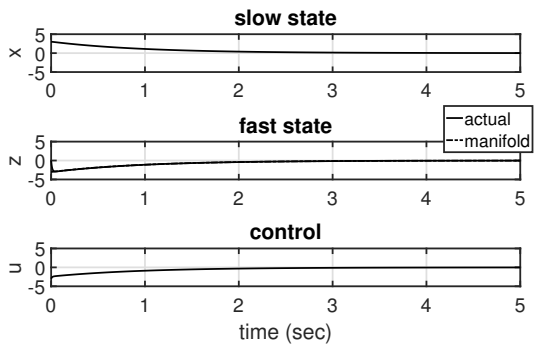

(a) full-state feedback

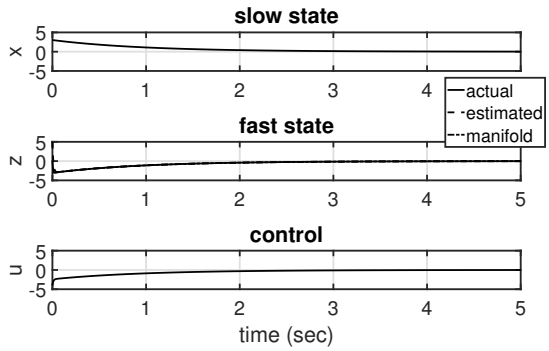

(b) output feedback, slow state measured

Figure 4.2: Comparison in the slow time-scale between full-state feedback and output feedback with slow state measured

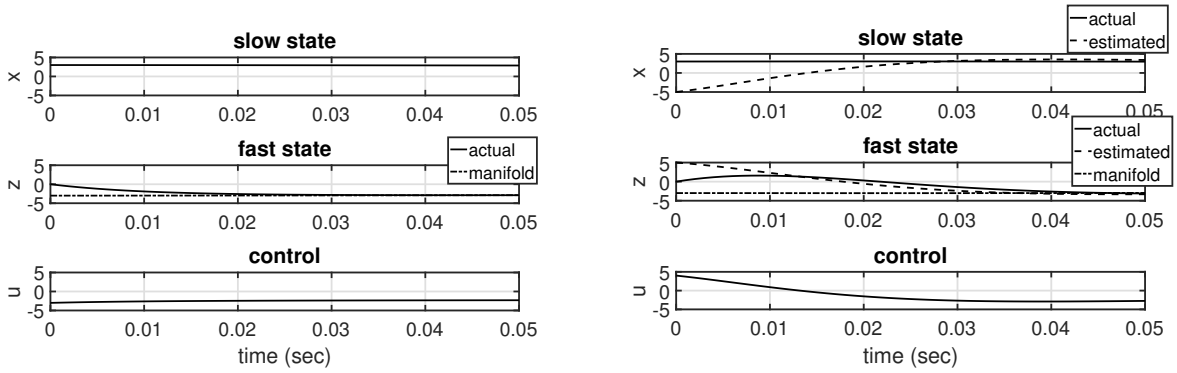

(a) full-state feedback

(b) output feedback, combination of states measured

Figure 4.3: Comparison in the fast time-scale between full-state feedback and output feedback with combination of slow and fast states measured

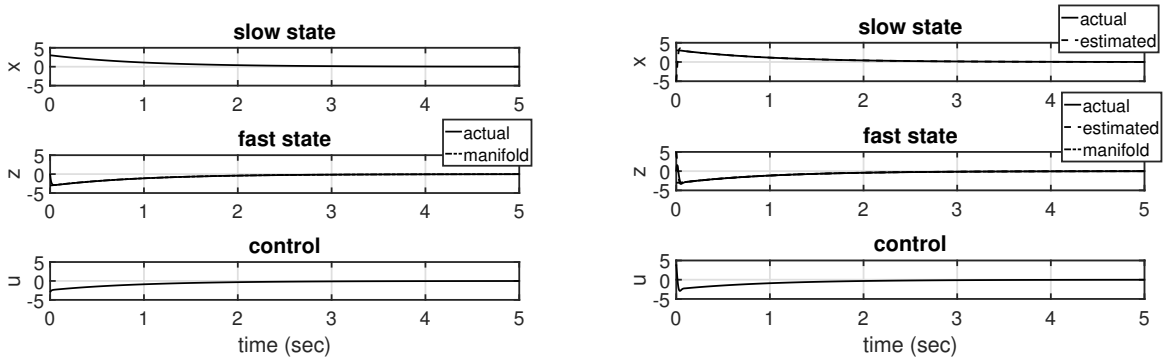

(a) full-state feedback

(b) output feedback, combination of states measured

Figure 4.4: Comparison in the slow time-scale between full-state feedback and output feedback with combination of slow and fast states measured

Table 4.1 shows a numerical comparison of the bounds of ε for full-state and output feedback. The system parameters and controller gains are kept the same. However, the weights of composite Lyapunov function are different as seen in Theorems 3.1 - 3.3. They are chosen such that all of the sufficient conditions stated in the Theorems are satisfied. It can be seen from Table 4.1 that it is

possible to obtain acceptable upper bounds ε^* and ε^{***} by selecting the gains and weights suitably. 'Acceptable' is defined here as the results being valid in the worst case when fast dynamics are evolving only 10 times faster than the slow dynamics.

	Full-state feedback	Output feedback $y = x$	Output feedback $y = c_1x + c_2z$
Bound of nonlinearity	$\theta_f = 1$	$\theta_f = 1$	$\theta_f = 1$
Known parameter	$p = 0.8$	$p = 0.8$	$p = 0.8$
Controller gains	$k_1 = 1$ $k_2 = 1$	$k_1 = 1$ $k_2 = 1$	$k_1 = 1$ $k_2 = 1$
Weights of Lyapunov functions	$w_1 = 0.1$ $w_2 = 0.1$	$\alpha_1 = 0.1$ $\alpha_2 = 0.1$ $\alpha_3 = 0.05$	$\beta_1 = 0.03$ $\beta_2 = 0.01$ $\beta_3 = 0.001$ $\beta_4 = 0.01$
Observer gains	none	no separate observer gain	$l_1 = 1$ $l_2 = 0.6$
Candidate bounds of ε	$\varepsilon^* = 1$	$\varepsilon_1^{***} = 1.2$ $\varepsilon_2^{***} = 0.6$	$\varepsilon_1^{***} = 0.1$ $\varepsilon_2^{***} = 0.1$ $\varepsilon_3^{***} = 0.2$
Bound of ε	$\varepsilon^* = 1$	$\varepsilon^{***} = 0.6$	$\varepsilon^{***} = 0.1$

Table 4.1: Comparison of stability bounds

4.3 Slow State Tracking Using Output Feedback of a Class of Uncertain Nonlinear Nonstandard Four-Time-Scale Systems

This section develops the theory of output feedback slow state tracking control design for the following class of four-time-scale, nonlinear nonstandard systems with uncertainties and actuator dynamics:

$$\begin{aligned}
\dot{x} &= B_{xx} f_{xx}(y) + F_{xx_U}(y) x_U + B_{xz} F_{xz}(y) z + \gamma_x(t, x, \xi, z) \\
&\quad + \Lambda_{x\delta_s} G_{x\delta_s}(y)\delta_s + \Lambda_{x\delta_f} G_{x\delta_f}(y)\delta_f \\
\dot{x}_U &= f_{x_U}(y) + F_{x_U x_U}(y) x_U + G_{x_U\delta_s}(y)\delta_s + G_{x_U\delta_f}(y)\delta_f \\
\dot{\xi} &= F_{\xi z}(y) z \\
\sigma\dot{\delta}_s &= B_{\delta_s} f_{\delta_s}(y) + \Lambda_{\delta_s u_s} G_{\delta_s u_s}(y) u_s \\
\varepsilon\dot{z} &= \sum_k B_z^k f_z^k(y) + \gamma_z(t, x, \xi, z) + \Lambda_{z\delta_f} G_{z\delta_f}(y)\delta_f \\
\rho\dot{\delta}_f &= B_{\delta_f} f_{\delta_f}(y) + \Lambda_{\delta_f u_f} G_{\delta_f u_f}(y) u_f. \\
y &= \begin{bmatrix} x & h(x, x_U) & \xi & \delta_s & z & \delta_f \end{bmatrix}^T.
\end{aligned} \tag{4.77}$$

This class of systems is similar to the one assumed for full-state feedback design in Section 2.6, but a few important modifications are made. The kinetic slow state vector now has two components. There are n measured slow states, forming the *measured* slow state vector x. In addition, there are n^* slow states which are not directly measured with sensors. The vector of *unmeasured* slow states is represented by x_U. Even though these states are not explicitly measured, part of the measurement vector y are nonlinear functions of the measured and unmeasured states, represented by $h(.)$. It is only the measured kinetic slow states x which are tracked, apart from the kinematic slow states ξ. The unmeasured slow states are not tracked, and are assumed to have stable dynamics. In the evolution of the measured slow states, the influence of the unmeasured slow states is via the matrix F_{xx_U}. The constant but unknown parameter matrices in the evolution of the measured slow states are $B_{xx}, B_{xz}, \Lambda_{x\delta_f}, \Lambda_{z\delta_f}$. It is to be noted that none of the terms in the dynamics has a product of an uncertain parameter and an unmeasured state. Any individual term can have at most

one unknown quantity. Furthermore, the evolution of the unmeasured slow state do not have any constant but unknown parameter matrix. The evolution of the unmeasured slow states have one component $f_{x_U}(.)$ which is known from the measurement, and another component which is linear in the unmeasured states via the influence matrix $F_{x_U x_U}$. It is known that $\lambda_{\max}(F_{x_U x_U}) \leq v_0$ for some known v_0. The kinematic slow states ξ, the fast states z, the slow actuators δ_s and the fast actuator δ_f are the same as those for full-state feedback.

The parameter matrix B_{xz} is such that its largest singular value satisfies $\bar{\sigma}(B_{xz}) \leq v_1$, where v_1 is a known constant. Both $f_{x_M x_M}$ and F_{xz} are assumed to consist of known, smooth functions. In addition, the matrix F_{xz} is such that its largest singular value satisfies $\bar{\sigma}(F_{xz}) \leq v_2$, where v_2 is a known constant. The matrices $G_{x\delta_s}$ and $G_{x\delta_f}$ respectively. Both of these matrices consist of known, smooth functions, and the matrix $G_{x\delta_s}$ is nonsingular. It is known that $\bar{\sigma}(\Lambda_{x\delta_s}) \leq v_3, \bar{\sigma}(G_{x\delta_s}) \leq v_4, \bar{\sigma}(\Lambda_{x\delta_f}) \leq v_5, \bar{\sigma}(G_{x\delta_s}) \leq v_6$ for some known constants v_3, v_4, v_5, v_6. The vector of functions $\gamma_x(t, x, \xi, z)$ represent the time-dependent and state-dependent uncertainties in slow dynamics. This is an additive uncertainty, and the Euclidean norm of this vector satisfies $\left\|\gamma_x(t, x, \xi, z)\right\|_2 \leq \kappa_1 \|x_M\|_2 + \kappa_2 \|\xi\|_2 + \kappa_3 \|z\|_2$ for some known constants $\kappa_1, \kappa_2, \kappa_3 \geq 0$. In addition to kinetic slow states x, the kinematic slow states ξ evolve in the slowest time-scale t. Their evolution depends solely on the fast state vector z through the influence matrix $F_{\xi z}$. This matrix is assumed nonsingular. It consists of known, smooth functions, and its largest singular value satisfies $\bar{\sigma}(F_{\xi z}) \leq v_7$ for some known constant v_7.

The fast dynamics have a combination of k constant but unknown parameter matrices B_z^k multiplied by known vectors of functions $f_z^k(.)$. The functions $f_z^k(.)$ represent the dependence of the fast dynamics on the slow and fast states. This vector is assumed to consist of known, smooth functions. The parametric uncertainties in the control distribution are captured in the constant but unknown matrix $\Lambda_{z\delta_f}$. The dependence of the fast dynamics on the fast actuators is represented by the matrix $G_{z\delta_f}$, which is assumed to be nonsingular and consisting of known, smooth functions. The largest singular values of these matrices satisfy $\bar{\sigma}(\Lambda_{z\delta_f}) \leq v_8, \bar{\sigma}(G_{z\delta_f}) \leq v_9$ for some known constants v_8 and v_9. The vector of functions $\gamma_z(t, x, \xi, z)$ captures the time-dependent and

state-dependent uncertainties in the fast dynamics. This is another additive uncertainty, and the Euclidean norm of this uncertainty satisfies $\left\|\gamma_z(t,x,\xi,z)\right\|_2 \leq \kappa_4\|x\|_2 + \kappa_5\|\xi\|_2 + \kappa_6\|z\|_2$ for some known constants $\kappa_4, \kappa_5, \kappa_6 \geq 0$. The matrices $B_{\delta_s}, \Lambda_{\delta_s u_s}, B_{\delta_f}, \Lambda_{\delta_f u_f}$ represent constant but unknown parameters in the evolution of slow and fast actuators. Each of the constant but unknown parameters in the parameter matrices are assumed to be within lower and upper bounds; i.e. $p_{ij} \in [\underline{p}_{ij}, \bar{p}_{ij}]$, where p_{ij} is any of the constant but unknown parameters. The vector of functions $f_{\delta_s}, f_{\delta_f}$ represent how the actuator rates depend on the current actuator deflections. The matrices $G_{\delta_s u_s}, G_{\delta_f u_f}$ represent how the actuator rates depend on the control commands u_s and u_f respectively. The matrices $G_{\delta_s u_s}$ and $G_{\delta_f u_f}$ are assumed to be nonsingular.

The control objective is to design the slow control vector u_s and the fast control vector u_f such that the kinetic slow state vector $x(t)$ tracks a twice differentiable reference trajectory $x_r(t)$, and the kinematic slow state vector $\xi(t)$ tracks a twice differentiable reference trajectory $\xi_r(t)$. In order to achieve this objective using the geometric singular perturbation approach, the fast states z need to be stabilized on a suitable manifold z^0, the slow actuators δ_s need to be stabilized on a suitable manifold δ_s^0, and the fast actuators need to be stabilized on a suitable manifold δ_f^0. Define error variables $e_x \coloneqq x - x_r, e_\xi \coloneqq \xi - \xi_r, e_z \coloneqq z - z^0, e_{\delta_s} \coloneqq \delta_s - \delta_s^0, e_{\delta_f} \coloneqq \delta_f - \delta_f^0$. The tracking problem becomes an equivalent stabilization problem in the error coordinates. Leaving out the evolution of the unmeasured slow states, the full-order system (4.119) in the error co-ordinates become

$$\begin{aligned}
\dot{e}_x &= B_{xx} f_{xx} + F_{xx_U} x_U + B_{xz} F_{xz}(e_z + z^0) + \gamma_x \\
&\quad + \Lambda_{x\delta_s} G_{x\delta_s}(e_{\delta_s} + \delta_s^0) + \Lambda_{x\delta_f} G_{x\delta_f}(e_{\delta_f} + \delta_f^0) - \dot{x}_r \\
\dot{e}_\xi &= F_{\xi z}(e_z + z^0) - \dot{\xi}_r \\
\sigma\dot{e}_{\delta_s} &= B_{\delta_s} f_{\delta_s} + \Lambda_{\delta_s u_s} G_{\delta_s u_s} u_s - \sigma\dot{\delta}_s^0 \\
\varepsilon\dot{e}_z &= \sum_k B_z^k f_z^k + \gamma_z + \Lambda_{z\delta_f} G_{z\delta_f}(e_{\delta_f} + \delta_f^0) - \varepsilon\dot{z}^0 \\
\rho\dot{e}_{\delta_f} &= B_{\delta_f} f_{\delta_f} + \Lambda_{\delta_f u_f} G_{\delta_f u_f} u_f - \rho\dot{\delta}_f^0.
\end{aligned} \tag{4.78}$$

The following subsections develop a four-time-scale control law based on lower-order reduced

subsystems obtained from (4.78) and prove the boundedness of errors.

4.3.1 Development of Control Law Using Reduced Subsystems

The development is similar to the one for full-state feedback with one modification. In addition to using the estimates of the constant but unknown parameters, the reduced slow subsystem also uses estimates of the unmeasured states. Mathematically, the estimate $\hat{x}_U$ is used instead of the actual states x_U. The four steps of the development are mentioned below so as to list the reduced subsystem, the Lyapunov function and the selected design variable at each step.

4.3.1.1 Design of Manifold of Fast States and Slow Actuators in the Slowest Time-Scale

Using estimates of unknown parameters and unmeasured states, the reduced subsystem in the slowest time-scale is

$$\begin{aligned} \dot{e}_x &= \hat{B}_{xx} f_{xx} + F_{xx_U} \hat{x}_U + \hat{B}_{xz} F_{xz} z^0 - \dot{x}_r + \hat{\Lambda}_{x\delta_s} G_{x\delta_s} \delta_s^0 + \hat{\Lambda}_{x\delta_f} G_{x\delta_f} \delta_f^0|_{z^0} \\ \dot{e}_\xi &= F_{\xi z} z^0 - \dot{\xi}_r. \end{aligned} \tag{4.79}$$

A positive-definite candidate Lyapunov function for subsystem (4.79) can be selected as

$$V_1 = \frac{1}{2} e_x^T e_x + \frac{1}{2} e_\xi^T e_\xi. \tag{4.80}$$

Its time-derivative with respect to the slowest time-scale t is

$$\dot{V}_1 = e_x^T \dot{e}_x + e_\xi^T \dot{e}_\xi. \tag{4.81}$$

Along the trajectories of subsystem (4.79), the time-derivative of the Lyapunov function V_1 is

$$\begin{aligned} \dot{V}_1|_{(4.79)} = e_x^T (\hat{B}_{xx} f_{xx} + + F_{xx_U} \hat{x}_U + \hat{B}_{xz} F_{xz} z^0 + \hat{\Lambda}_{x\delta_s} G_{x\delta_s} \delta_s^0 + \hat{\Lambda}_{x\delta_f} G_{x\delta_f} \delta_f^0|_{z^0} - \dot{x}_r) \\ + e_\xi^T (F_{\xi z} z^0 - \dot{\xi}_r). \end{aligned} \tag{4.82}$$

Suppose that the manifold of the fast states z^0 is selected as

$$z^0 = F_{\xi z}^{-1}(\dot{\xi}_r - K_\xi e_\xi). \tag{4.83}$$

and that the manifold of the slow actuators δ_s^0 is selected as

$$\delta_s^0 = G_{x\delta_s}^{-1}\hat{\Lambda}_{x_{\delta_s}}^{-1}(\dot{x}_r - \hat{B}_{xx}f_{xx} - F_{xx_U}\hat{x}_U - \hat{B}_{xz}F_{xz}z^0 - \hat{\Lambda}_{x\delta_f}G_{x\delta_f}\delta_f^0|_{z^0} - K_x e_x) \tag{4.84}$$

where $\hat{\Lambda}_{x_{\delta_s}}$ is assumed nonsingular, and $\delta_f^0|_{z^0}$ is yet to be determined. For these choices, the time-derivative of the Lyapunov function V_1 for the reduced subsystem (4.79) becomes

$$\dot{V}_1|_{(4.79)} = -e_x^T K_x e_x - e_\xi^T K_\xi e_\xi. \tag{4.85}$$

This is negative-definite for any positive-definite K_x and K_ξ, indicating that the equilibrium $e_x = 0, e_\xi = 0$ of the reduced subsystem (4.79) is Lyapunov-stable.

4.3.1.2 Design of Slow Control in the Second Slowest Time-Scale

the reduced subsystem in the second slowest time-scale is

$$\grave{e}_{\delta_s} = \hat{B}_{\delta_s}f_{\delta_s} + \hat{\Lambda}_{\delta_s u_s}G_{\delta_s u_s}u_s. \tag{4.86}$$

A positive-definite candidate Lyapunov function for this subsystem can be selected as

$$V_2 = \frac{1}{2}e_{\delta_s}^T e_{\delta_s}. \tag{4.87}$$

Its time-derivative with respect to the second slowest time-scale is

$$\grave{V}_2 = e_{\delta_s}^T \grave{e}_{\delta_s}. \tag{4.88}$$

Along the trajectories of the reduced subsystem (4.86), the time-derivative is

$$\dot{V}_2|_{(2.138)} = e_{\delta_s}^T(\hat{B}_{\delta_s} f_{\delta_s} + \hat{\Lambda}_{\delta_s u_s} G_{\delta_s u_s} u_s). \tag{4.89}$$

If the vector of slow controls u_s is selected as

$$u_s = G_{\delta_s u_s}^{-1} \hat{\Lambda}_{\delta_s u_s}^{-1}(-\hat{B}_{\delta_s} f_{\delta_s} - K_{\delta_s} e_{\delta_s}) \tag{4.90}$$

then the derivative of the Lyapunov function V_2 with respect to the second slowest time-scale becomes

$$\dot{V}_2|_{(2.138)} = -e_{\delta_s}^T K_{\delta_s} e_{\delta_s} \tag{4.91}$$

which is negative-definite for any positive-definite K_{δ_s}. Thus the equilibrium $e_{\delta_s} = 0$ of the reduced subsystem (4.86) is Lyapunov-stable.

4.3.1.3 Design of Manifold of Fast Actuators in the Second Fastest Time-Scale

The reduced subsystem in the second fastest time-scale is

$$e_z' = \sum_k \hat{B}_z^k f_z^k + \hat{\Lambda}_{z\delta_f} G_{z\delta_f} \delta_f^0 \tag{4.92}$$

A positive-definite candidate Lyapunov function for this subsystem is

$$V_3 = \frac{1}{2} e_z^T e_z. \tag{4.93}$$

Its time-derivative with respect to the time-scale t_z is

$$V_3' = e_z^T e_z'. \tag{4.94}$$

Along the trajectories of subsystem (4.92), the time-derivative is

$$V_3'|_{(4.92)} = e_z^T(\sum_k \hat{B}_z^k f_z^k + \hat{\Lambda}_{z\delta_f} G_{z\delta_f} \delta_f^0) \tag{4.95}$$

If the manifold of the fast actuators is selected as

$$\delta_f^0 = G_{z\delta_f}^{-1} \hat{\Lambda}_{z\delta_f}^{-1}(-\sum_k \hat{B}_z^k f_z^k - K_z e_z) \tag{4.96}$$

where $\hat{\Lambda}_{z_{\delta_f}}$ is assumed nonsingular, then the time-derivative of the Lyapunov function V_3 becomes

$$V_3'|_{(2.144)} = -e_z^T K_z e_z \tag{4.97}$$

which is negative-definite for any positive-definite K_z. This ensures that the equilibrium $e_z = 0$ of the reduced subsystem (4.92) is Lyapunov-stable. Moreover, the special case of the fast actuator manifold is

$$\delta_f^0|_{z^0} = -G_{z\delta_f}^{-1} \hat{\Lambda}_{z\delta_f}^{-1} \sum_k \hat{B}_z^k f_z^k|_{z=z^0} \tag{4.98}$$

4.3.1.4 Design of Fast Control in the Fastest Time-Scale

The reduced subsystem in the fastest time-scale is

$$\breve{e}_{\delta_f} = \hat{B}_{\delta_f} f_{\delta_f} + \hat{\Lambda}_{\delta_f u_f} G_{\delta_f u_f} u_f. \tag{4.99}$$

A positive-definite candidate Lyapunov function for the subsystem (4.99) can be selected as

$$V_4 = \frac{1}{2} e_{\delta_f}^T e_{\delta_f}. \tag{4.100}$$

Its time-derivative with respect to the fast actuator time-scale is

$$\breve{V}_4 = e_{\delta_f}^T \breve{e}_{\delta_f}. \tag{4.101}$$

Along the trajectories of the reduced subsystem (4.99), the time-derivative becomes

$$\breve{V}_4|_{(2.151)} = e_{\delta_f}^T(\hat{B}_{\delta_f} f_{\delta_f} + \hat{\Lambda}_{\delta_f u_f} G_{\delta_f u_f} u_f). \tag{4.102}$$

If the fast actuator command vector u_f is selected as

$$u_f = G_{\delta_f u_f}^{-1} \hat{\Lambda}_{\delta_f u_f}^{-1}(-\hat{B}_{\delta_f} f_{\delta_f} - K_{\delta_f} e_{\delta_f}) \tag{4.103}$$

then the derivative of the Lyapunov function V_4 becomes

$$\breve{V}_4|_{(4.99)} = -e_{\delta_f}^T K_{\delta_f} e_{\delta_f} \tag{4.104}$$

which is negative-definite for any positive-definite K_{δ_f}. Thus the equilibrium $e_{\delta_f} = 0$ of the reduced subsystem (4.99) is Lyapunov-stable.

4.3.2 Stability Analysis of the Full-Order System: Parameter Update Laws, State Observation Law, Boundedness of Errors

The parameter error matrices are defined the same as in Section 2.6. In addition, the state observation error is defined as

$$\tilde{x}_U := x_U - \hat{x}_U \tag{4.105}$$

A positive-definite candidate Composite Lyapunov function is

$$\begin{aligned} V_c = {} & \alpha_1 V_1 + \alpha_2 V_2 + \alpha_3 V_3 + \alpha_4 V_4 + \frac{1}{2}\alpha_5 \sum_i \sum_j \tilde{b}_{xx_{ij}}^2 + \frac{1}{2}\alpha_6 \sum_i \sum_j \tilde{b}_{xz_{ij}}^2 + \frac{1}{2}\alpha_7 \sum_i \sum_j \tilde{\lambda}_{x\delta_{s_{ij}}}^2 \\ & + \frac{1}{2}\alpha_8 \sum_i \sum_j \tilde{\lambda}_{x\delta_{f_{ij}}}^2 + \frac{1}{2}\alpha_9 \sum_i \sum_j \tilde{b}_{\delta_{s_{ij}}}^2 + \frac{1}{2}\alpha_{10} \sum_i \sum_j \tilde{\lambda}_{\delta_s u_{s_{ij}}}^2 + \frac{1}{2} \sum_k \alpha_{11k} \sum_i \sum_j \tilde{b}_{z_{ij}}^{k^2} \\ & + \frac{1}{2}\alpha_{12} \sum_i \sum_j \tilde{\lambda}_{z\delta_{f_{ij}}}^2 + \frac{1}{2}\alpha_{13} \sum_i \sum_j \tilde{b}_{\delta_{f_{ij}}}^2 + \frac{1}{2}\alpha_{14} \sum_i \sum_j \tilde{\lambda}_{\delta_f u_{f_{ij}}}^2 + \frac{1}{2}\alpha_{15} \tilde{x}_U^T \tilde{x}_U. \end{aligned} \tag{4.106}$$

where $\alpha_i > 0; i = 1, ..., 15$. This function captures the tracking errors, the manifold errors, all the parameter estimation errors and the state observation errors. Considering full-order and reduced-order dynamics and making necessary substitutions, the derivative of this composite Lyapunov function can be evaluated as

$$\begin{aligned}
\dot{V}_c = & -\alpha_1(e_x^T K_x e_x + e_\xi^T K_\xi e_\xi) - \frac{\alpha_2}{\sigma} e_{\delta_s}^T K_{\delta_s} e_{\delta_s} - \frac{\alpha_3}{\varepsilon} e_z^T K_z e_z - \frac{\alpha_4}{\rho} e_{\delta_f}^T K_{\delta_f} e_{\delta_f} \\
& + \alpha_1 e_x^T [B_{xz} F_{xz} e_z + \gamma_x + \Lambda_{x\delta_s} G_{x\delta_s} e_{\delta_s} + \Lambda_{x\delta_f} G_{x\delta_f} (e_{\delta_f} + \delta_f^0 - \delta_f^0|_{z^0})] + \alpha_1 e_\xi^T F_{\xi z} e_z \\
& + \frac{\alpha_3}{\varepsilon} e_z^T (\gamma_z + \Lambda_{z\delta_f} G_{z\delta_f} e_{\delta_f}) - \alpha_2 e_{\delta_s}^T \dot{\delta}_s^0 - \alpha_3 e_z^T \dot{z}^0 - \alpha_4 e_{\delta_f}^T \dot{\delta}_f^0 \\
& + \sum_i \sum_j \tilde{b}_{xx_{ij}} (\alpha_1 e_{x_i} f_{xx_j} - \alpha_5 \dot{\hat{b}}_{xx_{ij}}) + \sum_i \sum_j \tilde{b}_{xz_{ij}} (\alpha_1 (e_{x_i} (F_{xz} z^0)_j - \alpha_6 \dot{\hat{b}}_{xz_{ij}}) \\
& + \sum_i \sum_j \tilde{\lambda}_{x\delta_{s_{ij}}} (\alpha_1 (e_{x_i} (G_{x\delta_s} \delta_s^0)_j - \alpha_7 \dot{\hat{\lambda}}_{x\delta_{s_{ij}}}) + \sum_i \sum_j \tilde{\lambda}_{x\delta_{f_{ij}}} (\alpha_1 (e_{x_i} (G_{x\delta_f} \delta_f^0|_{z^0})_j - \alpha_8 \dot{\hat{\lambda}}_{x\delta_{f_{ij}}}) \\
& + \frac{1}{\sigma} \sum_i \sum_j \tilde{b}_{\delta_{s_{ij}}} (\alpha_2 e_{\delta_{s_i}} f_{\delta_{s_j}} - \alpha_9 \dot{\hat{b}}_{\delta_{s_{ij}}}) + \frac{1}{\sigma} \sum_i \sum_j \tilde{\lambda}_{\delta_s u_{s_{ij}}} (\alpha_2 e_{\delta_{s_i}} (G_{\delta_s u_s} u_s)_j - \alpha_{10} \dot{\hat{\lambda}}_{\delta_s u_{s_{ij}}}) \\
& + \frac{1}{\varepsilon} \sum_k \sum_i \sum_j \tilde{b}_{z_{ij}}^k (\alpha_3 e_{z_i} f_{z_j}^k - \alpha_{11k} \dot{\hat{b}}_{z_{ij}}^{k\prime}) + \frac{1}{\varepsilon} \sum_i \sum_j \tilde{\lambda}_{z\delta_{f_{ij}}} (\alpha_3 e_{z_i} (G_{z_{\delta_f}} \delta_f^0)_j - \alpha_{12} \dot{\hat{\lambda}}'_{z\delta_{f_{ij}}}) \\
& + \frac{1}{\rho} \sum_i \sum_j \tilde{b}_{\delta_{f_{ij}}} (\alpha_4 e_{\delta_{f_i}} f_{\delta_{f_j}} - \alpha_{13} \breve{\hat{b}}_{\delta_{f_{ij}}}) + \frac{1}{\rho} \sum_i \sum_j \tilde{\lambda}_{\delta_f u_{f_{ij}}} (\alpha_4 e_{\delta_{f_i}} (G_{\delta_f u_f} u_f)_j - \alpha_{14} \breve{\hat{\lambda}}_{\delta_f u_{f_{ij}}}) \\
& + \alpha_1 e_x^T F_{xx_U} \tilde{x}_U + \alpha_{15} \tilde{x}_U (f_{x_U} + F_{x_U x_U} x_U + G_{x_U \delta_s} \delta_s + G_{x_U \delta_f} \delta_f - \dot{\hat{x}}_U).
\end{aligned} \tag{4.107}$$

Suppose that the parameter update laws are selected the same as the ones for the full-state feedback design in Section 2.6. The last part of the time-derivative involving state observation error $\tilde{x}_U$ can be written as

$$\begin{aligned}
& \alpha_1 e_x^T F_{xx_U} \tilde{x}_U + \alpha_{15} \tilde{x}_U (f_{x_U} + F_{x_U x_U} x_U + \Lambda_{x\delta_s} G_{x_U \delta_s} \delta_s + \Lambda_{x\delta_f} G_{x_U \delta_f} \delta_f - \dot{\hat{x}}_U) \\
& = \alpha_{15} \tilde{x}_U^T (\frac{\alpha_1}{\alpha_{15}} F_{xx_U}^T e_x + f_{x_U} + F_{x_U x_U} x_U + G_{x_U \delta_s} \delta_s + G_{x_U \delta_f} \delta_f - \dot{\hat{x}}_U)
\end{aligned} \tag{4.108}$$

Suppose that the nonlinear state observer dynamics are selected as

$$\dot{\hat{x}}_U = \frac{\alpha_1}{\alpha_{15}} F_{xx_U}^T e_x + f_{x_U} + F_{x_U x_U} \hat{x}_U + G_{x_U \delta_s} \delta_s + G_{x_U \delta_f} \delta_f - L(\hat{x}_U - x_U^0) \tag{4.109}$$

where L is a positive-definite matrix, and x_U^0 is a desired variable. It can be seen that part of the observer dynamics are chosen to cancel or mimic some terms present in the original dynamics, and the remaining is to drive the estimates to some desired x_U^0 with desired rates specified by the L matrix. One way to specify the rates for each unmeasured state is to select L to be a diagonal matrix and choose the diagonal entries of L carefully. With these parameter update laws and observer dynamics, the time-derivative of the composite Lyapunov function can be simplified as

$$\begin{aligned}
\dot{V}_c = & -\alpha_1(e_x^T K_x e_x + e_\xi^T K_\xi e_\xi) - \frac{\alpha_2}{\sigma} e_{\delta_s}^T K_{\delta_s} e_{\delta_s} - \frac{\alpha_3}{\varepsilon} e_z^T K_z e_z - \frac{\alpha_4}{\rho} e_{\delta_f}^T K_{\delta_f} e_{\delta_f} \\
& + \alpha_1 e_x^T [B_{xz} F_{xz} e_z + \gamma_x + \Lambda_{x\delta_s} G_{x\delta_s} e_{\delta_s} + \Lambda_{x\delta_f} G_{x\delta_f} (e_{\delta_f} + \delta_f^0 - \delta_f^0|_{z^0})] + \alpha_1 e_\xi^T F_{\xi z} e_z \\
& + \frac{\alpha_3}{\varepsilon} e_z^T (\gamma_z + \Lambda_{z\delta_f} G_{z\delta_f} e_{\delta_f}) - \alpha_2 e_{\delta_s}^T \dot{\delta}_s^0 - \alpha_3 e_z^T \dot{z}^0 - \alpha_4 e_{\delta_f}^T \dot{\delta}_f^0 \\
& + \theta_1 \sum_i \sum_j \tilde{b}_{xx_{ij}} (\hat{b}_{xx_{ij}} - b_{xx_{ij}}^0) + \theta_2 \sum_i \sum_j \tilde{b}_{xz_{ij}} (\hat{b}_{xz_{ij}} - b_{xz_{ij}}^0) \\
& + \theta_3 \sum_i \sum_j \tilde{\lambda}_{x\delta_{s_{ij}}} (\hat{\lambda}_{x\delta_{s_{ij}}} - \lambda_{x\delta_{s_{ij}}}^0) + \theta_4 \sum_i \sum_j \tilde{\lambda}_{x\delta_{f_{ij}}} (\hat{\lambda}_{x\delta_{f_{ij}}} - \lambda_{x\delta_{f_{ij}}}^0) \\
& + \frac{\theta_5}{\sigma} \sum_i \sum_j \tilde{b}_{\delta_{s_{ij}}} (\hat{b}_{\delta_{s_{ij}}} - b_{\delta_{s_{ij}}}^0) + \frac{\theta_6}{\sigma} \sum_i \sum_j \tilde{\lambda}_{\delta_s u_{s_{ij}}} (\hat{\lambda}_{\delta_s u_{s_{ij}}} - \lambda_{\delta_s u_{s_{ij}}}^0) \\
& + \frac{\theta_7}{\varepsilon} \sum_k \sum_i \sum_j \tilde{b}_{z_{ij}}^k (\hat{b}_{z_{ij}}^k - b_{z_{ij}}^{k^0}) + \frac{\theta_8}{\varepsilon} \sum_i \sum_j \tilde{\lambda}_{z\delta_{f_{ij}}} (\hat{\lambda}_{z\delta_{f_{ij}}} - \lambda_{z\delta_{f_{ij}}}^0) \\
& + \frac{\theta_9}{\rho} \sum_i \sum_j \tilde{b}_{\delta_{f_{ij}}} (\hat{b}_{\delta_{f_{ij}}} - b_{\delta_{f_{ij}}}^0) + \frac{\theta_{10}}{\rho} \sum_i \sum_j \tilde{\lambda}_{\delta_f u_{f_{ij}}} (\hat{\lambda}_{\delta_f u_{f_{ij}}} - \lambda_{\delta_f u_{f_{ij}}}^0) \\
& + \alpha_{15} \tilde{x}_U^T F_{x_U x_U} \tilde{x}_U + \alpha_{15} \tilde{x}_U^T L (\hat{x}_U - x_U^0).
\end{aligned} \tag{4.110}$$

Since the unmeasured states are assumed to have stable dynamics, it can be assumed that $x_{U_i} \in [\underline{x}_{U_i}, \bar{x}_{U_i}]$ for the i^{th} unmeasured state. If L is chosen to be a diagonal matrix, i.e. $L = diag[L_i]; i = 1, ..., n^*$, then

$$\begin{aligned}
\alpha_{15} \tilde{x}_U^T L (\hat{x}_U - x_U^0) &= \alpha_{15} \sum_i L_i \tilde{x}_{U_i} (\hat{x}_{U_i} - x_{U_i}^0) \\
&\leq \frac{1}{2} \alpha_{15} \sum_i L_i (x_{U_i}^+ - x_{U_i}^2) \\
&= \frac{\alpha_{15}}{2} \sum_i L_i x_{U_i}^+ - \frac{\alpha_{15}}{2} \sum_i L_i \tilde{x}_{U_i}^2
\end{aligned} \tag{4.111}$$

where $x_{U_i}^+ := \max_{\underline{x}_{U_i} \le x_{U_i} \le \bar{x}_{U_i}} (x_{U_i} - x_{U_i}^0)^2$. As a result,

$$\begin{aligned}
\alpha_{15}\tilde{x}_U^T F_{x_U x_U}\tilde{x}_U + \alpha_{15}\tilde{x}_U^T L(\hat{x}_U - x_U^0) &\le \alpha_{15}\lambda_{\max}(F_{x_U x_U})\tilde{x}_U^T\tilde{x}_U + \frac{\alpha_{15}}{2}\sum_i L_i x_{U_i}^+ - \frac{\alpha_{15}}{2}\sum_i L_i \tilde{x}_{U_i}^2 \\
&\le \alpha_{15} v_0 \tilde{x}_U^T\tilde{x}_U + \frac{\alpha_{15}}{2}\sum_i L_i x_{U_i}^+ - \frac{\alpha_{15}}{2}\sum_i L_i \tilde{x}_{U_i}^2 \\
&= \frac{\alpha_{15}}{2}\sum_i L_i x_{U_i}^+ - \frac{\alpha_{15}}{2}\sum_i (L_i - 2v_0)\tilde{x}_{U_i}^2 \\
&= \frac{\alpha_{15}}{2}\sum_i L_i x_{U_i}^+ - \frac{\alpha_{15}}{2}\sum_i \bar{L}_i \tilde{x}_{U_i}^2
\end{aligned} \tag{4.112}$$

where $\bar{L}_i := L_i - 2v_0$. If the observer gain matrix L is chosen such that $L_i > 2v_0$, and the parameter update laws are chosen the same as Section 2.6, then the time-derivative of the composite Lyapunov function simplifies to

$$\begin{aligned}
\dot{V}_c \le & -\alpha_1(e_x^T K_x e_x + e_\xi^T K_\xi e_\xi) - \frac{\alpha_2}{\sigma} e_{\delta_s}^T K_{\delta_s} e_{\delta_s} - \frac{\alpha_3}{\varepsilon} e_z^T K_z e_z - \frac{\alpha_4}{\rho} e_{\delta_f}^T K_{\delta_f} e_{\delta_f} \\
& + \alpha_1 e_x^T [B_{xz} F_{xz} e_z + \gamma_x + \Lambda_{x\delta_s} G_{x\delta_s} e_{\delta_s} + \Lambda_{x\delta_f} G_{x\delta_f}(e_{\delta_f} + \delta_f^0 - \delta_f^0|_{z^0})] + \alpha_1 e_\xi^T F_{\xi z} e_z \\
& + \frac{\alpha_3}{\varepsilon} e_z^T(\gamma_z + \Lambda_{z\delta_f} G_{z\delta_f} e_{\delta_f}) - \alpha_2 e_{\delta_s}^T \dot{\delta}_s^0 - \alpha_3 e_z^T \dot{z}^0 - \alpha_4 e_{\delta_f}^T \dot{\delta}_f^0 \\
& - \frac{\theta_1}{2}\sum_i\sum_j \tilde{b}_{xx_{ij}}^2 - \frac{\theta_2}{2}\sum_i\sum_j \tilde{b}_{xz_{ij}}^2 - \frac{\theta_3}{2}\sum_i\sum_j \tilde{\lambda}_{x\delta_{s_{ij}}}^2 - \frac{\theta_4}{2}\sum_i\sum_j \tilde{\lambda}_{x\delta_{f_{ij}}}^2 \\
& - \frac{\theta_5}{2\sigma}\sum_i\sum_j \tilde{b}_{\delta_{s_{ij}}}^2 - \frac{\theta_6}{2\sigma}\sum_i\sum_j \tilde{\lambda}_{\delta_s u_{s_{ij}}}^2 - \frac{\theta_7}{2\varepsilon}\sum_k\sum_i\sum_j \tilde{b}_{z_{ij}}^{k^2} \\
& - \frac{\theta_8}{2\varepsilon}\sum_i\sum_j \tilde{\lambda}_{z\delta_{f_{ij}}}^2 - \frac{\theta_9}{2\rho}\sum_i\sum_j \tilde{b}_{\delta_{f_{ij}}}^2 - \frac{\theta_{10}}{2\rho}\sum_i\sum_j \tilde{\lambda}_{\delta_f u_{f_{ij}}}^2 - \frac{\alpha_{15}}{2}\sum_i \bar{L}_i \tilde{x}_{U_i}^2 + \mu_0.
\end{aligned} \tag{4.113}$$

where

$$\begin{aligned}
\mu_0 := & \frac{\theta_1}{2}\sum_i\sum_j b_{xx_{ij}}^+ + \frac{\theta_2}{2}\sum_i\sum_j b_{xz_{ij}}^+ + \frac{\theta_3}{2}\sum_i\sum_j \lambda_{x\delta_{s_{ij}}}^+ + \frac{\theta_4}{2}\sum_i\sum_j \lambda_{x\delta_{f_{ij}}}^+ \\
& + \frac{\theta_5}{2\sigma}\sum_i\sum_j b_{\delta_{s_{ij}}}^+ + \frac{\theta_6}{2\sigma}\sum_i\sum_j \lambda_{\delta_s u_{s_{ij}}}^+ + \frac{\theta_7}{2\varepsilon}\sum_k\sum_i\sum_j b_{z_{ij}}^{k^+} \\
& + \frac{\theta_8}{2\varepsilon}\sum_i\sum_j \lambda_{z\delta_{f_{ij}}}^+ + \frac{\theta_9}{2\rho}\sum_i\sum_j b_{\delta_{f_{ij}}}^+ + \frac{\theta_{10}}{2\rho}\sum_i\sum_j \lambda_{\delta_f u_{f_{ij}}}^+ + \frac{\alpha_{15}}{2}\sum_i L_i x_{U_i}^+.
\end{aligned} \tag{4.114}$$

Invoking the concept of compact sets and extreme value theorem, and using all the algebraic manipulations performed in Section 2.6 to bound the cross-terms, the final form of the time-derivative of the composite Lyapunov function is

$$\begin{aligned}\dot{V}_c \leq & -\beta_1 e_x^T e_x - \beta_2 e_\xi^T e_\xi - \beta_3 e_{\delta_s}^T e_{\delta_s} - \beta_4 e_z^T e_z - \beta_5 e_{\delta_f}^T e_{\delta_f} \\ & - \frac{\theta_1}{2}\sum_j \tilde{b}_{xx_{ij}}^2 - \frac{\theta_2}{2}\sum_i\sum_j \tilde{b}_{xz_{ij}}^2 - \frac{\theta_3}{2}\sum_i\sum_j \tilde{\lambda}_{x\delta_{s_{ij}}}^2 - \frac{\theta_4}{2}\sum_i\sum_j \tilde{\lambda}_{x\delta_{f_{ij}}}^2 \\ & - \frac{\theta_5}{2\sigma}\sum_i\sum_j \tilde{b}_{\delta_{s_{ij}}}^2 - \frac{\theta_6}{2\sigma}\sum_i\sum_j \tilde{\lambda}_{\delta_s u_{s_{ij}}}^2 - \frac{\theta_7}{2\varepsilon}\sum_k\sum_i\sum_j \tilde{b}_{z_{ij}}^{k^2} \\ & - \frac{\theta_8}{2\varepsilon}\sum_i\sum_j \tilde{\lambda}_{z\delta_{f_{ij}}}^2 - \frac{\theta_9}{2\rho}\sum_i\sum_j \tilde{b}_{\delta_{f_{ij}}}^2 - \frac{\theta_{10}}{2\rho}\sum_i\sum_j \tilde{\lambda}_{\delta_f u_{f_{ij}}}^2 - \frac{\alpha_{15}}{2}\sum_i \bar{L}_i \tilde{x}_{U_i}^2 + \mu\end{aligned} \tag{4.115}$$

Inspection of the final form indicates that tracking errors, manifold errors, parameter estimation errors and state observation errors will be ultimately bounded. Given an ultimate bound, the resulting inequalities similar to Section 2.6 will lead to the bounds σ_{***}, σ^{***}, ε_{***}, ε^{***}, ρ_{***}, ρ^{***} of the time-scale separation parameters $\sigma, \varepsilon, \rho$ respectively.

4.3.3 Numerical Results

The output feedback slow state tracking control laws developed in Subsection 4.3.1 - 4.3.2 are implemented on a nonlinear 6-DOF generic F-16A, which is commanded to perform two different large-amplitude combined longitudinal and lateral/directional maneuvers. The functions and matrices used for the control synthesis are given in Appendix B. Uncertainties for this aircraft are assumed as follows. The initial estimate of each of the inertias $I_{xx}, I_{yy}, I_{zz}, I_{xz}$ is assumed 15% below its actual value. The initial estimate of each of the control derivatives $C_{x_{\delta_e}}, C_{y_{\delta_a}}, C_{y_{\delta_r}}, C_{z_{\delta_e}}$, $C_{m_{\delta_e}}, C_{l_{\delta_a}}, C_{l_{\delta_r}}, C_{n_{\delta_a}}, C_{n_{\delta_r}}$ is assumed 20% below its actual value. The engine time-constant is assumed 25% above its actual value. No uncertainty is assumed for the stability derivatives and the time-constants of the elevator, aileron and rudder.

Furthermore, it is assumed that the angle-of-attack α and the sideslip angle β are not measured. Instead, the body-axis components of velocity U, V, W are measured. A state observer is designed to estimate the angles α and β. These angles are known to evolve in the slowest time-scale, and

the state observer updates the estimates in the slowest time-scale, starting from the initial estimates $\hat{\alpha}(0) = 0$ and $\hat{\beta}(0) = 0$. However, angular rates evolve in a faster time-scale, and the aerodynamic terms appearing in the angular rate dynamics are functions of α and β. In the fast time-scale, these angles do not change significantly, so they are $evaluated$ from measurements of the body-axis velocity components U, V, W using the standard relations:

$$\begin{aligned} \alpha &= \arctan(\frac{W}{U}) \\ \beta &= \arcsin(\frac{V}{\sqrt{U^2 + V^2 + W^2}}). \end{aligned} \tag{4.116}$$

4.3.3.1 Aircraft Evaluation Maneuver I: Sequential 90 Degree Left and Right Turn Maneuver of a Generic F-16A

The first evaluation maneuver is from a previous work of Valasek [36]. For this evaluation maneuver, the generic F-16A is initially at trim in straight and level flight with a velocity of 800 ft/s at an altitude of 15,000 ft. The trim angle-of-attack and elevator deflection are 0.9 deg and -1.6 deg respectively. The thrust at trim is 3265.0 lbf, which is 18.34% of the maximum military thrust of 17,800 lbf. To ensure straight and level flight, the pitch attitude angle at trim is the same as the trim angle-of-attack. All other angles, rates and control surface deflections are zero at trim. The aircraft is commanded to perform a 90 deg left turn followed by a 90 deg right turn. The heading angle is desired to change by 90 deg in 10 seconds for each turn. Bank angle and pitch attitude angle associated with each turn are commanded to reach a maximum from zero, and then come back to zero as the turn is complete. The maximum bank angle and pitch attitude angle associated with each turn are 75 deg and 15 deg respectively. Velocity is commanded to be close to its trim value of 800 ft/s throughout the maneuver.

The controller gains are selected as $K_x = 10$, $K_\xi = diag[1.2, 1.2, 1]$, $K_{\delta_s} = 1$, $K_z = diag[100, 100, 100]$, $K_{\delta_f} = diag[0.5, 2, 0.05]$. To design the parameter estimator, gains are selected as $\alpha_1 = 10^{-13}, \alpha_2 = 10^{-14}, \alpha_3 = 10^{-15}, \alpha_8 = 1, \alpha_9 = 1, \alpha_{10} = 1, , \alpha_{111} = 1, \alpha_{112} = 1, \alpha_{12} = 1, \theta_i = 0.1; i = 4, 5, 6, 7, 8$. The design variables corresponding to the final value of the estimates

in the parameter update laws are chosen such that the inertias, control derivatives and engine time-constant are 5% above the actual values. For state observer design, the gains are selected as $\alpha_{15} = 1, L = diag[1000, 500]$. The design variables corresponding to the final values of the estimated states were set to equal the equivalent α, β corresponding to the measurements U, V, W. To see the performance of the output feedback controller when measurements are imperfect, the following perturbations are added in simulation to the body-axis velocities U, V, W and angular rates p, q, r:

$$\begin{aligned} \delta U &= 80\sin(10t) \\ \delta V &= 5\sin(10t) \\ \delta W &= 5\sin(10t) \\ \delta p &= 0.6\sin(10t) \\ \delta q &= 0.3\sin(10t) \\ \delta r &= 0.15\sin(10t) \end{aligned} \tag{4.117}$$

Each velocity perturbation is in ft/s, and each angular rate perturbation is in deg/s. The perturbation amplitudes are selected such that the velocity perturbations are about 10% of the expected maximum, and the angular rate perturbations are about 1% of the expected maximum. The perturbation frequency is selected such that it is significantly higher than that of the reference. The simulation is run for 75 sec.

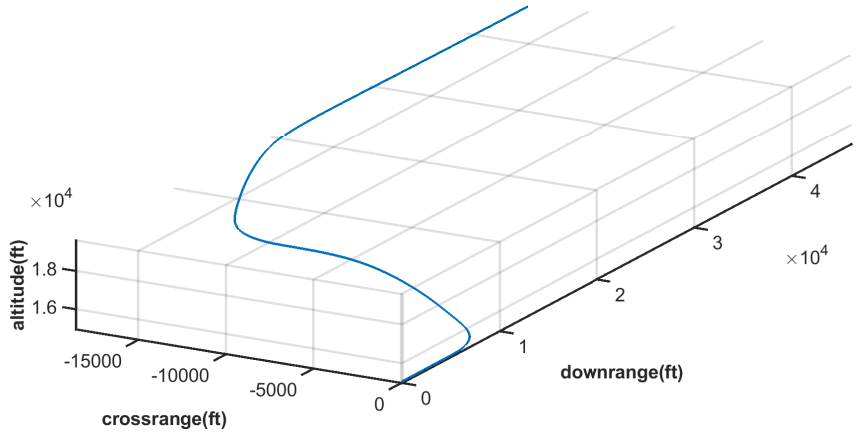

Figure 4.5: Trajectory of the generic F-16A during left and right turn

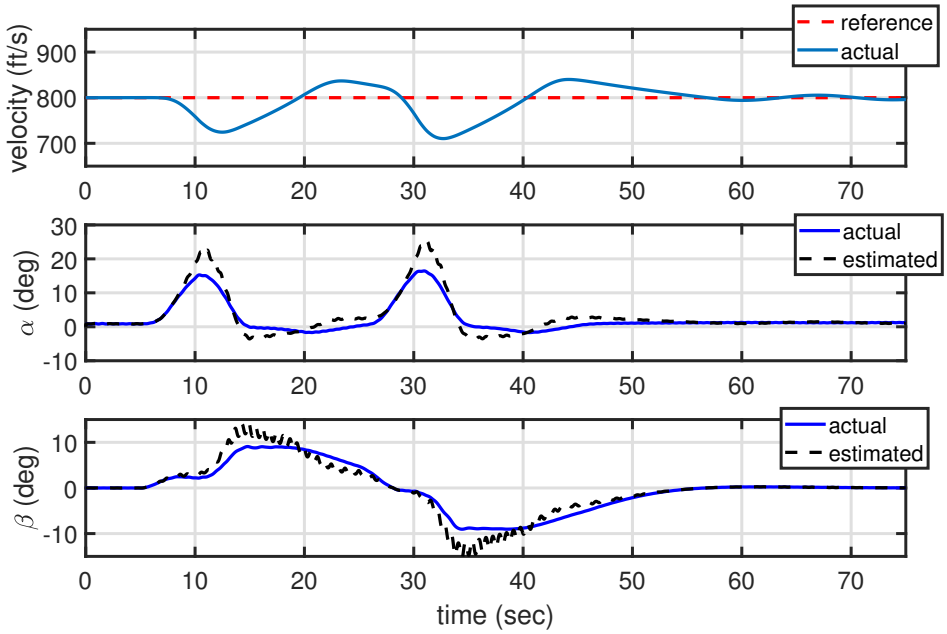

Figure 4.6: Velocity, angle-of-attack and sideslip angle during left and right turn

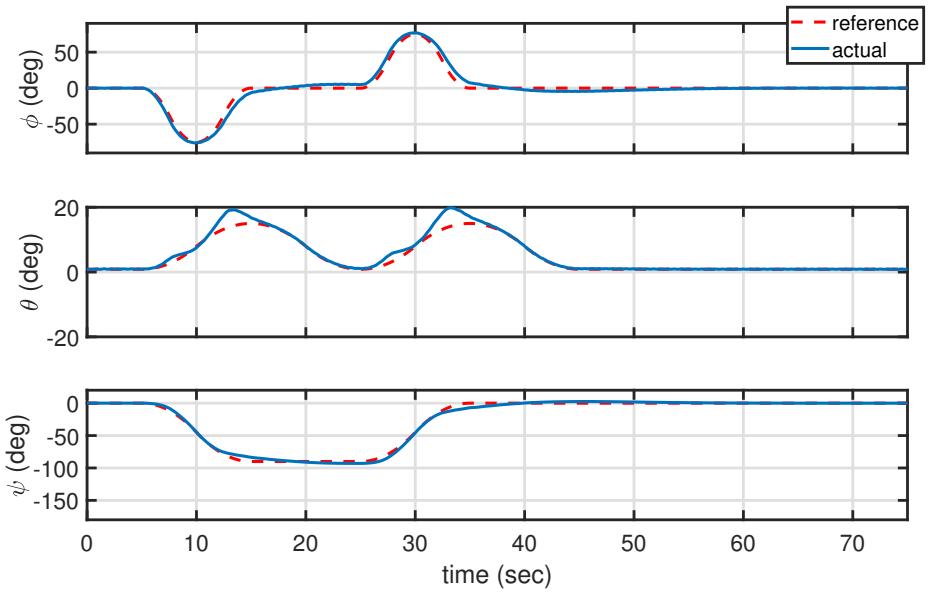

Figure 4.7: Bank angle, pitch attitude angle and heading angle during left and right turn

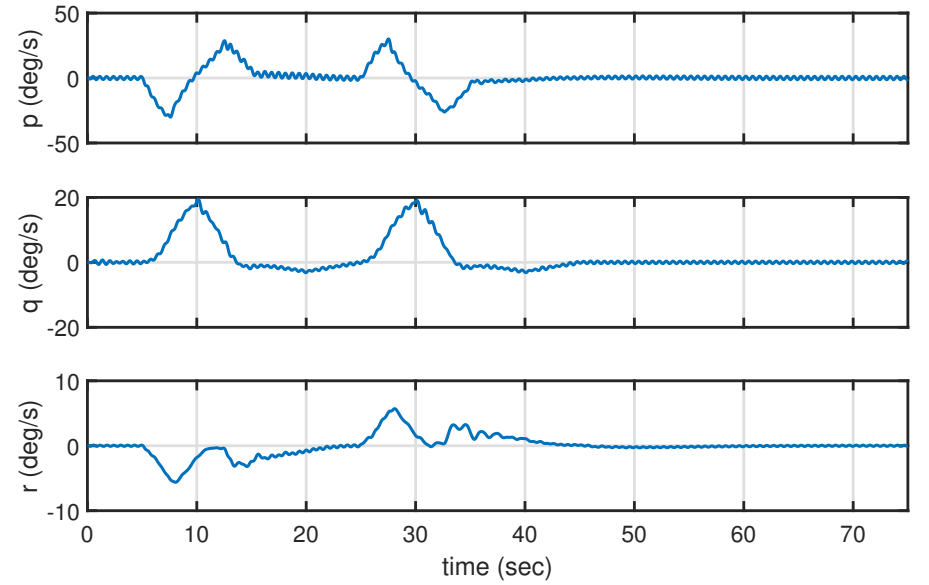

Figure 4.8: Body-axis roll, pitch and yaw rates during left and right turn

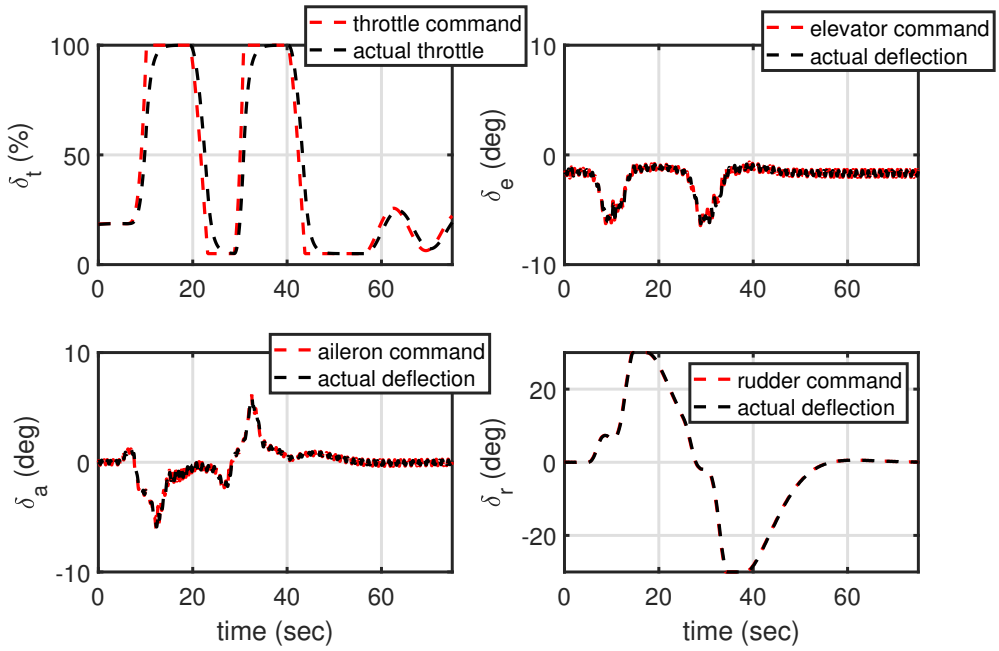

Figure 4.9: Throttle, elevator, aileron and rudder deflections during left and right turn

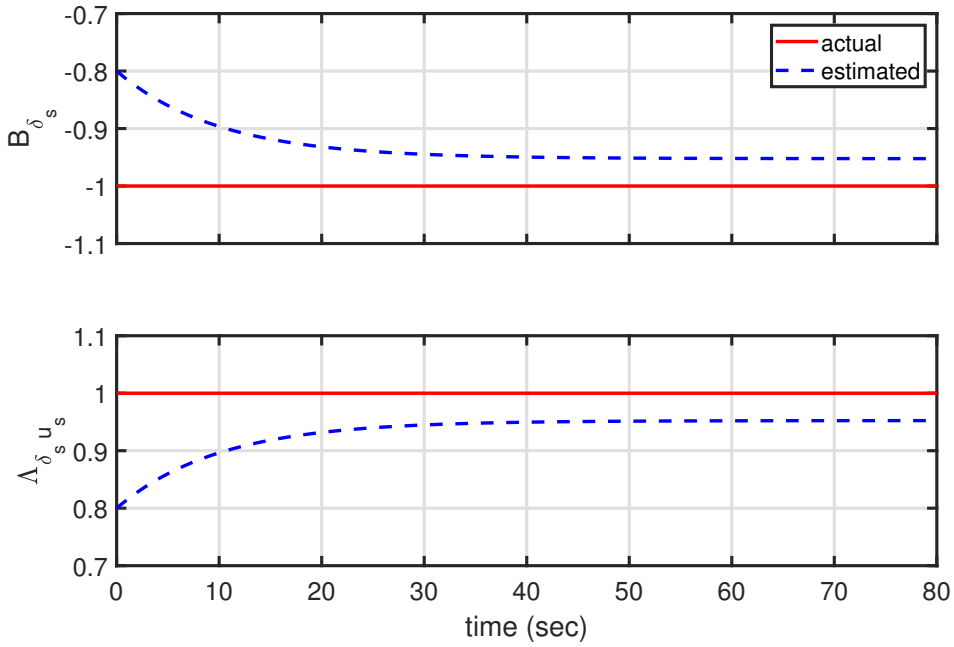

Figure 4.10: Uncertain parameters B_{δ_s} and $\Lambda_{\delta_s u_s}$ during left and right turn

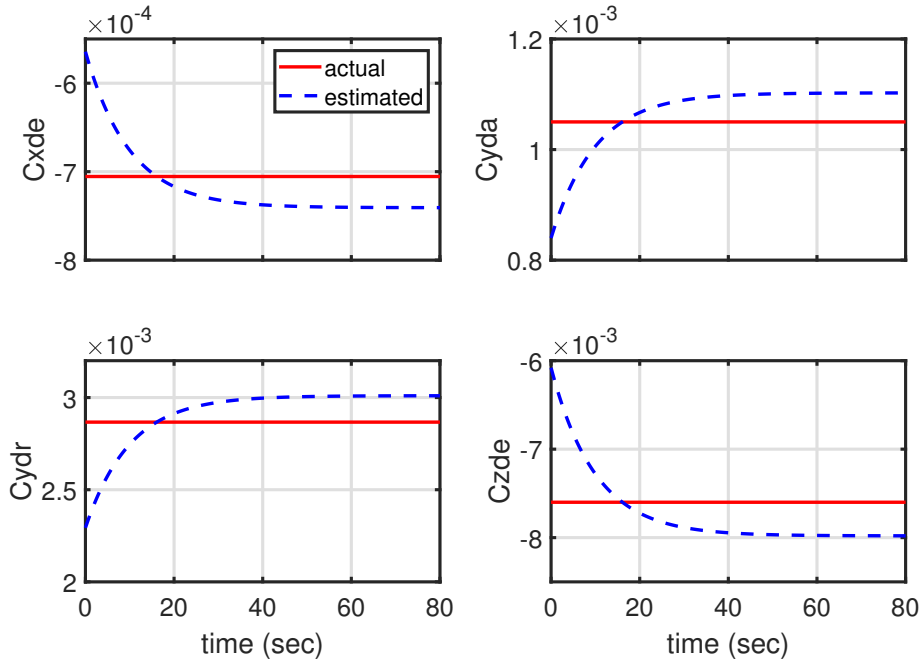

Figure 4.11: Uncertain parameters $C_{x_{\delta_e}}, C_{y_{\delta_a}}, C_{y_{\delta_r}}, C_{z_{\delta_e}}$ during left and right turn

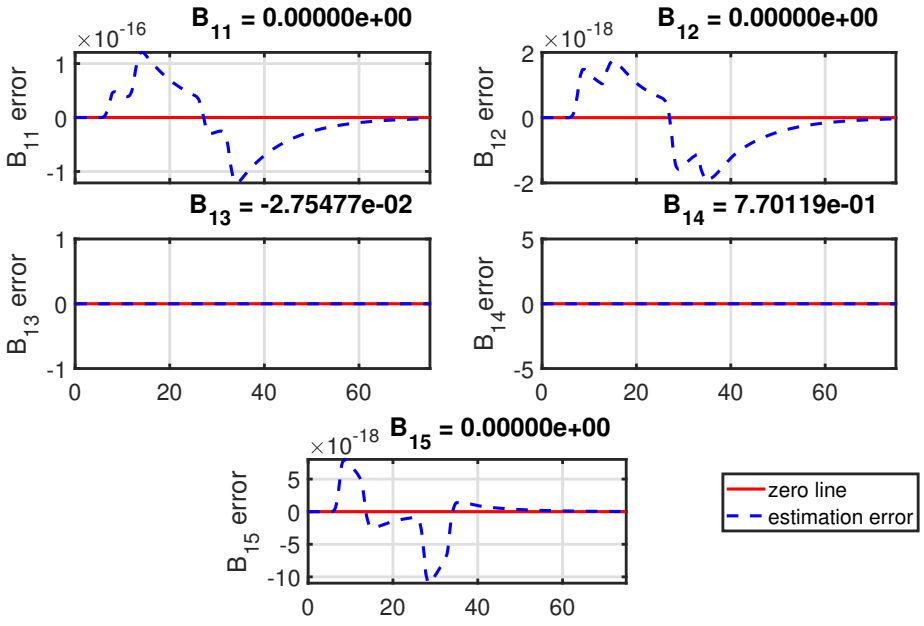

Figure 4.12: Uncertain parameters $B_{11} - B_{15}$ during left and right turn; the x-axis for each graph representing time in seconds

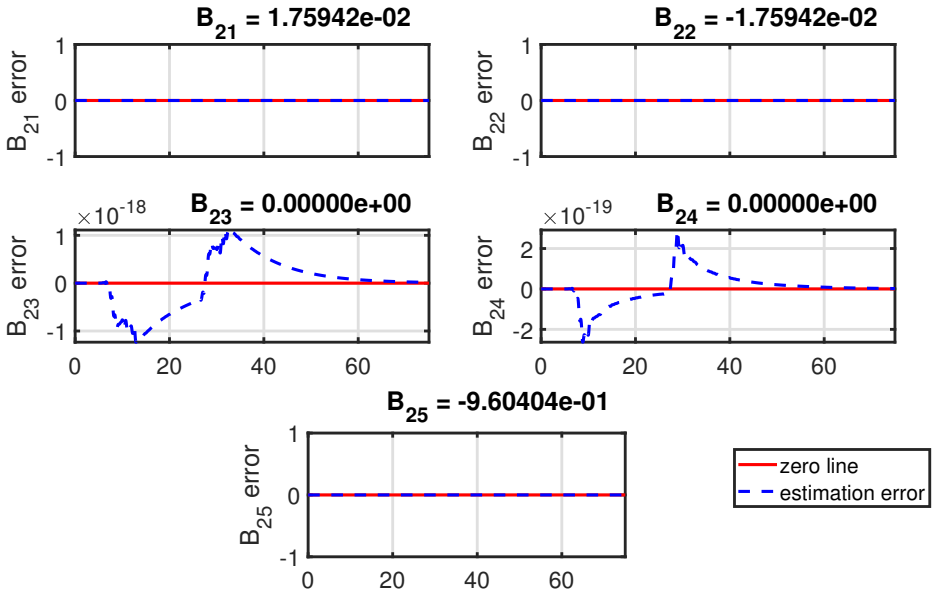

Figure 4.13: Uncertain parameters $B_{21} - B_{25}$ during left and right turn; the x-axis for each graph representing time in seconds

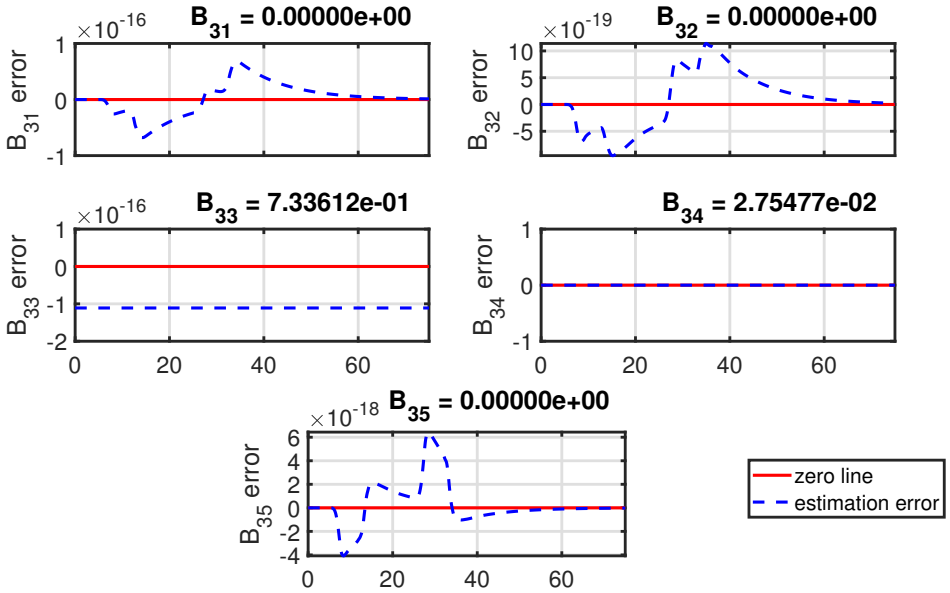

Figure 4.14: Uncertain parameters $B_{31} - B_{35}$ during left and right turn; the x-axis for each graph representing time in seconds

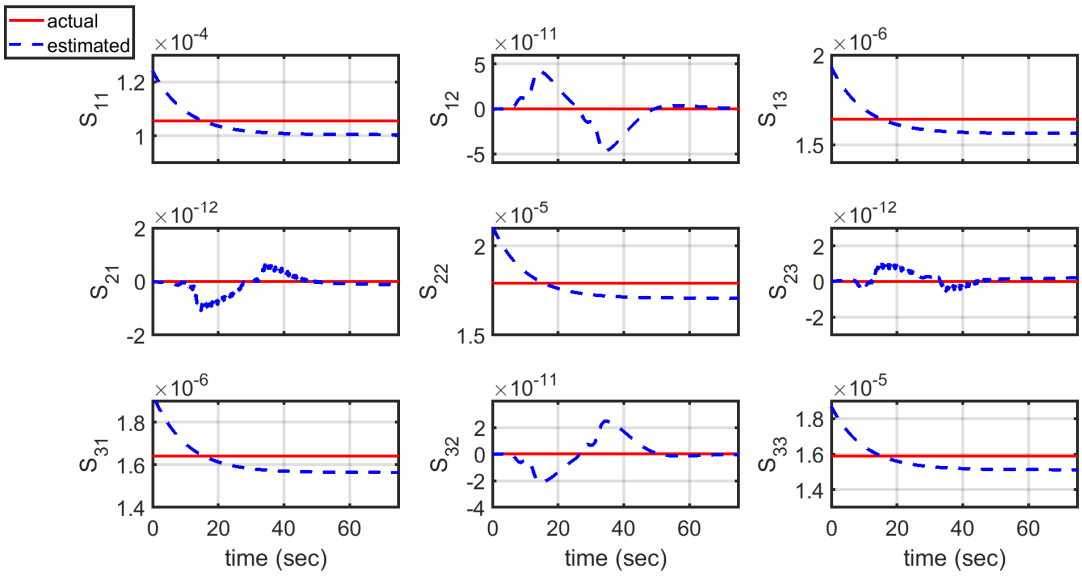

Figure 4.15: Uncertain parameters $S_{31} - S_{33}$ during left and right turn

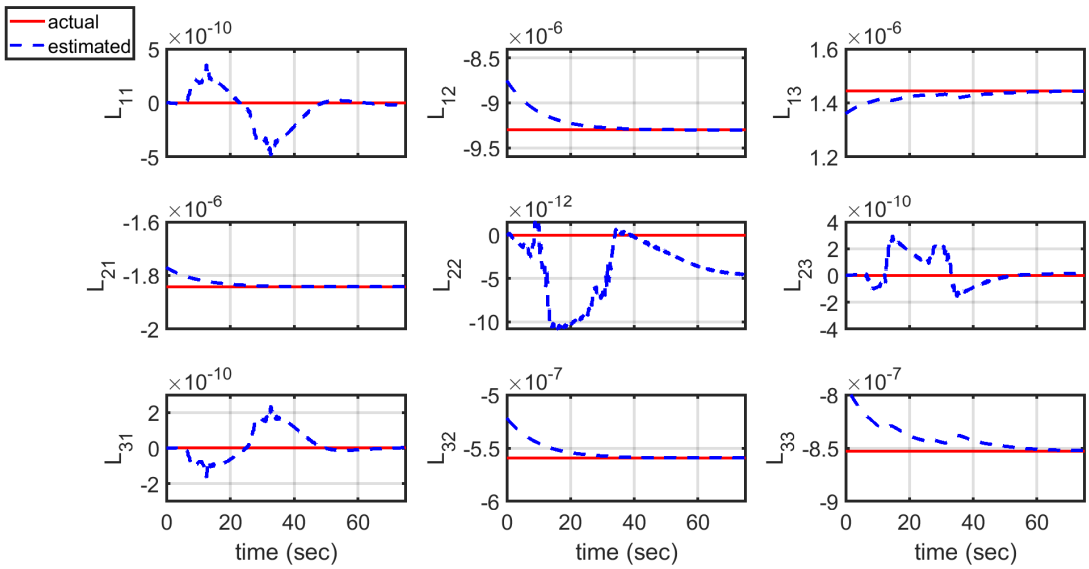

Figure 4.16: Uncertain parameters $L_{11} - L_{33}$ during left and right turn

Figures 4.5 - 4.9 show the time-history of the aircraft states and controls. Figure 4.5 shows the aircraft performing a 90 deg left turn followed by a 90 deg right turn. Figure 4.6 shows that the

loss of airspeed during the maneuver is within 50 ft/s. The lost airspeed is recovered as soon as each turn is complete. Additionally, the angle-of-attack and sideslip angle estimates remain very close to the actual angles throughout the simulation. Figure 4.7 show that kinematic angles are well-tracked. Figure 4.9 shows that the throttle goes from trim to full once each turn is initiated, and back to trim once each turn is complete. Because of the slow engine dynamics, the actual throttle follows the commanded throttle with a time lag. In contrast, the aerodynamic controls are seen respond much faster to a change in the control commands. It can be seen from Figures 4.7, 4.8 and 4.9 that the angle-of-attack, sideslip angle and body-axis rates are bounded, and that the control surface deflections are within acceptable limits.

Figures 4.10 - 4.16 show the evolutions of the uncertain parameters. It can be seen that the parameter estimation errors remain bounded. Specifically, for the B matrix which is obtained by multiplying inertia matrix with its inverse, the estimation errors are significantly small in magnitude. Overall, Figures 4.5 - 4.16 show a successful turn maneuver with bounded and small parameter estimation errors and accurate observations of angle-of-attack and sideslip angle.

4.3.3.2 Aircraft Evaluation Maneuver II: A Turn Maneuver Performed in an Engineering Flight Simulator

The second evaluation maneuver was generated by flying a generic F-16A in the XPlane 10 engineering flight simulator in the Vehicle Systems & Control Laboratory. For this maneuver, the generic F-16A is initially at trim in straight and level flight with a velocity of 500 knots, i.e. 843.9 ft/s at an altitude of 15,000 ft. The trim angle-of-attack and elevator deflection are 0.6 deg and -1.5 deg respectively. The thrust at trim is 3630.3 lbf, which is 20.4% of the maximum military thrust of 17,800 lbf. The pitch attitude angle at trim is the same as the trim angle-of-attack so the flight path angle is zero. The initial heading angle of the aircraft is 100 deg. All other angles, rates and control surface deflections are zero at trim. In flight simulator the aircraft is commanded to perform a left turn changing its heading angle to about 80 deg and then a right turn to change the heading to about 110 deg. Each heading change is commanded to occur over a time span of 5 sec. The maximum bank angle and pitch attitude angle are within 60 deg and 10 deg respectively. The

velocity stays within 50 ft/s of the trim value throughout the maneuver. Uncertainties are assumed exactly the same as the ones for the previous evaluation maneuver.

To simulate this maneuver, the controller gains are selected as $K_x = 5$, $K_\xi = diag[2, 4, 2]$, $K_{\delta_s} = 1$, $K_z = diag[15, 15, 15]$, $K_{\delta_f} = diag[1, 1, 1]$. To design the parameter estimator, gains are chosen as $\alpha_1 = 10^{-13}, \alpha_2 = 10^{-14}, \alpha_3 = 10^{-15}, \alpha_8 = 1, \alpha_9 = 1, \alpha_{10} = 1, , \alpha_{111} = 1, \alpha_{112} = 1, \alpha_{12} = 1, \theta_i = 1; i = 4, 5, 6, 7, 8$. The design variables corresponding to the final value of the estimates in the parameter update laws are chosen such that the inertias, control derivatives and engine time-constant are 5% above the actual values. For state observer design, the gains are selected as $\alpha_{15} = 1, L = diag[500, 100]$. The design variables corresponding to the final values of the estimated states were set to equal the equivalent α, β corresponding to the measurements U, V, W. To see the performance of the output feedback controller when measurements are imperfect, the following perturbations are added in simulation to the body-axis velocities U, V, W and angular rates p, q, r:

$$\begin{aligned} \delta U &= 40 \sin(10t) \\ \delta V &= 2.5 \sin(10t) \\ \delta W &= 2.5 \sin(10t) \\ \delta p &= 30 \sin(10t) \\ \delta q &= 3 \sin(10t) \\ \delta r &= 1.5 \sin(10t) \end{aligned} \tag{4.118}$$

Each velocity perturbation is in ft/s, and each angular rate perturbation is in deg/s. The perturbation amplitudes are selected such that the velocity perturbations are about 5% of the expected maximum, and the angular rate perturbations are about 10% of the expected maximum. The perturbation frequency is selected such that it is significantly higher than that of the reference. The simulation is run for 22 sec.

Figures 4.17 - 4.21 shows the time-history of the aircraft states and controls during the maneuver.

Figure 4.17 shows a left turn causing the heading angle to decrease to 80 degrees, followed by a right turn causing the heading angle to increase to 110 degrees. Figure 4.18 shows that the actual velocity is very close to the reference throughout the maneuver. This also shows that the estimated angle-of-attack and sideslip angle are very close to the actual angles. Figure 4.19 show that kinematic angles are well-tracked. Figure 4.21 shows the throttle responding to the change in command with a small time-delay due to the slow engine dynamics, whereas the aerodynamic controls respond much faster to any change in command. It can be seen from Figures 4.19, 4.20 and 4.21 that the angle-of-attack, sideslip angle and body-axis rates are bounded, and that the control surface deflections are within acceptable limits.

Figures 4.22 - 4.28 show the evolutions of the uncertain parameters. It can be seen that the parameter estimation errors remain bounded. Specifically, for the B matrix which is obtained by multiplying inertia matrix with its inverse, the estimation errors are significantly small in magnitude. Similar to the previous aircraft turn maneuver, Figures 4.17 - 4.28 show a successful slow state tracking maneuver with bounded and small parameter estimation errors and accurate observations of α and β.

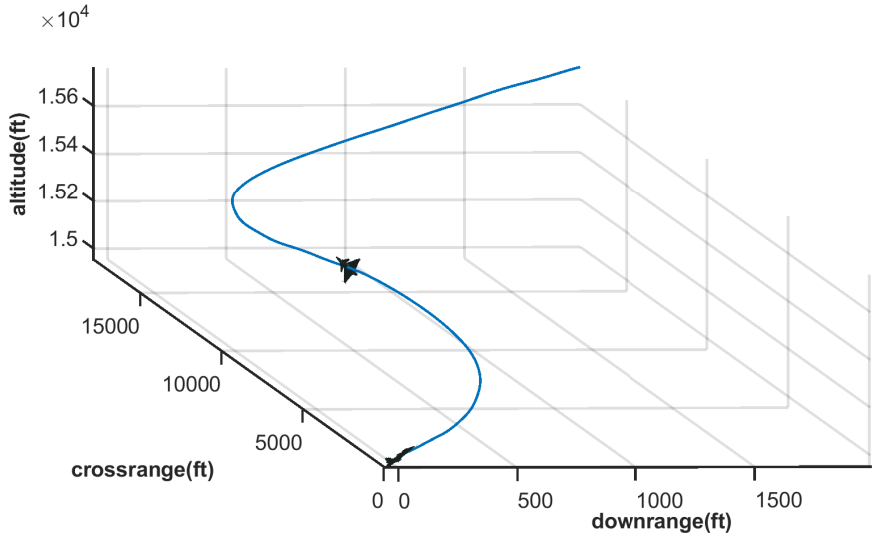

Figure 4.17: Trajectory of the generic F-16A during the flight simulator maneuver

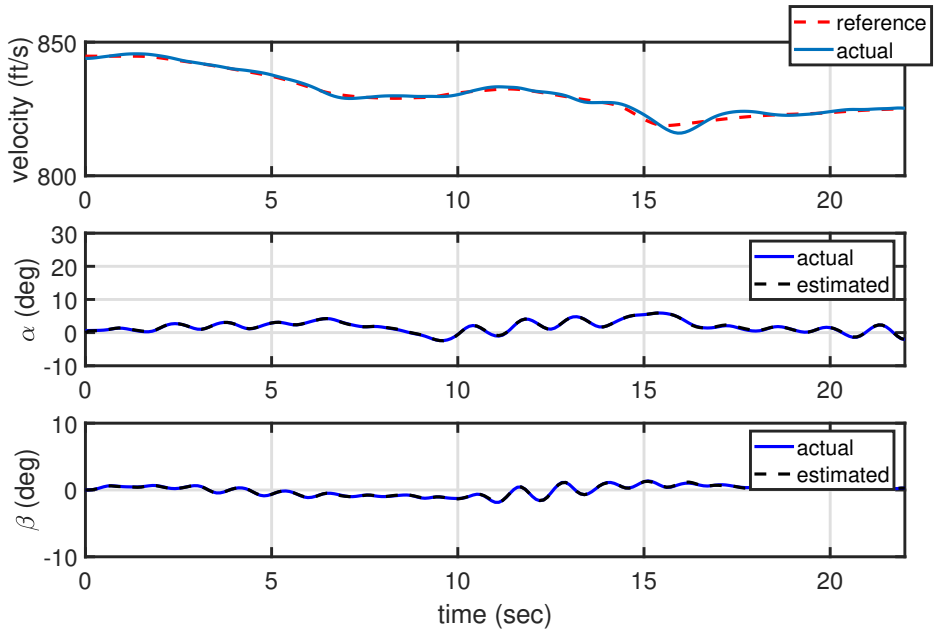

Figure 4.18: Velocity, angle-of-attack and sideslip angle during the flight simulator maneuver

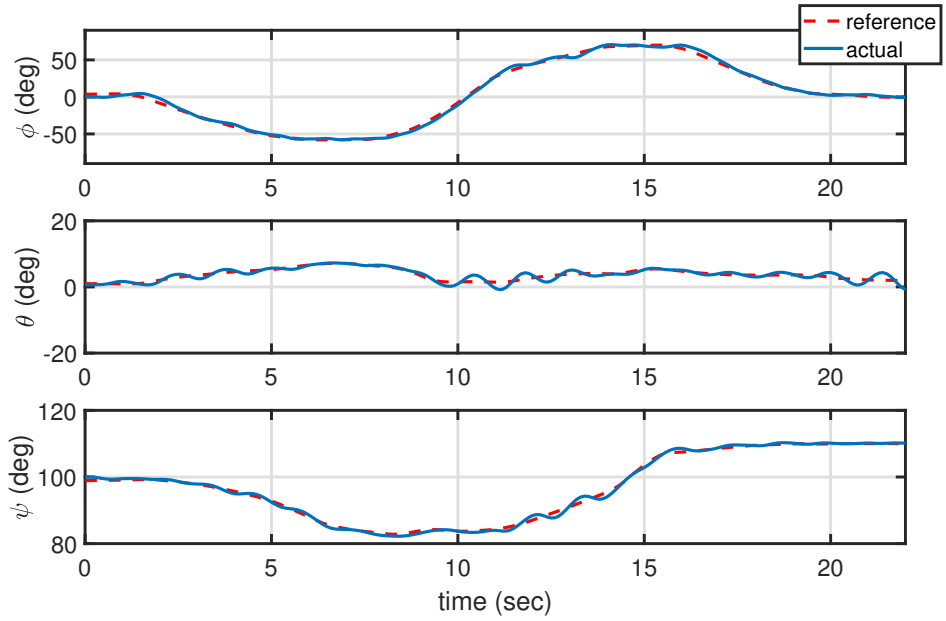

Figure 4.19: Bank angle, pitch attitude angle and heading angle during the flight simulator maneuver

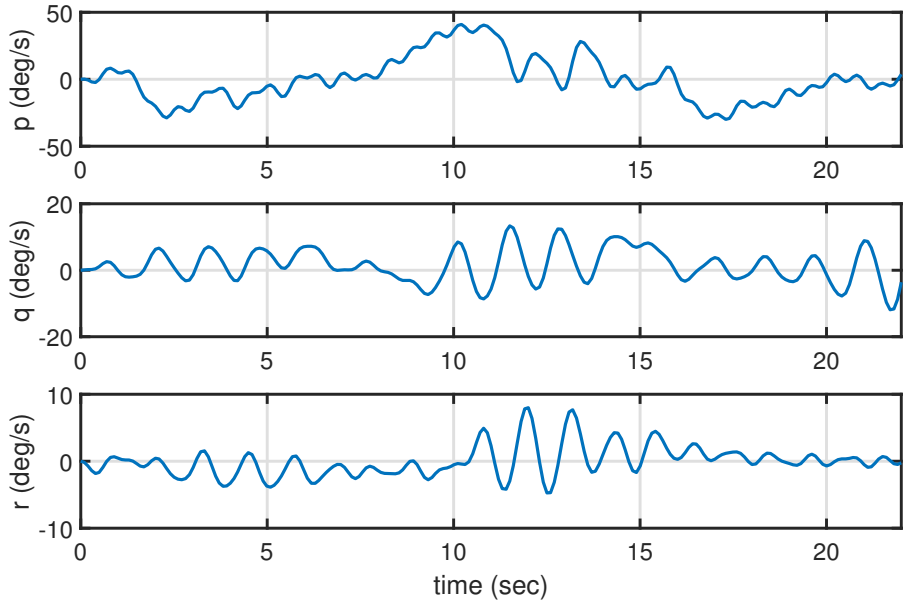

Figure 4.20: Body-axis roll, pitch and yaw rates during the flight simulator maneuver

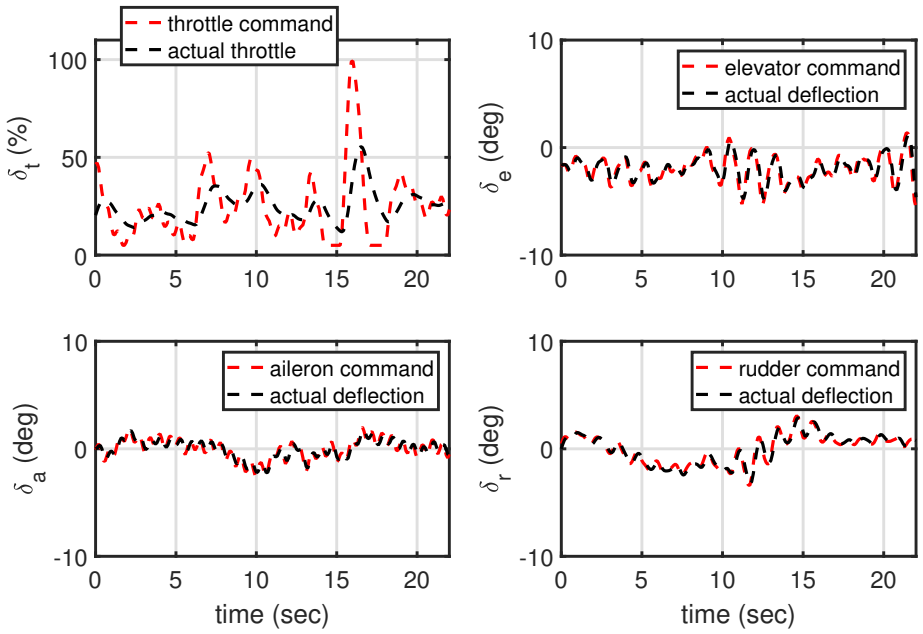

Figure 4.21: Throttle, elevator, aileron and rudder deflections during the flight simulator maneuver

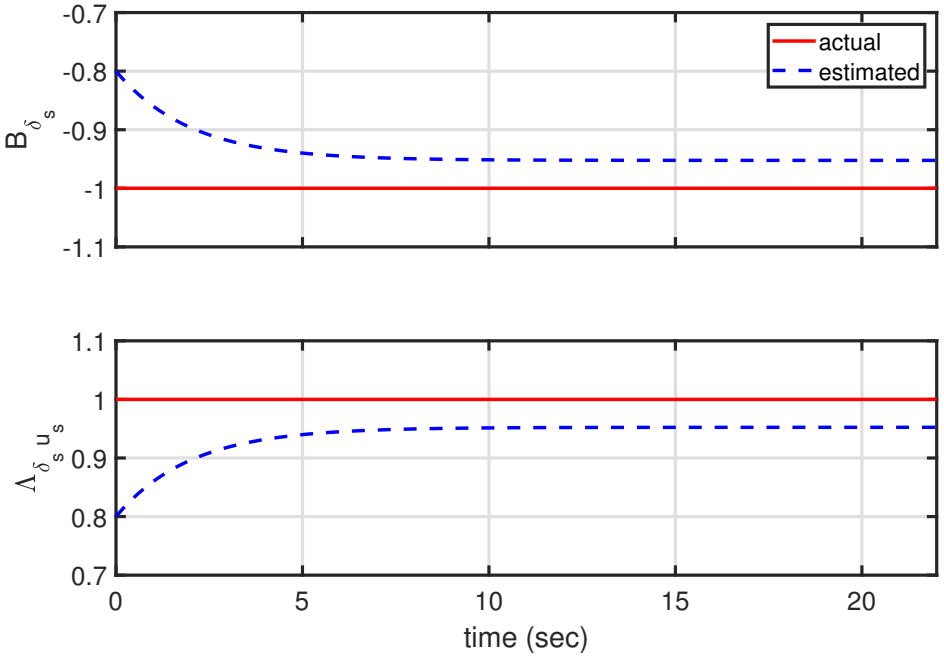

Figure 4.22: Uncertain parameters B_{δ_s} and $\Lambda_{\delta_s u_s}$ during the flight simulator maneuver

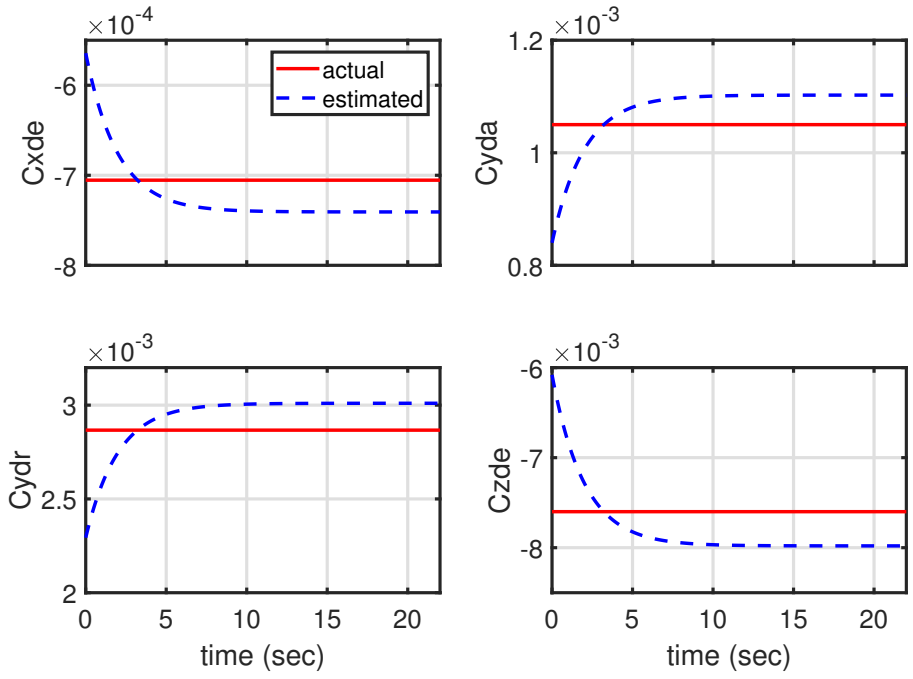

Figure 4.23: Uncertain parameters $C_{x_{\delta_e}}, C_{y_{\delta_a}}, C_{y_{\delta_r}}, C_{z_{\delta_e}}$ during the flight simulator maneuver

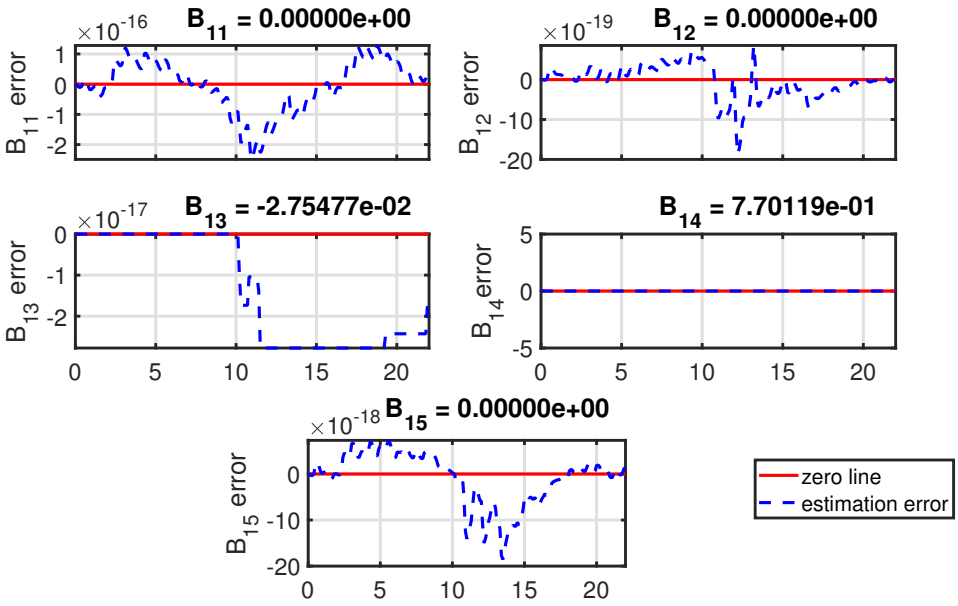

Figure 4.24: Uncertain parameters $B_{11} - B_{15}$ during the flight simulator maneuver

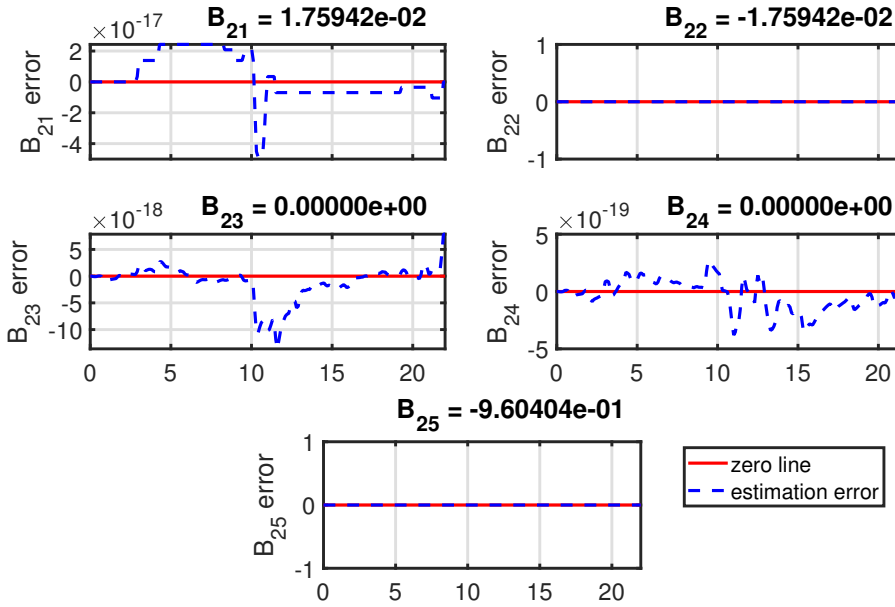

Figure 4.25: Uncertain parameters $B_{21} - B_{25}$ during the flight simulator maneuver; the x-axis for each graph representing time in seconds

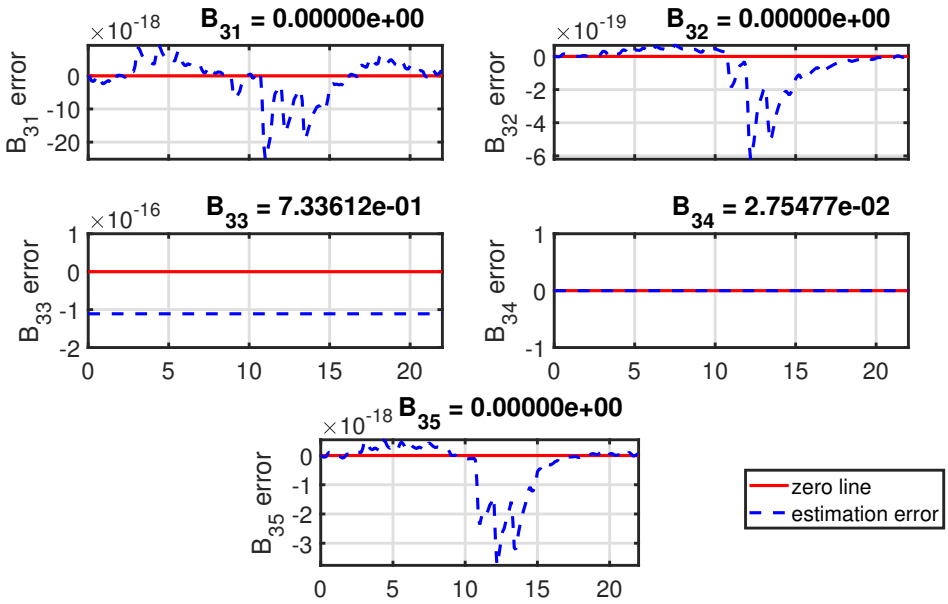

Figure 4.26: Uncertain parameters $B_{31} - B_{35}$ during the flight simulator maneuver; the x-axis for each graph representing time in seconds

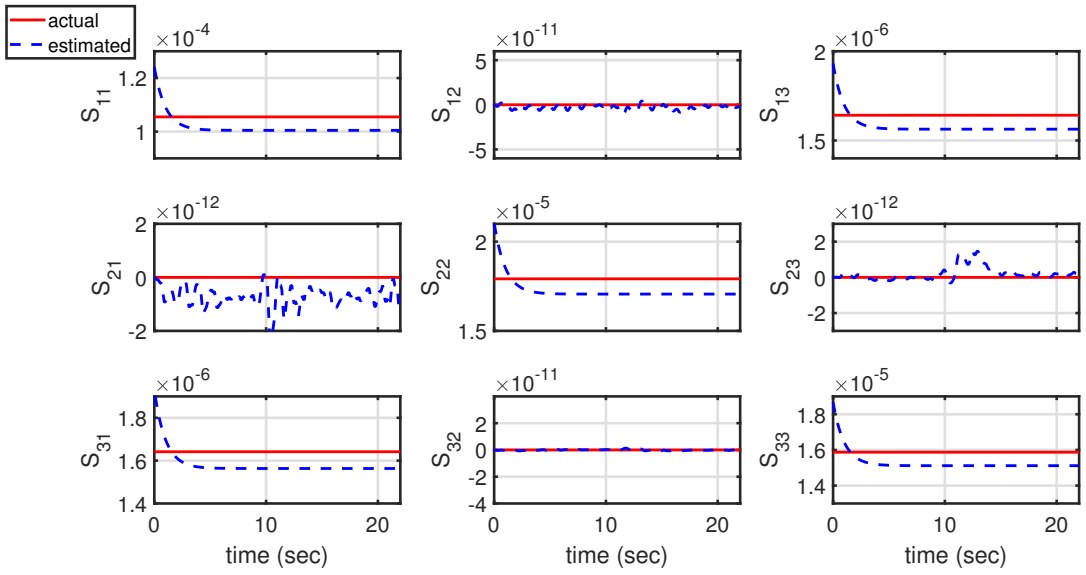

Figure 4.27: Uncertain parameters $S_{31} - S_{33}$ during the flight simulator maneuver; the x-axis for each graph representing time in seconds

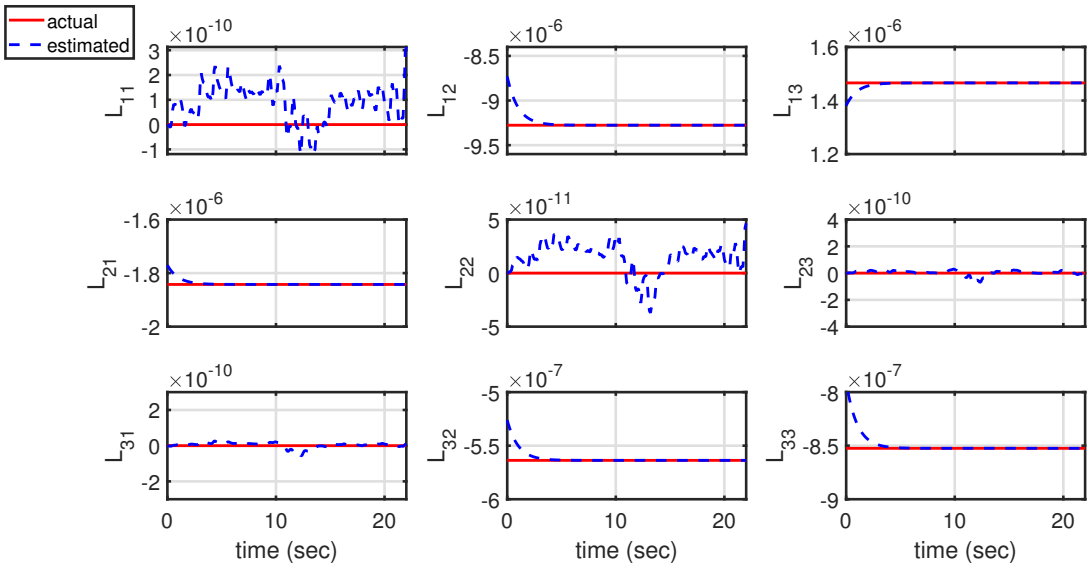

Figure 4.28: Uncertain parameters $L_{11} - L_{33}$ during the flight simulator maneuver

4.4 Simultaneous Slow and Fast State Tracking with Uncertainties and Actuator Dynamics Using Output Feedback

This section develops an output feedback controller for simultaneous slow and fast state tracking of a class of nonlinear, nonstandard four-time-scale system with slow and fast actuator dynamics and uncertainties. The class of systems is very similar to the one in Section 4.3, with the exception that the kinematic slow states are not considered for control design. Instead, the fast states are to be tracked. The slow states are divided into measured and unmeasured slow states. The measured slow states are tracked; the unmeasured slow states are assumed to have stable dynamics. The

four-time-scale system is

$$\begin{aligned}
\dot{x} &= B_x f_x(y) + F_{xx_U}(y)x_U + \gamma_x(t,x,\xi,z) + \Lambda_{x\delta_s}G_{x\delta_s}(y)\delta_s + \Lambda_{x\delta_f}G_{x\delta_f}(y)\delta_f \\
\dot{x}_U &= f_{x_U}(y) + F_{x_Ux_U}(y)x_U + G_{x_U\delta_s}(y)\delta_s + G_{x_U\delta_f}(y)\delta_f \\
\sigma\dot{\delta}_s &= B_{\delta_s}f_{\delta_s}(y) + \Lambda_{\delta_s u_s}G_{\delta_s u_s}(y)u_s \\
\varepsilon\dot{z} &= \sum_k B_z^k f_z^k(y) + \gamma_z(t,x,\xi,z) + \Lambda_{z\delta_f}G_{z\delta_f}(y)\delta_f \\
\rho\dot{\delta}_f &= B_{\delta_f}f_{\delta_f}(y) + \Lambda_{\delta_f u_f}G_{\delta_f u_f}(y)u_f. \\
y &= \begin{bmatrix} x & h(x,x_U) & \xi & \delta_s & z & \delta_f \end{bmatrix}^T.
\end{aligned} \tag{4.119}$$

4.4.1 Control, Parameter Update and State Observation Laws

The control objective is to drive the measured slow states $x(t)$ to a twice differentiable reference trajectory $x_r(t)$ and to drive the fast states $z(t)$ to a twice differentiable reference trajectory $z_r(t)$. The control law development in four time-scales using reduced subsystems is very similar to Section 3.3, except for the fact that the manifold of the slow actuator uses the estimates of the unmeasured slow states instead of the actual states. The parameter update laws are exactly the same as the ones in Section 3.3. The nonlinear observer can be designed from Composite Lyapunov analysis, and boundedness of errors can be proved in the same way as in Section 4.3. In this section, only the laws used for the simulation are provided for the reader's convenience.

4.4.1.1 Control Laws

The slow actuator manifold is selected as

$$\delta_s^0 = G_{x\delta_s}^{-1}\hat{\Lambda}_{x_{\delta_s}}^{-1}(\dot{x}_r - \hat{B}_x f_x - F_{xx_U}\hat{x}_U - \hat{\Lambda}_{x\delta_f}G_{x\delta_f}\delta_f^0|_{z_r} - K_x e_x) \tag{4.120}$$

where

$$\delta_f^0|_{z_r} = -G_{z\delta_f}^{-1}\hat{\Lambda}_{z\delta_f}^{-1}\sum_k \hat{B}_z^k f_z^k(x,z_r). \tag{4.121}$$

and K_x is positive-definite. The slow control is selected as

$$u_s = G_{\delta_s u_s}^{-1} \hat{\Lambda}_{\delta_s u_s}^{-1} (-\hat{B}_{\delta_s} f_{\delta_s} - K_{\delta_s} e_{\delta_s}) \tag{4.122}$$

where K_{δ_s} is positive-definite. The fast actuator manifold is selected as

$$\delta_f^0 = G_{z\delta_f}^{-1} \hat{\Lambda}_{z\delta_f}^{-1} (z_r' - \sum_k \hat{B}_z^k f_z^k - K_z e_z) \tag{4.123}$$

where K_z is positive-definite. The fast control is selected as

$$u_f = G_{\delta_f u_f}^{-1} \hat{\Lambda}_{\delta_f u_f}^{-1} (-\hat{B}_{\delta_f} f_{\delta_f} - K_{\delta_f} e_{\delta_f}) \tag{4.124}$$

where K_{δ_f} is positive-definite.

4.4.1.2 Dynamics of Parameter Estimator and Nonlinear Observer

The composite Lyapunov function is

$$\begin{aligned} V_c = {} & \alpha_1 V_1 + \alpha_2 V_2 + \alpha_3 V_3 + \alpha_4 V_4 + \frac{1}{2}\alpha_5 \sum_i \sum_j \tilde{b}_{x_{ij}}^2 + \frac{1}{2}\alpha_6 \sum_i \sum_j \tilde{\lambda}_{x\delta_{s_{ij}}}^2 \\ & + \frac{1}{2}\alpha_7 \sum_i \sum_j \tilde{\lambda}_{x\delta_{f_{ij}}}^2 + \frac{1}{2}\alpha_8 \sum_i \sum_j \tilde{b}_{\delta_{s_{ij}}}^2 + \frac{1}{2}\alpha_9 \sum_i \sum_j \tilde{\lambda}_{\delta_s u_{s_{ij}}}^2 + \frac{1}{2} \sum_k \alpha_{10k} \sum_i \sum_j \tilde{b}_{z_{ij}}^{k^2} \\ & + \frac{1}{2}\alpha_{11} \sum_i \sum_j \tilde{\lambda}_{z\delta_{f_{ij}}}^2 + \frac{1}{2}\alpha_{12} \sum_i \sum_j \tilde{b}_{\delta_{f_{ij}}}^2 + \frac{1}{2}\alpha_{13} \sum_i \sum_j \tilde{\lambda}_{\delta_f u_{f_{ij}}}^2 + \frac{1}{2}\alpha_{14} \tilde{x}_U^T \tilde{x}_U \end{aligned} \tag{4.125}$$

The estimates of constant but unknown parameters are updated as

$$\begin{aligned} \dot{\hat{b}}_{x_{ij}} &= \frac{\alpha_1}{\alpha_5} e_{x_i} f_{x_j} - \frac{\theta_1}{\alpha_5} (\hat{b}_{x_{ij}} - b_{x_{ij}}^0) \\ \dot{\hat{\lambda}}_{x\delta_{s_{ij}}} &= \frac{\alpha_1}{\alpha_6} e_{x_i} (G_{x\delta_s} \delta_s^0)_j - \frac{\theta_2}{\alpha_6} (\hat{\lambda}_{x\delta_{s_{ij}}} - \lambda_{x\delta_{s_{ij}}}^0) \\ \dot{\hat{\lambda}}_{x\delta_{f_{ij}}} &= \frac{\alpha_1}{\alpha_7} e_{x_i} (G_{x\delta_f} \delta_f^0|_{z_r})_j - \frac{\theta_3}{\alpha_7} (\hat{\lambda}_{x\delta_{f_{ij}}} - \lambda_{x\delta_{f_{ij}}}^0) \end{aligned} \tag{4.126}$$

$$\begin{aligned}\dot{\hat{b}}_{\delta_{sij}} &= \frac{\alpha_2}{\alpha_8} e_{\delta_{si}} f_{\delta_{sj}} - \frac{\theta_4}{\alpha_8}(\hat{b}_{\delta_{sij}} - b^0_{\delta_{sij}}) \\ \dot{\hat{\lambda}}_{\delta_s u_{sij}} &= \frac{\alpha_2}{\alpha_9} e_{\delta_{si}} (G_{\delta_s u_s} u_s)_j - \frac{\theta_5}{\alpha_9}(\hat{\lambda}_{\delta_s u_{sij}} - \lambda^0_{\delta_s u_{sij}})\end{aligned} \tag{4.127}$$

$$\begin{aligned}\hat{b}^{k'}_{z_{ij}} &= \frac{\alpha_3}{\alpha_{10k}} e_{z_i} f^k_{z_j} - \frac{\theta_6}{\alpha_{10k}}(\hat{b}^k_{z_{ij}} - b^{k^0}_{z_{ij}}) \\ \hat{\lambda}'_{z\delta_{f_{ij}}} &= \frac{\alpha_3}{\alpha_{11}} e_{z_i} (G_{z\delta_f} \delta^0_f)_j - \frac{\theta_7}{\alpha_{11}}(\hat{\lambda}_{z\delta_{f_{ij}}} - \lambda^0_{z\delta_{f_{ij}}})\end{aligned} \tag{4.128}$$

$$\begin{aligned}\breve{\hat{b}}_{\delta_{f_{ij}}} &= \frac{\alpha_4}{\alpha_{12}} e_{\delta_{f_i}} f_{\delta_{f_j}} - \frac{\theta_8}{\alpha_{12}}(\hat{b}_{\delta_{f_{ij}}} - b^0_{\delta_{f_{ij}}}) \\ \breve{\hat{\lambda}}_{\delta_f u_{f_{ij}}} &= \frac{\alpha_4}{\alpha_{13}} e_{\delta_{f_i}} (G_{\delta_f u_f} u_f)_j - \frac{\theta_9}{\alpha_{13}}(\hat{\lambda}_{\delta_f u_{f_{ij}}} - \lambda^0_{\delta_f u_{f_{ij}}})\end{aligned} \tag{4.129}$$

The nonlinear state observer is designed as

$$\dot{\hat{x}}_U = \frac{\alpha_1}{\alpha_{14}} F^T_{xx_U} e_x + f_{x_U} + F_{x_U x_U} \hat{x}_U + G_{x_U \delta_s} \delta_s + G_{x_U \delta_f} \delta_f - L(\hat{x}_U - x^0_U) \tag{4.130}$$

where $\alpha_i > 0; i = 1, ..., 14; \theta_i > 0; i = 1, ..., 9$. In addition, the observer gain matrix L is selected diagonal such that its diagonal elements satisfy $L_i > 2v_0$ where v_0 is such that $\lambda_{\max}(F_{x_U x_U}) \leq v_0$. On selecting the update laws, the time-derivative of the composite Lyapunov function becomes of the form

$$\begin{aligned}\dot{V}_c \leq & -\beta_1 e^T_x e_x - \beta_2 e^T_{\delta_s} e_{\delta_s} - \beta_3 e^T_z e_z - \beta_4 e^T_{\delta_f} e_{\delta_f} \\ & - \frac{\theta_1}{2} \sum_j \tilde{b}^2_{x_{ij}} - \frac{\theta_2}{2} \sum_i \sum_j \tilde{\lambda}^2_{x\delta_{sij}} - \frac{\theta_3}{2} \sum_i \sum_j \tilde{\lambda}^2_{x\delta_{f_{ij}}} \\ & - \frac{\theta_4}{2\sigma} \sum_i \sum_j \tilde{b}^2_{\delta_{sij}} - \frac{\theta_5}{2\sigma} \sum_i \sum_j \tilde{\lambda}^2_{\delta_s u_{sij}} - \frac{\theta_6}{2\varepsilon} \sum_k \sum_i \sum_j \tilde{b}^{k^2}_{z_{ij}} \\ & - \frac{\theta_7}{2\varepsilon} \sum_i \sum_j \tilde{\lambda}^2_{z\delta_{f_{ij}}} - \frac{\theta_8}{2\rho} \sum_i \sum_j \tilde{b}^2_{\delta_{f_{ij}}} - \frac{\theta_9}{2\rho} \sum_i \sum_j \tilde{\lambda}^2_{\delta_f u_{f_{ij}}} - \frac{\alpha_{14}}{2} \sum_i \bar{L}_i \tilde{x}^2_{U_i} + \mu.\end{aligned} \tag{4.131}$$

This indicates ultimate boundedness of tracking errors, manifold errors, parameter estimation errors and state observation errors.

4.4.2 Numerical Results: Climb and Roll Maneuver of a Generic F-16A

This section demonstrates simultaneous slow and fast tracking for a nonlinear 6-DOF aircraft with actuator dynamics and uncertainties using output feedback. The control and estimation laws in the previous Subsection is implemented on a nonlinear 6-DOF generic F-16A commanded to perform the same climb and roll maneuver as the one in Chapter 3. Velocity is the commanded slow state, whereas the body-axis roll, pitch and yaw rates are the commanded fast states. The difference between the earlier and the current simulations is that the angle-of-attack and sideslip angles are not measured in this simulation; they are observed using the state observation laws derived from the composite Lyapunov analysis.

At time zero, the generic F-16A is at steady level trim with a velocity of 800 ft/s at an altitude of 15,000 ft. The trim angle-of-attack and elevator deflection are 0.9 deg and -1.6 deg respectively. The thrust at trim is 3265.0 lbf, which is 18.34% of the maximum military thrust of 17,800 lbf. All other angles, rates and control surface deflections are zero at trim. A climb is commanded at a pitch rate of 15 deg/s followed by a roll at a rate of 20 deg/s while maintaining zero yaw rate and velocity 800 ft/s. The reference pitch rate increases smoothly from zero to 15 deg/s, then goes back to zero and reaches -15 deg/s before becoming zero again. Similarly the commanded roll rate goes from zero to 20 deg/s, then decreases to zero, reaches -20 deg/s, and finally becomes zero again.

The uncertainties are assumed as follows. The initial estimate of each of the inertias I_{xx}, I_{yy}, I_{zz}, I_{xz} is assumed 15% below its actual value. The initial estimate of each of the control derivatives $C_{x_{\delta_e}}, C_{y_{\delta_a}}, C_{y_{\delta_r}}, C_{z_{\delta_e}}, C_{m_{\delta_e}}, C_{l_{\delta_a}}, C_{l_{\delta_r}}, C_{n_{\delta_a}}, C_{n_{\delta_r}}$ is assumed 50% below its actual value. The engine time-constant is assumed 25% above its actual value. No uncertainty is assumed for the stability derivatives and the time-constants of the elevator, aileron and rudder.

The controller gains are selected as $K_x = 100$, $K_{\delta_s} = 0.005$, $K_z = diag[500, 1000, 500]$, $K_{\delta_f} = diag[1, 1, 1]$. To design the parameter estimator, gains are selected as $\alpha_1 = 10^{-13}, \alpha_2 = 10^{-14}, \alpha_3 = 10^{-15}, \alpha_7 = 1, \alpha_8 = 1, \alpha_9 = 1, , \alpha_{101} = 1, \alpha_{102} = 1, \alpha_{11} = 1, \theta_i = 0.5; i = 4, 5, 6, 7, 8$. The design variables corresponding to the final value of the estimates in the parameter update laws are chosen such that the inertias, control derivatives and engine time-constant are

5% above the actual values. For state observer design, the gains are selected as $a_{15} = 1, L = diag[5000, 500]$. The design variables corresponding to the final values of the estimated states were set to equal the equivalent α, β corresponding to the measurements U, V, W. To see the performance of the output feedback controller when measurements are imperfect, the following perturbations are added in simulation to the body-axis velocities U, V, W and angular rates p, q, r:

$$\begin{aligned} \delta U &= 80\sin(10t) \\ \delta V &= 5\sin(10t) \\ \delta W &= 5\sin(10t) \\ \delta p &= 6\sin(10t) \\ \delta q &= 3\sin(10t) \\ \delta r &= 1.5\sin(10t) \end{aligned} \tag{4.132}$$

Each velocity perturbation is in ft/s, and each angular rate perturbation is in deg/s. The perturbation amplitudes are selected such that the velocity perturbations are about 5% of the expected maximum, and the angular rate perturbations are about $5-10\%$ of the expected maximum. The perturbation frequency is selected such that it is significantly higher than that of the reference. The simulation is run for 40 sec.

Figures 4.29 - 4.33 show the time-histories of the states and controls during the maneuver. Figures 4.29 and 4.30 show that the loss of airspeed during climb is within 10%, and that the velocity comes back to the trim value of 800 ft/s once it levels out at its new altitude of 18,000 ft. 4.30 also shows that the estimated angle-of-attack and sideslip angle are very close to the actual angles. Good tracking of the body-axis roll, pitch and yaw rates can be observed in Figure 4.32. The tracking errors for the rates are seen to be are almost zero at all times. Figure 4.33 shows that the throttle goes from trim to full as the climb starts, and comes back to trim as the new altitude is reached. The inclusion of engine dynamics results in a smoother profile of the actual throttle, in contrast to the spikes in the commanded throttle profile. All the other states and the controls

remain bounded and within acceptable limits.

Figures 4.34 - 4.40 show the time-histories of the uncertain parameters for the climb and roll maneuver. Similar to the slow state tracking maneuvers, it can be observed that the parameter estimation errors remain bounded and small. Overall, the desired objective of simultaneous slow and fast state tracking has been accomplished using output feedback, with accurate estimates of the unmeasured states, and small and bounded parameter estimation errors.

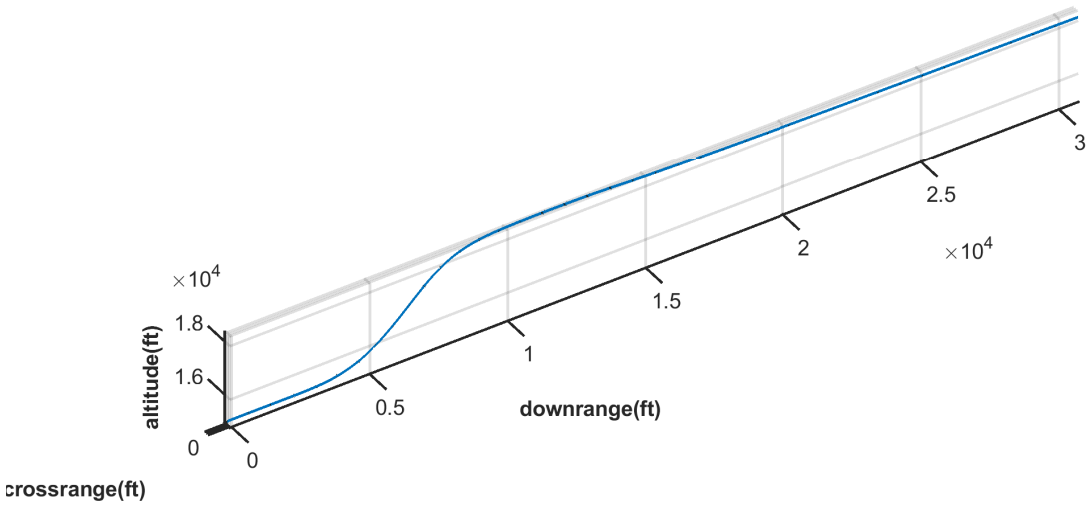

Figure 4.29: Trajectory of the generic F-16A during the climb and roll maneuver

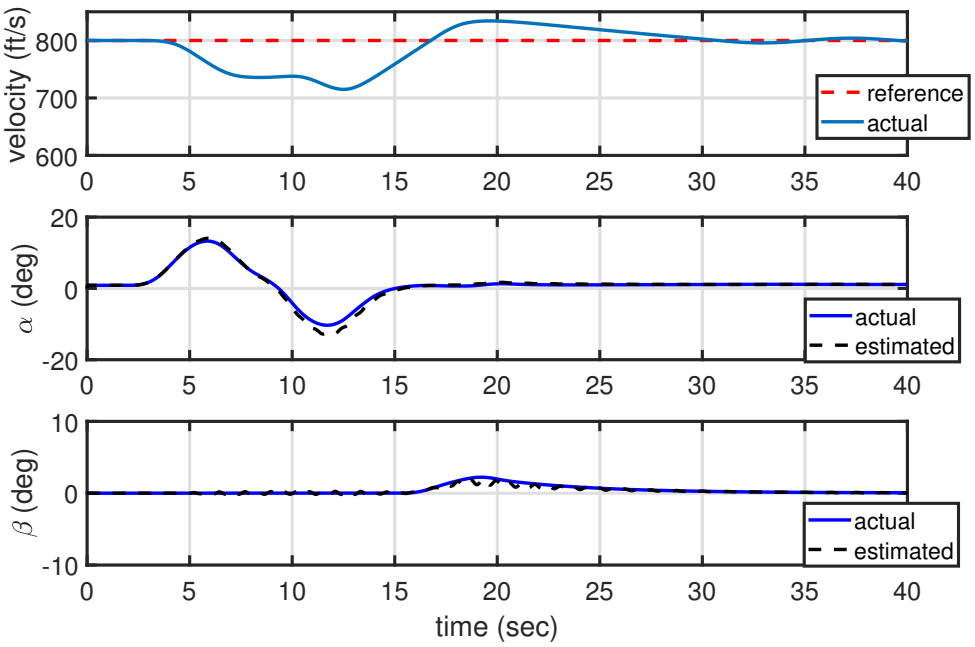

Figure 4.30: Velocity, angle-of-attack and sideslip angle during the climb and roll maneuver

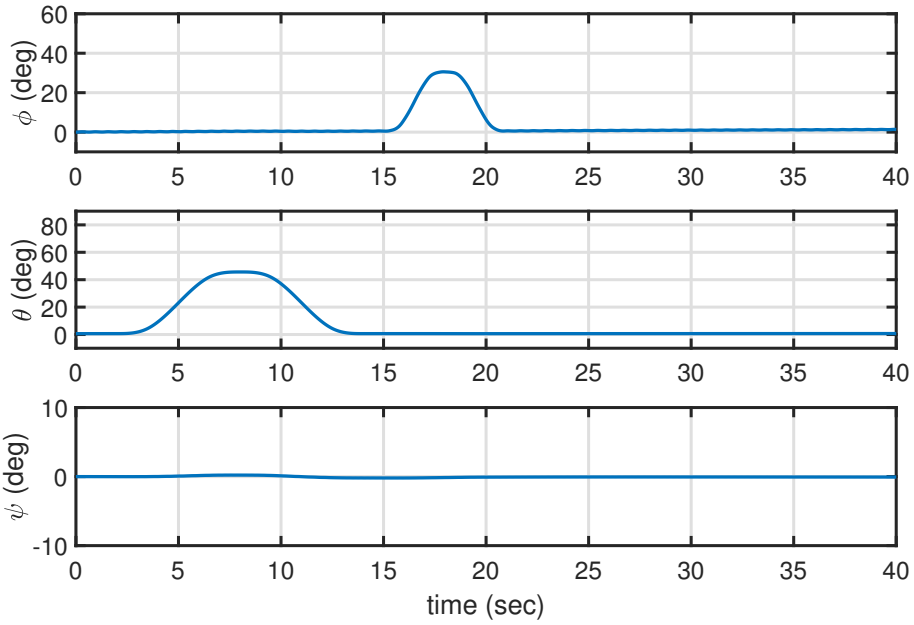

Figure 4.31: Bank angle, pitch attitude angle and heading angle during the climb and roll maneuver

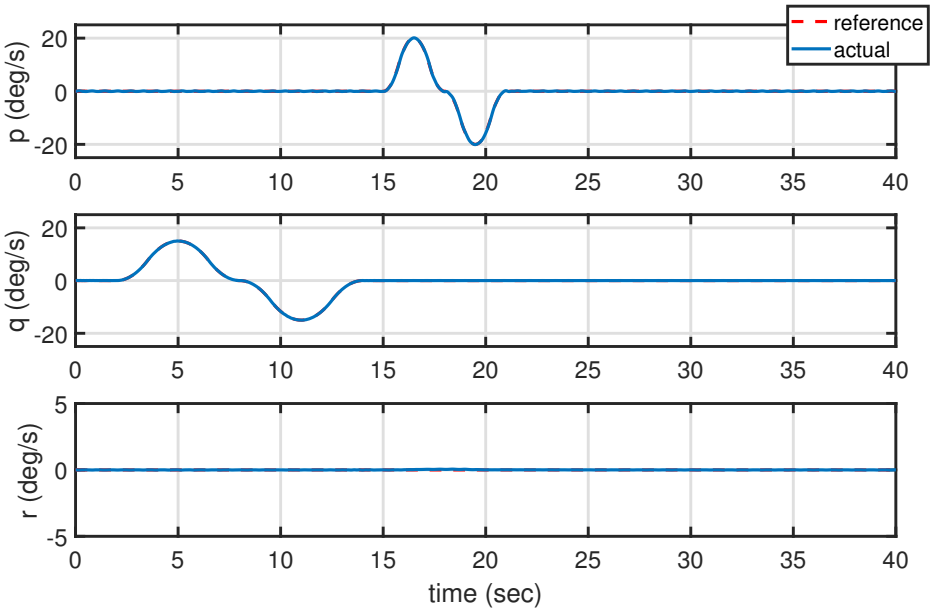

Figure 4.32: Body-axis roll, pitch and yaw rates during the climb and roll maneuver

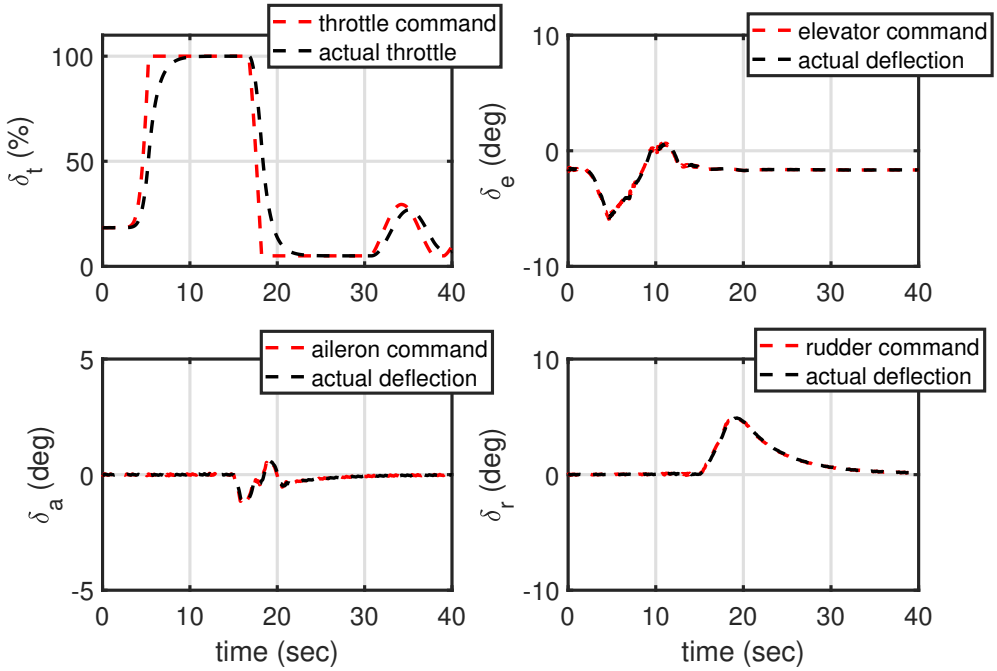

Figure 4.33: Throttle, elevator, aileron and rudder deflections during the climb and roll maneuver

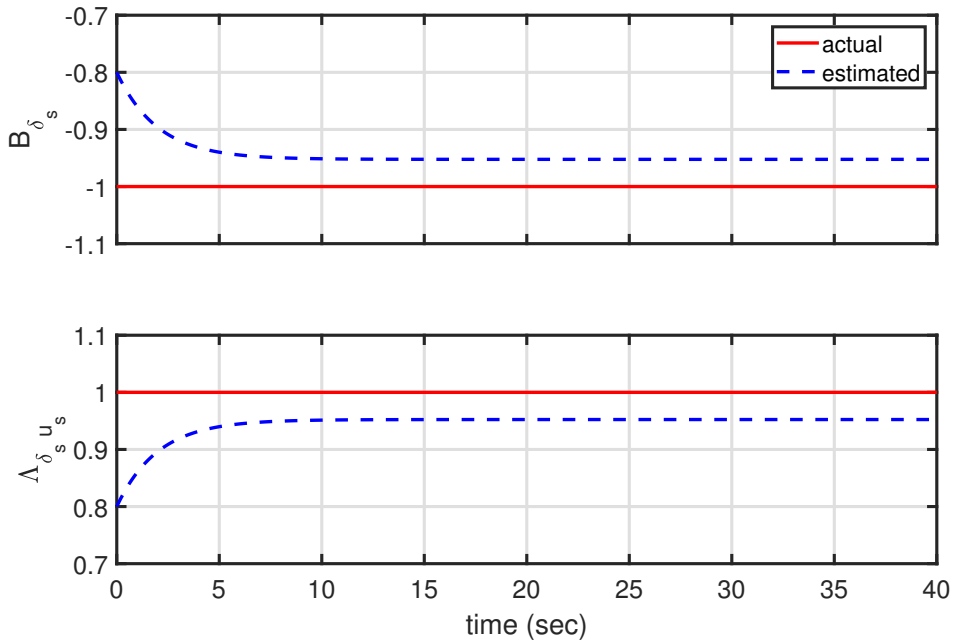

Figure 4.34: Uncertain parameters B_{δ_s} and $\Lambda_{\delta_s u_s}$ during the climb and roll maneuver

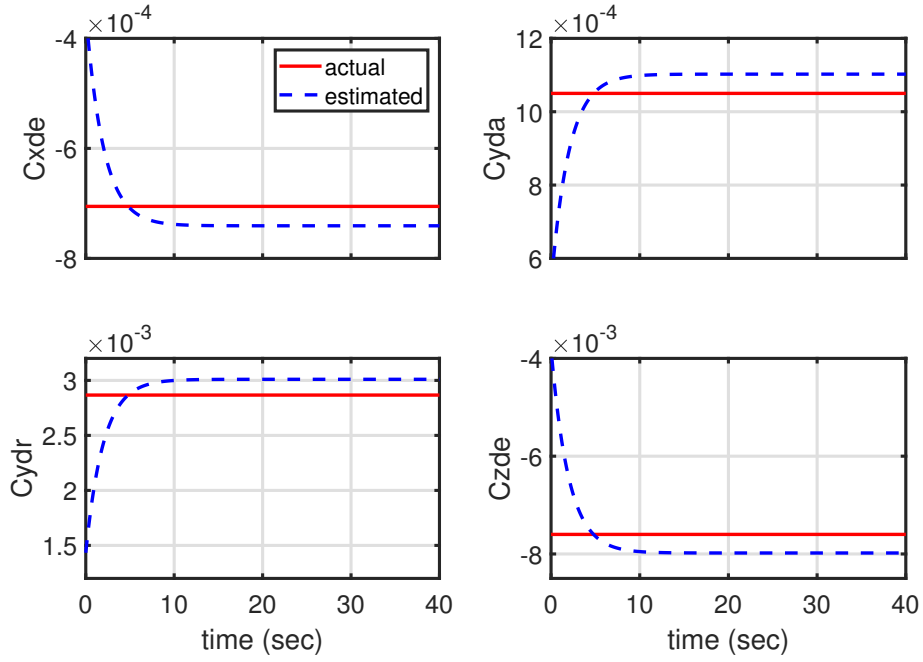

Figure 4.35: Uncertain parameters $C_{x_{\delta_e}}, C_{y_{\delta_a}}, C_{y_{\delta_r}}, C_{z_{\delta_e}}$ during the climb and roll maneuver

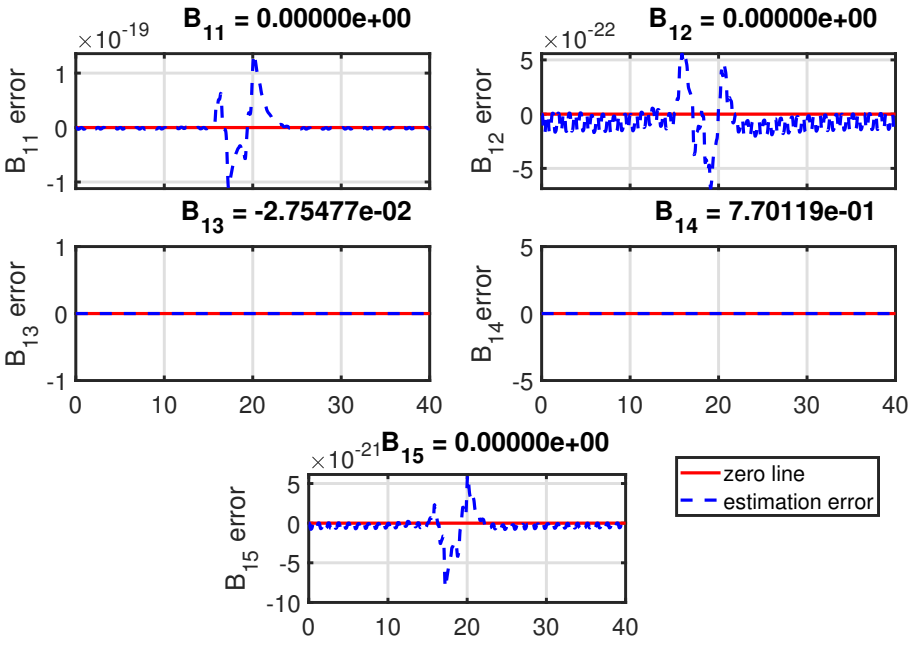

Figure 4.36: Uncertain parameters $B_{11} - B_{15}$ during the climb and roll maneuver; the x-axis for each graph representing time in seconds

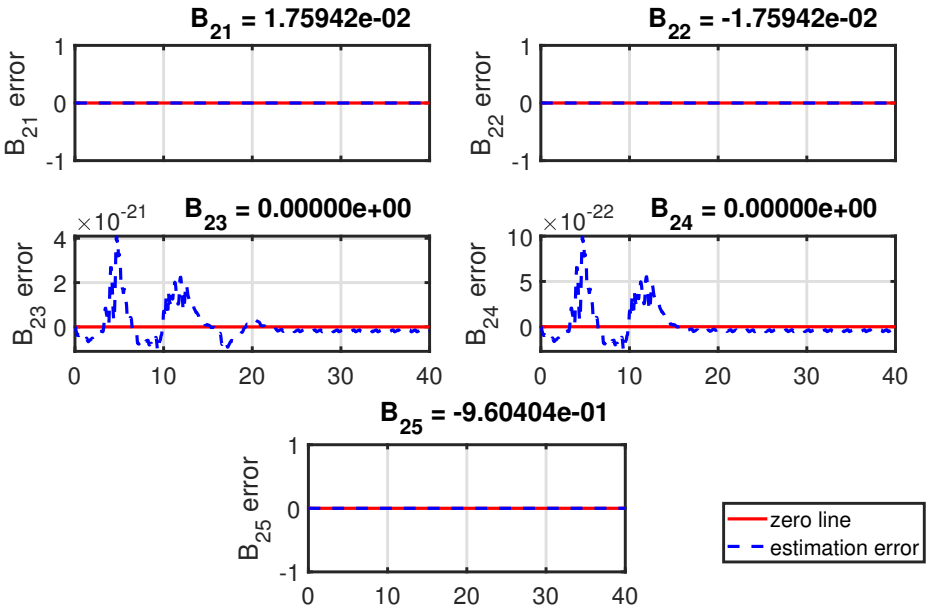

Figure 4.37: Uncertain parameters $B_{21} - B_{25}$ during the climb and roll maneuver; the x-axis for each graph representing time in seconds

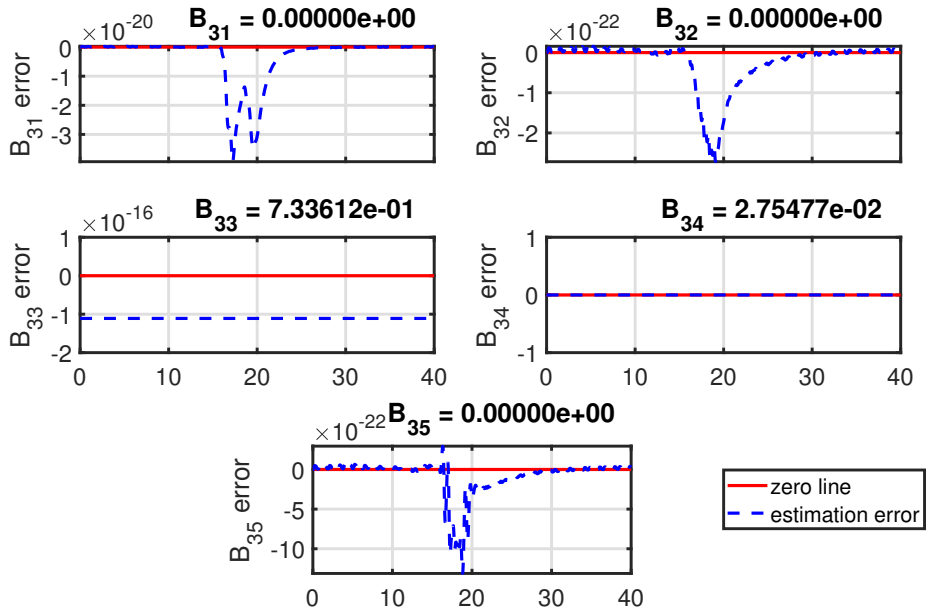

Figure 4.38: Uncertain parameters $B_{31} - B_{35}$ during the climb and roll maneuver; the x-axis for each graph representing time in seconds

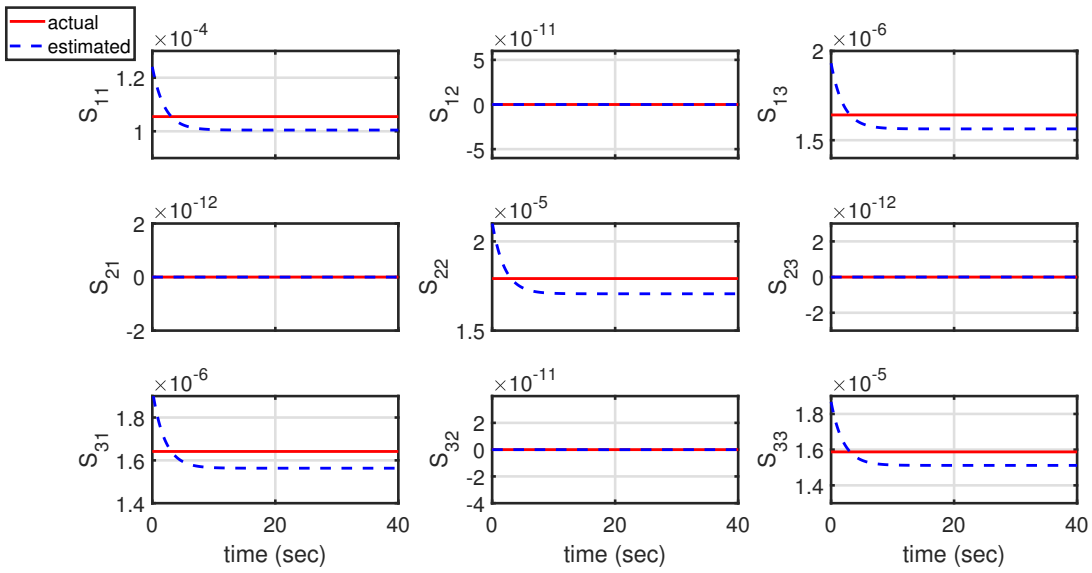

Figure 4.39: Uncertain parameters $S_{31} - S_{33}$ during the climb and roll maneuver

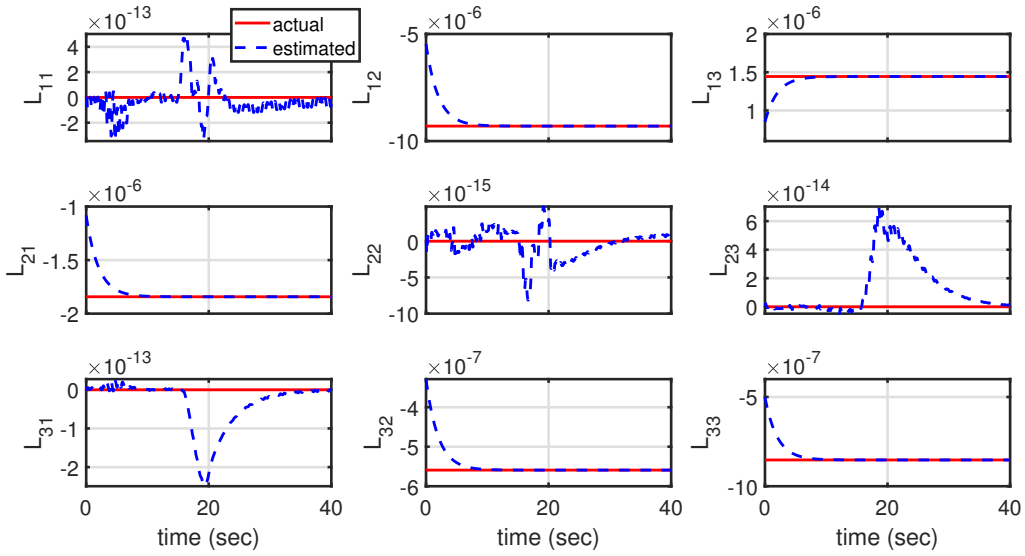

Figure 4.40: Uncertain parameters $L_{11} - L_{33}$ during the climb and roll maneuver

4.5 Concluding Remarks for the Chapter

This chapter investigated and developed a theory of output feedback control of a class of finite-dimensional, nonlinear, nonstandard multiple-time-scale systems with uncertainties in model structure and parameters. For a simpler system with two-time-scales, three cases of measurement was investigated: (a) only the slow state being measured, (b) only the fast state being measured, (c) a linear combination of the slow and the fast states being measured. For a more complex system with four time-scales and uncertainties, the slow states were classified as measured and unmeasured. The measurement vector was composed of all the states except the unmeasured slow states. A tracking controller used the estimates of the parameters and the unmeasured states. An online parameter estimator as well as a nonlinear state observer were designed based on the composite Lyapunov analysis to update the parameter and state estimates respectively. Based on the results presented in the chapter, the following conclusions can be drawn.

The transition from full-state feedback to output feedback did not need an entirely new design from the beginning. The earlier approach of time-scale controller and online parameter estimator

was modified and supplemented with a nonlinear state observer. Both of the parameter estimator and nonlinear state observer were designed using the composite Lyapunov analysis. The state observation laws followed a structure similar to the parameter update laws. This structure was essentially the sum of two components: one component to mimic or cancel terms in the dynamics, and a second component to allow each estimate to reach a desired final value following a first-order dynamics at a desired rate.

Using composite Lyapunov analysis it was proved that the tracking error of the slow states, the manifold error of the fast states and actuators, and the estimation error of the unknown parameters remain ultimately bounded. To ensure ultimate boundedness, this method established new bounds of the time-scale separation parameters: $\sigma_{***}, \sigma^{***}, \varepsilon_{***}, \varepsilon^{***}, \rho_{***}, \rho^{***}$. The explicit differentiations of the manifolds was cumbersome for this class of four-time-scale systems. The use of compact sets and extreme value theorem helped avoid the explicit differentiation and simplified the boundedness proof.

For the case of four time-scales, it was shown that the approach developed in Chapters 2 and 3 for full-state feedback could be extended to output feedback using state observers, with some important modifications made to the original class of systems. A number of functions used to represent the dynamics were considered to be functions of the known states and measurements. The dynamics were assumed such that no term contained products of uncertain parameters and unmeasured states. An improved version of the current theory is needed to handle a more general case of uncertainties. Moreover, the theory needs to be updated when uncertain parameters are present in the dynamics of the unmeasured states.

While this method considered actuator dynamics and thereby actuator rate limits, magnitude limits of actuators were not realistically accounted for in the control design. The control signals were kept within acceptable limits implicitly with gains. An improved version of the theory is needed to handle actuator magnitude limits realistically in the design.

Uncertainties were assumed in the deterministic sense instead of stochastic. While parametric uncertainties and modeling errors could be taken care of, handling certain types of disturbances

such as gust and turbulence in aircraft requires an improved version of the theory with stochastic uncertainties. A major challenge to overcome is to rigorously prove stability using stochastic Lyapunov functions.

This method relied on several parameter estimate matrices being invertible, especially the ones appearing in the control distribution. A way to ensure invertibility was to wisely choose the initial conditions and design parameters corresponding to final values of the estimates. An updated version of the theory is needed to realistically account for singularities in control distribution.

5. CONCLUSIONS

This dissertation investigated and developed novel theories of control design for three classes of finite-dimensional, nonlinear, nonstandard, multiple-time-scale systems. The first class of systems had two time-scales, and the fast state was the mathematical derivative of the slow state. The second class of systems had three time-scales, and the third class had four time-scales. The four time-scales included two for the slow and fast states of the system, and two more for the slow and fast actuators. In addition to the number of time-scales, complexity was progressively introduced in terms of the functions used in the dynamics, and uncertainties. Two different control objectives were accomplished for four-time-scale systems: (i) slow state tracking and (ii) simultaneous slow and fast state tracking. Based on the work, the following conclusions can be drawn.

1. The capability of the multiple-time-scale sequential control method based on geometric singular perturbation theory was extended to address actuator dynamics and uncertainties. The theory accounted for parametric uncertainties in the dynamics and the control distribution of all of the following: slow states, slow actuators, fast states, and fast actuators. Furthermore, additive uncertainties in the evolutions of the slow and the fast states were also accounted for.

2. The two control objectives of slow state tracking and simultaneous slow and fast state tracking were accomplished for the case when full-state feedback was not available. For a simpler two-time-scale system, a Lyapunov-based observer was designed using lower-order reduced subsystems. For a more complex system, a nonlinear observer was designed using the composite Lyapunov analysis. The observer dynamics were chosen similar to the parameter update laws. They had one component to mimic or cancel terms in the dynamics, and a second component to allow each estimate to reach a desired final value following a first-order dynamics at a desired rate.

3. Using composite Lyapunov analysis, the tracking errors, manifold errors, parameter estimation

errors and state observation errors were proved to be ultimately bounded. New bounds of the time-scale separation parameters $\sigma, \varepsilon, \rho$ were established to ensure the ultimate boundedness. The use of compact sets and the extreme value theorem alleviated the issue of differentiating the manifolds, and simplified the stability proofs.

4. The theory accounted for four time-scales with actuator dynamics and uncertainties, and therefore it was applicable for large-amplitude combined longitudinal and lateral/directional maneuvers of aircraft with some of the major sources of uncertainties: inertias, control derivatives, and speed of response of the engine. Nonlinear six-degree-of-freedom aircraft simulations demonstrated that the control laws were adequate to achieve tracking even when the initial estimates of the unknown parameters were off by 15% or more. In some simulations, the initial estimates of the control derivatives were off by 50%, and the control law still ensured good tracking. A simpler version of the slow state tracking control design accounted for three time-scales with actuator dynamics and uncertainties, and therefore it was applicable for large-amplitude attitude maneuvers of a spacecraft with uncertain inertias. Nonlinear simulations demonstrated that the control and estimation laws were adequate to achieve tracking even when the initial estimates of the inertias were off by 20%.

5. The output feedback control synthesis accounted for four time-scales with actuator dynamics and uncertainties, along with some of the slow states not being measured. This was applicable for large-amplitude aircraft maneuvers when the angle-of-attack and sideslip angle were not measured. Given the trim condition, the initial estimates of the unmeasured states were close to the actual values. This in addition to judicious choice of gains helped keep the estimated states very close to the actual states throughout the simulation.

6. RECOMMENDATIONS

The following are some potential directions of research in the future.

1. In this work uncertainties were assumed in a deterministic form. Some important uncertainties such as gust and turbulence for aircraft can be handled if the four-time-scale model assumes uncertainties in a stochastic form. A nonlinear version of the Kalman Filter such as the Unscented Kalman Filter (UKF) or the Ensemble Kalman Filter (EnKF) can be used to estimate the states to be used by the controller. Stochastic Lyapunov functions can be used to prove the stability of the full-order system.

2. Both of the parameter estimator and the state observer provided dynamic compensation. Although the bounds of time-scale separation were established by the stability proofs, for dynamic compensation in a time-scale any other than the slowest one, the corresponding time-scale separation parameter was to be known. Aircraft and spacecraft models used forced singular perturbation. The time-scale separation parameters were introduced artificially, and for simulation all three of $\sigma, \varepsilon, \rho$ were assumed to be unity. It is an open problem to perform dynamic compensation without needing to know these parameters in the first place. A possible approach is to start with the assumption that lower and upper bounds exist for $\sigma, \varepsilon, \rho$, and select dynamic compensator gains in terms of the bounds which are to be computer later in the development.

3. While this work accounted for actuator dynamics and thereby rate limits of actuators, magnitude limits of actuators were not accounted for realistically. At the best the gains were selected so as not to exceed the actuator magnitude limits, or in some simulations the controls were seen to be saturated. In the previous spacecraft simulations the controller was designed using the structured adaptive model inversion approach. It can be investigated how this approach may be extended in multiple time-scales.

4. This work did not realistically account for singularities in the control distribution. The parameter estimates in the control distribution were 'stopped' from becoming singular by using gains and other design variables judiciously. For each of these parameters, a better approach is to modify the update law such that the case of the estimate becoming zero is considered separately, or to insert in the update law a component which will automatically stop the estimate from becoming zero.

5. For output feedback, a more realistic controller should consider the presence of an uncertain parameter and an unmeasured state on the same term in the dynamics. Lower and upper bounds of the unknown parameter can be assumed, and it can be investigated if the nonlinear observer can use either or both of the bounds.

6. In addition to measured and unmeasured slow states, a more generic output feedback controller design should account for measured and unmeasured fast states. This can be handled by a slow observer updating the estimates of unmeasured slow states in the slowest time-scale, and the fast observer updating the estimates of the unmeasured fast states in the second-fastest time-scale.

REFERENCES

[1] F. -C. Chen and H. K. Khalil, "Two-Time-Scale Longitudinal Conrol of Airplanes Using Singular Perturbation", *Journal of Guidance*, vol. 13, no. 6, pp. 952 - 960, 1990.

[2] M. Shahravi and M. Azimi, "Attitude and Vibration Control of Flexible Spacecraft Using Singular Perturbation Approach", *ISRN Aerospace Engineering*, vol. 2014, no. 163870, 2014.

[3] A. Tavasoli, M. Eghtesad and H. Jafarian, "Two-Time Scale Control and Observer Design for Trajectory Tracking of Two Cooperating Robot Manipulators Moving a Flexible Beam", *Robotics and Autonomous Systems*, vol. 57, pp. 212 - 221, 2009.

[4] P. W. Sauer, "Time-Scale Features and Their Applications in Electric Power Systems Dynamic Modeling and Analysis", pp. 4155 - 4159, Proceedings of the American Control Conference, San Francisco, CA, June 29 - July 01, 2011.

[5] B. Mélykúti, J. P. Hespanha and M. Khammash, "Equilibrium Distributions of Simple Biochemical Reaction Systems for Time Scale Separation in Stochastic Reaction Networks", *Journal of the Royal Society Interface*, vol. 11, no. 97, 2014.

[6] S. R. Shimjith, A. P. Tiwari and B. Bandyopadhyay, "**Modeling and Control of a Large Nuclear Reactor: A Three-Time-Scale Approach**", Lecture Notes in Control and Information Sciences, vol. 431, Springer, Berlin, 2013.

[7] H. Mete Soner, "Singular Perturbations in Manufacturing", *SIAM Journal on Control and Optimization*, vol. 31, no. 1, pp. 132 - 146, 1993.

[8] N. Fenichel, "Geometric Singular Perturbation Theory for Ordinary Differential Equations", *Journal of Differential Equations*, vol. 31, pp. 53 - 98, 1979.

[9] P. Kokotovic, H. K. Khalil and J. O'Reilly, "**Singular Perturbation Methods in Control: Analysis and Design**", Society of Industrial and Applied Mathematics, 1986.

[10] H. K. Khalil, "**Nonlinear Systems**", 3rd ed., Prentice Hall, 2002.

[11] A. Narang-Siddarth and J. Valasek, "**Nonlinear Time Scale Systems in Standard and Nonstandard Forms: Analysis and Control**", Society of Industrial and Applied Mathematics, 2014.

[12] P. V. Kokotovic, R. E. O'Malley and P. V. Sannuti, "Singular Perturbation Methods and Order Reduction in Control Theory - An Overview", *Automatica*, vol. 12, pp. 123 - 132, 1976.

[13] D. S. Naidu, A. J. Calise, "Singular Perturbations and Time Scales in Guidance and Control of Aerospace Systems: A Survey", *Journal of Guidance, Control and Dynamics*, vol. 24, no. 6, November – December 2001.

[14] D. S. Naidu, "Singular Perturbations and Time-Scales in Control Theory and Applications", *Dynamics of Continuous, Discrete and Impulsive Systems Series B: Applications & Algorithms*, vol. 9, pp. 233 - 278, 2002.

[15] R. E. O'Malley, Jr., "**Singular Perturbation Methods for Ordinary Differential Equations**", Springer-Verlag, New York, 1991.

[16] R. E. O'Malley, Jr., "**Historical Developments in Singular Perturbations**", Springer International Publishing, 2014.

[17] A. N. Tikhonov, "Systems of Differential Equations Containing Small Parameters Multiplying Some of the Derivatives", *Mathematic Sbovenic*, vol. 31, no. 73, pp. 575 – 586, 1952.

[18] A. B. Vasileva, "Asymptotic Behavior of Solutions to Certain Problems Involving Nonlinear Ordinary Differential Equations Containing a Small Parameter Multiplying the Highest Derivatives", *Russian Mathematical Surveys*, vol. 18, pp. 13 – 84, 1963.

[19] Y. Liu and B. D. O. Anderson, "Singular Perturbation Approximation of Balanced Systems", *International Journal of Control*, vol. 50, no. 4, pp. 1379 - 1405, 1989.

[20] L. T. Grujic, "Singular Perturbations and Large-Scale Systems", *International Journal of Control*, vol. 29, no. 1, pp. 159 - 169, 1979.

[21] P. V. Kokotovic and P. Sannuti, “Singular Perturbation Method for Reducing Model Order in Optimal Control Design”, *IEEE Transactions on Automatic Control*, vol. 13, pp. 377 – 384, 1968.

[22] P. Sannuti and P. V. Kokotovic, “Near Optimum Design of Linear Systems by Singular Perturbation Method”, *IEEE Transactions on Automatic Control*, vol. 14, pp. 15 – 22, 1969.

[23] P. Sannuti, “Singular Perturbation Method in the Theory of Optimal Control”, Ph.D. Dissertation, University of Illinois, Urbana-Champaign, IL, 1968.

[24] A. Vigodner, “Limits of Singularly Perturbed Control Problems with Statistical Dynamics of Fast Motions”, *SIAM Journal on Control and Optimization*, vol. 35, no. 1, pp. 1 - 28, 1997.

[25] F. Bagagiolo and M. Bardi, “Singular Perturbation of a Finite Horizon Problem with State-Space Constraints”, *SIAM Journal on Control and Optimization*, vol. 36, no. 6, pp. 2040 - 2060, 1998.

[26] N. Forcadel and Z. Rao, “Singular Perturbation of Optimal Control Problems on Multidomains”, *SIAM Journal on Control and Optimization*, vol. 52, no. 5, pp. 2917 - 2943, 2014.

[27] D. S. Naidu and D. B. Price, “Singular Perturbation and Time Scale Approaches in Discrete Control Systems”, *Journal of Guidance*, vol. 11, no. 6, pp. 592 - 594, 1994.

[28] P. K. Rajagopalan and D. S. Naidu, “A Singular Perturbation Method for Discrete Control Systems”, *International Journal of Control*, vol. 32, no. 5, pp. 925 - 935, 1980.

[29] D. Zheng, W.-F. Xie, X. Ren and J. Na, “Identification and Control for Singularly Perturbed Systems Using Multi-Time-Scale Neural Networks”, *IEEE Transactions on Neural Networks and Learning Systems*, vol. 28, no. 2, pp. 321 - 333, February 2017.

[30] P. A. Lagerstrom and R. G. Casten, “Basic Concepts Underlying Singular Perturbation Techniques”, *SIAM Review*, vol. 14, no. 1, pp. 63 - 120, January 1972.

[31] O. R. B. de Oliviera, "The Implicit and Inverse Function Theorems: Easy Proofs", *Real Analysis Exchange*, vol. 39, no. 1, pp. 207 - 218, 2013.

[32] A. Narang-Siddarth and J. Valasek, "Kinetic State Tracking for a Class of Singularly Perturbed Systems", *Journal of Guidance, Control and Dynamics*, vol. 34, no. 3, pp. 734 - 749, 2011.

[33] A. Narang-Siddarth and J. Valasek, "Global Tracking Control Structures for Nonlinear Singularly Perturbed Aircraft Systems", AIAA-2010-8159, Proceedings of the 1st CEAS Specialist Conference on Guidance, Navigation and Control (Euro GNC 2011), Munich, Germany, 13 April 2011.

[34] A. Narang-Siddarth, "Analysis and Control of Non-Affine, Non-standard, Singularly Perturbed Systems", Ph.D. Dissertation, Texas A&M University, College Station, TX, December 2012.

[35] D. Saha, J. Valasek, D. Famularo and M. M. Reza, "Combined Longitudinal and Lateral/Directional Maneuvers of a Generic F-16A Using Multiple-Time-Scale Control", AIAA-2018-1335, Proceedings of the 2018 AIAA Guidance, Navigation, and Control Conference: AIAA Science and Technology Forum, Kissimmee, FL, 8 - 12 January 2018.

[36] J. Valasek, "A Study of a Modified Torsional Agility Metric Using Simulation Methods", M.S. Thesis, University of Kansas, Lawrence, KS, 1990.

[37] D. Saha and J. Valasek, "Two-Time-Scale Slow and Fast State Tracking of a Generic F-16A Using Slow and Fast Controls", AIAA-2017-1256, Proceedings of the 2017 AIAA Guidance, Navigation, and Control Conference: AIAA Science and Technology Forum, Grapevine, TX, 7 - 13 January 2017.

[38] P. Krishnamurthy and F. Khorrami, "A Singular Perturbation Based Global Dynamic High Gain Scaling Control Design for Systems With Nonlinear Input Uncertainties", *IEEE Transactions on Automatic Control*, vol. 58, no. 10, pp. 2686 - 2692, 2013.

[39] A. Chakrabortty and M. Arcak, “Time-Scale Separation Redesign for Stabilization and Performance Recovery for Uncertain Nonlinear Systems”, *Automatica*, vol. 45, pp. 34 - 44, 2009.

[40] M. Asadi and A. Khayatiyan, “Singular Perturbation Theory in Control of Nonlinear Systems with Uncertainties”, 24th Iranian Conference on Electrical Engineering (ICEE), Shiraz, Iran, 10 - 12 May 2016.

[41] J. E. Hurtado, “**Elements of Spacecraft Control**”, Lulu Press Inc., 2009.

[42] M. R. Akella, “Structured Adaptive Control: Theory and Applications to Trajectory Tracking in Aerospace Systems”, Ph.D. Dissertation, Texas A&M University, College Station, TX, 1998.

[43] K. Subbarao, “Structured Adaptive Model Inversion: Theory and Applications to Trajectory Tracking for Nonlinear Dynamical Systems”, Ph.D. Dissertation, Texas A&M University, College Station, TX, 2001.

[44] A. Ashayeri, M. Eghtesad, M. Farid and F. Shabani, “Two-Time Scale Fuzzy Logic Controller and Observer Design for Trajectory Tracking of Two Cooperating Robot Manipulators Handling a Flexible Beam”, Eurocon 2007, The International Conference on "Computer as a Tool", Warsaw, September 9 - 12, 2007.

[45] S.-T. Pan and C.-F. Chen, “Genetic Algorithm and Time-Scale Separation on the Reduced-Order Observer-Based Control Design for a Class of Discrete Systems”, *Opportunities and Challenges for Next-Generation Applied Intelligence*, vol. 214 of the series ‘Studies in Computational Intelligence’, pp. 127 - 132, 2009.

[46] S.-J. Pan, J.-H. Tsai, S.-T. Pan, “Application of Genetic Algorithm on Observer-Based D-Stability Control for Discrete Multiple Time-Delay Singularly Perturbation Systems”, *International Journal of Innovative Computing, Information and Control*, vol. 7, no. 6, pp. 3345 - 3358, 2011.

[47] P. R. Moghaddam and H. Zarabadipour, “Optimal Two Time-Scale Controller for a Missile Autopilot”, *International Journal of Research in Mechanical Engineering and Technology*, vol. 2, no. 1, pp. 45 - 48, April 2012.

[48] J. -S. Chiou, “Design of Controllers and Observer-Based Controllers for Time-Delay Singularly Perturbed Systems via Composite Control”, *Journal of Applied Mathematics*, vol. 2013, no. 813598, 2013.

[49] Y. Wang and W. Liu, “Observer-Based Feedback Control for Lipschitz Singularly Pertured Systems”, *Mathematical Problems in Engineering*, vol. 2015, no. 585301, 2015.

[50] H. Hofmann and S. R. Sanders, “Speed-Sensorless Vector Torque Control of Induction Machines Using a Two Time-Scale Approach”, *IEEE Transactions on Industry Applications*, vol. 34, no. 1, pp. 169 - 177, January - February 1998.

[51] D. Saha and J. Valasek, “Observer-Based Sequential Control of a Nonlinear Two-Time-Scale Spring-Mass-Damper System”, AIAA-2016-0361, Proceedings of the 2016 AIAA Guidance, Navigation, and Control Conference: AIAA Science and Technology Forum, San Diego, CA, 4 - 8 January 2016.

[52] D. Saha and J. Valasek, “Observer-Based Sequential Control of a Nonlinear Two-Time-Scale Spring-Mass-Damper System with Multiple Slow and Fast States”, 10th IFAC Symposium on Nonlinear Control Systems, IFAC-PapersOnLine, vol. 49, pp. 684 - 689, 2016.

[53] K. Vijayaraghavan, “Nonlinear Observer for Simultaneous States and Unknown Parameter Estimation”, *International Journal of Control*, vol. 86, no. 12, pp. 2263 - 2273, 2013.

[54] M. Krstic and P. V. Kokotovic, “Adaptive Nonlinear Output Feedback Schemes with Marino-Tomei Controller”, *IEEE Transactions on Automatic Control*, vol. 41, no. 2, pp. 274 - 280, February 1996.

[55] H. K. Khalil, “Adaptive Output Feedback Control of Nonlinear Systems Represented by Input-Output Models”, *IEEE Transactions on Automatic Control*, vol. 41, no. 2, pp. 177 - 188, February 1996.

[56] D. Saha, J. Valasek and M. M. Reza, "Two-Time-Scale Control of a Low-Order Nonlinear, Nonstandard System with Uncertain Dynamics", pp. 3720 - 3725, Proceedings of the American Control Conference, Milwaukee, WI, 27-29 June 2018.

[57] J. E. Slotine and W. Li, "**Applied Nonlinear Control**", Prentice Hall, 1991.

[58] M. D. Tandale and J. Valasek, "Structured Adaptive Model Inversion Control with Actuator Saturation Constraints Applied to Tracking Spacecraft Maneuvers", Proceeding of the American Control Conference, Boston, MA, 30 June - 02 July, 2004.

[59] M. D. Tandale and J. Valasek, "Adaptive Dynamic Inversion Control with Actuator Saturation Constraints Applied to Tracking Spacecraft Maneuvers", *The Journal of the Astronautical Sciences*, vol. 52, no. 4, 2004, presented at the 6th International Conference on Dynamics and Control of Systems and Structures in Space, Riomaggiore, Italy, 18-22 July 2004.

[60] D. Saha and J. Valasek, "Nonlinear Multiple-Time-Scale Attitude Control of a Rigid Spacecraft with Uncertain Inertias", to present at the 2019 AIAA Guidance, Navigation, and Control Conference: AIAA Science and Technology Forum, San Diego, CA, 7 - 11 January 2019.

[61] B. S. Park, S. J. Yoo, J. B. Park and Y. H. Choi, "Adaptive Tracking Control of Nonholonomic Mobile Robots Considering Actuator Dynamics: Dynamic Surface Design Approach", Proceedings of the American Control Conference, St. Louis, MO, June 10-12, 2009.

[62] W. Dong and K. D. Kuhnert, "Robust Adaptive Control of Nonholonomic Mobile Robot with Parameter and Nonparameter Uncertainties",*IEEE Transactions on Robotics*, vol. 21, no. 2, pp. 261 - 266, April 2005.

[63] D. Swaroop, J. C. Gerdes, P. P. Yip and J. K. Hedrick,"Dynamic Surface Control of Nonlinear Systems", Proceedings of the American Control Conference, Albuquerque, NM, June 1997.

[64] D. Swaroop, J. K. Hedrick, P. P. Yip and J. C. Gerdes, "Dynamic Surface Control for a Class of Nonlinear Systems", *IEEE Transactions on Automatic Control*, vol. 45, no. 10, pp. 1893 - 1899, October 2000.

[65] P. P. Yip and J. K. Hedrick, “Adaptive Dynamic Surface Control: A Simplified Algorithm for Adaptive Backstepping Control for Nonlinear Systems”, *International Journal of Control*, vol. 71, no. 5, pp. 959 - 979, 1998.

[66] Z. Cao, L. Yin, Y. Fu and Z. S. Dai,“Adaptive Dynamic Surface Control for Vision-Based Stabilization of an Uncertain Electrically Driven Nonholonomic Mobile Robot”,*Robotica*, vol. 34, pp. 449 - 467, 2016.

[67] S. R. Vadali, “Solution of the Two-Point Boundary Value Problems of Optimal Spacecraft Rotational Maneuvers”, Ph.D. Dissertation, Virginia Polytechnic Institute and State University, Blacksburg, VA, December 1982.

[68] H. Schaub and J. L. Junkins, “**Analytical Mechanics of Space Systems**”, AIAA Education Series, 2nd ed., 2009.

[69] R. Kristiansen and D. Hagen, “Modelling of Actuator Dynamics for Spacecraft Attitude Control”, *Journal of Guidance, Control, and Dynamics*, vol. 32, no. 3, pp. 1022 - 1025, May-June 2009.

[70] B. L. Stevens and F. L., Lewis, “**Aircraft Control and Simulation**”, John Wiley & Sons Inc., 2nd ed., 2003.

APPENDIX A

PARAMETER MATRIX B FOR THREE-TIME-SCALE SLOW STATE TRACKING

The matrix product $-\mathcal{S}\omega^{\times}\mathcal{I}\omega$ can be evaluated as

$$-\mathcal{S}\omega^{\times}\mathcal{I}\omega = -\begin{bmatrix}\mathcal{S}_{11} & \mathcal{S}_{12} & \mathcal{S}_{13}\\ \mathcal{S}_{21} & \mathcal{S}_{22} & \mathcal{S}_{23}\\ \mathcal{S}_{31} & \mathcal{S}_{32} & \mathcal{S}_{33}\end{bmatrix}\begin{bmatrix}0 & -\omega_3 & \omega_2\\ \omega_3 & 0 & -\omega_1\\ -\omega_2 & \omega_1 & 0\end{bmatrix}\begin{bmatrix}\mathcal{I}_{11} & \mathcal{I}_{12} & \mathcal{I}_{13}\\ \mathcal{I}_{12} & \mathcal{I}_{22} & \mathcal{I}_{23}\\ \mathcal{I}_{13} & \mathcal{I}_{23} & \mathcal{I}_{33}\end{bmatrix}\begin{bmatrix}\omega_1\\ \omega_2\\ \omega_3\end{bmatrix}. \tag{A.1}$$

Using the fact that the matrix $\mathcal{S}$ being inverse of the symmetric inertia matrix $\mathcal{I}$ is also symmetric, the final matrix product becomes

$$-\mathcal{S}\omega^{\times}\mathcal{I}\omega = \begin{bmatrix}B_{11} & B_{12} & B_{13} & B_{14} & B_{15} & B_{16}\\ B_{21} & B_{22} & B_{23} & B_{24} & B_{25} & B_{26}\\ B_{31} & B_{32} & B_{33} & B_{34} & B_{35} & B_{36}\end{bmatrix}\begin{bmatrix}\omega_1^2\\ \omega_2^2\\ \omega_3^2\\ \omega_1\omega_2\\ \omega_2\omega_3\\ \omega_3\omega_1\end{bmatrix} \tag{A.2}$$

with the elements B_{ij} given by

$$\begin{aligned} B_{11} &= -(\mathcal{S}_{13}\mathcal{I}_{12} - \mathcal{S}_{12}\mathcal{I}_{13})\\ B_{21} &= -(\mathcal{S}_{23}\mathcal{I}_{12} - \mathcal{S}_{22}\mathcal{I}_{13})\\ B_{31} &= -(\mathcal{S}_{33}\mathcal{I}_{12} - \mathcal{S}_{32}\mathcal{I}_{13}) \end{aligned} \tag{A.3}$$

$$
\begin{aligned}
B_{12} &= -(\mathcal{S}_{11}\mathcal{I}_{23} - \mathcal{S}_{13}\mathcal{I}_{12}) \\
B_{22} &= -(\mathcal{S}_{12}\mathcal{I}_{23} - \mathcal{S}_{23}\mathcal{I}_{12}) \\
B_{32} &= -(\mathcal{S}_{13}\mathcal{I}_{23} - \mathcal{S}_{33}\mathcal{I}_{12})
\end{aligned} \tag{A.4}
$$

$$
\begin{aligned}
B_{13} &= -(\mathcal{S}_{12}\mathcal{I}_{13} - \mathcal{S}_{11}\mathcal{I}_{23}) \\
B_{23} &= -(\mathcal{S}_{22}\mathcal{I}_{13} - \mathcal{S}_{12}\mathcal{I}_{23}) \\
B_{33} &= -(\mathcal{S}_{23}\mathcal{I}_{13} - \mathcal{S}_{13}\mathcal{I}_{23})
\end{aligned} \tag{A.5}
$$

$$
\begin{aligned}
B_{14} &= -(\mathcal{S}_{13}\mathcal{I}_{22} - \mathcal{S}_{13}\mathcal{I}_{11} + \mathcal{S}_{11}\mathcal{I}_{13} - \mathcal{S}_{12}\mathcal{I}_{23}) \\
B_{24} &= -(\mathcal{S}_{23}\mathcal{I}_{22} - \mathcal{S}_{23}\mathcal{I}_{11} + \mathcal{S}_{12}\mathcal{I}_{13} - \mathcal{S}_{22}\mathcal{I}_{23}) \\
B_{34} &= -(\mathcal{S}_{33}\mathcal{I}_{22} - \mathcal{S}_{33}\mathcal{I}_{11} + \mathcal{S}_{13}\mathcal{I}_{13} - \mathcal{S}_{23}\mathcal{I}_{23})
\end{aligned} \tag{A.6}
$$

$$
\begin{aligned}
B_{15} &= -(\mathcal{S}_{12}\mathcal{I}_{12} - \mathcal{S}_{13}\mathcal{I}_{13} - \mathcal{S}_{11}\mathcal{I}_{22} + \mathcal{S}_{11}\mathcal{I}_{33}) \\
B_{25} &= -(\mathcal{S}_{22}\mathcal{I}_{12} - \mathcal{S}_{23}\mathcal{I}_{13} - \mathcal{S}_{12}\mathcal{I}_{22} + \mathcal{S}_{12}\mathcal{I}_{33}) \\
B_{35} &= -(\mathcal{S}_{23}\mathcal{I}_{12} - \mathcal{S}_{33}\mathcal{I}_{13} - \mathcal{S}_{13}\mathcal{I}_{22} + \mathcal{S}_{13}\mathcal{I}_{33})
\end{aligned} \tag{A.7}
$$

$$
\begin{aligned}
B_{16} &= -(\mathcal{S}_{12}\mathcal{I}_{11} - \mathcal{S}_{11}\mathcal{I}_{12} + \mathcal{S}_{13}\mathcal{I}_{23} - \mathcal{S}_{12}\mathcal{I}_{33}) \\
B_{26} &= -(\mathcal{S}_{22}\mathcal{I}_{11} - \mathcal{S}_{12}\mathcal{I}_{12} + \mathcal{S}_{23}\mathcal{I}_{23} - \mathcal{S}_{22}\mathcal{I}_{33}) \\
B_{36} &= -(\mathcal{S}_{13}\mathcal{I}_{11} - \mathcal{S}_{13}\mathcal{I}_{12} + \mathcal{S}_{33}\mathcal{I}_{23} - \mathcal{S}_{23}\mathcal{I}_{33}).
\end{aligned} \tag{A.8}
$$

APPENDIX B

MATRICES USED IN AIRCRAFT FLIGHT CONTROL DESIGN

B.1 Aircraft Equations of Motion

The six kinetic and six kinematic equations of a nonlinear 6-DOF aircraft are

$$
\begin{aligned}
\dot{v}_A &= \frac{1}{m}[\cos\alpha\cos\beta(-mg\sin\theta + T_m\delta_t + F_{A_X}) + sin\beta(mg\cos\theta sin\phi + F_{A_y}) \\
&\quad + \sin\alpha\cos\beta(mg\cos\theta\cos\phi + F_{A_z})] \\
\dot{\alpha} &= q - p\cos\alpha\tan\beta - r\sin\alpha\tan\beta - \frac{\sin\alpha}{mv_A\cos\beta}(-mg\sin\theta + T_m\delta_t + F_{A_x}) \\
&\quad + \frac{\cos\alpha}{mv_A\cos\beta}(mg\cos\theta\cos\phi + F_{A_z}) \\
\dot{\beta} &= p\sin\alpha - r\cos\alpha - \frac{\sin\beta\cos\alpha}{mv_A}(-mg\sin\theta + T_m\delta_t + F_{A_x}) + \frac{\cos\beta}{mv_A}(mg\cos\theta\sin\phi + F_{A_y}) \\
&\quad - \frac{\sin\beta\sin\alpha}{mv_A}(mg\cos\theta\cos\phi + F_{A_z}) \\
I_{xx}\dot{p} &= (I_{yy} - I_{zz})qr + I_{xz}(\dot{r} + pq) + L_A \\
I_{yy}\dot{q} &= (I_{zz} - I_{xx})rp + I_{xz}(r^2 - p^2) + M_A \\
I_{zz}\dot{r} &= (I_{xx} - I_{yy})pq + I_{xz}(\dot{p} - qr) + N_A \\
\dot{\phi} &= p + \tan\theta(q\sin\phi + r\cos\phi) \\
\dot{\theta} &= q\cos\phi - r\sin\phi \\
\dot{\psi} &= (q\sin\phi + r\cos\phi)\sec\theta \\
\dot{x}_N &= v_A[\cos\alpha\cos\beta\cos\theta\cos\psi + \sin\beta(\sin\phi\cos\psi\sin\theta - \cos\phi\sin\psi) + \\
&\quad \sin\alpha\cos\beta(\cos\phi\sin\theta\cos\psi + \sin\phi\sin\psi)] \\
\dot{y}_N &= v_A[\cos\alpha\cos\beta\cos\theta\sin\psi + \sin\beta(\sin\phi\sin\psi\sin\theta + \cos\phi\cos\psi) + \\
&\quad \sin\alpha\cos\beta(\cos\phi\sin\theta\sin\psi - \sin\phi\cos\psi)] \\
\dot{h} &= v_A(\cos\alpha\cos\beta\sin\theta - \sin\beta\sin\phi\cos\theta - \sin\alpha\cos\beta\cos\phi\cos\theta).
\end{aligned}
\tag{B.1}
$$

The body-axis aerodynamic forces and moments are modeled using component build-up as

$$
\begin{aligned}
F_{A_x} &= [C_x(\alpha,\delta_e) + C_{x_q}\frac{q\bar{c}}{2v_A}]\bar{q}S \\
F_{A_y} &= [C_{y_\beta}\beta + C_{y_p}\frac{pb}{2v_A} + C_{y_r}\frac{rb}{2v_A} + C_{y_{\delta_a}}\delta_a + C_{y_{\delta_r}}\delta_r]\bar{q}S \\
F_{A_z} &= [C_z(\alpha,\beta) + C_{z_q}\frac{q\bar{c}}{2v_A} + C_{z_{\delta_e}}\delta_e]\bar{q}S \\
L_A &= [C_l(\alpha,\beta) + C_{l_p}\frac{pb}{2v_A} + C_{l_r}\frac{rb}{2v_A} + C_{l_{\delta_a}}\delta_a + C_{l_{\delta_r}}\delta_r]\bar{q}Sb \\
M_A &= [C_m(\alpha,\delta_e) + C_{m_q}\frac{q\bar{c}}{2v_A} + \frac{x_{cg_r}-x_{cg}}{\bar{c}}(C_z(\alpha,\beta) + C_{z_q}\frac{q\bar{c}}{2v_A} + C_{z_{\delta_e}}\delta_e)]\bar{q}S\bar{c} \\
N_A &= [C_n(\alpha,\beta) + C_{n_p}\frac{pb}{2v_A} + C_{n_r}\frac{rb}{2v_A} + C_{n_{\delta_a}}\delta_a + C_{n_{\delta_r}}\delta_r + \frac{x_{cg_r}-x_{cg}}{b}(C_{y_\beta}\beta + C_{y_p}\frac{pb}{2v_A} \\
&\qquad + C_{y_r}\frac{rb}{2v_A} + C_{y_{\delta_a}}\delta_a + C_{y_{\delta_r}}\delta_r)]\bar{q}Sb.
\end{aligned}
\tag{B.2}
$$

The nonlinear 6-DOF generic F-16A model and the definitions of all stability and control derivatives and parameters are contained in Stevens and Lewis [70]. Table B.1 gives the model parameters and constants.

The aerodynamic database contains the coefficients $C_x(.), C_z(.), C_l(.), C_m(.), C_n(.)$ as look-up tables for $-10\,\text{deg} \le \alpha \le 45\,\text{deg}, -30\,\text{deg} \le \beta \le 30\,\text{deg}, -25\,\text{deg} \le \delta_e \le 25\,\text{deg}$. For values of α, β, δ_e not included or outside the range, the nonlinear 6-DOF simulation has routines for interpolation and extrapolation.

B.2 Conversion to the Four-Time-Scale Form in Chapters 2 and 3

For full-state feedback control design in Chapters 2 and 3, the dependence on elevator deflection of the coefficients $C_x(.)$ and $C_m(.)$ need to be separated. Using linear least squares, these coefficients are approximated as

$$
\begin{aligned}
C_x(\alpha,\delta_e) &\approx C_{x_0} + C_{x_\alpha}\alpha + C_{x_{\delta_e}}\delta_e \\
C_m(\alpha,\delta_e) &\approx C_{m_0} + C_{m_\alpha}\alpha + C_{m_{\delta_e}}\delta_e
\end{aligned}
\tag{B.3}
$$

m	636.94 slug
g	32.17 ft/s^2
b	30 ft
S	300 ft^2
$\bar{c}$	11.32 ft
x_{cg_r}	$0.35\bar{c}$
x_{cg}	$0.30\bar{c}$
I_{xx}	$9,496$ slug-ft^2
I_{yy}	$55,814$ slug-ft^2
I_{zz}	$63,100$ slug-ft^2
I_{xz}	982 slug-ft^2
T_m	$17,800$ lbf
$\delta_{e_{max}}$	25 deg
$\delta_{a_{max}}$	20 deg
$\delta_{r_{max}}$	30 deg
C_{y_β}	-0.02 / deg
$C_{y_{\delta_a}}$	1.05×10^{-3} /deg
$C_{y_{\delta_r}}$	2.87×10^{-3} / deg
$C_{z_{\delta_e}}$	7.6×10^{-3} / deg

Table B.1: Parameters for the Generic F-16A

The kinetic slow state is $x = v_A$, the kinematic slow state vector is $\xi = \begin{bmatrix} \phi & \theta & \psi \end{bmatrix}^T$, the vector of fast states is $z = \begin{bmatrix} p & q & r \end{bmatrix}^T$, the slow actuator is $\delta_s = \delta_t$, the vector of fast actuators is $\delta_f = \begin{bmatrix} \delta_e & \delta_a & \delta_r \end{bmatrix}^T$. The velocity dynamics can be written as

$$\dot{x} = f_{xx}(x, \xi, \alpha, \beta) + f_{xz}^T(x, \alpha, \beta) z + g_{x_{\delta_s}}(\alpha, \beta)\delta_s + g_{x_{\delta_f}}^T(x, \alpha, \beta)\Lambda_{x_{\delta_f}}\delta_f \tag{B.4}$$

where

$$
\begin{aligned}
f_{xx}(.) &\triangleq g(-\cos\alpha\cos\beta\sin\theta + \sin\beta\cos\theta\sin\phi + \sin\alpha\cos\beta\cos\theta\cos\phi \\
&\quad + \frac{\bar{q}s}{m}[(C_{x_0} + C_{x_\alpha}\alpha)\cos\alpha\cos\beta + + C_{y_\beta}\beta\sin\beta + \bar{C}_z(\alpha,\beta)\sin\alpha\cos\beta] \\
f_{xz}(.) &\triangleq \begin{bmatrix} \frac{1}{m}C_{y_p}\frac{b}{2v_A}\bar{q}S\sin\beta \\ \frac{1}{m}C_{x_q}\frac{\bar{c}}{2v_A}\bar{q}S\cos\alpha\sin\beta + \frac{1}{m}C_{z_q}\frac{\bar{c}}{2v_A}\sin\alpha\cos\beta \\ \frac{1}{m}C_{y_r}\frac{b}{2v_A}\bar{q}S\sin\beta \end{bmatrix} \\
g_{x\delta_s}(.) &\triangleq \frac{T_m}{m}\cos\alpha\cos\beta \\
g_{x\delta_f} &\triangleq \frac{\bar{q}s}{m}\begin{bmatrix} \cos\alpha\cos\beta \\ \sin\beta \\ \sin\alpha\cos\beta \end{bmatrix} \\
\Lambda_{x\delta_f} &\triangleq \begin{bmatrix} C_{x_{\delta_e}} & 0 & 0 \\ 0 & C_{y_{\delta_a}} & C_{y_{\delta_r}} \\ C_{z_{\delta_e}} & 0 & 0 \end{bmatrix}.
\end{aligned}
\tag{B.5}
$$

The Euler angles evolve according to

$$
\begin{bmatrix} \dot{\phi} \\ \dot{\theta} \\ \dot{\psi} \end{bmatrix} = \begin{bmatrix} 1 & \sin\phi\tan\theta & \cos\phi\tan\theta \\ 0 & \cos\phi & -\sin\phi \\ 0 & \frac{\sin\phi}{\cos\theta} & \frac{\cos\phi}{\cos\theta} \end{bmatrix} \begin{bmatrix} p \\ q \\ r \end{bmatrix}. \tag{B.6}
$$

Equation (B.6) is in the form $\dot{\xi} = F_{\xi z}(\xi)z$.

The body-axis angular rates evolve according to

$$
\begin{aligned}
I_{xx}\dot{p} &= (I_{yy} - I_{zz})qr + I_{xz}(\dot{r} + pq) + L_A \\
I_{yy}\dot{q} &= (I_{zz} - I_{xx})rp + I_{xz}(r^2 + p^2) + M_A \\
I_{zz}\dot{r} &= (I_{xx} - I_{yy})pq + I_{xz}(\dot{p} - qr) + N_A
\end{aligned}
\tag{B.7}
$$

In vector-matrix form,

$$\begin{bmatrix} I_{xx} & 0 & -I_{xz} \\ 0 & I_{yy} & 0 \\ -I_{xz} & 0 & I_{zz} \end{bmatrix} \begin{bmatrix} \dot{p} \\ \dot{q} \\ \dot{r} \end{bmatrix} = \begin{bmatrix} (I_{yy} - I_{zz})qr + I_{xz}pq \\ (I_{zz} - I_x x)rp + I_{xz}(r^2 - p^2) \\ (I_{xx} - I_{yy})pq - I_{xz}qr \end{bmatrix} + \begin{bmatrix} L_A \\ M_A \\ N_A \end{bmatrix} \tag{B.8}$$

implying that

$$\begin{bmatrix} \dot{p} \\ \dot{q} \\ \dot{r} \end{bmatrix} = \mathcal{I}^{-1} \begin{bmatrix} 0 & 0 & I_{xz} & I_{yy} - I_{zz} & 0 \\ -I_{xz} & I_{xz} & 0 & 0 & I_{zz} - I_{xx} \\ 0 & 0 & I_{xx} - I_{yy} & -I_{xz} & 0 \end{bmatrix} \begin{bmatrix} p^2 \\ r^2 \\ pq \\ qr \\ rp \end{bmatrix} + \mathcal{I}^{-1} \begin{bmatrix} L_A \\ M_A \\ N_A \end{bmatrix} \tag{B.9}$$

where $\mathcal{I} := \begin{bmatrix} I_{xx} & 0 & -I_{xz} \\ 0 & I_{yy} & 0 \\ -I_{xz} & 0 & I_{zz} \end{bmatrix}$. Let $S := \begin{bmatrix} S_{xx} & S_{xy} & S_{xz} \\ S_{xy} & S_{yy} & S_{yz} \\ S_{xz} & S_{yz} & S_{zz} \end{bmatrix} := \mathcal{I}^{-1}$. The time-scale parameter ε is included artificially so the fast dynamics become

$$
\begin{aligned}
\varepsilon \begin{bmatrix} \dot{p} \\ \dot{q} \\ \dot{r} \end{bmatrix} = & \\
& - \begin{bmatrix} -S_{xy}I_{xz} & S_{xy}I_{xz} & S_{xx}I_{xz} + S_{xz}\Delta I_1 & S_{xx}\Delta I_2 - S_{xz}I_{xz} & S_{xy}\Delta I_3 \\ -S_{yy}I_{xz} & S_{yy}I_{xz} & S_{xy}I_{xz} + S_{yz}\Delta I_1 & S_{xy}\Delta I_2 - S_{yz}I_{xz} & S_{yy}\Delta I_3 \\ -S_{yz}I_{xz} & S_{yz}I_{xz} & S_{xz}I_{xz} + S_{zz}\Delta I_1 & S_{xz}\Delta I_2 - S_{zz}I_{xz} & S_{yz}\Delta I_3 \end{bmatrix} \begin{bmatrix} p^2 \\ r^2 \\ pq \\ qr \\ rp \end{bmatrix} \\
& + \begin{bmatrix} S_{xx} & S_{xy} & S_{xz} \\ S_{xy} & S_{yy} & S_{yz} \\ S_{xz} & S_{yz} & S_{zz} \end{bmatrix} \begin{bmatrix} (C_l(\alpha,\beta) + C_{l_p}\frac{pb}{2v_A} + C_{l_r}\frac{pb}{2v_A})\bar{q}sb \\ (C_{m_0} + C_{m_\alpha}\alpha + C_{m_q}\frac{q\bar{c}}{2v_A} + \frac{x_{cg_r}-x_{cg}}{\bar{c}}(\bar{C}_z(\alpha,\beta) + C_{z_q}\frac{q\bar{c}}{2v_A})\bar{q}s\bar{c} \\ (C_n(\alpha,\beta) + C_{n_p}\frac{pb}{2v_A} + \frac{x_{cg_r}-x_{cg}}{b}(C_{y_\beta}\beta + C_{y_p}\frac{pb}{2v_A} + C_{y_r}\frac{rb}{2v_A}))\bar{q}Sb \end{bmatrix} \\
& + \begin{bmatrix} S_{xx} & S_{xy} & S_{xz} \\ S_{xy} & S_{yy} & S_{yz} \\ S_{xz} & S_{yz} & S_{zz} \end{bmatrix} \begin{bmatrix} (C_{l_{\delta_a}}\delta_a + C_{l_{\delta_r}}\delta_r)\bar{q}sb + C_{y_r}\frac{rb}{2v_A})\bar{q}sb \\ (C_{m_{\delta_e}}\delta_e + \frac{x_{cg_r}-x_{cg}}{\bar{c}}C_{z_{\delta_e}}\delta_e)\bar{q}s\bar{c} \\ (C_{n_{\delta_a}}\delta_a + C_{n_{\delta_r}}\delta_r + \frac{x_{cg_r}-x_{cg}}{b}(C_{y_{\delta_a}}\delta_a + C_{y_{\delta_r}}\delta_r))\bar{q}sb \end{bmatrix}
\end{aligned}
\tag{B.10}
$$

with $\Delta I_1 := I_{xx} - I_{yy}$, $\Delta I_2 := I_{yy} - I_{zz}$, $\Delta I_3 := I_{zz} - I_{xx}$. This can be written as

$$
\begin{aligned}
\varepsilon \begin{bmatrix} \dot{p} \\ \dot{q} \\ \dot{r} \end{bmatrix} = & \begin{bmatrix} B_{11} & B_{12} & B_{13} & B_{14} & B_{15} \\ B_{21} & B_{22} & B_{23} & B_{24} & B_{25} \\ B_{31} & B_{32} & B_{33} & B_{34} & B_{35} \end{bmatrix} \begin{bmatrix} p^2 \\ r^2 \\ pq \\ qr \\ rp \end{bmatrix} + \begin{bmatrix} S_{xx} & S_{xy} & S_{xz} \\ S_{xy} & S_{yy} & S_{yz} \\ S_{xz} & S_{yz} & S_{zz} \end{bmatrix} \begin{bmatrix} f_{21}(x,z,\alpha,\beta) \\ f_{22}(x,z,\alpha,\beta) \\ f_{23}(x,z,\alpha,\beta) \end{bmatrix} \\
& + \begin{bmatrix} S_{xx} & S_{xy} & S_{xz} \\ S_{xy} & S_{yy} & S_{yz} \\ S_{xz} & S_{yz} & S_{zz} \end{bmatrix} P \begin{bmatrix} \delta_e \\ \delta_a \\ \delta_r \end{bmatrix} \bar{q}s
\end{aligned}
\tag{B.11}
$$

where $f_{21}(.), f_{22}(.), f_{23}(.)$ are the functions involving the stability derivatives as well as the damping

derivatives, and

$$P = \begin{bmatrix} 0 & C_{l_{\delta_a}} b & C_{l_{\delta_r}} b \\ (C_{m_{\delta_e}} \delta_e + \frac{x_{cg_r} - x_{cg}}{\bar{c}} C_{z_{\delta_e}} \delta_e) \bar{c} & 0 & 0 \\ 0 & (C_{n_{\delta_a}} + \frac{x_{cg_r} - x_{cg}}{b} C_{y_{\delta_a}}) b & (C_{n_{\delta_r}} + \frac{x_{cg_r} - x_{cg}}{b} C_{y_{\delta_r}}) b \end{bmatrix}.$$

Multiplying the inverse of the inertia matrix with the matrix involving the control derivatives, the fast dynamics can be written in this form:

$$\begin{aligned} \varepsilon \begin{bmatrix} \dot{p} \\ \dot{q} \\ \dot{r} \end{bmatrix} = \begin{bmatrix} B_{11} & B_{12} & B_{13} & B_{14} & B_{15} \\ B_{21} & B_{22} & B_{23} & B_{24} & B_{25} \\ B_{31} & B_{32} & B_{33} & B_{34} & B_{35} \end{bmatrix} \begin{bmatrix} p^2 \\ r^2 \\ pq \\ qr \\ rp \end{bmatrix} + \begin{bmatrix} S_{11} & S_{12} & S_{13} \\ S_{21} & S_{22} & S_{23} \\ S_{31} & S_{32} & S_{33} \end{bmatrix} \begin{bmatrix} f_{21}(x, z, \alpha, \beta) \\ f_{22}(x, z, \alpha, \beta) \\ f_{23}(x, z, \alpha, \beta) \end{bmatrix} \\ + \begin{bmatrix} L_{11} & L_{12} & L_{13} \\ L_{21} & L_{22} & L_{23} \\ L_{31} & L_{32} & L_{33} \end{bmatrix} \bar{q} s \begin{bmatrix} \delta_e \\ \delta_a \\ \delta_r \end{bmatrix} \end{aligned} \tag{B.12}$$

This is equivalent to

$$\varepsilon \dot{z} = B_z^1 f_z^1 + B_z^2 f_z^2 + \Lambda_{z\delta_f} G_{z\delta_f} \delta_f \tag{B.13}$$

where $B_z^1 := \begin{bmatrix} B_{ij} \end{bmatrix}_{3\times 5}$, $B_z^2 := \begin{bmatrix} S_{ij} \end{bmatrix}_{3\times 3}$, $f_z^1 = \begin{bmatrix} p^2 & r^2 & pq & qr & rp \end{bmatrix}^T$, $f_z^2 = \begin{bmatrix} f_{21} & f_{22} & f_{23} \end{bmatrix}^T$, $\Lambda_{z\delta_f} := \begin{bmatrix} L_{ij} \end{bmatrix}_{3\times 3}$, $G_{z\delta_f} := \bar{q} S$.

The engine, elevator, aileron and rudder are first-order actuators with time-constants T_{eng}, T_{el}, T_{ail}, T_{rud} respectively. The engine time-constant is uncertain. The perturbation parameters σ and ρ are introduced artificially in the actuator dynamics. As a result, the functions, matrices and parameters representing the actuator dynamics are $B_{\delta_s} := -\frac{1}{T_{eng}}$, $f_{\delta_s} := \delta_s$, $\Lambda_{\delta_s u_s} := \frac{1}{T_{eng}}$, $G_{\delta_s u_s} := 1$, $f_{\delta_f} := \begin{bmatrix} -\frac{1}{T_{el}}\delta_e & -\frac{1}{T_{ail}}\delta_a & -\frac{1}{T_{rud}}\delta_r \end{bmatrix}^T$, $G_{\delta_f u_f} := diag[\frac{1}{T_{el}}, \frac{1}{T_{ail}}, \frac{1}{T_{rud}}]$. For simultaneous slow

and fast tracking with uncertainties and actuator dynamics in Chapter 3, the function $f_x(.)$ in the velocity dynamics is

$$f_x(.) = f_{xx}(.) + f_{xz}^T(.)z. \tag{B.14}$$

The remaining parameters, functions and matrices are the same as the ones defined above.

B.3 Matrices Used for Two-Time-Scale Aircraft Tracking Control in Chapter 3

A few simplifications are made to the original equations to reduce them to the form in (3.1). The force coefficient $C_x(\alpha, \delta_e)$ and the moment coefficient $C_m(\alpha, \delta_e)$ do depend on the elevator deflection, but they are provided as look-up tables [70] rather than analytical functions of the elevator deflection. These two coefficients are therefore computed with the elevator δ_e at its trim value. Furthermore, the product of inertia I_{xz} is at least one order of magnitude smaller than the moments of inertia I_{xx}, I_{yy}, I_{zz}. Therefore, the I_{xz} terms in the rotational dynamics are neglected. As a consequence the elements of the vector $J(.)$ are

$$\begin{aligned}
J_1(.) &= \frac{1}{m}[mg(\cos\theta\sin\phi\sin\beta + \cos\theta\cos\phi\sin\alpha\cos\beta - \sin\theta\cos\alpha\cos\beta) \\
&\quad + \bar{q}S((C_x + C_{x_q}\frac{q\bar{c}}{2v_A})\cos\alpha\cos\beta + (C_{y_\beta}\beta + C_{y_p}\frac{pb}{2v_A} + C_{y_r}\frac{rb}{2v_A})\sin\beta \\
&\quad + (C_z + \frac{q\bar{c}}{2v_A}C_{z_q})\sin\alpha\cos\beta)] \\
J_2(.) &= p\sin\alpha - r\cos\alpha + \frac{g}{v_A}(\sin\theta\sin\beta\cos\alpha + \cos\theta\cos\beta\sin\phi - \cos\theta\cos\phi\sin\beta\sin\alpha) \\
&\quad + \bar{q}S(-(C_x + C_{x_q}\frac{q\bar{c}}{2v_A})\frac{\sin\beta\cos\alpha}{mv_A} + (C_{y_\beta}\beta + C_{y_p}\frac{pb}{2v_A} + C_{y_r}\frac{rb}{2v_A})\frac{\cos\beta}{mv_A} \\
&\quad - (C_z + C_{z_q}\frac{q\bar{c}}{2v_A})\frac{\sin\beta\sin\alpha}{mv_A}) \\
J_3(.) &= \frac{I_{zz} - I_{yy}}{I_{xx}}qr + \frac{\bar{q}Sb}{I_{xx}}(C_l + C_{l_p}\frac{pb}{2v_A} + C_{l_r}\frac{rb}{2v_A}) \\
J_4(.) &= \frac{I_{zz} - I_{xx}}{I_{yy}}rp + \frac{\bar{q}S\bar{c}}{I_{yy}}(C_m + C_{m_q}\frac{q\bar{c}}{2v_A} + \frac{x_{cg_r} - x_{cg}}{\bar{c}}(C_z + C_{z_q}\frac{q\bar{c}}{2v_A}))
\end{aligned} \tag{B.15}$$

and the matrix K is

$$K = \begin{bmatrix} \frac{T_m}{m}\cos\alpha\cos\beta & \frac{\bar{q}S}{m}\sin\alpha\cos\beta C_{z_{\delta_e}} & \frac{\bar{q}S}{m}C_{y_{\delta_a}}\sin\beta & \frac{\bar{q}S}{m}C_{y_{\delta_r}}\sin\beta \\ -\frac{\sin\beta\cos\alpha}{mv_A}T_m & -\frac{\sin\beta\sin\alpha}{mv_A}\bar{q}SC_{z_{\delta_e}} & \frac{\cos\beta}{mv_A}\bar{q}SC_{y_{\delta_a}} & \frac{\cos\beta}{mv_A}\bar{q}SC_{y_{\delta_r}} \\ 0 & 0 & \frac{\bar{q}Sb}{I_{xx}}C_{l_{\delta_a}} & \frac{\bar{q}Sb}{I_{xx}}C_{l_{\delta_r}} \\ 0 & \frac{\bar{q}S}{I_{yy}}(x_{cg_r}-x_{cg})C_{z_{\delta_e}} & 0 & 0 \end{bmatrix} \tag{B.16}$$

B.4 Matrices Used for Output Feedback Design in Chapter 4

The measured slow state is $x_M = v_A$. The vector of unmeasured slow state is $x_U = \begin{bmatrix} \alpha & \beta \end{bmatrix}^T$. The functions of angle-of-attack and sideslip angle in $\dot{v}_A, \dot{\alpha}, \dot{\beta}$ are converted in terms of the body-axis velocities. In addition to C_x and C_m, the other force and moment coefficients are approximated using least squares as

$$\begin{aligned} C_z(\alpha,\beta) &\approx C_{z_0} + C_{z_\alpha}\alpha + C_{z_\beta}\beta \\ C_l(\alpha,\beta) &\approx C_{l_0} + C_{l_\alpha}\alpha + C_{l_\beta}\beta \\ C_n(\alpha,\beta) &\approx C_{n_0} + C_{n_\alpha}\alpha + C_{n_\beta}\beta. \end{aligned} \tag{B.17}$$

The resulting matrices in the dynamics of the measured slow state (velocity) are

$$\begin{aligned} f_{xx} &:= \frac{U}{v_A}(-g\sin\theta) + \frac{V}{v_A}(g\cos\theta\sin\phi) + \frac{W}{v_A}(g\cos\theta\cos\phi) + \frac{1}{m}(\frac{U}{v_A}C_{x_0} + \frac{W}{v_A}C_{z_0})\bar{q}S \\ F_{xx_U} &:= \frac{\bar{q}S}{m}\begin{bmatrix} \frac{U}{v_A}C_{x_\alpha} + \frac{W}{v_A}C_{z_\alpha} & \frac{V}{v_A}C_{y_\beta} + \frac{W}{v_A}C_{z_\beta} \end{bmatrix} \\ F_{xz} &:= \begin{bmatrix} \frac{V}{v_A}C_{y_p}\frac{b}{2v_A} & (\frac{U}{v_A}C_{x_q} + \frac{W}{v_A}C_{z_q})\frac{\bar{c}}{2v_A} & \frac{V}{v_A}C_{y_r}\frac{b}{2v_A} \end{bmatrix} \\ g_{x\delta_s} &:= \frac{T_m}{m}\frac{U}{v_A} \\ g_{x\delta_f} &:= \frac{\bar{q}S}{m}\begin{bmatrix} \frac{U}{v_A} & \frac{V}{v_A} & \frac{W}{v_A} \end{bmatrix}^T \\ \Lambda_{x\delta_f} &:= \begin{bmatrix} C_{x_{\delta_e}} & 0 & 0 \\ 0 & C_{y_{\delta_a}} & C_{y_{\delta_r}} \\ C_{z_{\delta_e}} & 0 & 0 \end{bmatrix}. \end{aligned} \tag{B.18}$$

The vectors and matrices in the dynamics of the unmeasured states are as follows:

$$f_{x_U} := \begin{bmatrix} f_{x_{U_1}} & f_{x_{U_2}} \end{bmatrix}^T \tag{B.19}$$

where

$$\begin{aligned} f_{x_{U_1}} := q - \frac{UV}{U^2+W^2}p - \frac{VW}{U^2+W^2}r - \frac{W}{m(U^2+W^2)}(-mg\sin\theta + (C_{x_0} + C_{x_q}\frac{q\bar{c}}{2v_A})\bar{q}S \\ + \frac{U}{m(U^2+W^2)}(mg\cos\theta\cos\phi + (C_{z_0} + C_{z_q}\frac{q\bar{c}}{2v_A})\bar{q}S) \end{aligned} \tag{B.20}$$

$$\begin{aligned} f_{x_{U_2}} := \frac{W}{\sqrt{U^2+W^2}}p - \frac{U}{\sqrt{U^2+W^2}}r - \frac{UV}{mv_A^2\sqrt{U^2+W^2}}(-mg\sin\theta + (C_{x_0} + C_{x_q}\frac{q\bar{c}}{2v_A}\bar{q}S) \\ + \frac{\sqrt{U^2+W^2}}{mv_A^2}(mg\cos\theta\sin\phi + (C_{y_p}\frac{pb}{2v_A} + c_{y_r}\frac{rb}{2v_A})\bar{q}S) \\ - \frac{VW}{mv_A^2\sqrt{U^2+W^2}}(mg\cos\theta\cos\phi + (C_{z_0} + C_{z_q}\frac{q\bar{c}}{2v_A}\bar{q}S) \end{aligned} \tag{B.21}$$

and

$$\begin{aligned} F_{x_U x_U} &:= \frac{\bar{q}S}{m}\begin{bmatrix} -\frac{W}{U^2+W^2}C_{x_\alpha} + \frac{U}{U^2+W^2}C_{z_\alpha} & \frac{U}{U^2+W^2}C_{z_\beta} \\ -\frac{UV}{v_A^2\sqrt{U^2+W^2}}C_{x_\alpha} - \frac{UW}{v_A^2\sqrt{U^2+W^2}}C_{z_\alpha} & \frac{\sqrt{U^2+W^2}}{v_A^2}C_{y_\beta} - \frac{VW}{v_A^2\sqrt{U^2+W^2}}C_{z_\beta} \end{bmatrix} \\ G_{x_U\delta_s} &:= -\frac{T_m}{m}\begin{bmatrix} \frac{W}{m(U^2+W^2)} & \frac{UV}{v_A^2\sqrt{U^2+W^2}} \end{bmatrix}^T \\ G_{x_U\delta_f} &:\approx \begin{bmatrix} -\frac{W}{U^2+W^2} & 0 & \frac{U}{U^2+W^2} \\ -\frac{UV}{v_A^2\sqrt{U^2+W^2}} & \frac{\sqrt{U^2+W^2}}{mv_A^2} & -\frac{VW}{v_A^2\sqrt{U^2+W^2}} \end{bmatrix}\begin{bmatrix} \bar{C}_{x_{\delta_e}} & 0 & 0 \\ 0 & \bar{C}_{y_{\delta_a}} & \bar{C}_{y_{\delta_r}} \\ \bar{C}_{z_{\delta_e}} & 0 & 0 \end{bmatrix}. \end{aligned} \tag{B.22}$$

where $\bar{C}_{x_{\delta_e}}, \bar{C}_{y_{\delta_a}}, \bar{C}_{y_{\delta_r}}, \bar{C}_{z_{\delta_e}}$ represent the average values of those control derivatives. It is to be noted that every constant but unknown parameter are assumed to be within a specified minimum and maximum, so the average of the minimum and the maximum is taken as the parameter value for this approximation.

The vector of functions $f_z^2(.)$ in the angular rate dynamics is modified. Instead of $C_l(\alpha, \beta)$ and

$C_n(\alpha, \beta)$, their least-square approximations shown in equation (B.17) are used. This is because the angle-of-attack and the sideslip angle are evaluated from the measurements in the fast time-scale. The other vectors and matrices stay the same as in Section B.2. For simultaneous slow and fast tracking, $f_x := f_{xx} + F_{xz}z$. The remaining vectors and matrices stay the same.